JAVIER FERNÁNDEZ MARTÍNEZ

AN INTEGRATED GEOCHEMICAL AND ICHNOLOGICAL APPROACH TO RECONSTRUCTING THE FORMATION OF ORGANIC-CARBON-RICH SEDIMENTS AND SEDIMENTARY ROCKS: THE ROLE OF ANOXIA VERSUS PRODUCTIVITY DURING BLACK SHALE DEPOSITION

CO-DIRIGIDA POR EL DR. FRANCISCO JAVIER RODRÍGUEZ TOVAR Y LA DRA. FRANCISCA MARTÍNEZ RUÍZ

PROGRAMA DE DOCTORADO DE CIENCIAS DE LA TIERRA

DEPARTAMENTO DE ESTRATIGRAFÍA Y PALEONTOLOGÍA

UNIVERSIDAD DE GRANADA

2024

A mis padres y mi hermano.

A Belén, el amor de mi vida.

A David, a la Güela, al Paisano.

Από τον Ρούστικο διδάχτηκα […] να εξετάζω επακριβώς ένα θέμα και να μην αισθάνομαι ικανοποίηση μελετώντας το επιφανειακά, να μην συμφωνώ αμέσως με όσους μιλούν ανεύθυνα.

De Rústico aprendí […] a leer sin prisa y a no contentarme con entender un tema superficialmente, a no estar inmediatamente de acuerdo con quienes hablan irresponsablemente.

Marco Aurelio Antonino

Meditaciones (Τὰ εἰς ἑαυτόν), Libro I, Soliloquio 7

INDEX

XI

ABSTRACT

The multiproxy approach used in this research, based on an integrative geochemical and ichnological analysis, aims to advancing the understanding of processes which led to the deposition and preservation of organic matter and the formation of organic-rich sediments and sedimentary rocks, with especial focus on *black shales*. This type of deposits, although profusely studied, still remain poorly understood, and several questions arise when examining black shales. The main controversy refers to the role played by anoxic conditions, and their relationship with organic carbon burial. Other palaeoenvironmental features such as planktonic productivity, hydrographic circulation, and the influence of local versus global triggers, are also subject of debate. Within this context, two case studies of black shales sequences have been selected, representing different ages and depositional settings, thus, allowing for a general approach to investigate black shale deposition. First case study are Toarcian black shales (c. 184 Ma, Lower Jurassic), which are recorded worldwide, and linked to a period of widespread marine anoxia known as the Toarcian Oceanic Anoxic Event (T-OAE). Second case study corresponds to black shale beds from the Upper Pennsylvanian (c. 307 Ma, Upper Carboniferous), deposited in an epeiric sea known as the Late Pennsylvanian Midcontinent Sea during marine transgressions, thus related with large sea-level changes and glacio-eustatic dynamics.

The conducted research was aimed at covering the most debated aspects of black shale deposition. The obtained results have provided further evidence on the main open questions on black shale deposition: a) contrary to the classical assumption that strong anoxia is required for black shale formation, they can form under a broad spectrum of reductive redox conditions. The study cases show that organic-rich sediments can develop under both euxinic and slightly suboxic conditions, with frequent transitions between these stages over deposition; b) redox shifts during black shale deposition are typically sharp and abrupt. Calibration of geochemical proxies shows overlapping values across different redox stages, indicating rapid transitions from oxic/dysoxic to euxinic conditions in benthic environments. Intermediate redox conditions, such as suboxic or ferruginous, are often confined to a few centimetres in the sediment or water column, rendering them nearly imperceptible on a geological time scale; c) recovery of macrobenthic tracemakers following reductive conditions is consistently rapid. Ichnological proxies indicate that shortly after the end of reductive pulses associated with organic carbon burial, macrobenthic tracemaker communities swiftly reoccupy the seafloor, irrespective of whether post-event oxygen levels were predominantly oxic or slightly dysoxic (distinct ichnoassemblages indicate each redox stage); d) local triggers consistently wield a significant influence on black shale deposition in relation to previously considered global phenomena. The findings from both study cases underscore the crucial role played by local and regional factors such as topographic and palaeogeographic features in shaping the black shale record. While global causes are essential in creating conditions conductive to black shale deposition, their impact is localized to specific settings, highlighting the major importance of local and regional factors; and e) brief oxic pulses are commonly observed during black shale deposition, although their identification is not always straightforward. Black shales can accumulate under varying degrees of reductive conditions, interrupted, occasionally by brief oxic intervals irrespective of the specific redox stage during deposition.

Thus, the integration of geochemical and ichnological proxies provides complementary tools for reconstructing black shale depositional conditions. Future research focused on refining the calibration of these proxies will enhance their reliability and complementary utility.

RESUMEN

La presente tesis doctoral se basa en un enfoque multidisciplinar, basado en la integración de análisis icnológicos y geoquímicos, con el objetivo de avanzar en la comprensión de los procesos que condujeron al depósito y preservación de la materia orgánica y formación de sedimentos y rocas sedimentarias ricas en materia orgánica, en particular, las *black shales*. A pesar de haber sido ampliamente estudiadas, aún existen numerosas incógnitas sobre el origen de este tipo de rocas sedimentarias, especialmente en lo referido a sus modelos de formación. La principal controversia está relacionada con el papel que juegan las condiciones anóxicas en el fondo oceánico y su relación con la acumulación de carbono orgánico. Asimismo, otras características paleoambientales como la productividad planctónica, la circulación oceánica y la influencia de condiciones locales y globales, son objeto de debate. En este contexto, se han seleccionado dos casos de estudio de secuencias de *black shale*s que representan diferentes edades y ambientes de depósito, permitiendo así una aproximación general a la interpretación de este tipo de depósitos. El primer caso de estudio es el de las *black shales* del Toarciense (c. 184 Ma, Jurásico Inferior), ampliamente reconocidas a nivel mundial y asociadas a un período de anoxia marina generalizada conocido como el Evento Anóxico Oceánico del Toarciense (T-OAE, por sus siglas en inglés). El segundo caso de estudio corresponde a las capas de *black shales* del Pensilvaniense Superior (c. 307 Ma, Carbonífero superior) depositadas en un mar epicontinental conocido como el Mar del Epicontinental del Pensilvaniense Tardío durante transgresiones marinas, relacionadas con grandes cambios en el nivel del mar debido a dinámicas glacio-eustáticas.

La investigación se llevó a cabo con el objetivo de abordar algunos de los aspectos más controvertidos en el debate sobre el depósito de *black shales*. En general, los resultados obtenidos han permitido avanzar en aquellos aspectos más debatidos sobre la formación de *black shales*: a) Contrariamente a las ideas convencionales de la necesidad de condiciones estrictamente anóxicas para la formación de *black shales*, se ha demostrado que éstas pueden formarse en un amplio espectro de condiciones redox reductoras. Los casos de estudio muestran que los sedimentos ricos en materia orgánica pueden desarrollarse tanto bajo condiciones euxínicas como ligeramente subóxicas, con transiciones frecuentes entre estos dos estadios; b) los cambios redox durante el depósito de *black shales* suelen ser rápidos y abruptos. La calibración de los indicadores geoquímicos muestra valores superpuestos en diferentes estadios redox, indicando transiciones rápidas de condiciones óxicas/disóxicas a condiciones euxínicas en el fondo marino. Las condiciones redox intermedias, como subóxicas o ferruginosas, suelen estar confinadas a unos pocos centímetros en el sedimento o la columna de agua, haciéndolas casi imperceptibles a escala geológica; c) la recuperación de las comunidades macrobentónicas bioturbadoras tras las condiciones reductoras es muy rápida. El análisis icnológico indica que poco después del fin de los pulsos reductores asociados a la acumulación de carbono orgánico, las comunidades macrobentónicas reocupan rápidamente el substrato marino, independientemente de si los niveles de oxígeno post-evento fueron predominantemente óxicos o ligeramente disóxicos (diferentes icnoasociaciones indican cada estadio redox); d) los factores locales ejercen una influencia significativa en el depósito de *black shales* en comparación con los fenómenos de carácter global. Los resultados obtenidos en ambos casos de estudio subrayan el papel crucial desempeñado por factores locales y regionales como la topografía del lecho marino y las condiciones paleogeográficas en la configuración del registro de *black shales*. Si bien las causas globales son fundamentales para crear condiciones propicias para el depósito de este tipo de rocas sedimentarias, su impacto está localizado en entornos específicos, destacando la importancia fundamental de los factores locales y regionales; y e) breves pulsos óxicos son registrados comúnmente durante el depósito de *black shales*, aunque no siempre son identificados. Por tanto, las condiciones reductivas predominantes durante su depósito pueden ser interrumpidas por breves pulsos de mayor oxigenación.

La integración de indicadores geoquímicos e icnológicos se considera, por tanto, como una herramienta fundamental para el estudio de *black shales*, especialmente en la reconstrucción de los procesos implicados en su formación. Futuros avances en la investigación de rocas sedimentarias ricas en carbono orgánico empleando esta metodología permitirán mejorar la integración de ambos tipos de indicadores, aumentando su fiabilidad y utilidad.

PREFACE

I. MOTIVATION, HYPOTHESIS & OBJECTIVES

The preservation of *organic matter* in sediments has had significant historical importance in Earth Sciences. On a planetary scale, the accumulation of organic matter (OM) in sediments profoundly impacts the global carbon and oxygen cycles. The burial of OM results in a net decrease in atmospheric and oceanic CO_2 and an increase in O_2 levels (e.g., Berner, 1989; Hedges, 2002). Consequently, investigating the mechanisms that lead to the accumulation and preservation of OM in sediments is essential for advancing our understanding of atmospheric and oceanic dynamics.

Although organic carbon-rich facies, such as *black shales* and *sapropels*, constitute a minor fraction of the sedimentary record, their exceptionally high organic carbon content has attracted particular attention since they are valuable records of past environmental conditions and palaeoceanographic changes. Also, because of their exceptional high organic content, black shales hold significant economic interest as hydrocarbon source rocks. This interest has driven the development of specialized analytical tools to investigate their depositional mechanisms. Complementarily, these organic-rich facies are also pivotal for advancing our understanding of the organic matter cycle on a planetary scale. This focus has consequently given rise to numerous studies and sophisticated models aimed at deciphering their formation processes and broader implications. Furthermore, black shale deposition has been linked with biological crisis, which confers the study of these black facies a relevant role in the History of Life.

Notwithstanding, the mechanisms leading to the deposit of organic-rich facies remain poorly understood. The role of *oxygen* levels in the water column has long been regarded as one of the principal factors, alongside primary *productivity*, governing the accumulation of organic carbon in sediment. These premises have given rise to two primary models for the occurrence of anomalously high organic carbon deposition in sediment (i.e., the formation of organic-rich facies): the *preservation model* and the *high productivity model*. The key disparity between them, elaborated upon in the following sections, revolves around the interplay between organic matter *preservation* under anoxic conditions and elevated rates of organic carbon *accumulation* stemming from heightened plankton productivity. Both models are rooted in the examination of contemporary basins where organic carbon burial is ongoing. Nevertheless, the influence of oxygen dissolved in the water column, redox conditions, and other palaeoenvironmental factors harbours numerous subtleties that do not always align with modern analogues. Thus, the investigation of ancient organic-rich facies is indispensable for a comprehensive understanding of the diverse conditions underlying black shale deposition.

Against this backdrop, the primary aim of the present study is to enhance our understanding of the mechanisms underpinning the deposition of black shales and to precisely evaluate the palaeoenvironmental conditions governing the burial of organic matter. To achieve this, we propose an innovative methodology that integrates ichnological and geochemical analyses (Fig. 1). Within a benthic environment, a broad spectrum of redox conditions can be discerned in both bottom- and pore-waters. These conditions range from oxic and dysoxic —conducive to macrobenthic communities— to suboxic, anoxic, and euxinic (H_2S is present), representing inhospitable benthic habitats for macro-tracemakers. Consequently, detailed ichnological analysis, elucidating the *behaviour* of the tracemaker community, enables a precise characterization of oxic to dysoxic conditions and the response of tracemakers to redox fluctuations, primarily based on ichnological

features such as abundance, size, and diversity of ichnotaxa (e.g., Bromley & Ekdale, 1984; Savrda & Bottjer, 1986, 1991). Moreover, geochemical proxies facilitate the differentiation of various stages among reductive conditions, including suboxic, anoxic, and euxinic, through the evaluation of organic matter content, and major and trace elements (e.g., Jones & Manning, 1994; Tribovillard et al., 2006; Algeo & Li, 2020). By complementing this integrative approach with sedimentological-stratigraphic studies, the palaeoenvironmental conditions conducive to black shale deposition can be further constrained.

For this research, two case studies of black shale facies were selected to advance knowledge on organic matter accumulation, entailing a comprehensive characterization of the evolution of benthic redox conditions, their correlation with macrobenthic tracemaker communities, and the influence of local, regional, and global palaeoenvironmental factors —e.g. bottom topography, palaeogeography, and sea-level fluctuations. Target units were chosen to encompass a broad spectrum of depositional conditions and ages. The first case study focuses on Toarcian black shales (Lower Jurassic, c. 184 Ma), which are associated with a period of widespread marine anoxia, global sea-level rise, and greenhouse conditions known as the *Toarcian Oceanic Anoxic Event* (T-OAE) (Jenkyns, 1975). The second case study examines Pennsylvanian black shales (Upper Carboniferous, c. 305 Ma) deposited in an epeiric sea that covered much of present-day North America, characterized by cyclic deposits associated with glacio-eustatic sea-level fluctuations referred to as *cyclothems* (e.g., Heckel, 1986).

Despite the fact that the T-OAE has been widely studied, it remains poorly understood. Conventionally, it has been presumed to be nearly synchronous worldwide, characterized by uniformly anoxic benthic conditions in most basins (e.g., Jenkyns, 1985; Little & Benton, 1995; Bucefalo Palliani et al., 2002; Wignall et al., 2005; Mattioli et al., 2009). However, investigations over the past two decades have unveiled a wide spectrum of impacts of the T-OAE on both sedimentological and ecological dynamics (e.g., Hesselbo et al., 2000; Kemp et al., 2005; McElwain et al., 2005; Ruebsam et al.,
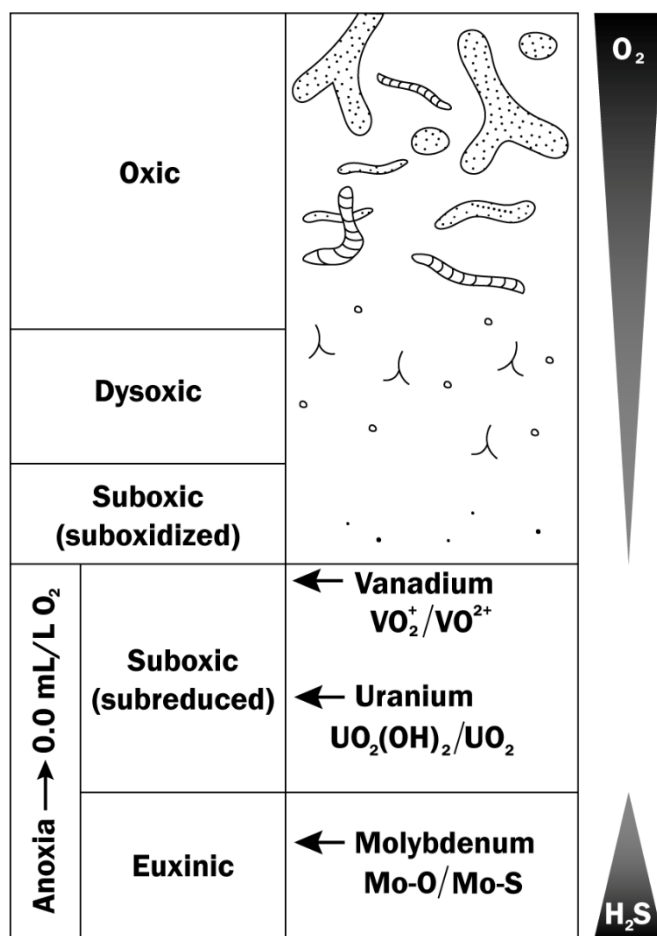
Figure 1. Scheme illustrating the redox ladder*, indicating the proxies used to assess each stage. Note that under suboxic-suboxidized conditions O_2 is still present, while is completely absent in suboxic-subreduced and euxinic (free H_2S) conditions. Abundance, size, and diversity of trace fossils are used to define oxic to dysoxic conditions, vanadium marks the onset of subreduced conditions, uranium indicates the threshold of anoxic-subreduced conditions, and molybdenum is used as a proxy for euxinia. Note that meio-tracemakers can inhabit suboxic benthos.*

2019; Reolid et al., 2021). Two competing models have been postulated to elucidate the triggers that determined black shale deposition during the T-OAE, one attributing it to local/regional factors, such as intense euxinia associated with sluggish hydrographic circulation (McArthur et al., 2008; McArthur, 2019; Remírez & Algeo, 2020), and the other advocating for a global mechanism, such as a worldwide sea-level rise and extensive anoxic conditions in bottom and pore waters (Thibault et al., 2018; Kemp et al., 2022).

Through the detailed study of two outcrops in the Asturian Basin (Northern Spain) (Fig. 2) and a

comprehensive review of literature encompassing data from twenty basins worldwide, this Thesis addresses specific objectives aimed at evaluating various aspects of the Toarcian Oceanic Anoxic Event, including:

- The evolution of redox conditions before, during, and after the event, and its link with black shale deposition.

- The response of macrobenthic tracemaker communities to shifts between anoxic and oxic conditions associated with the T-OAE.

- The intensity and duration of anoxic conditions.

- The significance of local versus global triggers (e.g., sea-level fluctuations, volcanism, tectonic processes, hydrographic circulation, productivity, anoxic bottom- and pore-waters).

The research conducted questions some classical assumptions proposed for the T-OAE, such as those positing persistent anoxia, synchronicity, the relationship to sea-level rise, the influence of massive volcanism, and the supposed absence of bioturbation in black facies.

The Pennsylvanian cyclothems are linked to the cyclical melting and growth phases of the Gondwanan ice sheets, resulting in sea-level fluctuations that profoundly influenced sedimentological dynamics in North America (Heckel, 1977, 1980; for a comprehensive review see Heckel, 2023). A typical cyclothem is characterized by the presence of two limestone units sandwiching a black shale bed, overlain by alternations of sandstone and shale bearing palaeosols. These sequences were deposited in the Late Pennsylvanian Midcontinent Sea (LPMS), which covered much of present-day North America during the Upper Carboniferous (Pennsylvanian) and Early Permian (e.g., Soreghan, 1994; Soreghan & Giles, 1999; Algeo & Heckel, 2008). This epeiric shallow sea featured a water mass circulation model conducive to anoxic conditions at benthic settings, resulting in black shale deposition at relatively shallow depths within a continental shelf (Algeo et al., 2008). While sandstone and shales have been extensively studied from an ichnological perspective, black shales remain poorly analysed, for which reason this Thesis investigates three consecutive cyclothems in five sedimentary records from diverse basins within the LPMS, with a specific focus on black shale facies.

Figure 2. Outcrop photography of a Toarcian black shale bed from Asturias, northern Spain.

The ichnological analysis of these cyclothems has yielded novel insights into the response of macrobenthic tracemaker communities to long-term sea-level changes. Moreover, a meticulous examination of the black shales, combining ichnological and geochemical proxies, enables the assessment of precise redox conditions during black facies deposition and the tracemakers' response to shifts between anoxic and oxic environments. This research also encompasses specific objectives aimed at characterizing palaeoenvironmental features associated with the cyclothems, including:

o   Investigating the role of sea-level transgressions and episodes of anoxic/euxinic conditions during black shale deposition.

o   Assessing the response of macrobenthic tracemaker communities to long-term sea-level fluctuations during black shale deposition.

o   Examining the redox conditions during black shale deposition and identifying their palaeoenvironmental triggers.

o   Evaluating the response of tracemaker communities to abrupt changes in redox conditions.

o   Developing an ichnological model for the cyclothems, focused on the role of anoxic conditions and sea-level changes.

Results and conclusions obtained from the integrated ichnological and geochemical analyses of the Toarcian and Pennsylvanian black shales are complemented with available data in the literature from black shale facies deposited in diverse settings, in an aim to develop a general model for the reconstruction of palaeoenvironmental conditions during the deposition of black shale facies.

II. LAYOUT

The present dissertation is divided into seven chapters, comprising an introduction (Chapter I), and results already published or prepared for publication, including: a study of the T-OAE in the Asturian Basin

(Chapter II), along an analysis of the relationship of the ichnogenus *Halimedides* and the T-OAE (Chapter III); a study of the palaeoenvironmental dynamics during the Toarcian, assessing global vs local triggers (Chapter IV); a study of the North American cyclothems (Chapter V) with specific analysis of their black shales (Chapter VI); and the final remarks integrated in the discussion and conclusion (Chapter VII). The results already published correspond to scientific papers in high impact journals, including *Sedimentary Geology* and *Global and Planetary Change*, and one *Special Publication of the Geological Society*.

Chapter I: Introduction and case studies. This section is aimed at providing the fundamental framework necessary for a comprehensive understanding of the subsequent sections. The introduction offers an overview of the organic matter in sedimentary environments, a concise presentation of the redox conditions prevalent in aquatic systems, and an exploration of the debates surrounding black shale deposition. It outlines the classical models proposed for such deposition, emphasising the significance of these facies in elucidating organic matter accumulation and oceanic dynamics, among other factors.

Chapter II: The T-OAE in the Asturian Basin. This chapter investigates the ichnological and sedimentological changes recognized in two sections from the Asturian Basin (Northern Spain) during the Toarcian Oceanic Anoxic Event (Lower Jurassic). Through detailed bed-by-bed analysis, the study revealed fluctuations in oxygen levels impacting the macrobenthic tracemaker community during the T-OAE and the fauna's response to these redox shifts. The findings document an abundant and diverse trace fossil assemblage before and after the event, with trace fossils absent or scarce during the T-OAE, evidencing alternations between oxic, dysoxic, and anoxic conditions. The ichnological data provide valuable insights into palaeoenvironmental conditions and the T-OAE's impact on benthic ecosystems. These results underscore the importance of ichnology as a tool for enhancing palaeoenvironmental reconstruction based on sedimentological facies analyses.

Chapter III: The record of the ichnogenus Halimedides *and its relationship with the T-OAE*. This chapter focus on the particular record of *Halimedides* Lorenz von Liburnau 1902, just above the black shales marking the end of the T-OAE. This trace fossil indicates the recovery of the tracemaker community with the return of oxic conditions. The occurrence of *Halimedides* post-T-OAE, not previously recorded, highlights its close association with oxygen levels, similar to other anoxic events like the Cretaceous OAE-1a and OAE-2. Additionally, there is a correlation between morphometric and palaeoenvironmental parameters: larger, densely chambered specimens are found in darker, weakly oxygenated facies, whereas smaller, sparsely chambered forms are present in lighter, better-oxygenated sediments.

Chapter IV: Palaeoenvironmental dynamics during the Toarcian: global vs local triggers. This section delves into the extent of anoxia during the T-OAE across various global marine basins. Through the analysis of molybdenum (Mo) and total organic carbon (TOC), the study evaluates local hydrographic restriction and redox conditions in the Asturian Basin (northern Spain) and compares these findings with data from other sections worldwide. The results indicate significant variability in euxinic conditions and water mass restriction across different regions, with certain areas exhibiting pronounced local water mass restriction amidst a broader context of global seawater Mo drawdown. This research enhances our understanding of the intricate interplay between local and global factors influencing oceanic anoxia during the T-OAE.

Chapter V: The Pennsylvanian cyclothems: sea-level changes, transgressive black shales, and the response of benthic fauna. The ichnoassemblages of Upper Pennsylvanian cyclothems in the North American Midcontinent region and their relationship to long-term sea-level changes remain poorly understood. This chapter presents a comprehensive ichnological and sedimentological analysis of three complete cyclothemic transgressive-regressive sequences, focusing on the Hertha, Swope, and Dennis cyclothems in the Illinois Basin and the Midcontinent Shelf. Biogenic structures such as *Planolites*, *Palaeophycus*, *Chondrites*, and ?*Conichnus* are found in nearshore units, while *Zoophycos* and *Chondrites* are characteristic of black shale beds. The integration of ichnological and sedimentological data has identified various depositional settings, ranging from subtidal to intertidal, defined by 12 lithofacies. Despite significant lateral lithological variation across the basins, ichnoassemblages are consistent for equivalent facies. The recovery of oxic conditions after highstand anoxic pulses is evidenced by deep-tier biogenic structures, influenced by the basin's connection to the open ocean.

Chapter VI: Cyclic sedimentation in Pennsylvanian black shales. This chapter is focused on the integration of geochemical and ichnological analyses to precisely characterise redox conditions during the deposition of the Stark and Hushpuckney shales. A prominent euxinic pulse is observed in the lower part of the black shale beds during sea level transgression, followed by a weaker euxinic pulse in the early regressive phase. The uppermost part transitions abruptly to suboxic conditions, progressing to dysoxic facies in the overlying grey shale bed. Geochemical analyses show diverse redox trends tied to glacio-eustatic sea level changes and high-frequency climatic fluctuations. A robust pycnocline during transgressive, highstand, and early regressive stages corresponds with euxinic pulses in the lower black beds, while decreased sea levels and continental input weaken the pycnocline, leading to suboxic and dysoxic conditions in the uppermost black beds and grey shale bed. Low ichnodiversity indicates predominantly dysoxic conditions during grey shale deposition. The abundance and distribution of ichnotaxa suggest regional recovery following euxinic pulses, with variations in benthic colonisation patterns influenced by pycnocline strength and freshwater input.

Chapter VII: Final remarks and conclusions. This final chapter integrates all the results obtained during the conducted research, presenting and asking the main questions regarding black shale deposition. Seven main conclusions were reached, most of them common to all types of black shales, such as the major role played by local factors or the large range of reductive redox conditions under which black shales can be deposited.

CHAPTER I

INTRODUCTION AND CASE STUDIES

1. INTRODUCTION

Organic-rich sediments and sedimentary rocks have been the subject of numerous studies in diverse Earth Science fields. They are characterized by significant amounts of organic carbon and formed in a variety of continental and marine settings. Most interest in organic-rich sedimentary rocks is due to their nature as *source rocks* generating hydrocarbons that eventually accumulated in other sedimentary *reservoir rocks*. However, the deposition of organic-rich sediments responded to substantial changes in environmental conditions controlling the production of organic material, sedimentation rates, and deep-water oxygenation. Thus, further interest in organic-rich sedimentary deposits stems from the information they may offer to infer past environmental conditions regarding, among others, palaeoclimate, ocean circulation, palaeoproductivity, and redox conditions. Among such deposits, black shales hold special interest because they are linked to past biotic crises and a major extinction of species. Yet black shales "are amongst the least understood of all sedimentary rock types" (Wignall, 1994), the depositional mechanisms leading to their formation still poorly understood and subject to extensive debate. Within this context, the present research aims to advance our understanding of processes and mechanisms involved in back shale deposition. To this end, several examples of black shales of different ages and depositional settings were examined under a multiproxy approach that integrates ichnological and geochemical analyses. This introductory chapter covers various general aspects of black shale deposition to provide a solid framework for the subsequent chapters.

1.1. Organic matter in the sediment

In general, the amount of organic matter fixed in sediments represents only a minimal fraction of that globally produced. *Remineralization* (transformation of organic C into minerals or new nutrients) affects c. 99% of the total production; therefore, mechanisms inhibiting remineralization and/or favouring the preservation of OM in sediments are only effective in a minimal fraction (1 to 0.1%) of the total production in oceanic and continental environments (Eglinton & Repeta, 2006; Burdige, 2007). Classically, oceanic primary productivity and anoxic conditions have been considered the main factors controlling organic C fixation in marine sediments (e.g., Wignall, 1994; Hedges & Keil, 1995; Killops & Killops, 2005; Piper & Calvert, 2009). However, advancements in the study of the C cycle and organic-rich sediments have shown that many other factors play a crucial role in OM burial (e.g., Brumsack, 2006; Burdige, 2007; Gómez et al., 2008; Kolesnikov et al., 2009; Reolid et al., 2014). Indeed, organic C is present in almost all sedimentary rocks as disseminated kerogen, representing c. 1% of their composition (Eglinton & Repeta, 2006). Still, it represents an important fraction of the sediments only in facies like black shales or sapropels (> 2-5 %).

The origin of OM buried in marine sediments can be traced both to the continents and the ocean (Fig. I.1). Although terrestrial organic matter (TOM) is considered to be less reactive (i.e., less prone to remineralization) than its marine counterpart, it usually represents a minimal fraction of the buried organic C (Burdiger, 2005). The origin of the marine fraction relies mostly on phytoplankton debris (e.g., Alldredge et al., 1993; Alldredge & Silver, 1998), while other compounds such as bacterial necromass and recycled kerogen particles can represent considerable portions (e.g., Parkes et al., 1993; Keil & Fogel, 2001; Burdiger, 2007). As the product of plant and rock weathering, terrestrial OM is readily remineralized in the oceans, thus having a poor preservation potential; it only represents high fractions of the preserved OM in deltaic settings (Fig. I.1). Conversely, the higher reactivity of marine organic matter (MOM) is outweighed by higher production rates compared with TOM, and it is therefore the main compound of the total organic fraction of the sediments (e.g., Burdiger, 2005, 2007).

In order to understand organic C preservation in sediments, it is necessary to consider several mechanisms that may inhibit remineralization and enhance preservation of the OM, such as physical and chemical protection, the shuttle effect produced by Mn and Fe compounds, and the role of redox conditions. In terms of palaeoenvironmental features, the sedimentation rate, grain size, bathymetry, oxygen levels, redox conditions, and presence of tracemakers are the key aspects regulating organic matter preservation in marine
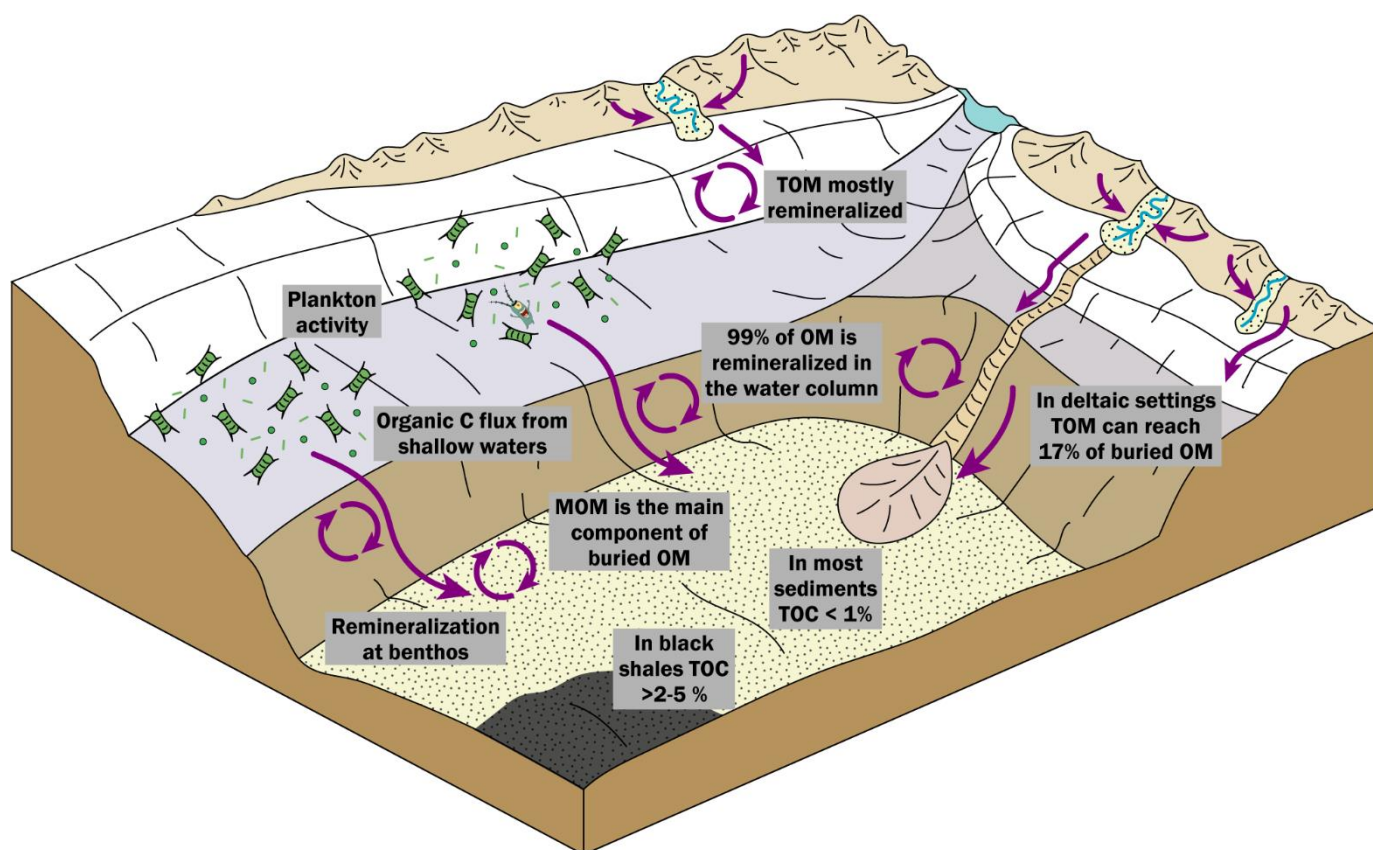
Figure I.1. Sketch illustrating a simplified version of the organic matter cycle (modified from Rebesco et al., *2014). MOM: marine organic matter, OM: organic matter, TOM: terrestrial organic matter.*

sediments. As detailed below, low sedimentation rates enhance OM remineralization due to longer exposure times of the organic compounds before burial. Thus, OM fixation mainly occurs in coastal settings and continental shelfs/margins, where sedimentation rates are higher (e.g., Wignall, 1994; Eglinton & Repeta, 2006; Burdige, 2007). Notably, in deltaic settings and continental margins, terrestrial OM can represent higher fractions (up to 70%) of the buried organic C, but it is also important to consider that most continental shelf sediments correspond to organic carbon-poor sandstones (e.g., Berner, 1989; Shum, 1996; Boudreau et al., 2001; Hedges, 2002; Jahnke et al., 2005; Burdige, 2007). Grain size plays a crucial role in OM preservation, as fine-grained sediments (mudrocks) can enhance preservation of organic compounds by providing physical protection from remineralization (within mineral grains or on mineral surfaces of clay minerals and Fe oxides) (e.g., Huettel & Webster, 2001; Burdige & Zimmerman, 2002; Reimers et al., 2004; Barber et al., 2017).

As mentioned above, anoxic conditions alongside with high primary productivity would classically be considered the main triggers for OM accumulation in marine sediments. However, it is well-known that OM degradation occurs both under oxic and anoxic conditions (e.g., Pendersen & Calvert, 1990; Wignall, 1991; Calvert et al., 1992; Hollander, 1992), with some biomolecules (certain proteins and carbohydrates) being remineralized only under oxygen-deprived circumstances (e.g., Ingalls, 2004). Therefore, not only oxygen levels control OM degradation; the biomolecular composition and *redox shifts* are also important factors controlling OM preservation. The classical assumption that organic compounds are better preserved under anoxic conditions conflicts with the evidenced importance of redox shifts: oxic pulses during pervasive anoxia can activate OM degradation not only during the oxic pulse but also by triggering subsequent anoxic consumption (e.g., Aller, 1994; Hedges & Keil, 1999) or reactivating the biogeochemical cycles of elements such as Mn and Fe, enhancing the fraction of OM that reaches the sediment (*shuttle effect*) (e.g., Tribovillard et al., 2012; Barber, 2017). Oxygen levels are, in turn, controlled by palaeoenvironmental features such as bathymetry, temperature, bioturbation of the

sediment, water mass stratification, or hydrographic circulation. Within this context, benthic tracemaker communities also control OM preservation. Burrowing activity tends to re-oxygenate the substratum (*bioirrigation*), thus extending the exposure of OM to oxidants (i.e., enhancing remineralization) (e.g., Demaison & Moore, 1980; Aller, 1996; Aller et al., 2001). Therefore, the balance between dissolved oxygen through the water column, sedimentation rates, redox changes, biogenic activity, and oceanic productivity is key to understanding the mechanisms of organic carbon burial.

1.2. The redox ladder

A firm understanding of the redox framework is essential for comprehending the mechanisms involved in black shale deposition. Redox conditions in the ocean can be conceptualized as a *redox ladder* (Tyson & Pearson, 1991; Yakushev & Newton, 2013; Grund et al., 2014; recent review in Algeo & Li, 2020), the *redox steps* being determined by the main oxidant (electron acceptor) used in redox reactions (Fig. I.2). These *steps* have been named differently by biologists, chemists, and geologists, alternating terminations in –aerobic and –oxic, in reference to environment facies, bio-redox facies, and redox facies (e.g., Rhoads & Morse, 1971; Tyson & Pearson, 1991; Levin et al., 2009).

Under oxic (aerobic) conditions, defined as having more than 0.2 mL/L of dissolved oxygen, benthic organisms (tracemakers) colonize the substratum, forming complex communities whose abundance and diversity primarily depend on oxygen availability (although factors like salinity may also be important). Hence, less abundant and diverse benthic communities may indicate a transition from oxic to dysoxic (hypoxic, dysaerobic) settings, with oxygen levels dropping to 0.2 mL/L. Suboxic (quasi-anaerobic) conditions occur when oxygen concentration falls to 0 mL/L, and suboxidized and subreduced stages can be distinguished: suboxidized facies still contain dissolved oxygen (up to a maximum of 0.2 mL/L). Under such conditions, only diminutive organisms (< 1 mm), known as meiofauna, can inhabit the benthos (represented as small dots in Figs. 1 and I.2). Below this threshold, tolerance for marine life is threatened, and oxygen-deprived conditions inhibit the development of benthic fauna. The sub-reduced boundary is reached when O_2 concentration drops to 0.0 mL/L (anoxic, anaerobic) without free hydrogen sulfide. The presence of free H_2S would then indicate euxinic conditions (anoxic, anaerobic).

In well-ventilated settings, oxygen is the main element serving as an *oxidant* in microbial processes. As dissolved O_2 in the water column falls, other elements begin to be preferably used as oxidants, characterizing each redox step (Fig. I.2). Suboxidized conditions are characterized by the use of nitrogen, subsequently substituted by manganese when O_2 is absent. Under subreduced conditions, other elements may be used as oxidants, such as vanadium and rhenium in the early stages, and uranium when well developed. Iron can indicate the onset of ferruginous facies within subreduced settings, although this facies is not always present. Finally, the use of sulfur as the main electron acceptor marks the onset of euxinic conditions. In this facies, molybdenum is readily fixed to the sediment linked to organic matter (see Chapter III).

Trace metal species present in the water column can be scavenged and fixed in sediments by means of several biotic and abiotic processes. "This variety of processes results in trace-element enrichments that mirror the specific [redox] conditions prevailing by the time of deposition and early diagenesis" (Tribovillard et al., 2006). Therefore, the study of trace metal concentration involves reconstruction of the redox steps prevailing during deposition (see section 1.6). In well-ventilated benthic environments, where trace element fixation is limited, biogenic activity of macro-tracemakers allows for characterization of oxic and dysoxic facies, as well as oxic-anoxic shifts. Meioturbation can be useful to characterize suboxidized settings, though under more reductive conditions ichnofossils are absent. The use of other oxidants leads to the subsequent accumulation of different trace metals (such as V, U, and Mo), which can be used to identify subreduced to euxinic conditions (Fig. I.2).
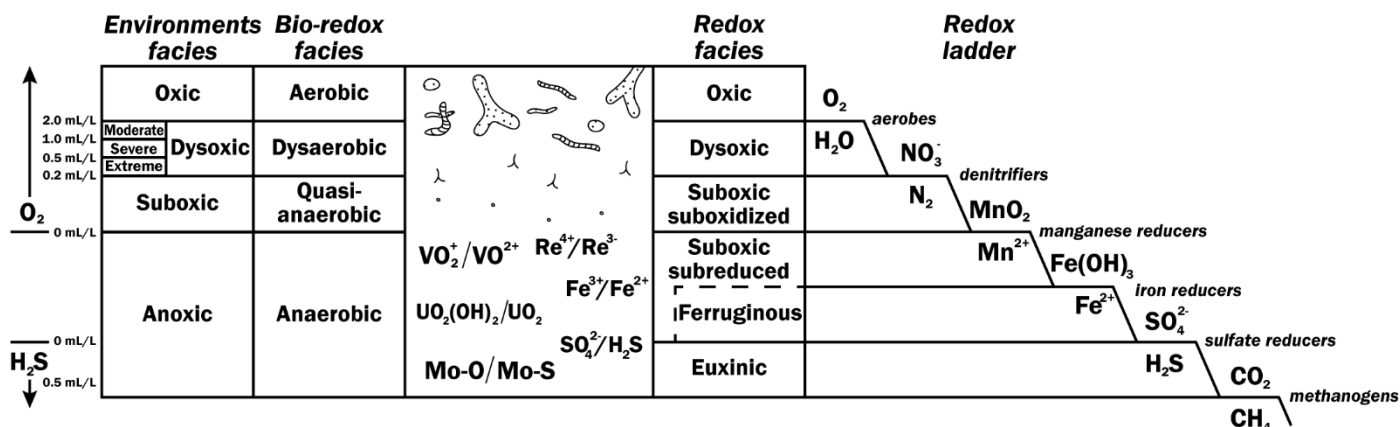
Figure I.2. Scheme indicating the different terminologies used for redox facies. Main oxidants and microbial activity are illustrated, as well as the ichnological and geochemical proxies for each redox stage. Modified from Sapkota et al., 2022.

1.3. Black shales: a short approach

As already mentioned, black shales are dark-coloured mudrocks of high organic matter content, attracting particular interest because they contain valuable geological information, including insights into past environmental conditions and climate changes; but they also hold economic interest, since they may have generated hydrocarbon. Many black shale units are also enriched in metals severalfold above expected amounts in ordinary shale. The name "black shales", also known as black mudstones, derives from their dark colour owing to the high organic matter content. In general, mudstones —sedimentary rocks containing more than 50% mud-sized grains— typically exhibit low total organic carbon (TOC) content, often below 1% (Lazar et al., 2012), while *black shales* (i.e., organic-rich mudstones) possess unique characteristics, their most notable features being their black colour and high organic carbon content (TOC exceeding 2-5%).

A common attribute of black shales is their planar, parallel lamination (Fig. I.3), a feature traditionally interpreted as evidence of steady mud debris accumulation. Yet several recent studies have empirically demonstrated that mud can accumulate under similar flow velocities as sandy sediments (Schieber et al., 2007), and mud floccules can form ripples. Notably, these ripple and cross-bedded structures may undergo deformation during diagenesis and compaction, resulting in planar lamination. Black shales may additionally exhibit bedding types such as wavy and curved, all displaying variable lateral continuity, and more or less

parallel structures (Lazar et al., 2012). Graded bedding, commonly upward-fining, plus compound sequences resulting from turbidite and tempestite flows, are also typical sedimentary structures of black shales.

Regarding mineralogy, the clay minerals that dominate black shales include illite, smectite, kaolinite, chlorite, and montmorillonite. Quartz silt and carbonates (calcite, dolomite, siderite, and ankerite, among others) can also be significant components. Additionally, various (more or less) minor components may represent significant fractions of black shales: detrital (e.g., plagioclase, K-feldspar, rutile, zircon), sulphide (e.g., pyrite), and phosphate minerals, as well as carbonate and quartz cementation (e.g., Lazar et al., 2012; Uffman et al., 2012; Abou El-Anwar, 2016; Ling et al., 2018; Vind & Tamm, 2021). Pyrite, for example, can constitute up to 20% of black shales (Fig. I.3), occurring as finely disseminated, tiny framboids. Microfossil tests, especially foraminifera and radiolaria, are commonly found in black shales, as faecal pellets. Bacterial mats have also been frequently identified. Three main types of porosity are recorded: phylosilicate framework pores, carbonate dissolution pores, and organic matter pores (Schieber, 2010). When TOC exceeds 10%, the phylosilicate framework pores can play a crucial role in organic matter preservation by encapsulating kerogen particles.

The organic matter in black shales comes from both terrestrial and marine sources (see review in Liu et al., 2022). Phytoplankton and bacterial debris are the main constituents, primarily composed of lipids, proteins, and carbohydrates. The terrigenous fraction
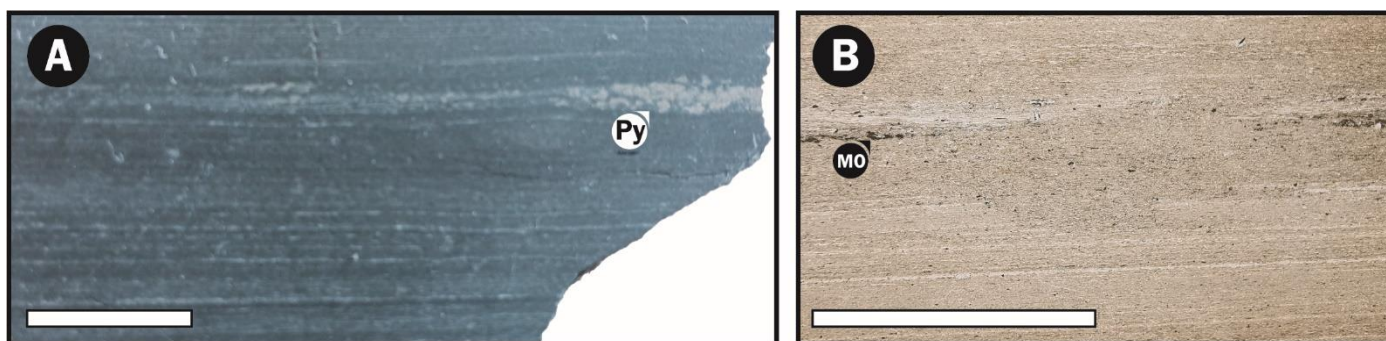
Figure I.3. Detailed black shale photographies from the Rodiles section (Toarcian, Early Jurassic) showing parallel planar lamination in a polished section (A), and in thin section (B). The presence of pyrite (Py) and disseminated organic matter (MO) is indicated; note the change from laminated to a massive texture in the thin section (B). Scale bar: 1 cm.

predominantly consists of plant detritus (mainly lignin), soil compounds, and a minor proportion of terrestrial organisms. Depending on the prevailing fraction of organic matter, hydrogen and oxygen rates can vary, allowing for the determination of organic matter origin by plotting against carbon in a van Krevelen diagram (Fig. I.4). Kerogens formed mainly from algal detritus are hydrogen-rich (Type I), while those with similar hydrogen and oxygen rates originate from phytoplankton debris with a minor fraction of terrestrial organic matter (Type II). Woody material leads to the formation of oxygen-rich kerogens (Type III), whereas highly reworked organic matter exhibits low values of both oxygen and hydrogen (Type IV). Detailed studies of the macerals comprising organic matter can help determine the precise origin of the organic carbon buried in black shales.

Early studies of fossil content in black shales assumed that "benthic-like taxa […] were pseudoplanktonic/pseudopelagic forms that had become detached from floating objects in the water column" (Wignall, 1994). This assumption was based on the generalized acceptance that anoxic benthic conditions were mandatory for black shale deposition. But since the late 1970s, the development of the redox biofacies model, and the demonstration that organic-rich facies can be deposited under oxygen-deprived conditions, have led many studies to consider these fossils as records of in-situ communities. The most characteristic taxa found in black shales are the *paper pectens* (Wignall, 1990), flat-valved, thin bivalves whose lifestyle has been the subject of long debates. The most celebrated example is the Posidonia Shale from Germany (Toarcian, Lower Jurassic), where the occurrence of bivalve-rich horizons
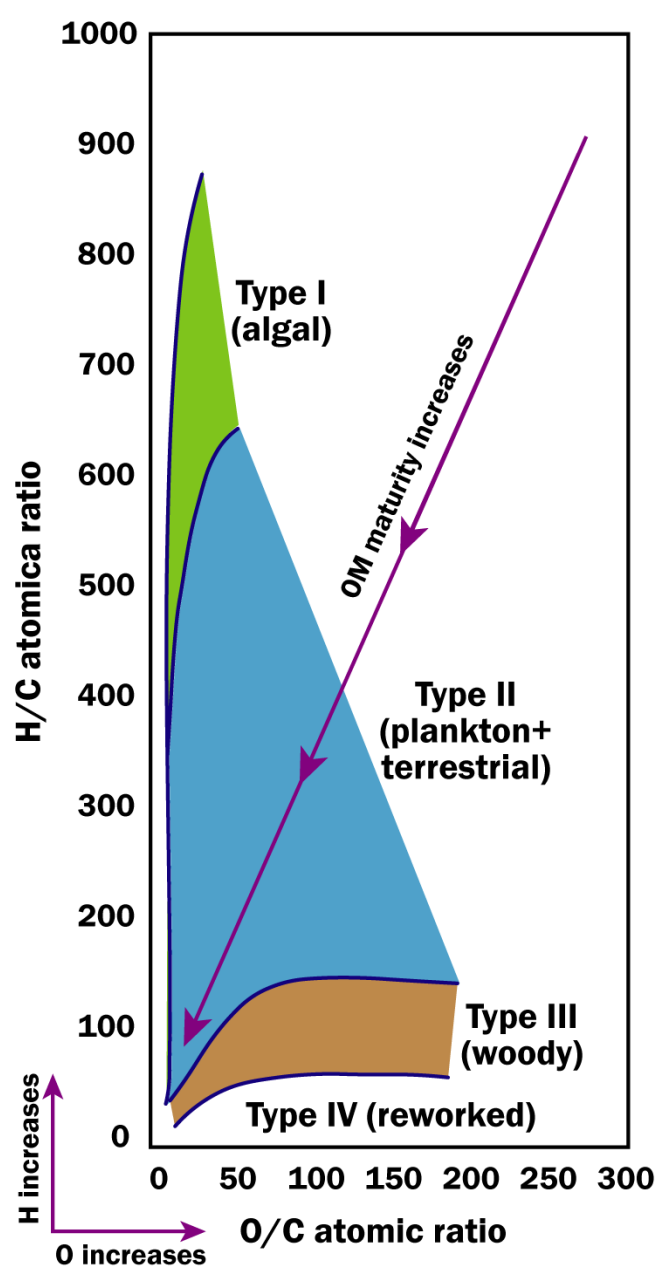
Figure I.4. Modified Van Krevelen diagram illustrating the different types of kerogens and their H-O-C atomic ratios.
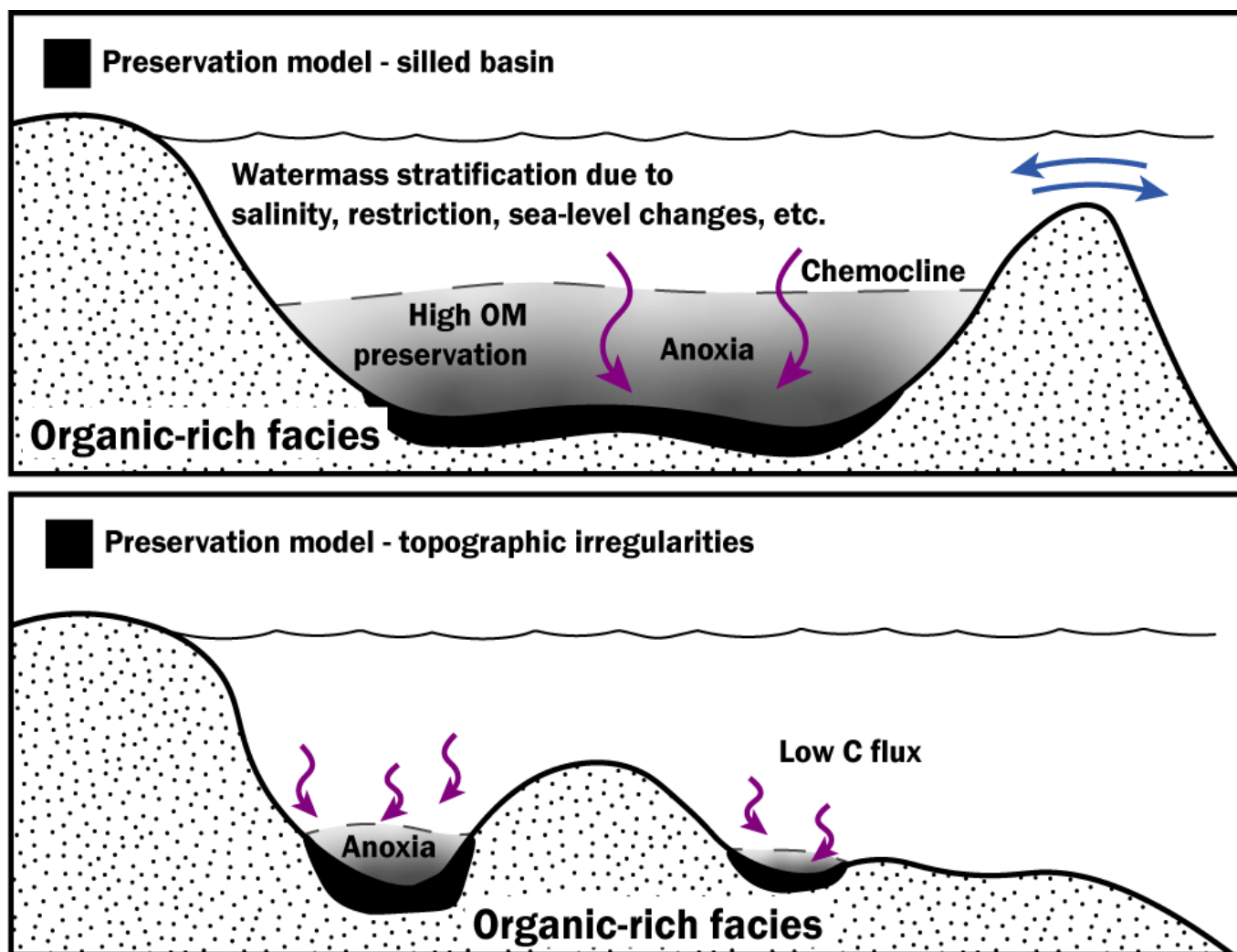
Figure I.5. Simplified versions of the preservation model for silled basins (up) and irregular bottom topography (down).

allows for precise assessment of fluctuations in benthic oxygen levels (e.g., Röhl & Schmid-Röhl, 2001, 2005). Ammonoids are also common planktonic/nektonic taxa found in black shales, along with some foraminifera, graptolites, fish remains and belemnite hooks. Overall, anoxic conditions and fine-grained sediments make black shales excellent candidates for recording extremely well-preserved fossils (*konservatlagerstätte*), including specimens of both vertebrate and invertebrate taxa (e.g., Xiaofeng et al., 2008).

Due to their organic content, since the late 19th century black shales have been the focus of considerable economic interest as hydrocarbon *source rocks*. Exceptional examples are the New Albany and Chatanooga shales, exploited for oil and gas in the U.S.A. since the 1860s (Selley & Sonnenberg, 2015), or the formations Vaca Muerta (Argentina) and La Luna (Colombia-Venezuela), which represent nowadays large

oil plays (Páez-Reyes et al., 2021; Paz, 2021). Aside from their potential economic interest, black shales play a crucial role in Earth history because they are often linked to past biocrisis and widespread anoxic conditions. For example, the aforementioned Chatanooga Shale is a thick (up to 120 m) black shale deposit tied to the Upper Devonian (c. 370 Ma) mass extinction, which along its regional counterparts characterizes most of the Devono-Carboniferous deposits in eastern North American basins (e.g., Algeo et al., 2007). Also, several black shale intervals recorded worldwide are scattered throughout the Mesozoic, linked to widespread marine anoxia episodes, and usually associated with greenhouse conditions and marine transgressions, the so-called Oceanic Anoxic Events (OAEs) (Jenkyns, 1975). Some of these events have been profusely studied: the Posidonienschiefer event (T-OAE, Toarcian, Lower Jurassic c. 184 Ma), the Bonarelli event (OAE-2, Cenomanian–Turonian, Upper Cretaceous c. 93 Ma), or
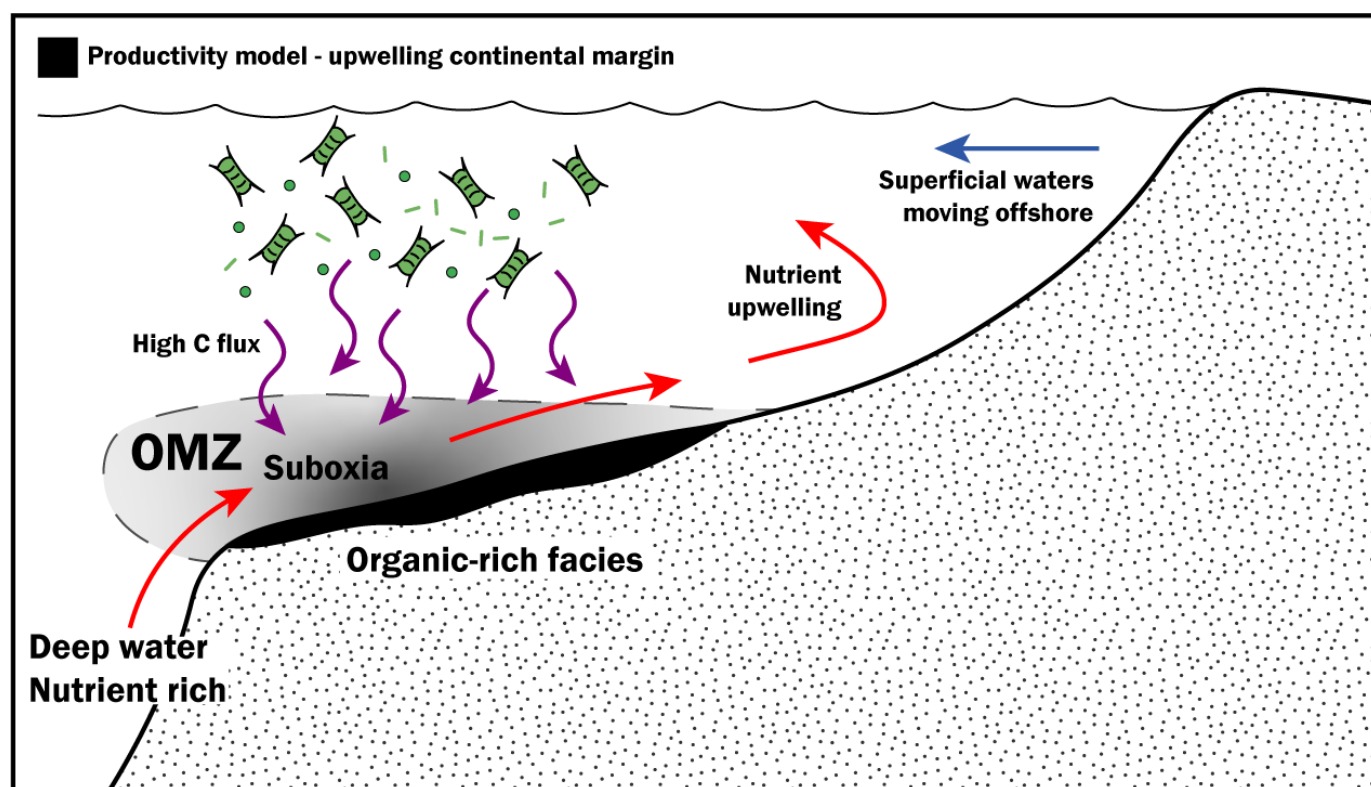
Figure I.6. Simplified versions of the productivity model. OMZ: oxygen minimun zone.

the Paquier event (OAE-1b, Albian, Upper Cretaceous c. 111 Ma) (see review in Jenkyns, 2010).

As mentioned above, depositional mechanisms involving organic rich facies in general, and black shales in particular, remain poorly understood. Thus, palaeoenvironmental conditions during the deposition of black shales are the subject of countless studies. The presence of pyrite and large amounts of organic matter led pioneer researchers to assume that anoxic conditions were required for black shale formation (e.g., Pompeckj, 1909; Woolnough, 1937). This assumption led to the *preservation model* for black shale deposition (e.g., Woolnough, 1937; Tyson, 1987; Canfield, 1989; Rabouille and Gaillard, 1991; Wignall, 1991; Paropkari et al., 1992) (Fig. I.5). In silled basins, the development of anoxic conditions at benthic settings inhibits organic matter degradation by oxygen-consuming microorganisms, thereby enhancing organic matter preservation. However, organic-rich sediments are also deposited in settings where anoxic conditions are not fully developed. In continental margins, a flux of deep waters —which are enriched in nutrients due to the absence of plankton below the photic zone— to shallower settings can give rise to enhanced levels of plankton production. In this context, oxygen

consumption by planktonic organisms produces oxygen-deprived conditions at benthic settings, where organic matter accumulates in the sediment due to the high flux of dead microorganisms. This depositional mechanism is known as the *productivity model* (e.g., Berger, 1979; Calvert, 1987; Morris, 1987; Bender et al., 1989; Pedersen & Calvert, 1990) (Fig. I.6). The key difference between the two models is that in the latter, oxygen deprived conditions do not cause the organic matter enrichment, which is instead due to high accumulation rates. Accordingly, oxygen levels, just as other environmental features, can vary during organic-rich black shale deposition.

Overall, several questions arise regarding the precise mechanisms behind black shale deposition, such as:

I.   Is anoxia a cause or a consequence of black shale deposition?

II. Are anoxic conditions persistent, or may brief oxic intervals occur during black shale deposition?

III. Are anoxic pulses related to sea-level transgressions, which can shallow the chemocline, or to regressions, which can isolate

silled basins causing high hydrographic restriction?

IV.   Are black shales deposited exclusively under marine salinities, or can they also be found in brackish settings?

V.   What role is played by the sedimentation rate? Although slow sedimentation rates have been widely reported for black shale units, high sedimentation rates enhance organic matter preservation by isolating it from the sediment-water interface, where most organic degradation occurs.

VI.   What role is played by water temperature? Several widespread black shale deposits are linked to a global rise in sea-water temperature.

VII.   Do tectonic mechanisms play a relevant role in black shale deposition? Horst and graben structures, as well as smaller bottom irregularities, can act as semi-restricted basins enhancing organic C burial.

The absence of modern analogues for several palaeoenvironmental configurations triggering organic carbon enrichment makes the study of black shales key for developing an accurate model for the global carbon cycle. However, there are still many open questions that make the origin of black shales a challenge in Earth Sciences.

1.4. Ichnology of black shales

Due to the prevalent oxygen-poor depositional conditions, ichnofossils in black shales are generally scarce. Most structures are light-coloured and occur in the upper part of the black beds, suggesting they were formed later, associated to post-black shale conditions. Therefore, the study of light-infilled trace fossils in black shales is a useful tool for examining the recovery of benthic communities after inhospitable conditions (e.g., Rodríguez-Tovar, 2021). In several cases, alternations between dark and light mudstones have led to the development of *palimpsest ichnofabrics* (e.g., Bromley & Ekdale, 1984; Jordan, 1985; Savrda & Bottjer, 1986),

where different ichnoassemblages can be identified, representing the behaviour of benthic fauna under variable redox conditions. In all cases, however,
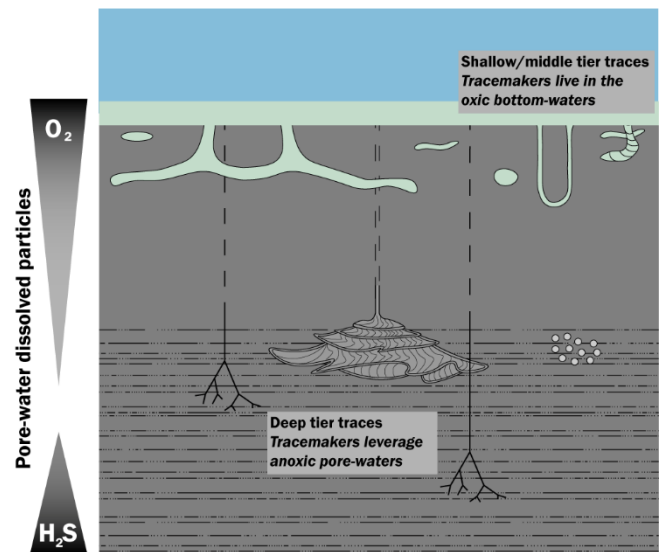
Figure I.7. Scheme illustrating the different biogenic structures which are commonly observed in black shales. Note the distribution of O_2 and H_2S within pore-waters.

bioturbation can be traced to organisms living in (or connected to) oxic waters.

Common trace fossils found in black shales include shallow/middle-tier structures like *Thalassinoides*, *Arenicolites*, *Diplocraterion*, and *Planolites*, but deep burrows such as *Chondrites* and *Zoophycos*-like structures are also found (e.g., Savrda & Bottjer 1991; Savrda & Ozalas 1993; Wetzel & Uchman 1998, 2012; Lazar et al., 2012; see recent review in Rodríguez-Tovar, 2021). Depending on the penetration of the burrow within the sediment, the relationship of their tracemaker with the anoxic facies varies (Fig. I.7). Deep burrows were developed in an aim to leverage suboxic/euxinic pore-waters, for example, to farm microorganisms such as sulfate-reducing bacteria, which could serve the tracemaker as food (agrichnia) or symbiont (chemosymbiosis) (e.g., Seilacher, 1990). These structures, developed to *leverage anoxic conditions*, could be considered as the black shale ichnofossils sensu stricto. Yet ichnotaxonomical characterization is hampered by the scarcity and weak visibility of the trace fossils; if burrows were produced during black shale deposition, they would showcase a dark infill in very poor contrast with the black host-bed. Conversely, shallow/middle-tier structures were developed under/in contact with oxic conditions regardless of the black sediment pore-waters, such as dwelling

(domichnia) or feeding structures (fodinichnia). The interpretation of these structures yields a relation with the oxic conditions after black facies deposition, therefore aiding post-event palaeoenvironmental reconstructions. The variations in size, diversity, abundance, penetration depth, and cross-cut relationships of trace fossils are keys for inferring benthic redox conditions during and after mudstone deposition, and how tracemaker communities responded to these redox shifts.

Recent works have highlighted the role of *meioturbation* in the study of mudstones, especially black shales (e.g., Schieber, 2003; Schieber & Wilson, 2021; Wilson et al., 2022; cf. crypto-bioturbation from e.g., Pemberton & Gringas, 2005; Pemberton et al., 2008, 2012). Meioturbation comprises biogenic structures produced by tiny organisms (< 1 mm), which can heavily modify the fabric of black shales (Schieber & Wilson, 2021). Some studies suggest that massive (i.e., non-laminated) black shale beds can result from the activity of *sediment swimmers* (Schieber, 2003), organisms that move through a thin layer within the sediment, developing non-discrete, black-in-black structures. The activity of these organisms erases the primary sedimentary structures, resulting in a homogenized fabric with invisible or very subtle structures. Not only does this fact have crucial sedimentological implications, it also implies that detailed analysis of previously considered anoxic black shale successions could result in the identification of oxic/dysoxic conditions. Moreover, experiments on consolidation rates of muds indicate that bioturbation would occur during the few weeks after deposition (Barret & Schieber, 1999), suggesting that suboxic/euxinic conditions did not prevail during deposition of this type of black facies. In addition, the activity of meiofauna can modify primary lamination, cutting the sets or altering the laminae path; thus, a detailed examination of a supposed parallel lamination may result in the identification of well-ventilated benthic settings.

1.5. Inorganic geochemistry of black shales

Relative to common mudstones or the average crust, black shales are known for being enriched in many redox-sensitive and/or sulfide-forming metals such as chromium, copper, molybdenum, or vanadium. As explained before, the complex redox conditions leading to organic carbon preservation is paired with the fixation of different chemical elements in the sediment. Thus, the concentration of trace elements in black shales *mirrors* the redox steps that prevailed during deposition. Other trace metals like barium and phosphorus can also be accumulated due to palaeoenvironmental variations (e.g., productivity). The analysis of elemental concentrations of black shales can therefore serve to trace both palaeoredox and palaeoenvironmental conditions.

Redoxsensitive elements are normally used as palaeoredox proxies (e.g., V, Re, Fe, Cu, Cr, Mo), since their fixation in sediments is mostly redox-dependant (e.g., Algeo & Maynard, 2004; Algeo & Lyons, 2006; Algeo & Tribovillard, 2006; Tribovillard et al., 2012; Little et al., 2015; Algeo & Li, 2020; Algeo & Liu, 2020). To estimate the enrichment of such elements, bulk concentrations are usually *normalized* to aluminium ($\%_{Element}/\%_{Al}$) (e.g., Brumsack, 1989; Calver & Pedersen, 1993). Moreover, in order to compare among different units, the trace element concentration can be represented as an *Enrichment Factor* (EF), based on the average trace element and Al concentration of global shales (GS): $Element_{EF} = [(Element/Al)_{sample}/(Element/Al)_{GS}]$ (Taylor & McLennan, 1985; Tribovillard et al., 2006); when the EF is > 1-3 the sample may be considered enriched (see Chapters III and V for more details). Further proxies based on other elements can be used to trace redox conditions. One good example is the Degree of Pyritization (DOP), which is based on iron speciation and is calculated following the equation: $DOP = Fe_{py}/(Fe_{py} + Fe_x)$, where Fe_x represents reactive iron and Fe_{py} represents pyrite iron, the latter calculated by multiplying $S\cdot0.871$ (Leventhal & Taylor; 1990). After Algeo & Liu (2020), total DOP (DOP_T) is commonly used, calculated as $(55.85/64.12)\cdot(S/Fe_T)$, where Fe_T is the total concentration of Fe. The C_{org}/P ratio is also used owing to its relationship with benthic redox conditions (Algeo & Ingall, 2007): the presence of oxygen enhances the oxidation of C and the presence of P in the sediment, whereas under anoxic conditions P is lost to the water column and C_{org} preservation in the sediment rises, giving high ratios for anoxic conditions and lower values for oxic environments (Fig. I.8). The C_{org}/P ratio is

calculated by dividing TOC and P values by its respective molar weight, following the equation $C_{org}/P = (TOC/12)/(P/30.97)$.

Among the trace metal proxies, molybdenum is one of the most useful and reliable. Molybdenum is fixed in sediments only under euxinic conditions, mostly linked to OM, so that it can be used to trace hydrographic restriction (Mo/TOC ratio). This proxy is based on the *reservoir effect* (Algeo & Lyons; 2006): because the main source of Mo in the seawater is the open ocean, the isolation of a silled basin during euxinic conditions leads to the fixation of Mo in sediments, with a subsequent decrease in total Mo due to the absence of water renewal (i.e., the absence of Mo flux in the basin from the open ocean). Hence, when sediment sequestrates Mo from the water, raising its concentration in sediments, aqueous Mo concentration will decrease if sediment fixation exceeds its replenishment in the basin (see Chapter III for a detailed description of this mechanism).

Regarding productivity, barium and marine barite have been broadly used as palaeoproductivity proxies (e.g., Dymond et al., 1992; Gingele and Dahmke,1994; Nürnberg et al., 1997; Eagle et al., 2003; Ma et al., 2015; Martínez-Ruiz et al., 2020). Mechanisms of barite production in the mesopelagic zone (200-600m) have been linked to microbial processes and organic matter degradation (e.g., Dehairs et al., 2008; Jacquet et al., 2011; Planchon et al., 2013; Martínez-Ruiz et al., 2018, 2019). Bacterially mediated processes for barite precipitation have also been demonstrated under experimental conditions (Gonzalez-Muñoz et al., 2012; Torres-Crespo et al., 2015). These bacterial processes are consistent with barite abundance at mesopelagic depths in the ocean where extracellular polymeric substances (EPS) play fundamental roles as nucleation sites. In general, diverse proxies based on Ba have been commonly used to trace past primary productivity in the oceans (e.g., Ba_{EF}, Ba/Al, Ba/Ti, or Ba_{bio}). While the estimation of palaeoproductivity in black shales is generally complicated by the strong diagenetic overprint of barite (e.g., Arndt et al, 2002), remobilized Ba and authigenic barite fronts may still serve as indicators for past marine barite occurrence and enhanced productivity.

Figure I.8. Several redox proxies and their relationship with the redox ladder. Modified from Algeo & Liu, 2020.

2. MATERIAL AND METHODS

The present dissertation is based on a multiproxy approach applied to the study of black shales from both outcrops and drill cores, encompassing fieldwork, geochemical analyses, and ichnological studies. While each chapter within this thesis contains a detailed methodological section, a brief summary is provided below.

Over the duration of this PhD project, several campaigns were conducted, most fieldwork being done during the first two years. Two sections along the Asturian coast in northern Spain, located at the Rodiles and Lastres cliffs, were studied and sampled. These sections contain two black shale beds associated with the Toarcian Oceanic Anoxic Event, intercalated within a sequence of light/dark marl alternations. During these field campaigns, observations were conducted bed-by-bed, focusing primarily on sedimentological and ichnological features. Additionally, samples were obtained for subsequent geochemical analyses and for polished and thin sections. Photographs were taken to document the main ichnological features of the studied sediments. Ichnological analyses were conducted both in the field and in the laboratory. In the field, the study focused specifically on the spatial distribution of trace fossils, including their vertical and lateral arrangement within the beds, as well as their crosscutting relationships with other layers and sedimentary structures. Size, abundance (measured using the Bioturbation Index, s. Taylor & Goldring, 1993), and diversity were assessed,

and preliminary taxonomic assignations were made. Then, detailed analysis of thin and polished sections improved the characterization of infill features (such as colour, presence of pellets, and wall structures), and their relationships with other sedimentary (e.g., lamination) and biogenic (ichnofossils) structures, providing for a more detailed ichnotaxonomical characterization. Additionally, image editing using common software (e.g., Adobe Photoshop) enhanced the visibility of trace fossils by increasing the colour contrast between biogenic structures and the host sediment, facilitating the recognition of various ichnological properties.

Collected samples underwent diverse geochemical analyses. Major element concentrations (e.g., Si, Al, Fe, K, Mn) were obtained using X-Ray Fluorescence (XRF), while trace element values (e.g., Mo, U, V, Cu) were determined by means of Inductively Coupled Plasma - Mass Spectrometry (ICP-MS). Total Organic Carbon (TOC) was obtained by Rock-Eval pyrolysis. Additionally, different iron species were determined, involving sequential acid dissolution of samples. Scanning Electron Microscopy (SEM) was used for mineralogical characterization of selected samples — for instance, to obtain high-resolution images of pyrite framboids.

Later on, drill cores stored in several US Geological Survey warehouses were studied. Although study of the spatial distribution of trace fossils is limited in core analysis, half-cut cores facilitated a detailed ichnological analysis, in a way similar to polished sections. The study units corresponded to thin black shale beds sandwiched within limestone or sandstone beds, deposited during the Pennsylvanian in a massive epeiric sea. Ichnological techniques resembling those mentioned were employed to investigate the different black shale deposits.

3. CASE STUDIES

As stated previously, environmental conditions resulting in the formation of organic-rich sediments do not always correspond to modern analogues. Some models are based on modern anoxic environments such as the Black Sea. But detailed studies of black shale

formation have revealed that the mechanisms leading to their deposition do not align with those observed in modern basins. To advance our understanding of the global carbon cycle and its variations it was therefore necessary to study records of ancient organic-rich sediments, among which black shales prove particularly noteworthy. In the present research effort, we examined two representative types of black shales whose depositional conditions have been broadly discussed and subjected to debate.

The first case study involves two black shale beds associated with one of the several oceanic anoxic events sparsely distributed throughout the Mesozoic, occurring during the Early Jurassic (T-OAE; Toarcian, c. 184 Ma). These events, including the T-OAE, were characterized by greenhouse conditions, massive volcanic activity, sea-level fluctuations, and widespread benthic anoxia, resulting in globally distributed black shale records. The second case study focuses on sediments from a Pennsylvanian epeiric sea (c. 307 Ma) that covered most of the North American continent. Sedimentological dynamics in basins within this epeiric sea were dominated by large sea-level changes driven by glacio-eustatic mechanisms, resulting in thin black shales intercalated within transgressive and regressive limestones. The studied black shales therefore represent challenging case studies of organic carbon accumulation in variable sedimentary environments, and diverse palaeoenvironmental factors are involved in their formation.

3.1. The Toarcian Oceanic Anoxic Event

In the late 1970s, several studies put forth that diverse black shale deposits across Europe were associated with the same depositional event. The first identified intervals of widespread black facies deposition occurred during the Cretaceous (Aptian/Albian and Cenomanian/Turonian), characterized by greenhouse conditions, rising sea-levels, and high productivity. These periods of significant palaeoenvironmental changes —recorded as extensive black shale deposits— were termed "Oceanic Anoxic Events" (OAEs) (Jenkyns, 1975; Schlanger & Jenkyns, 1976). Subsequently other examples were studied, primarily in Cretaceous

sediments (e.g., Ryan & Cita, 1977; Thiede & van Bandel, 1977; McCave, 1979; Arthur et al., 1984, 1990; Bréhéret, 1985; Jenkyns, 1985; Graciansky et al., 1986; Coccioni et al., 1987; Schlanger et al., 1987).

Among these, the most renowned non-Cretaceous OAE occurred during the Toarcian stage (Early Jurassic, c. 184 Ma), known as the Toarcian-OAE (T-OAE; Hallam & Bradshaw, 1979; Jenkyns, 1980, 1988). Early studies proposed a productivity model developed under global sea-level rise and greenhouse conditions, which expanded shelf areas, thereby enhancing planktonic productivity. Alternatively, proponents of the preservation model argued for stratified water columns in semi-silled basins, linked to cold freshwater inputs associated with ice-sheet melting and continental runoff (Seilacher & Westphal, 1971; Hallam, 1981; Bessereau et al., 1995).

However, more recent studies have invoked additional mechanisms influencing black shale accumulation during the T-OAE at both local and global scales. In line with the massive input of volcanogenic CO_2 from the Karoo and Ferrar large igneous provinces (McElwain et al., 2005), seawater temperatures rose by more than 10°C in certain regions (e.g., Gómez & Goy, 2011), and a global transgression has been recorded since the onset of the Toarcian stage (e.g., Krencker et al., 2019). Tectonic mechanisms also facilitated the destabilization of methane clathrates (e.g., Hesselbo et al., 2000), contributing to greenhouse conditions along with permafrost and ice-sheet melting (e.g., Ruebsam et al., 2019). At regional scales, water mass stratification due to salinity gradients (Remírez & Algeo, 2020a) enhanced hydrographic restriction (i.e., slow bottom-water renewal rates) in silled basins (e.g., McArthur et al., 2008).

These advancements have led to a more detailed understanding of the mechanisms involved in black shale deposition during the T-OAE. Consequently, the preservation vs productivity debate has gradually become obsolete, shifting discussions towards a global vs local dichotomy (e.g., Thibault et al., 2018; Remírez & Algeo, 2020b; Kemp et al., 2022). In this context, the present research underscores the importance of ichnology as a tool to upgrade sedimentological and redox facies analysis, interpreting the dynamics that affected the benthic setting of a carbonate platform in the

northwestern Tethys (Fernández-Martínez et al., 2021). Furthermore, the evolution of euxinic conditions during the Toarcian is addressed through the use of the Mo/TOC ratio (Fernández-Martínez et al., 2022), in a review that examined almost thirty basins worldwide to evaluate the role played by regional and global triggers in black shale deposition. Seeking to address some of the questions raised in the preceding chapters, geochemical and ichnological analyses are integrated and complemented with sedimentological data. Palaeoenvironmental features are characterized and compared, empirically assessing the role played by each factor in organic carbon accumulation during the T-OAE.

3.2. The Pennsylvanian cyclothems

During the Middle Pennsylvanian and Early Permian (315 - 270 Ma), a significant portion of the inner North American continent was submerged under a vast epeiric sea known as the Late Pennsylvanian Midcontinent Sea (LPMS). This shallow sea, comprised of several basins more or less isolated by submerged arches, experienced sedimentological dynamics strongly influenced by sea-level fluctuations. The fluctuations were primarily driven by glacio-eustatic mechanisms, resulting from the growth and melting cycles of the Gondwanan ice sheets. This led to the deposition of cyclic sedimentary sequences known as "cyclothems" (e.g., Heckel, 1977, 1980).

An ideal cyclothem typically consists of limestone facies deposited during subsequent transgressive and regressive stages, with thin black shale beds intercalated at the stage's boundary. The sequence is further characterized by alternations of sandstone and shale, interpreted as regressive/lowstand deposits, often capped by palaeosols. While limestone and sandstone/shale facies exhibit varying distributions across the basins comprising the LPMS, black shale beds demonstrate persistent lateral continuity. Therefore, the same black bed records the influence of different mechanisms depending on the palaeogeography of the basin within the LPMS (see Heckel, 2023 for a review).

Furthermore, comprehensive studies of the LPMS have revealed that this expansive epeiric sea was

characterized by a unique model of water circulation, termed the "superestuarine model" by Algeo & Heckel (2008). During flooding episodes, extensive anoxic conditions arose due to the westward influx of oxygen-depleted waters from Panthalassa, coupled with humid conditions triggering significant continental freshwater runoff from the east. This interplay within predominantly landlocked basins established a gradient of benthic redox conditions, with more pronounced anoxic pulses occurring in the inner, shallower regions of the LPMS (Illinois and Appalachian basins). Within these basins, regional precipitation and extensive continental runoff fostered the formation of a robust halocline and a deep pycnocline, restricting vertical water mixing and facilitating the development of anoxic conditions, preconditioned by the oxygen-depleted deep water mass from Panthalassa. Consequently, the emergence of anoxic conditions in the LPMS was highly susceptible to changes in climatic conditions (Algeo & Heckel, 2008, and references therein).

The LPMS cyclothems therefore represent unique examples of black shale accumulation. Modern examples of such an expansive epeiric sea no longer exist, and the intricate water circulation model of the LPMS presents an opportunity to address some of the challenges associated with black shale deposition. Widely distributed cores were selected to analyse the regional features influencing sedimentological dynamics, contrasting them against local features and sea-level fluctuations. Additionally, the effects of these palaeoenvironmental features on benthic tracemaker communities were studied. The study sections comprise three subsequent cyclothems (Swope, Hertha, and Dennis), thus enabling an evaluation of the roles played by different features both spatially and temporally (Fernández-Martínez et al., in press).

Figure I.9. Core photography of the black shale from the Dennis cyclothem (Upper Pennsylvanian). Box length is 3 ft (c. 90 cm).

CHAPTER II

THE T-OAE IN THE ASTURIAN BASIN

Bottom- and pore-water oxygenation during the early Toarcian Oceanic Anoxic Event (T-OAE) in the Asturian Basin (N Spain): Ichnological information to improve facies analysis

Javier Fernández-Martínez [a], Francisco J. Rodríguez-Tovar [a], Laura Piñuela [b], Francisca Martínez-Ruiz [c], José C. García-Ramos [b]

[a] Departamento de Estratigrafía y Palaeontología, Universidad de Granada, Granada, Spain

[b] Museo del Jurásico de Asturias (MUJA), Colunga, Asturias, Spain

[c] Instituto Andaluz de Ciencias de la Tierra CSIC-UGR, Granada, Spain
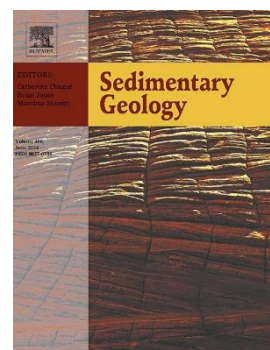
ABSTRACT

Detailed bed-by-bed ichnological and sedimentological analysis of the early Toarcian Oceanic Anoxic Event (T-OAE) in two sections from the Asturian Basin -Rodiles and Lastres- reveals changes in the macrobenthic tracemaker community mainly induced by oxygen fluctuations. Ichnological analysis enabled us to document an abundant and diverse trace fossil assemblage, with ten ichnogenera, probably corresponding to alternations between the *Zoophycos* ichnofacies and the distal expression of the *Glossifungites* ichnofacies: *Arenicolites*, *Chondrites*, *Diplocraterion*, *Halimedides, Palaeophycus, Planolites*, *Rhizocorallium*, *Thalassinoides, Trichichnus* and *Zoophycos*. Six ichnofabrics were differentiated: laminated?, *Diplocraterion-Thalassinoides*, *Chondrites*-mottled*, Chondrites-Palaeophycus-Planolites, Chondrites-Halimedides-Planolites* and *Chondrites*-laminated. Ichnological features (including ichnodiversity, distribution of traces and cross-cutting relationships) allowed us to characterise a well-developed multi-tiered macrobenthic tracemaker community, as well as distinguish different tiering models associated with variations in bottom- and pore-water oxygenation. Anoxic conditions associated with the T-OAE corresponded mainly, but not exclusively, to black shale facies. Minor-order oxygen fluctuations from suboxic/anoxic to disoxic/oxic conditions developed during the middle part of the T-OAE. Laminated intra-T-OAE dark and light grey marls show lithological features similar to those of bioturbated pre- and post-event marls; thus, the ichnological information provides evidence that the T-OAE had a larger effect on biota than on depositional features.

KEY WORDS

1. INTRODUCTION

The early Toarcian Oceanic Anoxic Event (T-OAE) is one of the most important environmental perturbations affecting marine ecosystems during Mesozoic times (e.g., Little & Benton, 1995; Bucefalo Palliani et al., 2002; Mattioli et al., 2009). The environmental perturbation has been documented globally and is marked by a negative carbon isotope excursion, reflecting a global carbon cycle perturbation (e.g., Hesselbo et al., 2000, see also review by Remírez & Algeo, 2020).

The causes of the negative ^{13}C isotope excursion are related to the emplacement of the Karoo-Ferrar Large Igneous Province (K-F LIP) (Fig. II.1A), in turn associated with extensional mechanisms and the production of volcanogenic CO_2 (McElwain et al., 2005), the dissociation of gas hydrates and methane clathrates (Hesselbo et al., 2000; Kemp et al., 2005), permafrost destabilisation and cryokasts (Ruebsam et al., 2019), and wetland methanogenesis (Them II et al., 2017).

Massive release of greenhouse gases to the atmosphere caused an increase in atmospheric CO_2 (McElwain et al., 2005), linked to a global temperature rise during the early Toarcian; e.g., the seawater temperature rose over 10 °C in the Mediterranean region during the T-OAE (Gómez & Goy, 2011; Ruebsam et al., 2020). Furthermore, a change in sea level influenced the deposition of organic-rich sediments, the early Toarcian being characterized by a global transgression related with melting permafrost and polar ice sheets (Hermoso et al., 2013; Krencker et al., 2019), which in turn released more greenhouse gases to the atmosphere during the thaw. Aside from the global-scale phenomena, local variations appear to control the magnitude of the event, and hydrographic restrictions (i.e., the watermass renewal rate) deeply influence the deposition of organic-rich sediments (e.g., McArthur, 2008; Remírez & Algeo, 2020).

Black shale deposits associated with the T-OAE are present all around the world, from the Panthalassa Ocean (e.g., Toyora area, actual west Japan; Izumi et al., 2012) to the Tethys Ocean (e.g., western Tethys'

European basins; see recent review by Rodríguez-Tovar, 2021). Records in Europe, North Africa, the Middle East, Siberia, Madagascar, Australian coasts, Japan, and North and South America have been well documented (e.g., Jenkyns et al., 2002; Them II et al., 2017; Ruebsam et al., 2018; Suan et al., 2018). Focusing on the western Tethys domain (Fig. II.1A), two major groups of basins can be differentiated depending on the T-OAE features: a) a central group known as the Western Europe Euxinic Basin (WEEB) (Gómez and Goy, 2011), where the magnitude of the event was higher, characterised by the presence of black shales having high total organic carbon (TOC) values (over 5%); and b) a peripheral group, comprising numerous and partially connected basins, including the Asturian Basin, those of the South Iberian Massif margin, and the ancient Moroccan Meseta, where black shales are less common, and TOC values are lower (e.g., 3% in the Asturian Basin) (Gómez et al., 2008).

Sediments associated with the event have been dated as early Toarcian (around 183 Myr ago), thus corresponding to the lower part of the ammonites *Harpoceras serpentinum* Zone in the subboreal, submediterranean and northwest European provinces, equivalent to the *Hildaites levisoni* Zone in the Mediterranean province (Bilotta et al., 2010; Rodríguez-Tovar & Uchman, 2010; Gómez & Goy, 2011). Depending on the basin, black shales may extend below the *Serpentinum* Zone boundary into the *Tenuicostatum* Zone, or upward through the *Serpentinum* Zone (e.g., Hermoso et al., 2013).

The T-OAE caused significant extinctions in several marine species, such as ammonites, belemnites, bivalves and gastropods, and affected other organisms, including foraminifera, ostracods, brachiopods, echinoderms, calcareous nannofossils and dinoflagellate cysts (e.g., Raup & Sepkoski, 1984; Sepkoski, 1996; Dera et al., 2010, 2011). Its impact on the endobenthic tracemaker community has been registered in trace fossil features (e.g., Rodríguez-Tovar & Uchman, 2010; Rodríguez-Tovar & Reolid, 2013; Miguez-Salas et al., 2018; Reolid et al., 2018; Fernández-Martínez et al., 2021), reflecting the importance of ichnological analysis as a proxy for the studies of the T-OAE. Indeed, detailed
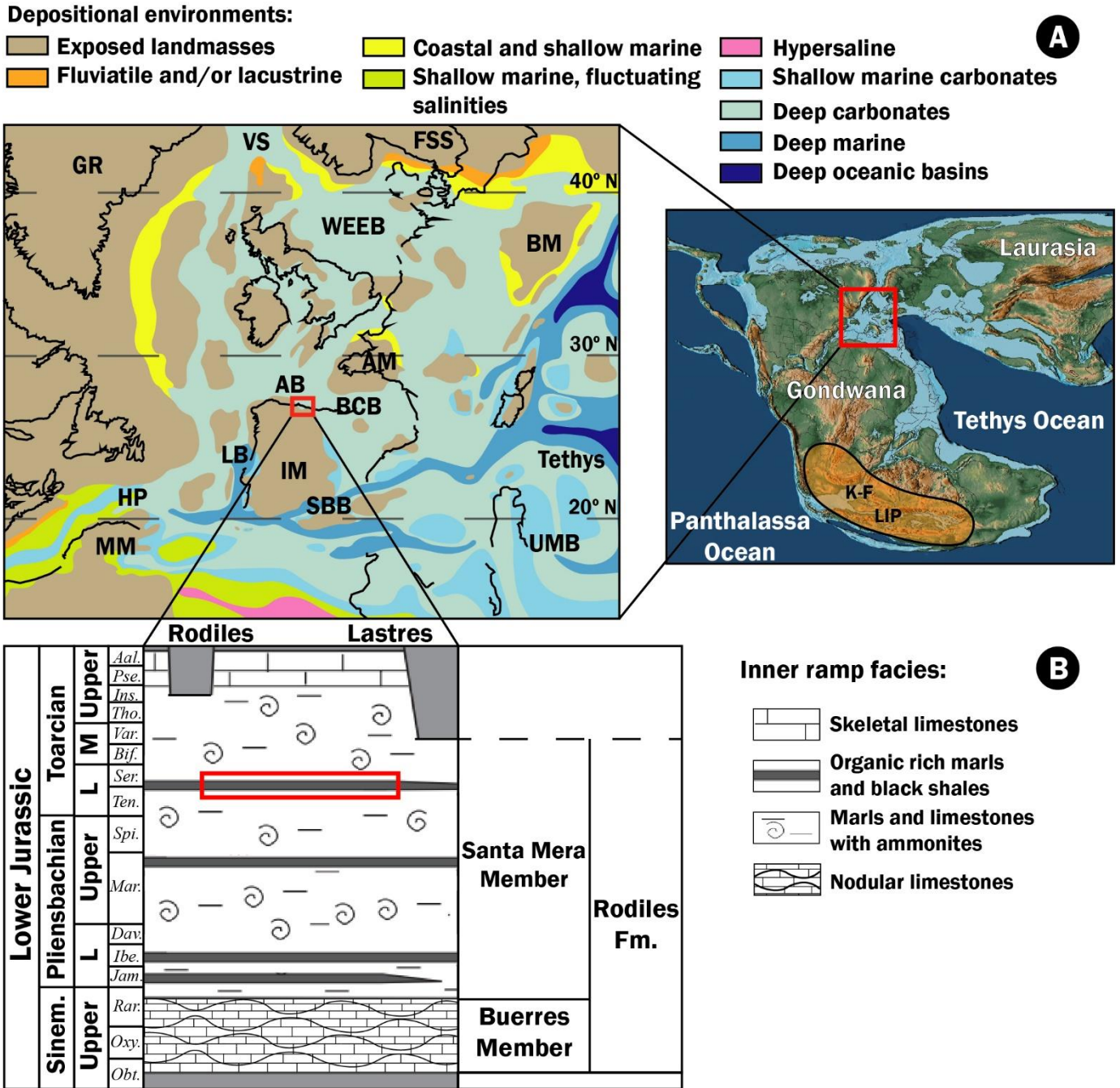
Figure II.1. (A) Palaeogeographic reconstruction of the Early Jurassic, showing the position of the Asturian Basin (red rectangle) in the Western Tethys (modified from Thierry et al., 2000; Dera et al., 2010; Gómez & Goy, 2011; Scotese, 2013, Rosales et al., 2018). AB: Asturian Basin, AM: Armorican Massif, BCB: Basque-Cantabrian Basin, BM: Bohemian Massif, FSS: Fenno-Scandian Shield, GR: Greenland, HP: Hispanic corridor, IM: Iberian Massif, K-F LIP: Karoo-Ferrar Large Igneous Province, LB: Lusitanian Basin, MM: Moroccan Meseta, WEEB: Western European Euxinic Basin, SBB: Sub-Betic Basins, VS: Viking Strait. (B) Facies distribution and formations of the Lower Jurassic of Asturias (not to scale, modified from Aurell et al., 2003; Deconinck et al., 2020). Studied interval marked in a red rectangle. Ammonite zones are indicated, from bottom to top: Obt.: Obtusum, Oxy.: Oxynotum, Rar.: Raricostatum, Jam.: Jamesoni, Ibe.: Ibex, Dav.: Davoei, Sto.: Stokesi, Mar.: Margaritatus, Spi.: Spinatum, Ten.: Tenuicostatum, Ser.: Serpentinum. Bif.: Bifrons, Var.: Variabilis, Tho.: Thouarsense, Ins.: Insigne, Pse.: Pseudoradiosa, Aal.: Aalensis. Other abbreviations are: Sinem.: Sinemurian, L: Lower, M: Medium.

study of ichnological features (i.e., composition and distribution of the trace fossil assemblages, abundance, infilling material, tiering, architectural designs and cross-cutting relationships) improve palaeoecological and depositional characterisation of the T-OAE, especially

regarding oxygen conditions (see recent review in Rodríguez-Tovar, 2021).

This study integrates ichnological and sedimentological analyses of two selected sections of the Asturian Basin, Rodiles and Lastres, underlining the presence of different ichnoassemblages in these lower Toarcian deposits. The aim of this research is to precisely delimit the T-OAE by assessing the evolution of its associated palaeoenvironmental changes, determining the seafloor oxygen availability in bottom- and pore-waters and its effect on the endobenthic tracemaker community. Results can provide vital insights into the development of oxygen-deficient conditions and their relation to black shale deposition during the T-OAE.

2. GEOLOGICAL SETTING

The studied outcrops are located along the Asturian cliffs, in an area known as the "Dinosaur Coast", a sector of the Jurassic Asturian Basin with abundant reptile footprints (García-Ramos et al., 2006). They occupy two cliffs (Fig. II.2A, B, C), one on the east part of Rodiles beach (43°32'19.7"N 5°22'25.5"W) and the other on the west part of Lastres beach (43°30'41.2"N 5°16'06.2"W). Both sections (Rodiles and Lastres), around 2 m thick each, consist of alternations of limestones with light and dark grey marls, and the noteworthy presence of organic matter-rich black shales associated with the T-OAE (Fig. II.2D, E) (García Joral & Goy, 2009; Gómez & Goy, 2011).

The two studied sections belong to the Rodiles Formation, which has two members: the lower Buerres Member, and the upper Santa Mera Member. They form part of the same homoclinal carbonate ramp, where the Buerres Member corresponds to a shallower setting, while the Santa Mera Member represents more distal environments, ranging between open marine and restricted depocentres. The latter, mainly consisting of marl and limestone alternations, is divided in two sub-

units. The studied organic rich-black shale deposits are in the lower sub-unit, at the boundary between *Tenuicostatum* and *Serpentinum* zones (indicated by a red rectangle in Fig. II.1B), and were accumulated in an intrashelf basin environment (Valenzuela et al., 1986, 1989; Armendáriz et al., 2012).

3. MATERIAL AND METHODS

The Rodiles and Lastres sections were studied bed-by-bed at the cliffs, focusing on their sedimentological and stratigraphic features, with special attention to ichnological characterisation. Analysis of the ichnological features in outcrop focused on ichnotaxobases (i.e., overall shape, orientation, ornamentation, internal structure; Bromley, 1996; Bertling et al., 2006). Ichnodiversity (ID) and abundance of the trace fossil assemblages were also studied, together with infilling material of burrows, size, depth from the bed surface, and cross-cutting relationships. The abundance of trace fossils is expressed by the Bioturbation Index (BI) (Taylor & Goldring, 1993), where grade 0 means no bioturbation and grade 6 designates completely bioturbated rock. In some cases, lamination was observed in the absence of bioturbation. Ichnodiversity and ichnodisparity were likewise evaluated: alpha ichnodiversity refers to the number of different ichnogenera present in a particular community (i.e., taxonomic richness), whereas ichnodisparity refers to variations in the morphology of structures (Buatois & Mángano, 2011, 2013). Both parameters can be used as proxies for palaeoenvironmental, evolutionary and ecosystem interpretations (e.g., Buatois & Mángano, 2011, 2018).

Detailed photographs were taken to characterise ichnotaxa, as well as the relationships of trace fossils with sedimentary structures, bed surfaces, and facies. Collected samples were studied in the laboratory on thin sections and polished sections. The polished sections were analysed using different lenses (x10 and x20) and a

Figure II.2. (A) Location of the studied sections of Rodiles and Lastres on the Asturian coast (modified from García Joral & Goy, 2009). (B) Rodiles beach and cliffs, red star marking the outcrop. (C) Lastres beach and cliffs, yellow star marking the outcrop. B and C modified from Google Earth. (D) Rodiles outcrop and (E) Lastres outcrop, red segments indicating T-OAE interval. Some level numbers are indicated.
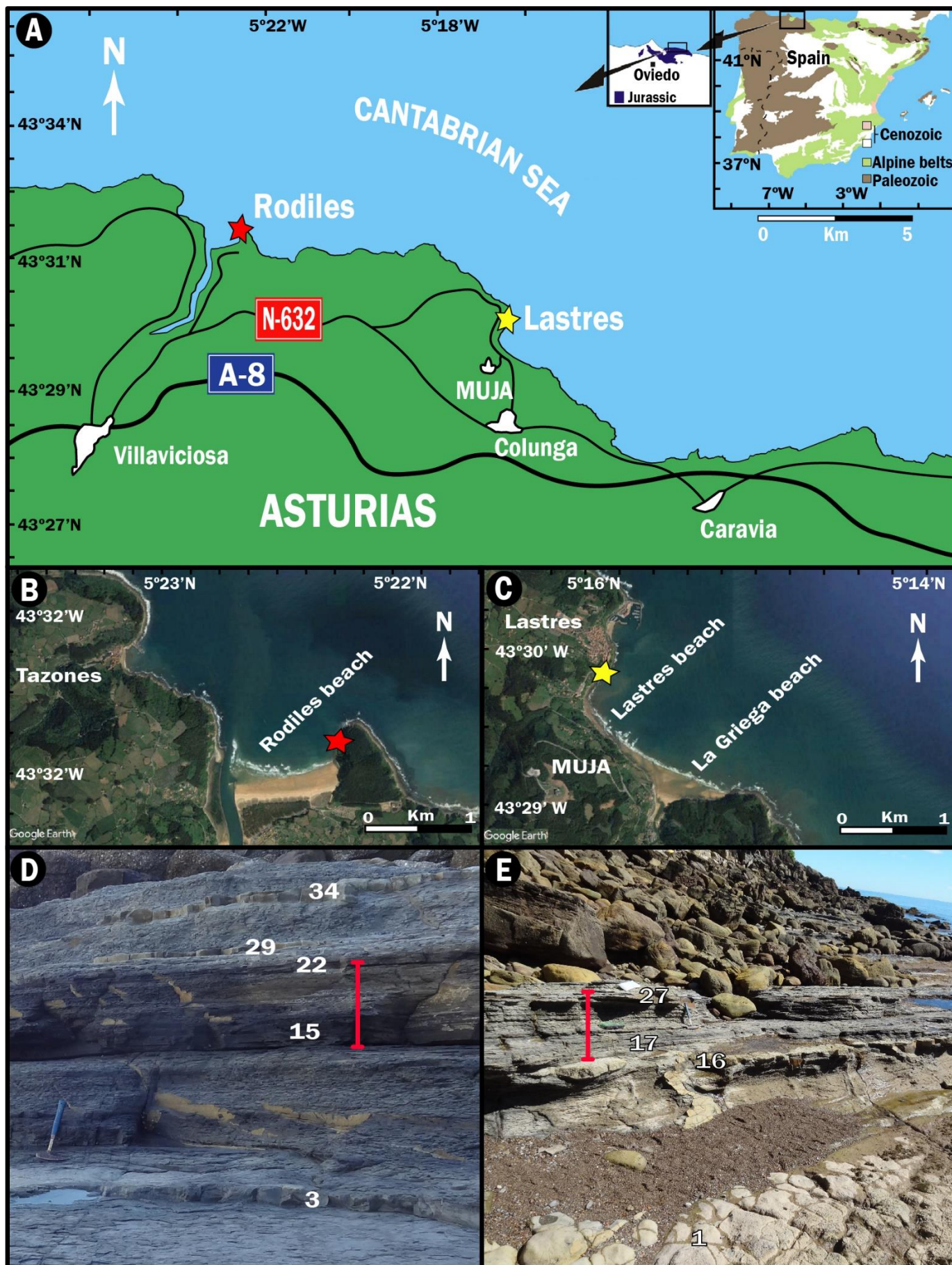
Dino-Lite Digital Microscope, paying special attention to black shales and laminated facies. Ichnological analysis was mainly focused on the infilling material, external features, and relationships with micro-scale lamination. Thin sections were studied using an OLYMPUS CX31 microscope, classifying the carbonate sediments following Dunham (1962). Some photographs were treated with Adobe Photoshop CS6 to enhance visibility of certain ichnological properties, according to the methodology proposed by Dorador & Rodríguez-Tovar (2018). Collected samples are housed in the *Departamento de Estratigrafía y Palaeontología* (University of Granada), labelled as L-1 to L-10 for Lastres and R-1 to R-11 for Rodiles.

4. RESULTS
4.1. Lithological characterisation
4.1.1. Stratigraphic description
The studied sections consist of alternating nodular to wavy limestones, showing lateral variations in thickness, and light and dark grey marls. Occasionally, black shale intervals are intercalated. Previous biostratigraphic studies at the Rodiles section allowed for identification of the *Tenuicostatum* (*Polymorphum*) and *Serpentinum* (*Levisoni*) zones of the early Toarcian (García Joral & Goy, 2009; Gómez & Goy, 2011; Gómez et al., 2016b).

The detailed bed-by-bed study revealed minor differences between the two sections investigated (Fig. II.3). The lowermost part of Rodiles section features a wavy limestone bed that is 9 cm thick and has sharp lower and upper contacts, followed by a light marl level. The overlying levels in Rodiles, and the lowermost part of the Lastres section, begin with a wavy limestone bed (10 cm thick) followed by alternating dark/light marls (56 cm thick in Rodiles and 62 cm thick in Lastres). Above, the first black shale interval (25 cm thick) is recognised, directly overlying marls in the Rodiles section and a 12 cm thick limestone bed in the Lastres section. Upward from the black shales, a second alternation of dark/light grey marls is observed in both sections, with a similar total thickness (around 26 cm). Then a second interval of black shales (8 cm thick in Rodiles and 9 cm thick in

Lastres) is recorded. Finally, the upper part of both sections consists of a third alternation of light/dark grey marls (20 cm thick), capped by a limestone bed (8 cm thick in Rodiles and 10 cm thick in Lastres) with sharp lower and upper contacts. The uppermost part of the Rodiles section consists of alternating light and dark marls (around 40 cm) overlain by a wavy limestone level (10 cm thick).

Carbon isotope analysis of the bulk organic matter (δ^{13}C, TOC) carried out on the sediments of the Rodiles section revealed the presence of a negative carbon isotope excursion spanning the *Tenuicostatum-Serpentinum* zonal boundary (Gómez et al., 2008, 2016a), which ranges from below the first black shale interval to the top of the second one (levels 9 to 22, Fig. II.3).

4.1.2. Lithofacies
Four lithofacies types were identified on the basis of sedimentological and ichnological observations made on polished slabs, petrographic thin sections (Fig. II.4), and field observations: highly bioturbated grey limestones (HBL), highly bioturbated light grey marls (HBM), variably bioturbated medium to dark grey marls (VBM), and laminated black shales (LBS).

The terms burrow-mottled or mottled background have been used by previous authors to describe diverse ichnofabrics having different bioturbation intensity and contrast. In the present work, this denomination is used specifically for ichnofabrics with high bioturbation index values (5-6) and whose burrows show poor colour contrast with respect to the host sediment.

4.1.2.1. Highly bioturbated grey limestones (HBL)
Their thickness is irregular, ranging from 0 to 11 cm, due to frequent wedging (Fig. II.3). The contacts with the underlying and overlying facies are often gradational, visible to the naked eye, due to pervasive bioturbation and progressive decrease in carbonate content. The contact is sharp only when the limestone beds are covered by overlying dark grey marls (VBM) or black shales (LBS) facies. Possible primary sedimentary features are disrupted or absent due to intense and diverse bioturbation (Figs. II.8D, II.9B, C, II.10A, C, G). Usually present is a highly mottled texture with
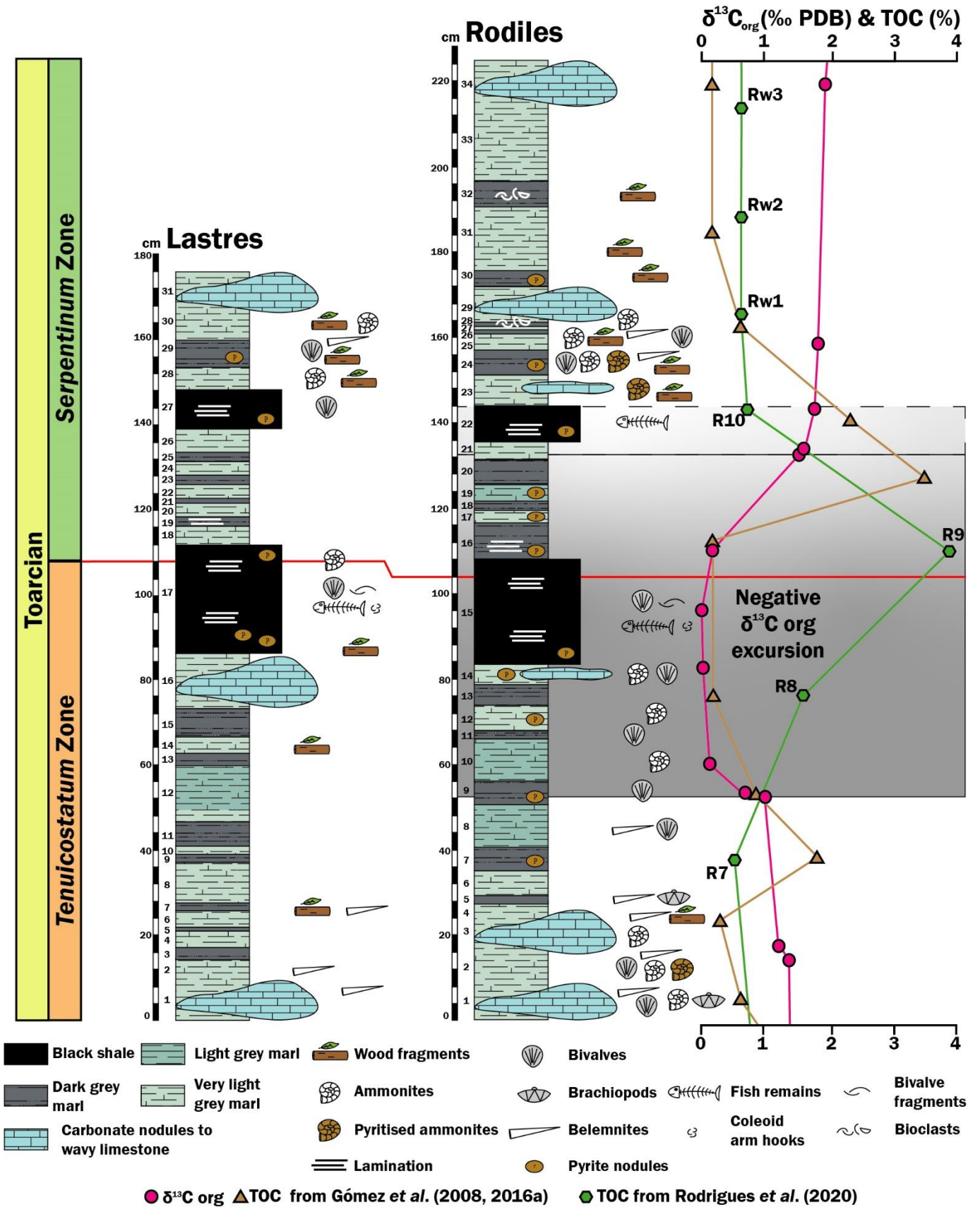
Figure II.3. Stratigraphic columns of both sections (Lastres and Rodiles), showing biostratigraphy (after Gómez et al., 2008, 2016a), lithology, lamination and palaeontological content. Levels are numbered. Note the different tonalities of light and dark marls. Rodiles section also shows variations in TOC and the negative ¹³C isotope excursion (Gómez et al., 2008, 2016a; Rodrigues et al., 2020).

superimposed dark-filled discrete trace fossils introduced from the overlying dark grey marls (VBM) facies (e.g., Figs. II.8D, II.9C). There are frequent lateral transitions between this facies and the bioturbated light marls (HBM) facies (Fig. II.3). TOC content is always low (< 0.5 %), as deduced from previous works (Gómez et al., 2008, 2016a; Rodrigues et al., 2020) (Fig. II.3). Microfacies indicate that the high bioturbated limestones represent a carbonate-cemented mudstone with scattered bioclasts.

This facies show typical composite ichnofabrics, including both varieties sensu Savrda (2016): autocomposite (formed by a single ichnocoenose) and heterocomposite material (originated by multiple communities of tracemakers). Most frequent ichnogenera are *Arenicolites*, *Chondrites*, *Diplocraterion*, *Planolites* and *Thalassinoides*.

The pervasive bioturbation (discrete traces on a burrow-mottled background), composite ichnofabric, pale-grey colour, and low organic matter content all suggest slow sedimentation rates and well-oxygenated conditions during deposition. However, the common presence of protrusive dark filled *Diplocraterion* cross-cutting the mottled background provides evidence of stiffground (associated with an overlying erosive surface covered by dark grey marly sediments of the variably bioturbated dark grey marls -VBM- facies). The high bioturbation index and the complex tiering structure (sensu Taylor et al., 2003), probably also reveal long hiatuses between successive depositional events. There is no evidence of mechanical compaction in this lithofacies, whereby the calcitic cement was precipitated during

early diagenetic times, prior to main compaction processes and significant burial. On the other hand, the lateral (wedging) and vertical transitions between this limestone lithofacies (HBL) and the light grey marl lithofacies (HBM) is gradual, not sharp, the weathering profile of the present outcrops exemplifying a common phenomenon mentioned by Ricken (1986). Moreover, the carbonate precipitation that generates the limestone beds partially distorts the primary sedimentary signals, as indicated by Westphal et al. (2008).

4.1.2.2. Highly bioturbated light grey marls (HBM)

Their thickness oscillates between 1 and 28 cm, but they usually form beds from 2 to 10 cm (Fig. II.3). Basal surfaces are gradational to dark grey marls (VBM) or black shales (LBS) facies, given a progressive decrease in bioturbation index. The highly bioturbated light grey marls represent a typical composite ichnofabric (Fig. II.11A). Indistinctive burrow-mottling, characteristic of this facies, is overprinted by well-defined discrete traces with dark grey marl infill, later emplaced on a stiff-to-firmground (Fig. II.11E). The phyllosilicate content is low and concentrated on the burrows infilled with dark grey marly sediment. The facies often passes laterally to a cemented limestone bed (HBL facies) through a progressive increase in the carbonate content during early diagenesis (Fig. II.3). According to the microfacies, it represents a calcareous-argillaceous mudstone with scattered bioclasts.

The most common trace fossils include *Arenicolites*, *Chondrites*, *Diplocraterion*, *Halimedides*, *Planolites* and *Thalassinoides*.

Figure II.4. Microphotographs (plane-polarised light) of thin sections of the differentiated facies: (A) Laminated black shale (LBS facies). Note small compacted intraclasts, organo-mineral aggregates and alternating millimetre to submillimetre silt and clay-rich laminae which suggest episodic deposition and erosion (Lastres level 17, i.e., L17). (B) Laminated black shales (LBS facies). Note some quartz-rich silty laminae with sharp-based boundaries and frequent framboidal pyrite and kerogenous components (Rodiles level 15, i.e., R15). (C-D) Highly bioturbated grey limestone (HBL facies). Note the burrow-mottled ichnofabric with homogenised aspect and the comminuted biogenic debris (R3 and R29, respectively). (E) Highly bioturbated light-grey marl (HBM facies). Note the dark filled burrows on a light grey matrix and the dispersed bioclasts (R23). (F) Highly bioturbated light grey marl (VBM facies). Note foraminifera (red circle) and several small bioclasts (L28). (G-H) Variably bioturbated medium to dark grey marl (VBM facies). Note in this case the fine parallel lamination, the high kerogenous and small pyrite framboid contents and absence of bioturbation (L23 and R16, respectively). (I) Upward gradual transition from laminated dark grey marl (VBM facies, L23) to bioturbated light marl (HBM facies, L24). (J) Bioturbated dark grey marl (VBM facies) showing Chondrites *with a light infill (R24). Scale bars are 200 μm for A-D and F-I and 500 μm for E and J. Top is always upwards.*
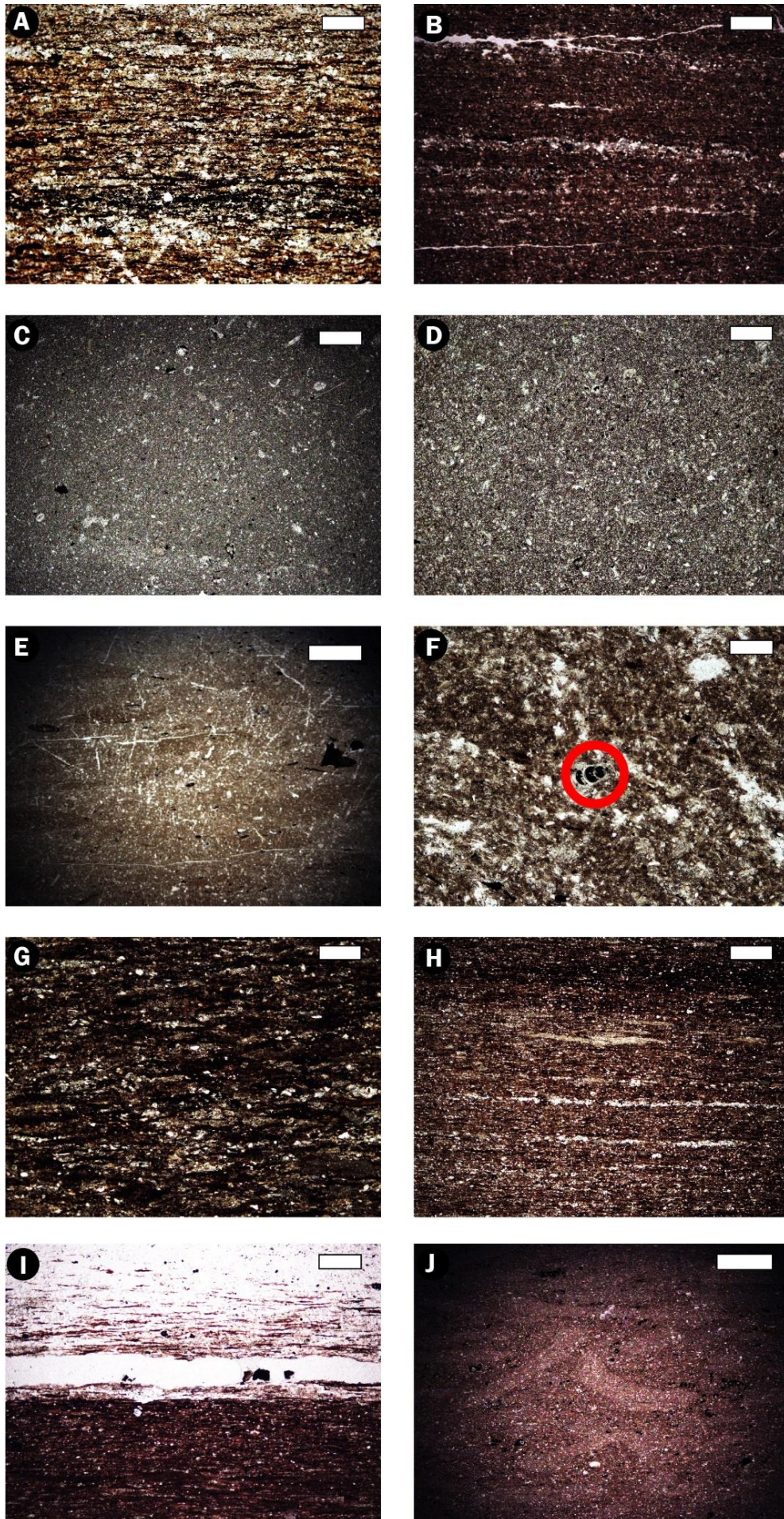
4.1.2.3. Variably bioturbated medium to dark grey marls (VBM)

Their thickness ranges from 1 to 10 cm, but most commonly from 4 to 7 cm (Fig. II.3). The basal contact with the underlying limestones (HBL) or light marls (HBM) facies is sharp and probably erosive, yet gradual with the underlying black shales (LBS) facies. The TOC content may be higher than in the black shales, as deduced from previous works (Gómez et al., 2008, 2016a; Rodrigues et al., 2020) (Fig. II.3). Bioturbation intensity shows a wide range between apparently unbioturbated (BI = 0) to highly bioturbated (BI = 5). The most bioturbated varieties show an upward increase in trace fossil content, size and diversity, and a gradual transition to the overlying high bioturbated light marls or limesotones facies. When bioturbated, the burrows are filled by pale grey marly sediments derived from the overlying light marls or limestones facies. Microfacies observations indicate a laminated argillaceous-calcareous and carbonaceous mudstone with scattered bioclasts. The phyllosilicate content, as also deduced from thin sections, is higher than in black shales and light marls facies.

The most common trace fossils are *Arenicolites*, *Chondrites*, *Diplocraterion*, *Planolites*, *Thalassinoides* and small *Zoophycos*.

4.1.2.4. Laminated black shales (LBS)

In the outcrops studied here, only two levels with laminated black shales facies are identified in each section. The lower level, 25 cm in thickness, appears unbioturbated to the naked eye, but the upper level (8-9 cm-thick) shows a progressive upward increase in trace fossil content and diversity. Black shales show a marked colour contrast between the light grey burrow fill and the dark grey host sediment. The sharp boundaries of the traces moreover suggest their emplacement in a stiffground.

Compared with the other facies, the

phyllosilicate content is more elevated here. The lower contacts with other facies are very sharp and the surfaces are planar and erosional, probably representing transgressive surfaces. The contact of the lower level with the overlying dark marls facies in the Rodiles section

is gradual and reflects an upward increase in organic matter content, which correlates with a decrease in phyllosilicate components. Flattened pyrite nodules are also common in this facies, along with several millimetre-scale laminar concentrations of parautochthonous disarticulated small bivalves, phosphatic fish debris, and some dispersed coleoid arm hooks. Microfacies analysis allows to characterize this facies as laminated silty and carbonaceous mudstone with well-developed fissility.

As also deduced from thin sections, the deep dark colouration is due to the combination of organic matter, common small pyrite framboids and framboidal aggregates. Lamination is due to laterally continuous millimetre-scale laminae of phyllosilicate-rich silty mudstones, originated from storm or distal hyperpycnal flows. The bases of both laminated black shale episodes most likely represent transgressive surfaces, in view of their sharp and erosive character, the presence in their lower parts of compacted intraclasts, relatively coarser particles, and reworked small fossil fragments. The upper parts of these levels, having more diffuse lamination and being more organic-rich, are interpreted as potential maximum flooding surfaces.

4.2. Ichnological analysis
4.2.1. Ichnotaxonomy, distribution and abundance of trace fossils

Rodiles and Lastres sections have a similar ichnoassemblage, consisting of ten ichnogenera: *Arenicolites*, *Chondrites*, *Diplocraterion*, *Halimedides*, *Palaeophycus*, *Planolites*, *Rhizocorallium*, *Thalassinoides*, *Trichichnus* and small *Zoophycos*, together with undetermined horizontal pyritised burrows (Figs. II.5-II.10, Table II.1).

The most abundant trace fossil is *Chondrites*, followed by *Planolites*, occurring throughout both sections. *Palaeophycus* is especially common in the limestones, whereas *Halimedides*, *Trichichnus*, *Rhizocorallium*, and small *Zoophycos* only occur locally. *Chondrites* occurs in patches or randomly in the bed, in some cases completely reworking other trace fossils (mainly *Arenicolites*, *Diplocraterion* and *Planolites* (e.g., Figs. II.8D, II.9B, C, D, F, II.10A, C, G).

There are significant variations in the distribution and abundance of trace fossils throughout the sections. The lower (below the first black shale interval) and upper parts (above the second black interval), corresponding to marls and limestones, feature an abundant and relatively diverse (high bioturbation index and ichnodiversity) trace fossil assemblage. The middle part (between the black shale levels; levels 15-22 in Rodiles and levels 17-27 in Lastres) shows lower bioturbation index values, and even the occasional absence of traces, with primary parallel lamination being present as well.

In the upper black shale levels, lamination disappears progressively due to bioturbation in the upper part (the bioturbation index increases from 0 to 5).

4.2.2. Ichnodiversity, ichnodisparity and architectural designs

Ichnodiversity varies in the studied sections — from 0 in the lower black shale and in some marly levels characterised by the absence of trace fossils, to 5-7 in some marly levels where a diverse trace fossil assemblage is recorded (Figs. II.5-II.6). Ichnodisparity is relatively high. The wide variety of morphologies in the recorded trace fossils can be classified into eight different architectural designs following Buatois et al. (2017): 1) vertical single U- and Y-shaped burrows (*Arenicolites*, *Diplocraterion*), 2) horizontal burrows with serial chambers (*Halimedides*), 3) passively filled horizontal burrows (*Palaeophycus*), 4) simple actively filled (massive) horizontal to oblique structures (*Planolites*), 5) maze and boxwork burrows (*Thalassinoides*), 6) burrows with horizontal spreiten (*Rhizocorallium*), 7) burrows with helicoidal spreiten (*Zoophycos*), and 8) burrows having a shaft or bunch with downward radiating probes (*Chondrites*, *Trichichnus*).

The ichnodiversity and ichnodisparity indices are directly related in the studied sections, showing a parallel evolution (either both are high or both are low) (Figs. II.5, II.6). Notwithstanding, the two indices show variations in the sections regardless of the bioturbation index. Lower values (usually between 0 and 1-2 in ichnodiversity) are recorded in the middle part of both sections, while higher values are observed in the lower and upper parts. Especially significant is the highest ichnodiversity value (6) recorded in the lower part of the Rodiles section.

4.2.3. Ichnofabric approach

Sedimentological and ichnological features — primary sedimentary structures, ichnodiversity, cross-cutting relationships and relative abundance of ichnotaxa— allowed us to discern six different ichnofabrics and their corresponding tiering structures (Figs. II.10, II.11): I) Laminated? ichnofabric, apparently showing no bioturbation (bioturbation index is 0), but with a primary parallel lamination present. II) *Diplocraterion-Thalassinoides* ichnofabric, characterised by a relatively diverse and abundant assemblage (bioturbation index 4-5), with dominant *Chondrites*, *Arenicolites*, *Diplocraterion*, *Planolites*, *Thalassinoides* and scarce small *Zoophycos*, and punctual *Rhizocorallium* and *Halimedides* (the latter in the upper part of the sections). Most of the ichnotaxa are cross-cut by *Chondrites*. Furthermore, variable cross-cutting relationships between *Thalassinoides, Planolites, Arenicolites* and *Diplocraterion* are observed (e.g., Figs. II.7I, II.8D, II.10A). Cross-cutting relationships in the *Diplocraterion-Thalassinoides* ichnofabric point to a shallower tier consisting of *Palaeophycus* and *Planolites*, a middle tier

---

Figure II.5. Ichnogenus and ichnofabric distribution at Rodiles section, showing the Bioturbation Index (BI) and ichnodiversity (ID) values. In ichnogenus distribution, light grey bars mean light infill and dark grey ones dark infill, pyritised infills (orange bars) also being considered. Segments with no BI, ID and ichnofabric values indicate levels where no polished sections were made, showing no bioturbation in outcrop. For legend see Fig. II.3. Other symbols: La: laminated, Mo: mottled, Ar: Arenicolites, Ch: Chondrites, Di: Diplocraterion, Ha: Halimedides, Pa: Palaeophycus, Pl: Planolites, Rh: Rhizocorallium, Th: Thalassinoides, Zo: Zoophycos, Tr: Trichichnus, *Ht: horizontal pyritized tubes,* Di-Th *ich:* Diplocraterion-Thalassinoides *ichnofabric,* Ch-Pa-Pl *ich:* Chondrites-Palaeophycus-Planolites *ichnofabric,* Ch-Ha-Pl *ich:* Chondrites-Halimedides-Planolites *ichnofabric,* Ch-*mo ich:* Chondrites-*mottled ichnofabric,* Ch-*la ich:* Chondrites-*laminated ichnofabric,* La? ich: *Laminated? ichnofabric.*
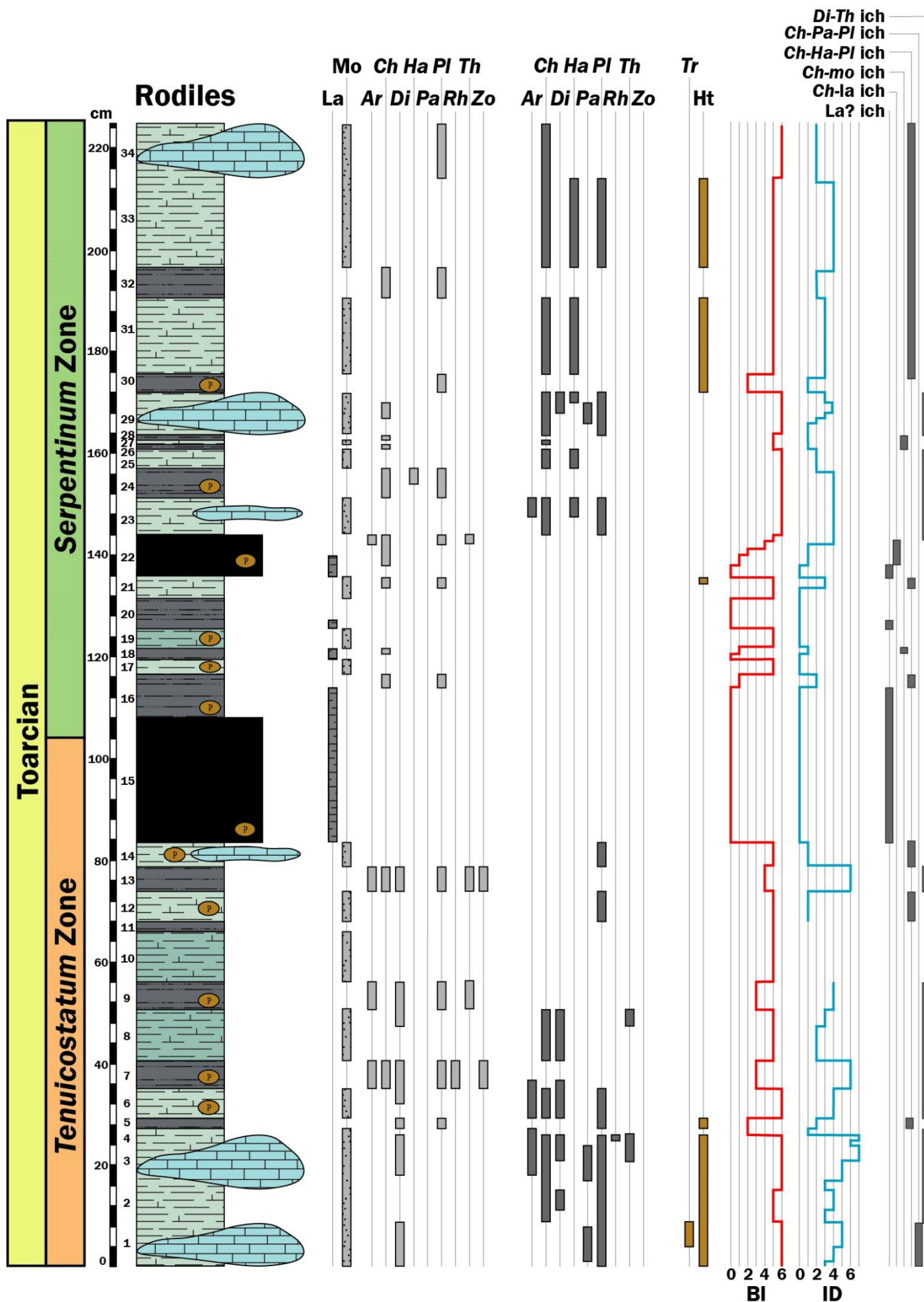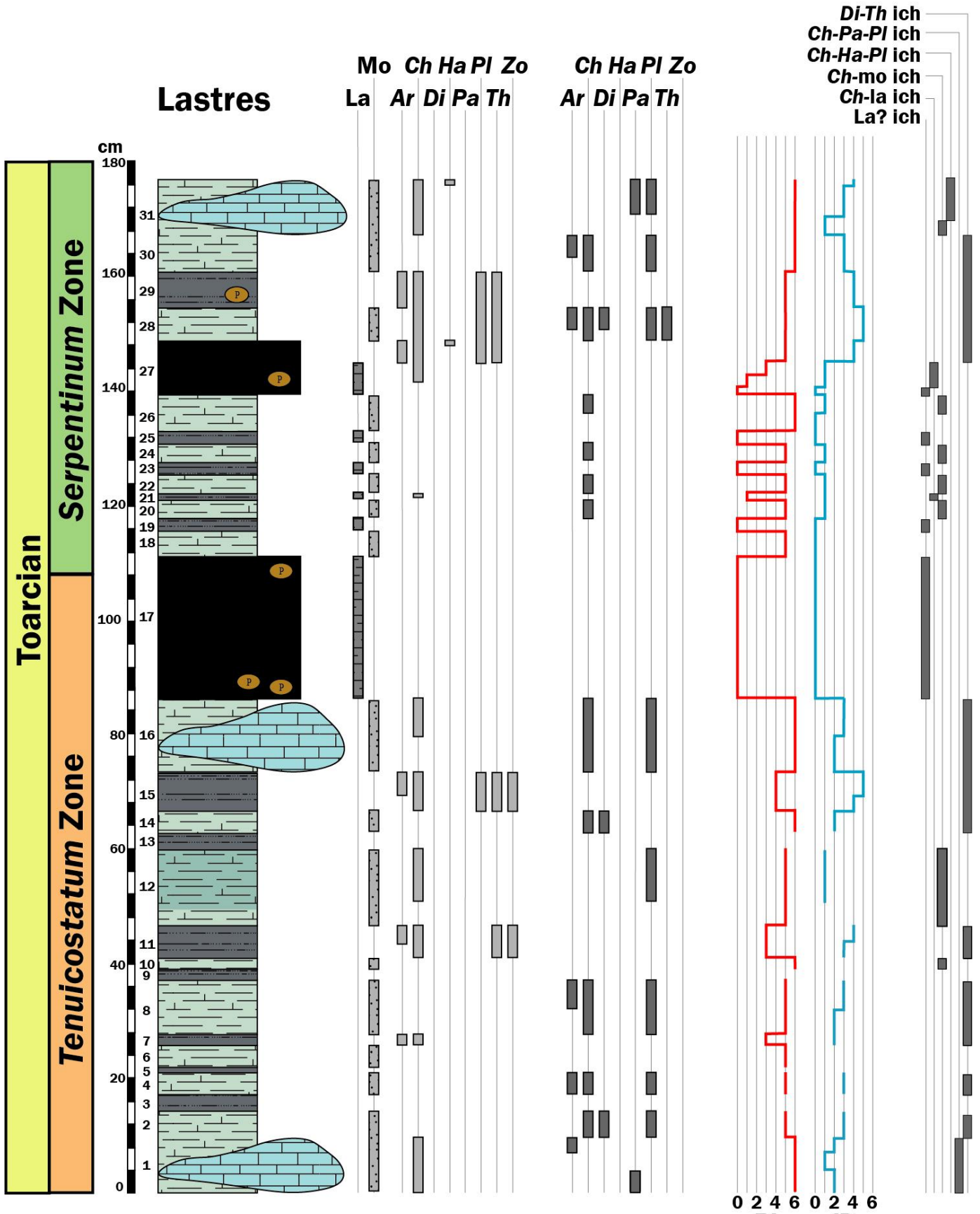
Figure II.6. Ichnogenus and ichnofabric distribution at Lastres section, showing the Bioturbation Index (BI) and ichnodiversity (ID) values. In ichnogenus distribution, the light grey rectangle means light infill, and dark grey ones dark infill. Segments with no BI, ID and ichnofabric values indicate levels where no polished sections were made, showing no bioturbation in outcrop analysis. For legend see Fig.II.3, other symbols as Fig. II.5

Ichnogenera	Identified ichnospecies	Outcrop and sample description	Size	Possible tracemakers	Ethology	Figure	References
Arenicolites	*A. sparsus*	Vertical and subparallel U-shaped burrows (pairs of circles in horizontal section). Full relief showing dark grey (dominant) or light grey infill	TD: 4 to 9 mm PD: 2 to 8 cm	Polychaetes or amphipod crustaceans	Domichnia	7I, 8A, D, E. 10A	Goldring, 1962; Fürsich, 1974; Rindsberg and Kopaska-Merkel, 2005
Chondrites	*C. targionii*	Circular to elliptical spots and horizontal to subhorizontal tubes; occurring in patches, scattered in the bed or reworking other traces	TD: < 1 to 5 mm	Vermiform (polychaetes), but also bivalves and other organisms	Fodinichnia, chemichnia or agrichnia	7A, D, E-I, 8C-D, 9A-G, 10A-D,F-G	Seilacher, 1990; Bromley, 1996; Bromley and Ekdale, 1984; Uchman, 1999; Uchman *et al.*, 2012; Rodríguez-Tovar and Uchman, 2010; Baucon *et al.*, 2020
Diplocraterion	*D. parallelum*	Perpendicular U-shaped tubes (pairs of circles on horizontal surfaces). Full relief showing light and dark grey infill and protusive *spreite*	TD: 5 to 10 mm PD: 2 to 8 cm	Polychaetes, echiurids and amphipods or other crustaceans	Equilibrichnia	8A, 10A	Goldring, 1962; Fürsich, 1974; Olóriz and Rodríguez-Tovar, 2000
Halimedides	*H. annulata*	Heart-chambered (dominant), semicircular and rectangular bodies separately distributed on the strings, which show no branching	TD: 1 to 6 mm CL: 0.7 to 1.7 cm CW: 0.6 to 2.2 cm	Unknown, though infaunal crustaceans are considered	Agrichnia and/or sequestrichnia	8F, 9F	Uchman, 1999; Gaillard and Olivero, 2009; Rodríguez-Tovar *et al.*, 2019; Fernández-Martínez *et al.*, 2021
Palaeophycus	*P. tubularis* *P. heberti*	Only observed in polished sections: circles and cylinders with dark grey wall and a light grey infilled tube	TD: 1 to 2 mm	Vermiform tracemakers, such as annelids or polychaetes like Nereidae	Domichnia	9A-B, H, 10G	Pemberton and Frey, 1982; Keighley and Pickerill 1997; Rodríguez-Tovar *et al.*, 2009
Planolites	*P. montanus* *P. beverleyensis*	Cylindrical tubes, sometimes sinuous, mainly horizontal and showing dark or light grey infill	TD: 1 to 9 mm	Wide variety of vermiform organisms	Fodinichnia or pascichnia	7I, 9A-C, 10C-D,G-H	Pemberton and Frey, 1982; Keighley and Pickerill, 1997; Knaust, 2017
Rhizocorallium	*R. commune*	Subhorizontal burrows, oblique to the bedding. Consisting of a light grey-infilled, U-shaped marginal tube and an inner *spreite* zone	TD: 0.8 to 1.2 cm	Decapod crustaceans and worm-like forms as annelids or larvae	Domichnia and fodinichnia, also agrichnia is considered	7G, 8D	Knaust, 2013
Thalassinoides	*T. suevicus*	Observed as circular to elliptic burrows. In cross section, without wall lining and with dominant Y-circular branches. Showing light and dark infill and an enlargement at the bifurcation points	TD: 0.5 to 6 cm (3 to 5 cm are dominant)	Mainly Malacostraca crustaceans (thalassinid shrimps), but also associated with arthropods, anemones, fish and other vermiform organisms	Domichnia and fodinichnia	7E, H-I, 8D	Ekdale and Bromley, 2003; Rodríguez-Tovar *et al.*, 2008, 2017
Trichichnus	--	Vertical and subvertical curved burrows, showing pyritized infill	TD: 1 to 2 mm	Annelids, probably chemiosymbionts	Domichnia	8B	Uchman, 1999
Zoophycos	--	Horizontal and subvertical burrows, showing meniscate light infill. Sometimes occurring as spirals, convoluted shapes or branching structures	TD: 0.5 cm PD: 2 to 5 cm	Associated with a vermiform organism like Sipuncula, or polychaetes as Echiura or Spionidae	Domichnia, fodinichnia pascichnia and/or agrichnia	7F, 9D-E	Bromley *et al.*, 1999; Olivero, 2007; Olivero and Gaillard, 2007; Knaust, 2009; Rodríguez-Tovar *et al.*, 2009

Table II.1. Ichnotaxa descriptions: table including a detailed description of the present ichnogenera and the identified ichnospecies. TD: tube diameter. CW: chamber width. CL: chamber length. PD: penetration depth.

with *Arenicolites*, *Diplocraterion*, *Thalassinoides* and *Halimedides*, and a deeper tier conformed by *Zoophycos* and *Chondrites*.

Several ichnofabrics that are characterised by dominant *Chondrites* show certain differences: III) *Chondrites*-mottled ichnofabric, with *Chondrites* from shallow to deep tiers, on a mottled background. IV) *Chondrites*-laminated, with *Chondrites* occurring as sparse and disperse patches (bioturbation index 1-2)

overprinting but not deforming primary lamination. V) *Chondrites-Halimedides-Planolites* ichnofabric, featuring *Chondrites* and *Planolites* and the local presence of *Halimedides* (bioturbation index 2-4); *Planolites* occupy the shallow tier while *Chondrites* occur in deeper tiers. VI) *Chondrites-Palaeophycus-Planolites* ichnofabric, with *Chondrites*, *Palaeophycus* and *Planolites*, and showing punctual *Trichichnus* or *Halimedides*, occurring only in

Figure II.7. Outcrop images from different levels: (A) Light Chondrites *isp. in a dark grey marl bed (R7). (B-C) Horizontal pyritised tubes (R2 and R21, respectively). (D) Dark infilled* Chondrites targionii *in a limestone bed (L16). (E) Y-type branching* Thalassinoides *near the top of the upper black shale (L27). (F)* Zoophycos *showing sinuous morphology in dark grey marl (R13). (G)* Rhizocorallium *isp. in dark grey marl (R7); note the presence of pellets. (H) Dark grey marl with vertical shafts of* Thalassinoides *(Th) and scattered* Chondrites *(Ch) (L29). (I) Highly bioturbated boundary between the upper black shale bed and the overlying light grey marl, showing recovery of oxic conditions just after T-OAE (L27-28); note the progressive increase in the bioturbation index (BI). Scale bars are 1 cm.*
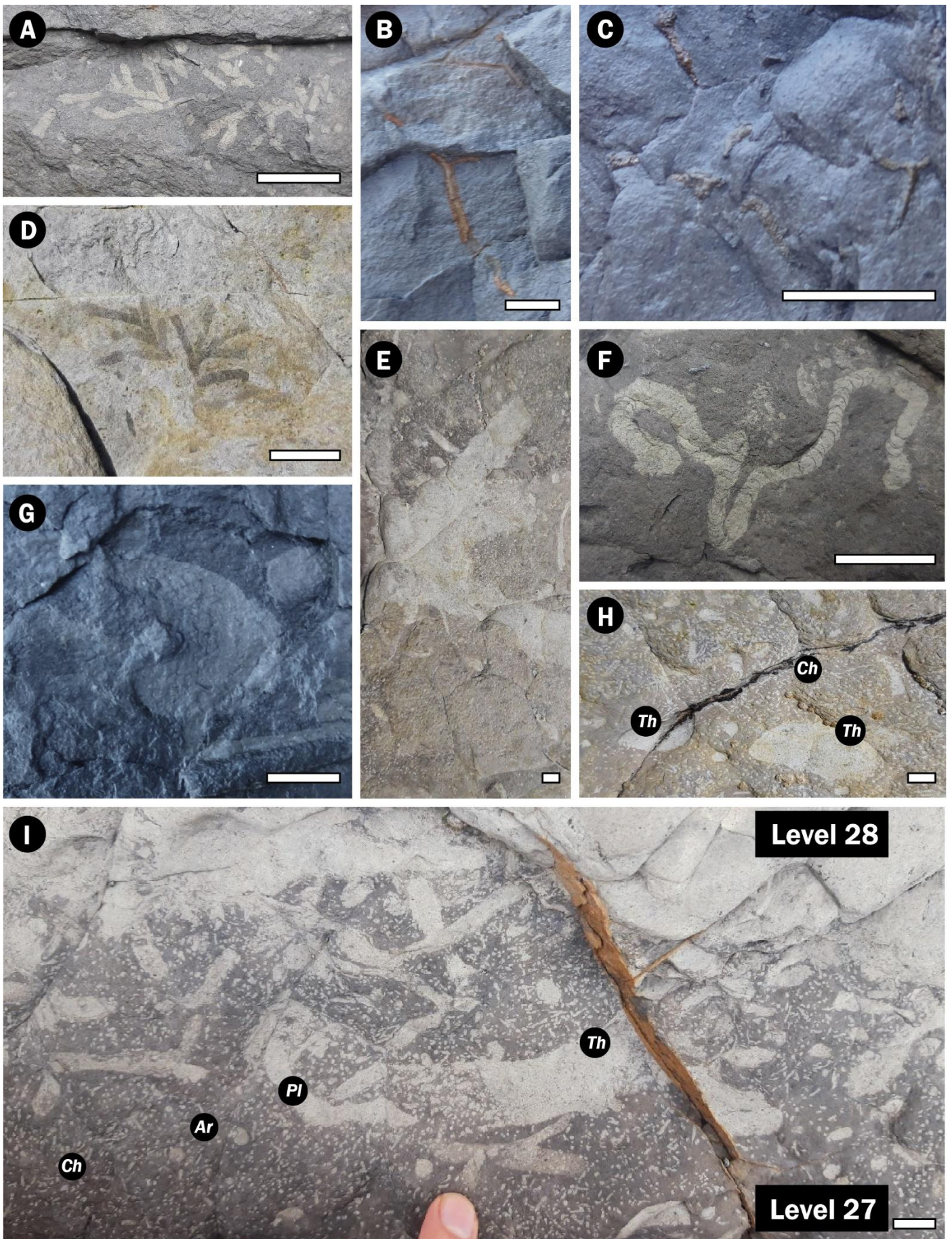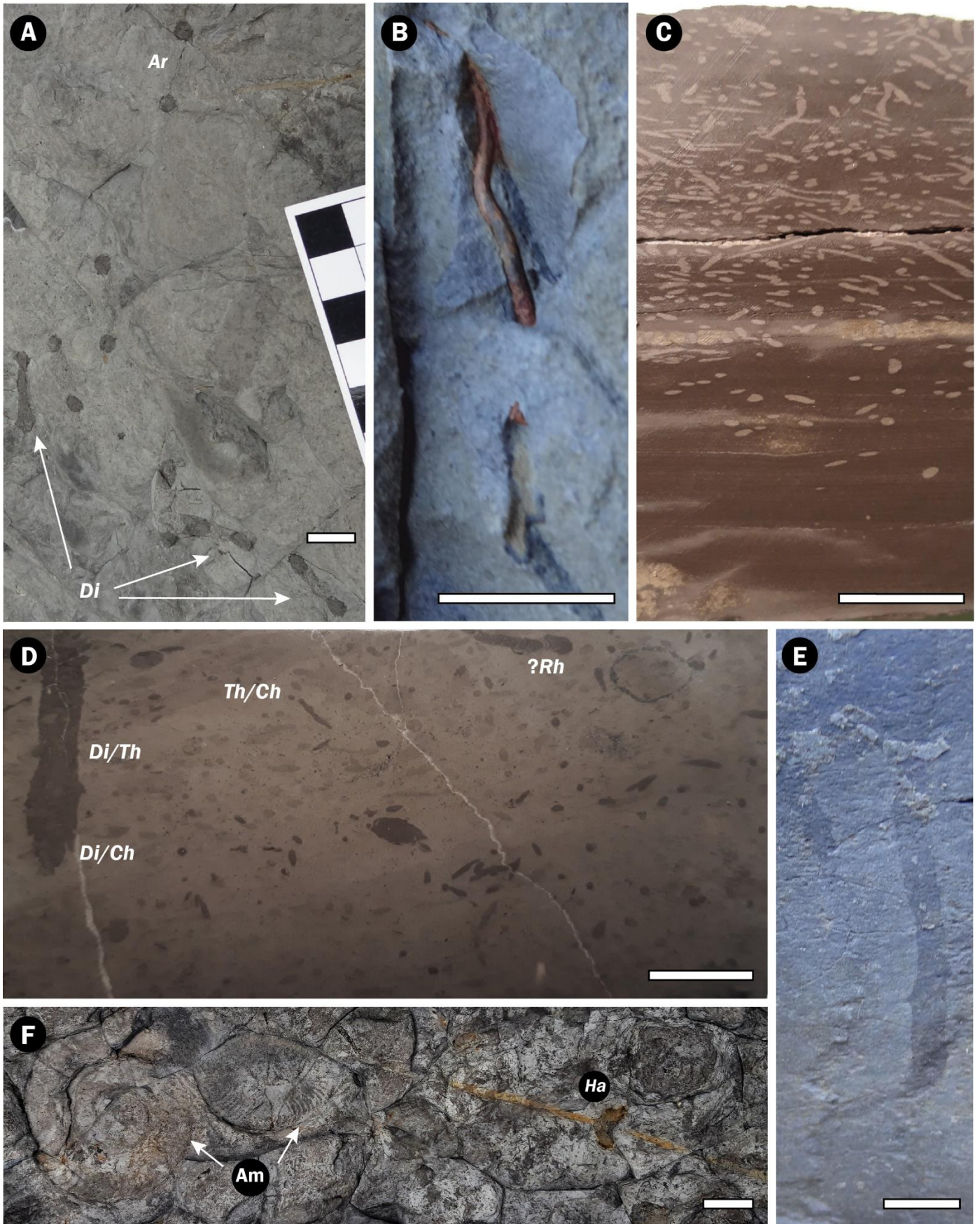
limestone beds (bioturbation index 4-5); *Planolites* and *Palaeophycus* occupy the shallow tier, *Halimedides* occur in the middle tier, and the deep tier consists of *Chondrites* and *Trichichnus*.

Laminated? And *Diplocraterion-Thalassinoides* ichnofabrics are the most abundant ones in terms of occupied thickness, the first occurring in the black shale intervals and in the dark marl levels among them, and the second mainly through the lower part of both sections (Figs. II.5, II.6). *Chondrites*-mottled ichnofabric mainly occupies light grey marls.

5. DISCUSSION
5.1. Macrobenthic tracemaker community and tiering models

The trace fossil assemblages are typical of *Zoophycos* (i.e., *Chondrites*, *Zoophycos*) and *Glossifungites* (i.e., *Arenicolites*, *Diplocraterion*, *Rhizocorallium*) ichnofacies, according to previous authors (Buatois & Mángano, 2011; MacEachern et al., 2012). These ichnofacies may appear in distal/deep marine settings, which is in concordance with the palaeoenvironment of a distal carbonate ramp inferred from the lithofacies analysis (Valenzuela et al., 1989; García-Ramos et al., 1992). *Glossifungites* ichnofacies is characterised by dominant vertical dwelling structures, especially U-tubes with or without spreite (like *Arenicolites* or *Diplocraterion*) and ramified burrows (such as *Thalassinoides* and *Chondrites*), corresponding to the identified architectural designs of the studied ichnoassemblage. As these trace fossils occur accompanied by *Zoophycos* (Figs. II.5, II.6), the present case could correspond to the distal expression of the

Glossifungites ichnofacies (Buatois & Mángano, 2011, and references therein). The *Zoophycos* ichnofacies is typically represented by dominant feeding structures occupying deep tiers, such as *Chondrites* and *Zoophycos*. The palaeoenvironment of this ichnofacies is highly variable (e.g., Buatois & Mángano, 2011; MacEachern et al., 2012, and references therein).

Ichnological features, with special attention to differentiated ichnofabrics, lead us to propose several tiering models and define the development of the endobenthic macrofauna in view of palaeoenvironmental (depositional and ecological) conditions during the early Toarcian in the Asturian Basin (Fig. II.12).

As shown by the bioturbation structures, the lower part of both sections (mainly dominated by the *Diplocraterion-Thalassinoides* ichnofabric) contains a relatively diverse ichnoassemblage. Mainly on the basis of cross-cutting relationships, the shallowest tier would correspond to the mottled texture, indicating a high bioturbation activity under favourable conditions, at the sea floor or just below, in a soupy ground -hence a mixed layer. Soupy conditions interfere with the preservation of discrete trace fossils, meaning the local presence of diffuse *Planolites* may be related to a slight increase in consistency (soupy/soft) in the lowermost part of the mixed layer (Fig. II.10D). The shallow-middle tier reflects the highest ichnodiversity, with well-defined *Planolites* in its upper part, and *Rhizocorallium* and *Palaeophycus* in its middle and lower parts. Deeper down, the middle tier is occupied by *Diplocraterion*, *Arenicolites* and *Thalassinoides*. Finally, the deepest tier is represented by *Chondrites* and small *Zoophycos* in the stiffest part, as the cross-cut relationships indicate, occurring with very

Figure II.8. Outcrop (A-B, E-F) and polished section (C-D) images from different levels: (A) Arenicolites *(Ar) and* Diplocraterion *(Di) occurring in the upper surface of a light grey marl (R6), some diffuse* spreite *making it difficult to differentiate between the two ichnotaxa. (B) Vertical section of a limestone bed (R1) showing* Trichichnus *isp. with pyritized infill. (C)* Chondrites *isp. in the upper black shale level (R22), the lower part still presenting lamination overprinted by scarce* Chondrites. *Note the domain of larger forms in the lower part. (D) Highly bioturbated limestone bed (R3) showing a composite ichnofabric: ?Rhizocorallium (?Rh),* Diplocraterion *(Di) and* Thalassinoides *(Th) completely reworked by* Chondrites *(Ch), also scattered in the substratum. Note the superposition of several ichnocoenoses, e.g.,* Diplocraterion *occur cross-cutting* Thalassinoides *burrows. (E)* Arenicolites sparsus *penetrating from a colonisation surface (stiffground) located in the boundary between the light grey marl and the overlying dark grey level (R6-7), funnel overtures not conserved. (F) Species of ammonites (Am) on the upper surface of a light grey marl level (R25), occurring just next to heart-chambered* Halimedides *(Ha). Scale bars are 1 cm and top is always upwards in B-E.*
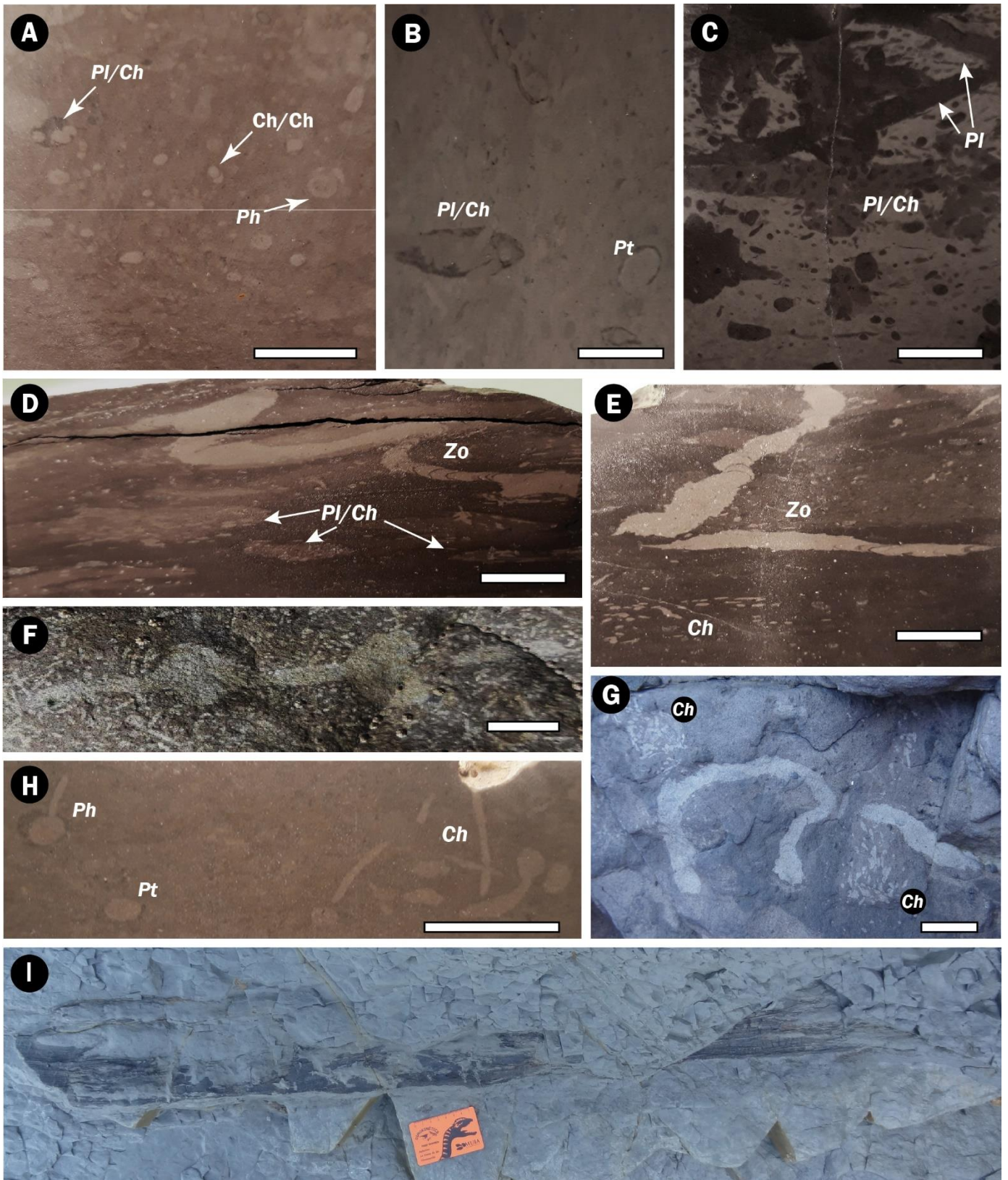
sparse *Trichichnus*. The high values of both bioturbation and ichnodiversity indices reflect good general palaeoenvironmental conditions with well oxygenated bottom- and pore-waters, and food availability, providing for the development of a relatively diverse tracemaker community.

The middle part of the sections is characterised by the presence of thin levels of dark grey marls with primary parallel lamination (laminated? ichnofabric) and an apparent absence of coetaneous bioturbation, reflecting unfavourable palaeoenvironmental conditions for the macrobenthic tracemaker community (Fig. II.12). The punctual record of sparse patches of small light grey *Chondrites*, cross-cutting primary lamination in some dark grey marl levels, indicates bioturbation from a more oxygenated upper level after the deposition of the laminated interval. Thus, *Chondrites* tracemakers determining the *Chondrites*-mottled and the *Chondrites*-laminated ichnofabrics show an opportunistic behaviour, colonising the shallowest levels of a poorly oxygenated substrate after the deposition of laminated sediments, during variable palaeoenvironmental conditions.

The upper black shale levels (R22 and L27) show an interesting succession of laminated?, *Chondrites*-laminated and *Diplocraterion-Thalassinoides* ichnofabrics (Figs. II.7I. II.8C, II.10F, II.12). Below there are no trace fossils, but exclusively lamination. Then, the upward presence of bioturbation progressively overprints laminations, leading first to a *Chondrites* community and then to the more diverse ichnoassemblage of the *Diplocraterion-Thalassinoides* ichnofabric, which definitively erases the original lamination. This provides evidence of the end of adverse conditions and the recovery of oxic bottom- and pore-waters.

The upper part of the sections shows an ichnoassemblage similar to that of the lower part, with minor variations (Fig. II.12): the ichnofabrics dominated by *Chondrites* are more common than the *Diplocraterion-Thalassinoides* ichnofabric. The shallow-middle tier is formed by *Planolites* (upper level) and *Diplocraterion*, *Arenicolites*, *Palaeophycus* and *Halimedides* (medium and lower levels). Deeper, only *Chondrites* tracemaker colonises the substrate. The diversity of this ichnoassemblage points to the recovery of a multi-tiered and well developed macrobenthic community that rapidly colonised the substrate after re-establishment of favourable oxygen conditions.

5.2. The T-OAE at the Asturian Basin: The role of the oxygenation crisis

The distribution of observed tiering models throughout the studied sections sheds light on palaeoenvironmental changes before, during and after the T-OAE, particularly regarding oxygen availability variations in bottom- and pore-waters as the main limiting factor controlling benthic activity during this event. The incidence of other parameters such as organic matter content, an important limiting condition in deep environment for the macrobenthic tracemaker community (Uchman & Wetzel, 2011, 2012; Wetzel & Uchman, 2012), cannot be totally discarded.

Based on these findings, the T-OAE in the Asturian Basin should not be viewed as a continuous suboxic/anoxic event, but rather as reflecting minor-

Figure II.9. Polished sections (A-E, H) and outcrop (F, G-I) images from different levels: (A) Limestone bed (L31) showing the typical mottled texture and composite ichnofabric. Note Chondrites *(Ch) cross-cutting themselves and reworking* Planolites *(Pl), also thick-walled* Palaeophycus heberti *(Ph). (B) Composite ichnofabric in a limestone bed (L1).* Note thin-walled P. tubularis *(Pt) and* Chondrites *(Ch) reworking* Planolites *(Pl). (C)* Planolites *(Pl) cross-cut by diverse-size* Chondrites *(Ch) in a limestone bed with mottled background in a characteristic composite ichnofabric (R29). (D) Composite ichnofabric in a dark grey marl (L15) with* Chondrites *(Ch) reworking* Planolites *(Pl) and* Zoophycos *(Zo). (E) Late emplaced* Zoophycos *(Zo) and flattened* Chondrites *(Ch) in a dark grey marl (L15). (F)* Halimedides *cross-cut by* Chondrites *in the top surface of the upper black shale; note the heart-shaped (right) and the ovalated (left) chambers (L27). (G) Small* Zoophycos *and* Chondrites *(Ch) patches in a dark grey marl (R7). (H) Mottled ichnofabric in a limestone bed (L31) with* Chondrites *(Ch),* Palaeophycus tubularis *(Pt) and* Palaeophycus heberti *(Ph). (I) Bedding plane view of a marl level showing a big size wood fragment, common in both sections (R30-31). Scale bars are 1 cm and top is always upwards. In image I, orange scale is 10 cm.*
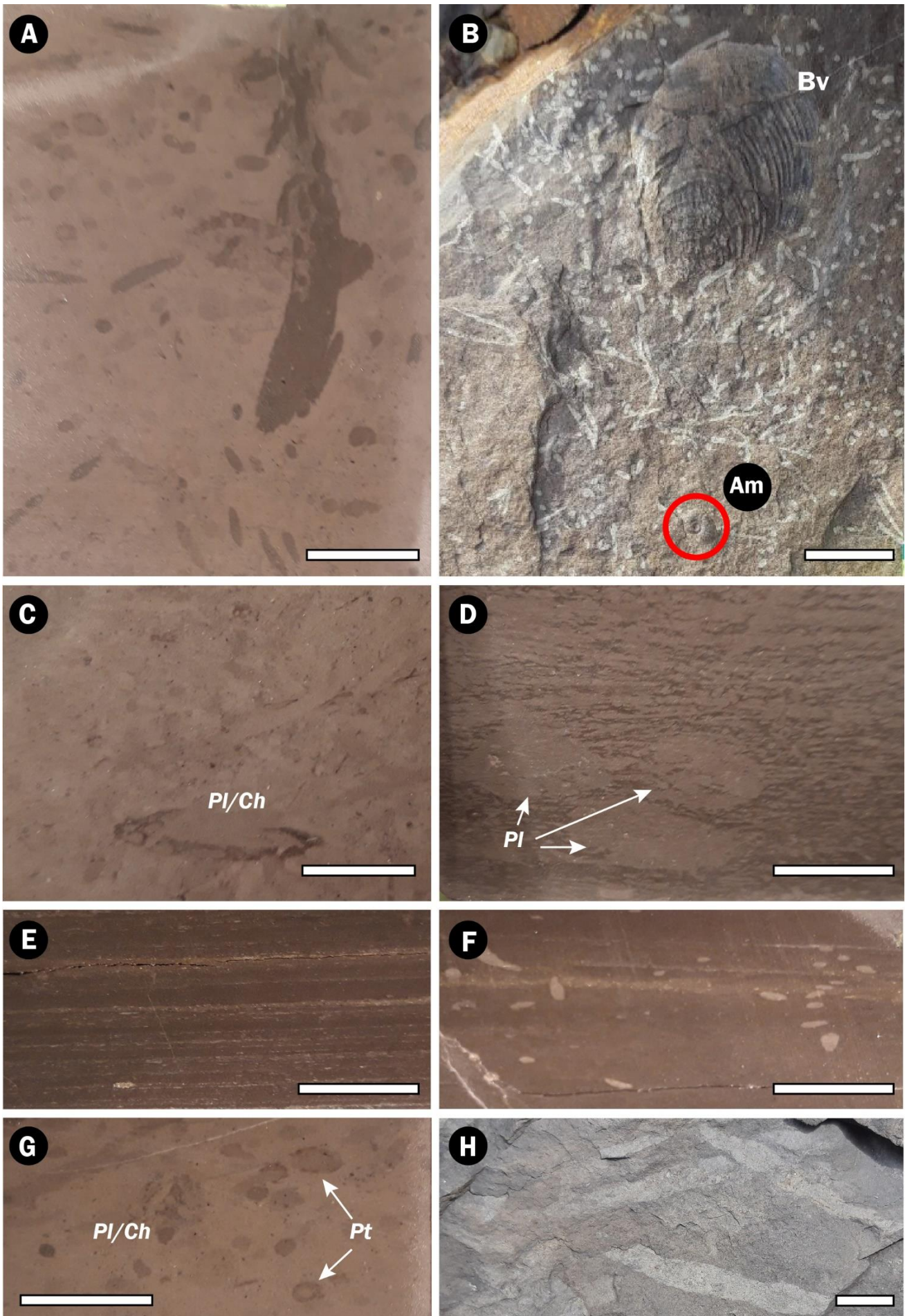
order fluctuations involving anoxic, dysoxic and oxic conditions, leading to successive ecological replacements in the endobenthic tracemaker community.

Suboxic/sporadic anoxic conditions are exclusive at the beginning of the event, characterised by laminated black shales and the absence of bioturbation, reflecting the beginning of the first major episode of the oxygenation crisis (Fig. II.12). Afterwards, during most of the T-OAE (characterised by the dark/light grey marl alternations), oxygenation fluctuates between suboxic/sporadic anoxic conditions (apparent absence of trace fossils, only laminated dark marls) and dysoxic/oxic conditions (presence of small *Chondrites*), representing minor episodes of the oxygenation crisis. Finally, the last part of the T-OAE is marked by a new short suboxic/sporadic anoxic period, representing the second major episode of the oxygenation crisis (Fig. II.12), followed by a quick re-establishment of oxic conditions in bottom- and pore-waters. Thus, ichnological analysis confirms oxygen fluctuations into the T-OAE that occurred during dark/light marl alternations under discontinuous deposition.

Noteworthy is the correlation between the tracemaker community development and the negative isotopic excursiom. As seen in Figures II.3 and II.12, the onset of the negative ^{13}C excursion occurred during a period of favourable environmental conditions for the tracemakers, as reflected by the bioturbation and ichnodiversity index values. Furthermore, the deposition of the laminated black shales (i.e., the first suboxic/sporadic anoxic pulse of the event) starts after the onset of the ^{13}C perturbation, indicating a retarded

effect of the negative excursion on both faunal and sedimentological dynamics.

5.3. A variable effect on biota: the role of temperature

As interpreted above, the T-OAE determined fluctuations in bottom- and pore-water conditions in the Asturian Basin, from anoxic to dysoxic, which significantly affected the benthic habitat, hence the ichnological features. However, the T-OAE had only a minor effect on the macrobenthic tracemaker community, which recovered quickly after the event. This is not a generalised biotic response for the Asturian Basin, where other groups of organisms responded very differently. The global temperature increase during early Toarcian bore deep impact on marine fauna: in the Rodiles section, δ^{18}O analysis conducted in belemnite rostra evidenced a seawater temperature variation from 16 °C up to 24 °C at the *Tenuicostatum-Serpentinum* zone boundary (Gómez & Goy, 2011). In other basins, such as the Subbetic and the Umbria-Marche Basins (Fig. II.1A), the sea surface temperature rose from 22 to 32 °C throughout the T-OAE (Ruebsam et al., 2020).

Previous research conducted in the Asturian Basin, including the Rodiles section, revealed changes in epifauna (brachiopods), pelagic macrofauna (ammonoids) and planktonic microfauna (calcareous nannofossils) interpreted as tied to an abrupt increase in temperature associated with the T-OAE (García Joral et al., 2011; Gómez & Goy, 2011; Fraguas et al., 2012; Gómez et al., 2016a, 2016b). Brachiopods were significantly affected, their reduction in diversity and abundance being correlated with an increase in

Figure II.10. Polished section (A, C-G) and outcrop (B, H) images from different levels, showing the different ichnofabrics: (A) Diplocraterion-Thalassinoides *composite ichnofabric in a limestone bed (R3). Note the dark infilled limb of* Diplocraterion *or* Arenicolites *completely reworked by* Chondrites*, occurring in various sizes. Note also the amalgamation of several ichnocoenoses. (B)* Chondrites-*laminated ichnofabric. Top of the upper black shale level showing small and medium-size* Chondrites*, ammonites (Am) and bivalves (Bv) (L27). (C)* Chondrites-Halimedides-Planolites *ichnofabric in a limestone bed (L1). Note light infilled* Chondrites *(Ch) reworking flattened* Planolites *(Pl). (D) Highly bioturbated ichnofabric in the boundary between a dark marl level and the overlying light grey marl. Note the dominance of* Chondrites *and some diffuse* Planolites *(Pl) in the lower part (R24-25). (E) Laminated? ichnofabric in the lower black shale level (R15). (F)* Chondrites-*laminated ichnofabric in the upper black shale level (R23). Note* Chondrites *overprinting but not deforming lamination. (G)* Chondrites-Palaeophycus-Planolites *ichnofabric in a limestone bed (R3). Note thin-walled* Palaeophycus tubularis *(Pt). (H) Inferred* Planolites *ichnofabric on the bedding plane of a light marl (R34). This ichnofabric is only tentatively considered due to its scarcity, so it is included in the* Chondrites-Halimedides-Planolites *ichnofabric. Scale bars are 1 cm and top is always upwards.*

Legend:

Lamination

Palaeophycus

Zoophycos

Arenicolites   Chondrites   Thalassinoides

Diplocraterion   Planolites   Halimedides

Horizontal
pyritised tubes   Rhizocorallium   Trichichnus
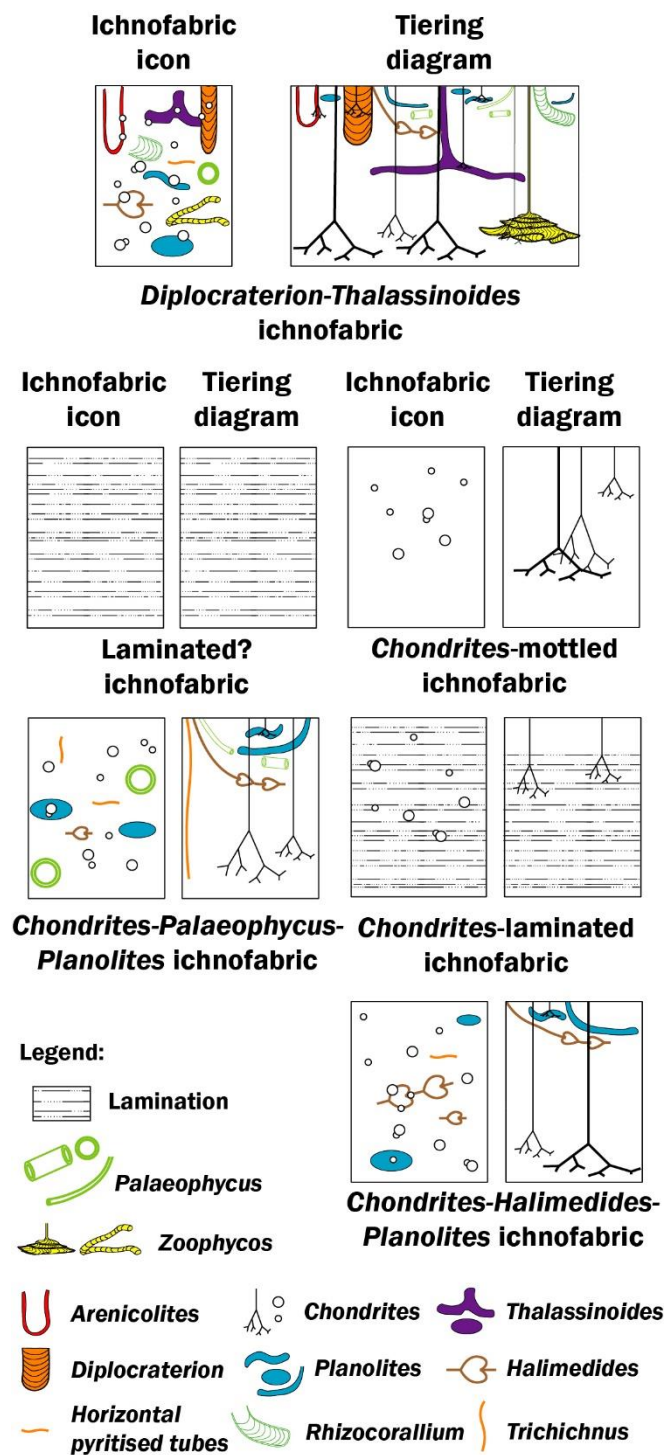
Figure II.11. Ichnofabric icons and the corresponding tiering diagram based on cross-cutting relationships

temperature before the T-OAE; their complete extinction would have taken place during the abrupt temperature rise at the onset of the event (García Joral & Goy, 2009; García Joral et al., 2011). Ammonoids show a substantial decrease in abundance and diversity owing to T-OAE effects, with recovery after the event. Calcareous nannoplankton species show different

responses to the event, including extinctions, but also the appearance of opportunistic forms (Gómez & Goy, 2011). Otherwise, according to Gómez & Goy (2011), the rise in temperature began at the *Tenuicostatum* zone (i.e., before the oxygenation crisis) and reached its maximum upwards of the *Tenuicostatum-Serpentinum* boundary (i.e., during and after the oxygenation crisis) (Fig. II.12). Therefore, the presence of similar ichnoassemblages irrespective of the temperature, with only *Halimedides* appearing as a new ichnotaxa after the *Tenuicostatum-Serpentinum* boundary, provides evidence of a minor effect of this palaeoenvironmental parameter on the macroendobenthic tracemaker community. The effect of the T-OAE on biota in the Asturian Basin would therefore depend on the environmental parameters and the particular habitat in volved. The biota inhabiting the water column are significantly affected (particular species even becoming extinct) mainly due to the increase in temperature, whereas the benthic habitat was mainly controlled by changes in oxygen availability, causing the punctual disappearance of the macrobenthic tracemaker community during certain phases of the T-OAE (i.e., the episodes of the oxygenation crisis).

Still, the rapid recovery of the endobenthic fauna, with a post-T-OAE trace fossil assemblage similar to that of pre-T-OAE times, underlines the absence of significant extinctions, hence the comparatively minor incidence of the event in endobenthic organisms. It is likely that displacement to refuges allowed the macrobenthic tracemaker community to be maintained during unfavourable conditions.

6. CONCLUSIONS

The Rodiles and Lastres sections in the Asturian Basin show similar distributions of facies, consisting of limestones, light and dark marl alternations, and black shales associated with the early Toarcian Oceanic Anoxic Event (T-OAE), all deposited in the outer part of a carbonate ramp.

Ichnological analysis made it possible to identify a diverse ichnoassemblage, comprising ten ichnogenera assigned to the *Zoophycos* ichnofacies and the distal expression of *Glossifungites* ichnofacies. Six ichnofabrics
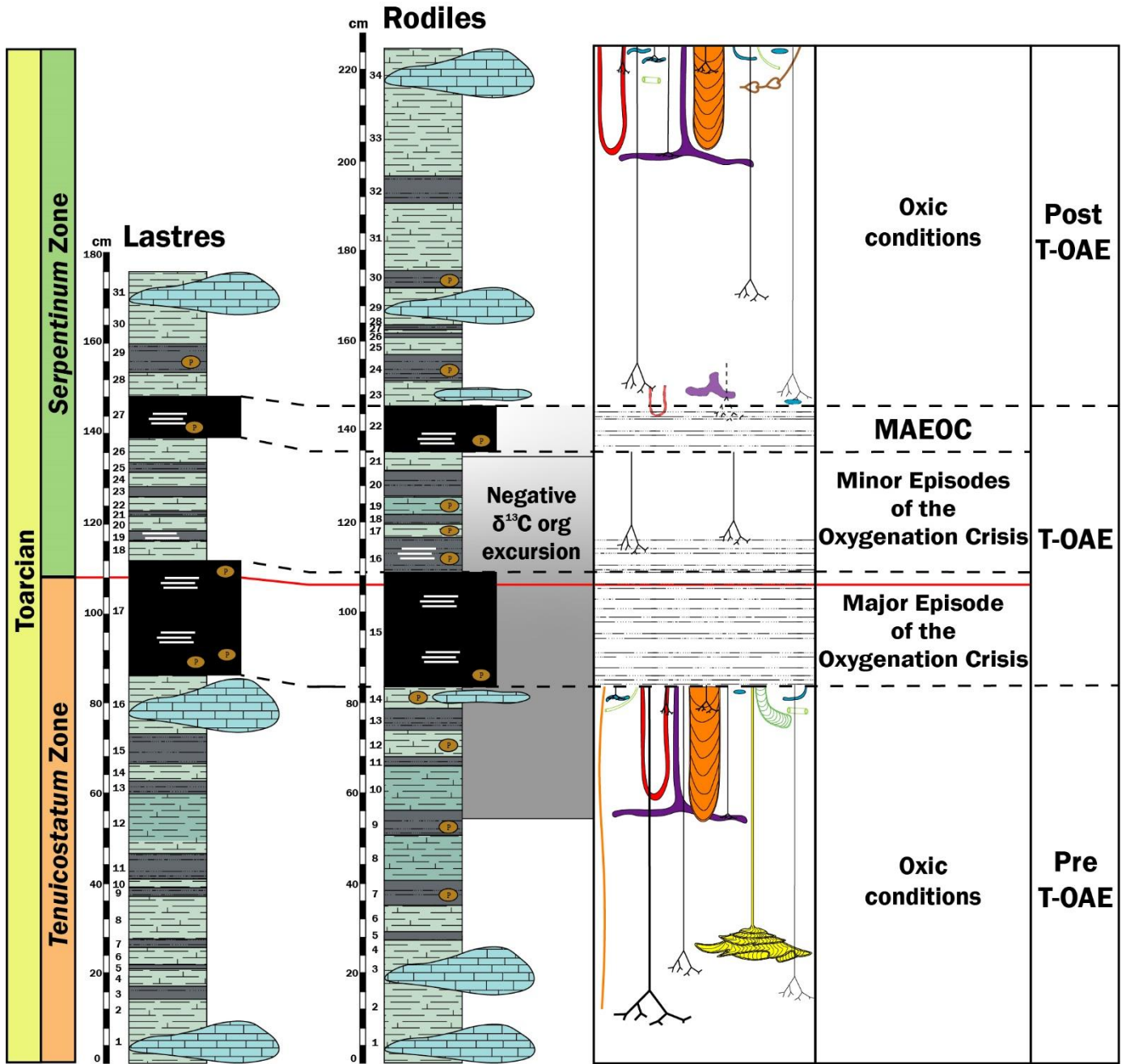
Figure II.12. Diagram showing tiering model distributions along both sections and their correspondence with the T-OAE stages. For legend see Figs. II.3 and II.11. MAEOC: Major episode of the oxygenation crisis.

were differentiated: laminated?, *Diplocraterion-Thalassinoides*, *Chondrites*-mottled, *Chondrites*-laminated, *Chondrites-Halimedides-Planolites* and *Chondrites-Palaeophycus-Planolites*. This allowed for the characterisation of four tiering models associated with sporadic anoxic, disoxic and oxic environments. Suboxic/sporadic anoxic tiering models are related to laminated facies (black shales and dark laminated marls) and the apparent absence of recognisable trace fossils, occurring in different phases of the T-OAE (mainly at the beginning, but punctually during and at the end of the

event). Minor-order oxygen fluctuations from suboxic/anoxic (dark marls) to disoxic/oxic (light marls) conditions developed during the middle part of the T-OAE. Thus, ichnological analysis is shown to be a tool providing for more precise T-OAE characterisation, improving upon approaches based exclusively on facies information.

With regard to the lithofacies, the genesis of alternations between the light grey marls (or limestones) and the dark grey marls may be related to high-frequency

palaeoclimatic changes and/or short-term minor relative sea level changes.

The macrobenthic tracemaker community showed fast recovery, as revealed by the high values found for the bioturbation index and ichnodiversity after the T-OAE, supporting the event´s comparatively minor effect and the rapid re-establishment of favourable oxic conditions in the bottom- and pore-waters of the Asturian Basin.

Acknowledgements

CHAPTER III

THE RECORD OF THE ICHNOGENUS *HALIMEDIDES* AND ITS RELATIONSHIP WITH THE T-OAE

The record of *Halimedides* at the Asturian Basin (northern Spain): supporting the T-OAE relationship

Javier Fernández-Martínez [a], Francisco J. Rodríguez-Tovar [a], Laura Piñuela [c], Francisca Martínez Ruíz [b], José C. García-Ramos [c]

[a] *Departamento de Estratigrafía y Palaeontología, Universidad de Granada, Granada, Spain*

[b] *Museo del Jurásico de Asturias (MUJA), Colunga, Asturias, Spain*

[c] *Instituto Andaluz de Ciencias de la Tierra CSIC-UGR, Granada, Spain*

Carbon Cycle and Ecosystem
Response to the Jenkyns Event
in the Early Toarcian (Jurassic)

Edited by
M. Reolid, L. V. Duarte, E. Mattioli and W. Ruebsam

Geological Society
Special Publication 514
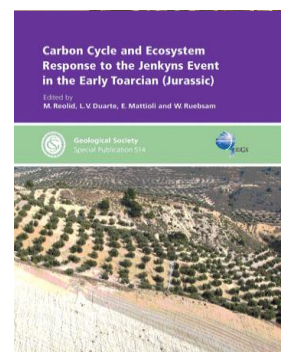
ABSTRACT

Recent ichnological analysis conducted in two sections (Rodiles and Lastres) of the Asturian Basin revealed the presence of *Halimedides* Lorenz von Liburnau 1902, which occurs just above the black shales related to the end of the T-OAE. *Halimedides* is associated with the recovery of the tracemaker community after the reestablishment of favourable, oxic, conditions. The appearance of *Halimedides* after the T-OAE event, previously not registered, supports the close relationship of the tracemaker with oxygen conditions, as occurs in other anoxic events including the Cretaceous OAE-1a and OAE-2. Also a relation between morphometric and paleoenvironmental parameters is observed, occurring larger and densely chambered specimens in darker, weakly oxygenated facies, while smaller and sparsely chambered forms are registered in lighter, better oxygenated sediments.

KEY WORDS

1. INTRODUCTION

The Toarcian Oceanic Anoxic Event (T-OAE) is an important perturbation that affected marine ecosystems during Early Jurassic times. The event is marked in the sedimentary record by a pronounced negative carbon isotope excursion (CIE) between two positive ones, and widely documented in records of organic-rich, black shale, sediments (e.g., Hesselbo et al. 2007; Suan et al. 2008, 2015; Jenkyns 2010; Hermoso et al. 2012). The associated mass extinction entailed the disappearance or reduction of many forms of ammonoids, ostracods, brachiopods, foraminifera, echinoderms and calcareous nannofossils (Dera et al. 2010; García Joral et al. 2011; Gómez & Goy 2011; Rita et al. 2016; Reolid et al. 2018, 2019; Slater et al. 2019, Soulimane et al. 2020).

This event has been profusely studied from various standpoints, paleontological information serving as a tool for its interpretation. Ichnological studies are comparatively scarce, though some detailed analyses have recently been published (e.g., Rodríguez-Tovar & Uchman 2010; Rodríguez-Tovar & Reolid 2013; Reolid et al. 2014; Miguez-Salas et al. 2017, 2018; Rodríguez-Tovar et al. 2017, 2019). Trace fossils, reflecting the behaviour of tracemakers in response to the paleoenvironment, provide useful information about ecological and depositional conditions, such as bottom water oxygenation, food availability, sedimentation rate, current energy or substrate consistency (e.g., McIlroy 2004; Miller III 2007; Buatois & Mángano 2011; Knaust & Bromley 2012). In this context, ichnological analysis is a very useful proxy when interpreting oceanic anoxic events such as the Faraoni Event (upper Hauterivian; Rodríguez-Tovar & Uchman 2017), the Bonarelli Event (Cenomanian-Turonian boundary; Uchman et al. 2008, 2013a, b; Rodríguez-Tovar et al. 2009a, b, 2020; Rodríguez-Tovar & Uchman 2011; Monaco et al. 2012, 2016), and the Toarcian Oceanic Anoxic Event (cites above).

In the case of the Lower Jurassic sediments from the Asturian Basin, black shale facies signal the T-OAE, although other facies are also associated. The first detailed ichnological analysis of the lower Toarcian sediments in selected sections (Rodiles and Lastres) of

the Asturian Basin allows for an ichnological characterization of the T-OAE transition (Fernández-Martínez et al. submitted). Of special interest in the registered trace fossil assemblage is the record of *Halimedides*, a trace fossil recently associated with the T-OAE (Rodríguez-Tovar et al. 2019). The present research studies the *Halimedides* record in detail to establish its relationship with oceanic anoxic events, particularly the T-OAE; its morphometric characteristics are analysed and related with the organic matter content and oxygen availability.

2. GEOLOGICAL SETTING

Research efforts were focused on two sections of the Asturian Basin, Lastres and Rodiles. The Lastres section is found in the western part of Lastres beach [43°30'41.2"N 5°16'06.2"W], and the Rodiles section in the eastern part of Rodiles beach [43°32'19.7"N 5°22'25.5"W] (Fig. ÍII.1a). Both sections, of around 1.5 m thick in Rodiles and 1.1 m in Lastres, consist of alternations of limestones with light and dark marls, and interbedded organic matter-rich black shales (Figs. ÍII.1b-d, ÍII.2), which have already been associated with the T-OAE (e.g., García Joral & Goy 2009; Gómez & Goy 2011), being the boundary between Tenuicostantum and Serpentinum zones located into the lower black shale level (Fig. ÍII.2., Gómez et al. 2008).

Both sections belong to the Santa Mera Member, of the Rodiles Formation, comprising rhythmites of marls and limestones, ranging from the intra upper Sinemurian to the lower Bajocian. Santa Mera Mb. is the distal part of a carbonate ramp deposited in offshore environments (Valenzuela et al. 1986, 1989; Armendáriz et al. 2012; Bádenas et al. 2013). It is divided in two sub-units. The lower one (intra upper Sinemurian to lower Toarcian) represents an offshore occasionally-restricted setting, with several organic-rich black shales, while the upper one (upper Toarcian to lower Bajocian) was deposited in more open and oxygenated waters (Fig. ÍII.1d).
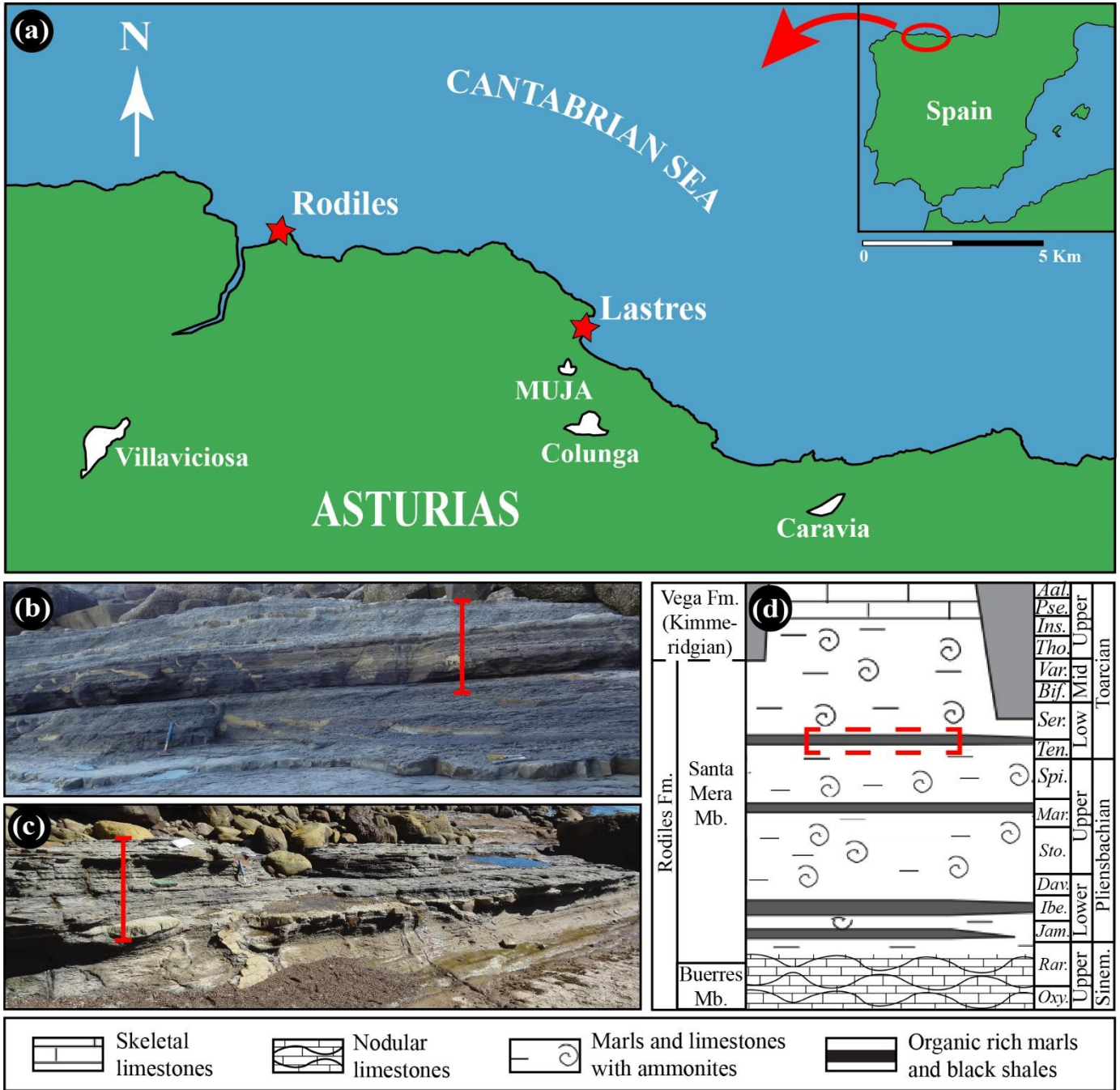
Figure III.1. Studied sections of the T-OAE in the Asturian Basin. (a) Location of the studied sections (red stars) in the Asturian coast (northern Spain). MUJA: Museo Jurásico de Asturias (Jurassic Museum of Asturias). (b) Outcrop view of the Rodiles section. (c) Outcrop view of the Lastres section. Note: red lines indicate the studied intervals, 160 cm in (b) Rodiles and 110 cm in (c) Lastres. (d) Simplified distribution of facies and formations in the Lower Jurassic of the Asturian Basin (not to scale, modified from Aurell et al. 2003 and Deconick et al. 2020). Ammonite zones are indicated, from bottom to top: Oxy.: Oxynotum, Rar.: Raricostatum, Jam.: Jamesoni, Ibe.: Ibex, Dav.: Davoei, Sto.: Stokesi, Mar.: Margaritatus, Spi.: Spinatum, Ten.: Tenuicostatum, Ser.: Serpentinum. Bif.: Bifrons, Var.: Variabilis, Tho.: Thouarsense, Ins.: Insigne, Pse.: Pseudoradiosa, Aal.: Aalensis. Studied interval marked in red.

3. ICHNOLOGICAL ANALYSIS: THE RECORD OF *HALIMEDIDES*

    A recent ichnological analysis of the T-OAE transition in Rodiles and Lastres sections revealed an abundant and diverse trace fossil assemblage consisting of eight ichnogenera: *Arenicolites*, *Chondrites*, *Diplocraterion*, *Halimedides*, *Palaeophycus*, *Planolites*, *Thalassinoides* and *Zoophycos*. Of particular interest is the record of *Halimedides* with regard to the T-OAE (Figs. ÍI.2-5).
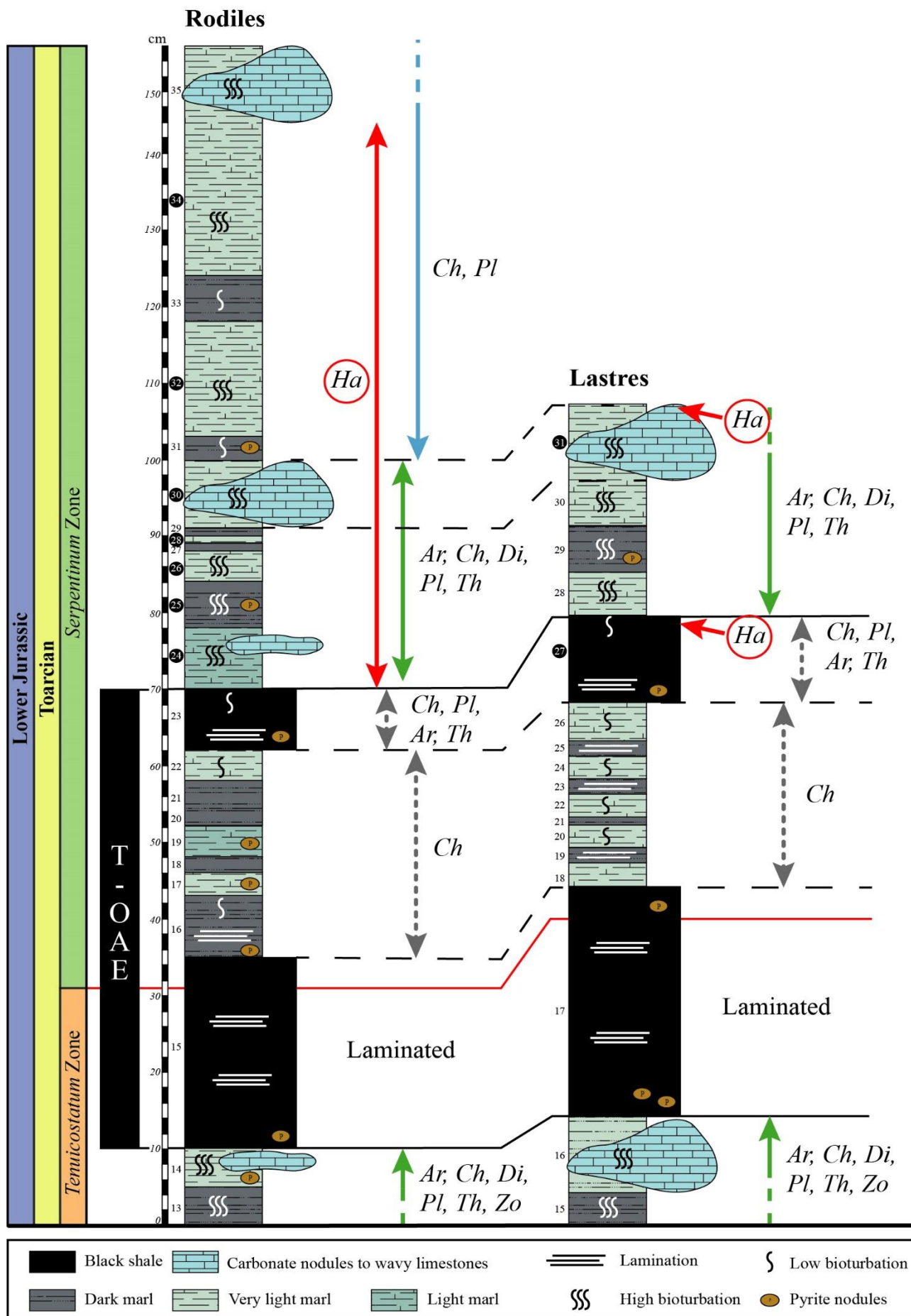
*Figure III.2. Lithological columns of the studied sections (*Tenuicostatum *and* Serpentinum *zones, lower Toarcian, after Gómez et al. 2008). Ichnoassemblages and distribution of* Halimedides *are indicated. Dashed grey line indicates discontinuous occurrence.*

Figure III.3. Close-up outcrop views of Halimedides *specimens, images (a-b) from Lastres and (c) from Rodiles: (a) L27B: light infill, densely chambered specimen crosscut by* Chondrites *at the top of the upper black shale. Chamber 1 is ovalated and chamber 2 is heart-shaped (cf. Fig. 4c in Gaillard & Olivero 2009). (b) L27A: light infill* Halimedides *at the top of the upper black shale, showing a rectangular chamber and crosscut by* Chondrites. *(c) R24C: specimen from a light marl with a heart-shaped chamber with a slightly curved tube, showing ferruginous infill. Scale bar: 1 cm.*

In the studied outcrops, a total of 60 specimens were found, 3 of them in Lastres (labelled as L) and 57 in Rodiles (labelled as R) (Table ÍII.1). The registered *Halimedides* are found toward the top of the sections, associated with the second (upper) black shale interval corresponding to the final T-OAE (Fig. ÍII.2). Specimens L27A and B occur at the top of the upper black shale in Lastres, and L31A appear at the top of the section in a limestone level, whereas the Rodiles *Halimedides* occurs above the upper black shale, in light (R24A-H, R26A-AI, R28A-B, R32A) and dark (R25A-I) marl alternations and in a limestone level (R30A-B).

The specimens show different infilling material than the host sediments: those preserved in dark facies (dark marl and black shale) show a light marl infill (Fig. ÍII.3a-b), yet those occurring in a light facies (light marl and limestone) show a dark marl infill (Figs ÍII.3d,

ÍII.4c). In both types of facies, several specimens show ferruginous infill (Figs. ÍII.3c, ÍII.4a-b), originally formed by pyrite (as organic matter enhances its precipitation) and now oxidized to goethite due to weathering.

Halimedides Lorenz von Liburnau 1902 refers to chamber-like structures showing several shapes (angular, trapezoidal, oval, arcuate —hearted— and/or hemispherical), regularly or irregularly distributed in a string, which is locally branched (following *Halimedides* annulata Vialov 1971 sensu Uchman 1999).

As in the diagnosis of the ichnogenus, the registered *Halimedides* at the Lastres and Rodiles sections consist of chamber-like structures distributed in a string. The well preserved chambers tend to be circular/oval and heart-shaped (e.g., specimen L27B (Fig. ÍII.3a) shows both types); also rectangular chambers were
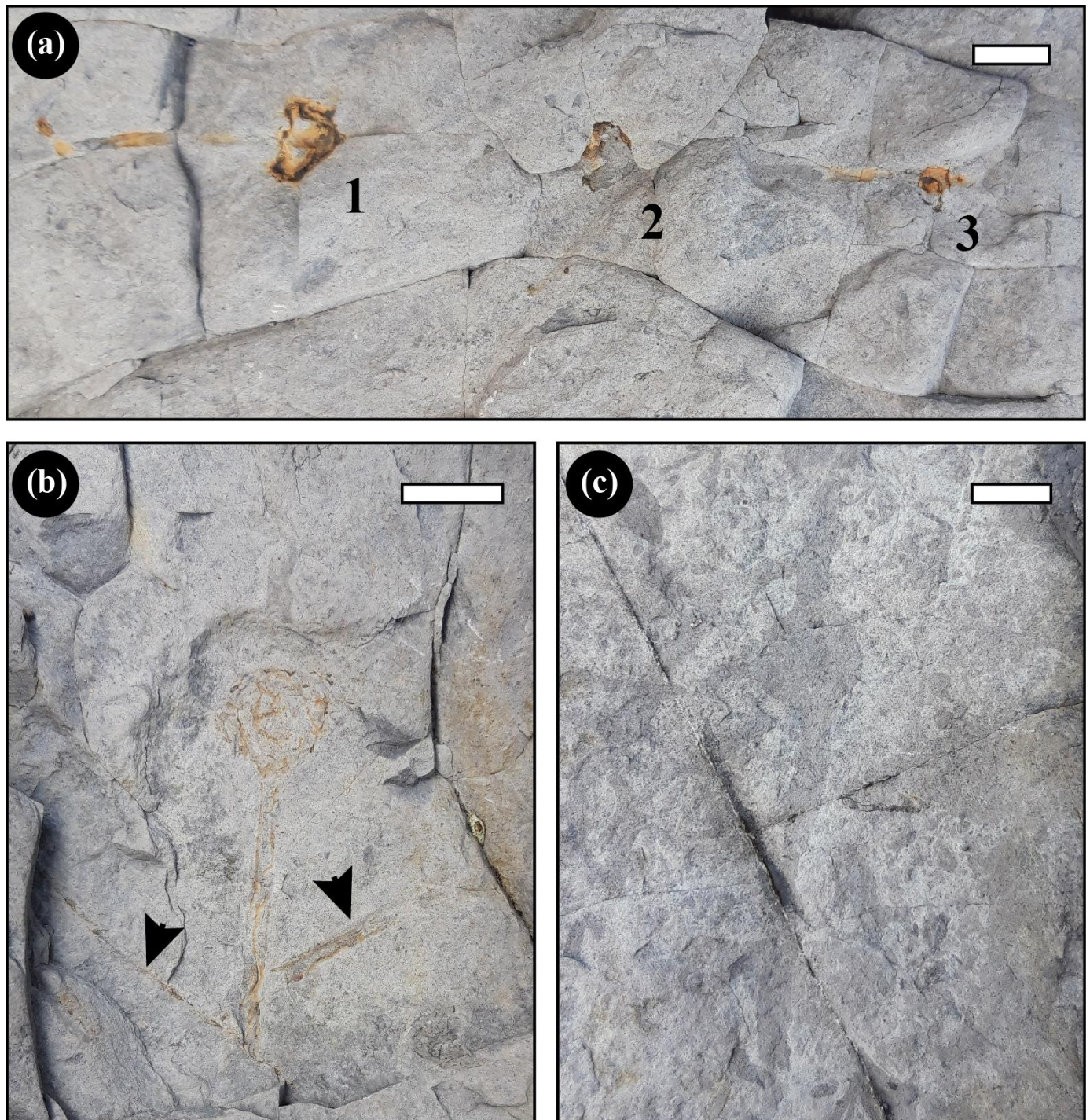
Figure III.4. Close-up outcrop views of Halimedides *specimens from the Rodiles section. Images (a-b) from light marls and (c) from limestone: (a) R26G: almost straight tube showing three chambers (1 and 2 heart-shaped, 3 totally deformed), with ferruginous infill. (b) R26H: circular chamber, showing partially-eroded ferruginous infill and a straight tube ramified (arrows) at both right and left sides with a 45° angle. (c) R30B: circular chamber and straight tube showing dark infill, crosscut by dark-infilled* Chondrites. *Scale bar: 1 cm.*

registered, in specimens L27A (Fig. ÍII.3b) and R26C. The horizontal tubes are straight or slightly curved, having the same infill as the chambers. Terminations of the tubes were not recognized, but some tubes showed marked curves or radiations in variable angles (e.g.,

specimen in Fig. ÍII.4b). The observed tube length varies from 0.40 (R26L) to 21.50 cm (R21E), while their diameters, with an average of 0.26 cm, varies between 0.10 (R24B, R26F, U) and 0.60 cm (R25I) (Table ÍII.1,

Measures in cm	L27 A	L27 B		L31 A	R24 A	R24 B	R24 C	R24 D	R24 E	R24 F	R24 G	R24 H	R25 A		R25 B	R25 C
Chamber Number		1	2										1	2		
Tube diameter	0.43	0.37		0.20	0.20	0.10	0.19	0.36	0.16	0.24	0.24	0.21	0.40		0.30	0.40
Tube length	7.24	5.40		2.00	2.10	4.00	7.12	6.29	8.33	3,00	8.75	4,00	6.30		1.10	2.60
Chamber lenght	1.61	1.00	0.80	0.90	0.8	0.70	0.92	1.12	0.94	0.76	1.09	0.74	1.3	1.00	1.10	1.30
Chamber width	2.14	1.10	1.20	1.00	1.3	0.90	1.23	1.6	0.88	1.03	1.22	0.79	1,00	1.1	1.20	2.00
Chamber spacing		1.20											3.50			

	R25 D	R25 E	R25 F	R25 G	R25 H	R25 I	R26 A	R26 B	R26 C	R26 D	R26 E	R26 F	R26 G			R26 H
Chamber Number													1	2	3	
Tube diameter	0.30	0.40	0.20	0.10	0.30	0.60	0.20	0.30	0.20	0.20	0.30	0.10	0.20			0.20
Tube length	4.00	3.00	3.50	3.80	3.90	2.41	10.00	0.40	1.70	2.30	1.30	0.60	13.65			3.70
Chamber lenght	0.80	0.90			0.9	1.40	1.20	0.50	0.90	0.40	1.10	1.00	1.00	0.80		1.70
Chamber width	1.10	1.20			1.50	2.10	1.00	0.60	1.20	0.90	1.60	1.20	1.30	1.00		1.40
Chamber spacing													3.50 (1-2) 4.00 (2-3)			

	R26 I	R26 J	R26 K	R26 L	R26 M	R26 N	R26 O	R26 P	R26 Q	R26 R	R26 S	R26 T	R26 U	R26 V	R26 W	R26 X
Tube diameter	0.30	0.30	0.30	0.20	0.30	0.30	0.20	0.30	0.40	0.20	0.15	0.30	0.10	0.20	0.20	0.30
Tube length	5.40	7.50	10.30	0.40	1.20	3.10	2.00	4.50	2.50	1.80	2.50	2.50	3.40	0.70	4.50	9.60
Chamber lenght	1.00	1.00		0.70	0.80				0.90	0.90	0.80		0.80	1.10	1.40	1.00
Chamber width	1.00	1.00		1.40	0.90				1.10	1.20	1.00		1.00	1.20	1.50	1.00

	R26 Y	R26 Z	R26 AA	R26 AB	R26 AC	R26 AD	R26 AE	R26 AF	R26 AG	R26 AH	R26 AI	R28 A	R28 B	R30 A	R30 B	R32 A
Tube diameter	0.20	0.30	0.20	0.40	0.20	0.21	0.20	0.20	0.24	0.32	0.18	0.30	0.30	0.30	0.40	0.20
Tube length	2.40	1.60	5.60	17.50	1.50	2.92	14.40	5.70	18.50	21.50	2.00			3.50	6.30	
Chamber lenght	1.00		1.00	1.00	0.80	1.17	0.90	1.00	0.50	1.00	1.03	0.90	0.90	1.00	1.10	1.00
Chamber width	1.00		1.50	1.60	1.00	1.25	1.60	1.43	1.20	1.46		1.20	1.00	1.10	1.10	1.30

Table III.1. Parameters measured for the Halimedides *specimens in Lastres and Rodiles sections. Labels of specimens corresponds to: L (Lastres) or R (Rodiles), the number of the level where it occurs, and a letter for each specimen in the same level; in case of two or more chambers they are also numbered. Each colour represents one different level: L27 is black shale; R25 is dark marl; R24, R26, R28 and R32 are light marls; and R30 is limestone. ND (no data).*
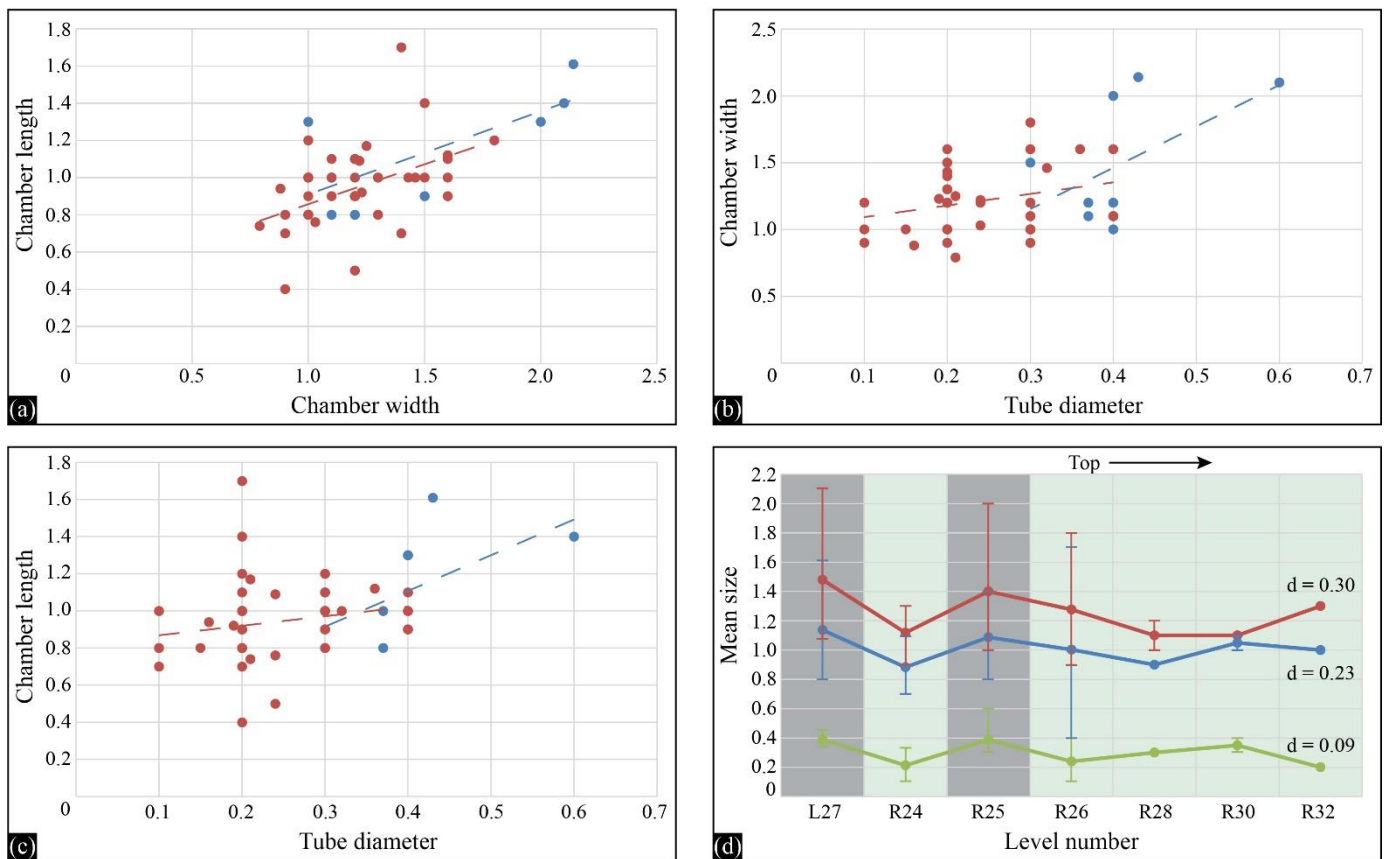
Figure III.5. Representation of the measured parameters: (a) Chamber length vs chamber width. (b) Chamber width vs tube diameter. (c) Chamber length vs tube diameter. (d) Stratigraphic variations of chamber width, chamber length and tube diameter at Lastres (level L27) and Rodiles (levels R24-26, R28, R30 and R32) sections. Note: Bar colour indicates dark (grey) or light (light green) facies. Measures are in cm, obtained only from complete specimens. d: normal deviation. See text for explanation.

Fig. ĺII.5d). The tubes do not show scratches or faecal pellets. The chambers have an average length of 1.01 cm and an average width of 1.25 cm (Table ĺII.1). Chambers show no scratches or radiating tubes. Only one chamber was observed in most tubes, though few specimens showed two or even three chambers (e.g., Figs. ĺII.3a, ĺII.4a): in L27B (chamber spacing of 1.2 cm between chambers 1 and 2), R25A (3.5 cm between chambers 1 and 2) and R26G (3.5 cm between chambers 1 and 2, and 4 cm between 2 and 3). The specimens from the Asturian Basin are similar in size to those registered in the Lusitanian Basin (Toarcian of Portugal: Rodríguez-Tovar et al. 2019) and larger than *Halimedides* from the southern Alps in Puez area (Barremian-Aptian of Italy; Lukeneder et al. 2012), from Digne, Dieulefit and Como areas (Hauterivian-early Aptian of SE France, Switzerland and N Italy, respectively; Gaillard & Olivero 2009), from the Sztoinia and the Leszczawa sections (uppermost Cenomanian and Oligocene, Polish Carpathians, Uchman et al. 2013a and Kotlarczyk & Uchman 2012, respectively), and from Ontario (Upper Ordovician; Stanley & Pickerill 1993).

A variable correlation is seen between the measured parameters (Fig. ĺII.5). According to the difference in deviation between corresponding measures, chamber length vs chamber width show a good correlation (Fig. ĺII.5a), yet chamber length and chamber width vs tube diameter are less correlated (Fig. ĺII.5b-c). Also is significant the low dispersion of tube diameter values (0.09), while chamber width and length show higher deviations (0.30 and 0.23 respectively), indicating more variation in chamber size than in tube diameter among the different specimens.

Significantly, as it is seen in Fig. ĺII.5d, specimens from dark facies (dark marls and black shales) are larger than those from light facies (light marls and limestones). This difference is specially observed in the tube diameter (Fig. ĺII.5b-c), since the dark facies specimens occurs with larger tube sizes. On the other hand, the differences in chamber size are less relevant, with similar values in dark and light facies (though three specimens from dark facies have significantly greater chambers, Fig. ĺII.5a). Well preserved chambers are

mainly heart-shaped or circular/oval, showing an undifferentiated occurrence in both dark and light facies.

The chamber spacing is notably higher in the marls specimens (R25A, 3.5 cm; R26G, 3.5 and 4 cm) than in the black shale one (L27B, 1.2 cm). Even so, following the definition from Gaillard and Olivero (2009), all specimens should be classified as sparsely chambered. Orientation of some specimens was measured showing two main directions, N124E and N166E (Fig. ĺII.6).

Several specimens (L27A-B, R25A-D and G-I, R26J and R30A-B) are crosscut by *Chondrites*, occurring both in the same as in different infill colour than the *Halimedides* specimen (Figs ĺII.3a-b, ĺII.4c). It is remarkable that most of these crosscut specimens appear in dark levels, and the *Chondrites* occur crosscutting the *Halimedides* while occupying all the substratum, not reworking the trace fossil.
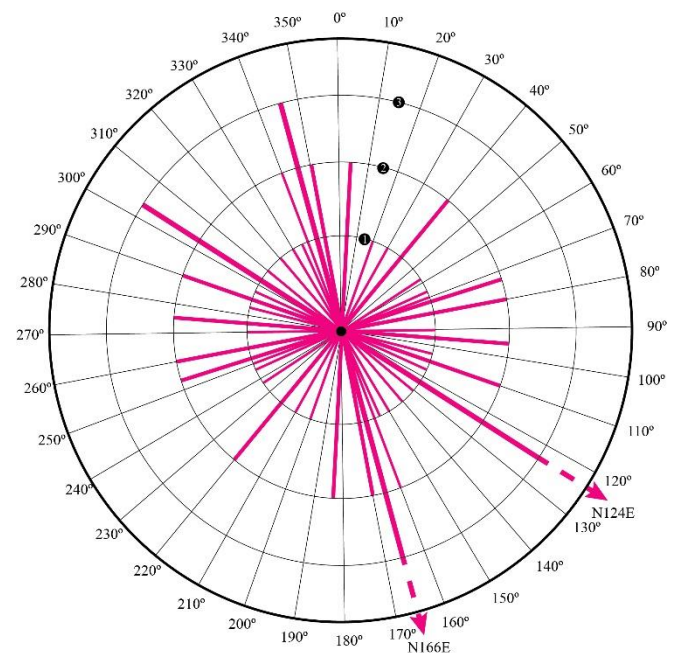
Figure III.6. Surface orientation of Halimedides *specimens, showing two principal directions at N124E and N166E.*

Halimedides co-occurs with several trace fossils, according to particular facies (Fig. ĺII.2): a) in the black shale from the Lastres section (level L27), with *Chondrites*, *Planolites*, and sparse *Thalassinoides* and *Arenicolites*; b) in the light/dark marl and limestone alternations just overlying the T-OAE from the Rodiles section (levels R24-30), with *Arenicolites*, *Chondrites*,

Diplocraterion, *Planolites* and *Thalassinoides*; and c) in the upper Rodiles light/dark marl and limestone alternation (levels R31-35), with *Chondrites* and *Planolites*.

4. DISCUSSION

Previous ichnological analysis at the studied sections confirmed the existence of minor-order fluctuations involving anoxic, dysoxic to oxic conditions, associated with the T-OAE at the Asturian Basin. Most of the event is related to the black shale intervals and the alternation of light and dark marls: the beginning of the event is characterized by anoxic conditions and the record of the lower black shale interval; the end of the T-OAE also reveals a short anoxic period during deposition of most of the upper black shale interval. After that, a fast reestablishment of oxic conditions at the bottom- and pore-waters is registered, corresponding to the top of the sections.

There is not a clear relationship between size of specimens and the type of host sediment, although most of the larger specimens occur in dark facies (which show wider tubes, in some cases larger chambers). Facies analysis compared with TOC (Fig. ÍII.7) and isotopic data from previous works (Gómez et al. 2008, 2016, and Rodrigues et al. 2020), leads to the conclusion that most of the specimens of *Halimedides* occurred when TOC values decrease (after level R23), i.e., when T-OAE finished and oxygen availability increased.

Thus, in the Asturian Basin, the larger and densely chambered specimens occur in darker sediments, probably enriched in organic matter and then poorly oxygenated; in contrast, the smaller and sparsely chambered specimens occur in light levels where the organic matter content is probably lower and oxygen availability higher. This difference is even more notorious between marl and black shale levels. This finding agrees with the interpretation presented in Gaillard & Olivero (2009), showing a correspondence between a poorly oxygenated substratum and larger, closer chambers in specimens found in Cretaceous pelagic alternations of marls and limestones.

The record of *Halimedides* immediately after the T-OAE in the studied sections (Fig. ÍII.2) supports
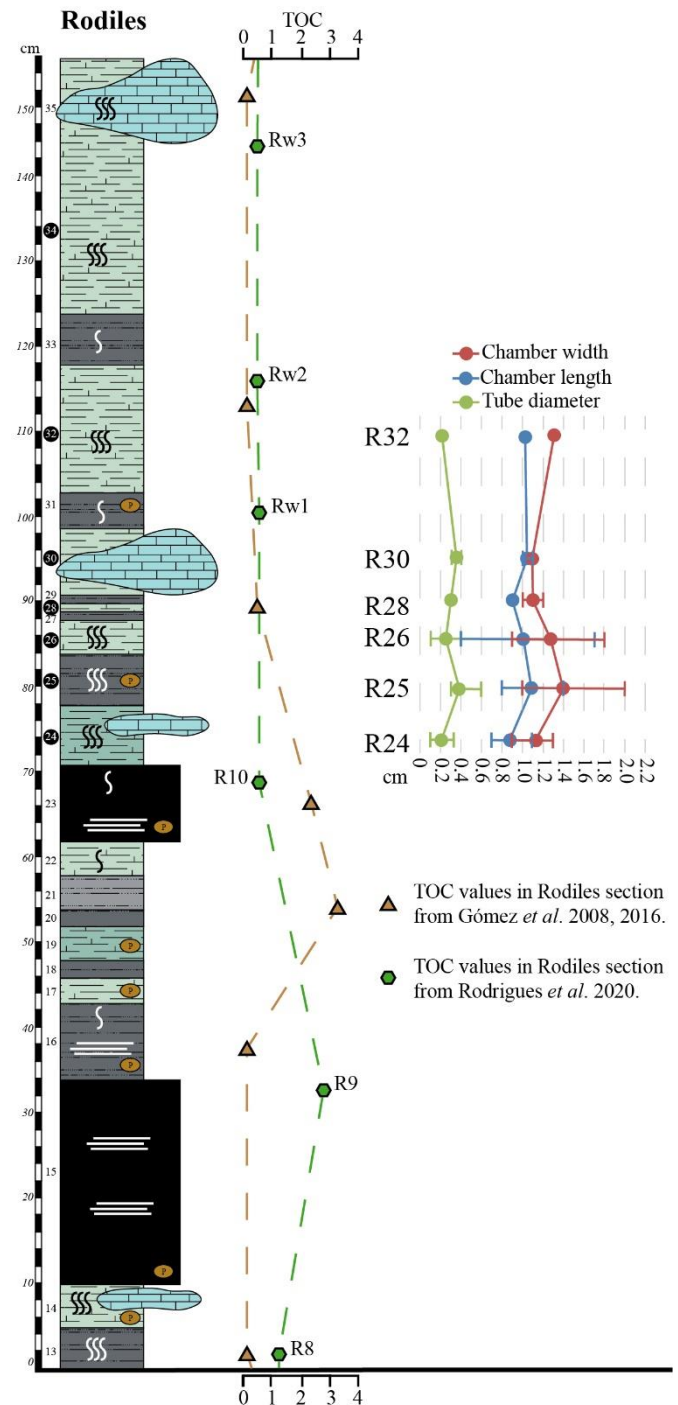
Figure III.7. Lithological column of the Rodiles section showing the approximate location of TOC values (after Gómez et al. 2008, 2016; Rodrigues et al. 2020) correlated with the mean measures of the Halimedides *specimens from each level (black circles in the log). For lithologic symbols see Fig. ÍII.2.*

previous interpretations on the relationship of the tracemaker and the global event (Rodríguez-Tovar et al. 2019 for the record at the Lusitanian Basin). However, in the case of the specimens from the Lusitanian Basin, oxygenation was not interpreted as a major factor determining the presence of *Halimedides* tracemakers;

neither sedimentological nor ichnological data support a significant change in the oxygen conditions (from anoxic/dysoxic to oxic) during the *Halimedides* interval with respect to previous T-OAE facies (Rodríguez-Tovar et al. 2019). In the former case, *Halimedides* was associated with comparatively oligotrophic seafloors favouring an agrichnial/sequestrichnia behaviour. In the case presented here, the appearance of *Halimedides* in the Asturian Basin is clearly related to the reestablishment of oxic conditions in the bottom- and pore-waters, as indicated by geochemistry and the relatively abundant and diverse trace fossil assemblage (*Arenicolites*, *Chondrites*, *Diplocraterion*, *Halimedides*, *Planolites*, and *Thalassinoides*) after the upper black shale interval (Figs. ÍII.2, ÍII.7). The inferred relationship between the *Halimedides* of the Asturian Basin and the increasing in oxygen conditions agrees with previous research of *Halimedides* in oceanic anoxic event intervals: specially with the T-OAE in the Posidonia Shales (S. Germany, Brenner & Seilacher 1978), where *Halimedides* is found at the top of a "bituminous shale" level, just like in the Lastres section, and with the case presented in Kotlarczyk & Uchman (2012) (Oligocene, Polish Carpathians), where *Halimedides* specimens occur marking an improvement in oxygenation. This also agree with data from the early Aptian, OAE-1a (Lehmann et al. 2016) and the late Cenomanian, OAE-2 (Uchman et al. 2013a), where *Halimedides* disappear just before the oxygen depletion.

Orientation of the specimens in two main directions (N124E and N166E) (Fig. ÍII.6), could be related with the bottom water currents, as interpreted in previous studies (Rodríguez-Tovar et al. 2019).

5. CONCLUSIONS

The study of two sections (Rodiles and Lastres) in the Asturian Basin revealed the presence of several *Halimedides* specimens related to the T-OAE. Because they occur just over the upper black shale levels representing the end of the event, they reveal a close relationship with the reestablishment of oxic conditions after the anoxic event. The occurrence of some trace fossils during the T-OAE is followed by a more diverse

ichnoassemblage, indicating the reestablishment of favourable conditions for the tracemaker community. Such findings are in line with previous works proposing a link between oxygenation and the record of *Halimedides* associated to anoxic events (e.g., T-OAE, OAE-1 and OAE-2).

Analysis of morphometric features of the studied *Halimedides* reveals a tentative relationship with sedimentological and geochemical data, with larger, densely chambered specimens registered in dark, poorly oxygenated facies, and smaller, sparsely chambered specimens, mainly occurring in lighter, well oxygenated sediments.

Acknowledgments

CHAPTER IV

PALAEOENVIRONMENTAL DYNAMICS DURING THE TOARCIAN: GLOBAL VS LOCAL TRIGGERS

Euxinia and hydrographic restriction in the Tethys Ocean: Reassessing global oceanic anoxia during the early Toarcian

Javier Fernández-Martínez [a], Francisca Martínez Ruíz [b], Francisco J. Rodríguez-Tovar [a], Laura Piñuela [c], José C. García-Ramos [c], Thomas J. Algeo [d, e, f]

[a] *Departamento de Estratigrafía y Palaeontología, Universidad de Granada, Granada, Spain*

[b] *Instituto Andaluz de Ciencias de la Tierra CSIC-UGR, Granada, Spain*

[c] *Museo del Jurásico de Asturias (MUJA), Colunga, Asturias, Spain*

[d] *State Key Laboratory of Geological Processes and Mineral Resources, China University of Geosciences, Wuhan 430074, China*

[e] *State Key Laboratory of Biogeology and Environmental Geology, China University of Geosciences, Wuhan 430074, China*

[f] *Department of Geosciences, University of Cincinnati, Cincinnati, OH 45221-0013, USA*

ABSTRACT

Despite carbon-cycle perturbations at a global scale during the Early Toarcian, the extent of anoxia during the ~182 Ma Toarcian Oceanic Anoxic Event (T-OAE) remains in debate. A common factor in the development of oceanic anoxia is watermass restriction, which is thought to have been important in the NW European Seaway, but whose influence elsewhere is relatively unstudied. Here, we analyze Mo/TOC (a proxy for watermass restriction) and redox proxies (e.g., C_{org}/P) in two sections of the Asturian Basin (northern Iberian Palaeomargin), and we integrate these results with data from a suite of global Toarcian sections in order to reassess the relationship of euxinia and local hydrographic restriction during the T-OAE. The Asturian Basin study sections accumulated in oxic to dysoxic waters, punctuated by two episodes of intermittently euxinic bottomwaters or porewaters around the *Tenuicostatum/Serpentinum* zonal boundary. This area was an unrestricted carbonate ramp during the T-OAE that was not sufficiently reducing for its Mo/TOC ratios (2.3-4.5) to accurately record the degree of watermass restriction. Regionally, Lower Toarcian black shales exhibit elevated Mo and TOC concentrations (21-42 ppm Mo, 12-18% TOC) along with exceptionally low $m_{Mo/TOC}$ (e.g., ~0.3 in the Paris Basin, ~0.4 in the Cleveland Basin, and ~2.0 in the Qiangtang Basin), providing evidence of highly restricted, euxinic bottomwaters in Northwestern (epicontinental intrashelf troughs) and Eastern (barrier-lagoon) Tethyan settings. In contrast, in other basins across the SW Tethys and Panthalassic oceans, low contents of Mo and TOC (mostly <5 ppm Mo, <3% TOC) indicate unrestricted watermass conditions and at most intermittent bottomwater or porewater euxinia in pelagic to hemipelagic environments, although intermittently euxinic bottomwaters developed also in deep open-marine settings. The results of our analysis support both (1) a major role for hydrographic restriction in modulating the local expression of the T-OAE in various regions globally, and (2) a substantial drawdown of aqueous Mo in the global ocean during the T-OAE, indicating that existing hypotheses regarding the nature of the T-OAE event are not mutually exclusive.

KEY WORDS

1. INTRODUCTION

During the Early Toarcian (*ca.* 183 to 174 Ma; Early Jurassic), massive atmospheric inputs of volcanogenic CO_2 led to climatic warming, sea-level rise, and widespread deposition of black shales. This event, known as the Toarcian Oceanic Anoxic Event (T-OAE) (Jenkyns, 1985), represents a major perturbation to the global carbon cycle expressed as a negative carbon isotopic excursion (NCIE) that has been linked to release of isotopically light carbon from the Karoo, Ferrar, and Chon Aike Large Igneous Provinces (Percival et al., 2015; see NCIE review by Remírez & Algeo, 2020a). This event was associated with the release of greenhouse gases (e.g., CO_2, CH_4) that drove global warming, a rise in sea-surface temperatures, dissociation of seafloor methane clathrates, wetland methanogenesis, permafrost and glacier destabilization, and a global sea-level transgression during the T-OAE (Kemp et al., 2005; McElwain et al., 2005; Krencker et al., 2019; Ruebsam et al., 2019, 2020a). The T-OAE was also associated with widespread deposition of organic-rich black shales in marine settings, reflecting extensive development of bottomwater anoxia/euxinia (e.g., Wignall et al., 2005). These environmental changes contributed to a marine biocrisis that severely impacted many animal clades including ammonoids, belemnites, foraminifera, brachiopods, calcareous nannofossils, and ostracods (e.g., Raup & Sepkoski, 1984; Sepkoski, 1996; Dera et al., 2010, 2011; Jiang et al., 2020), and that also markedly altered endobenthic faunal dynamics (see review by Rodríguez-Tovar, 2021).

The present work intends to address one of the main debates concerning the T-OAE, which is the cause of exceptionally low molybdenum (Mo) concentrations in many Lower Toarcian black shales deposited during this event and, specifically, their relationship to local hydrographic restriction versus expanded global-ocean euxinia. Two competing models have been proposed to account for observations of low Mo concentrations in T-OAE black shales, one invoking aqueous Mo drawdown at a local scale, and the other aqueous Mo drawdown at a global scale. In the 'local restriction model' (McArthur et al., 2008; McArthur, 2019; Remírez & Algeo, 2020b), bottomwaters within silled, semi-restricted marine basins, especially those in NW Europe, became Mo-depleted owing to strong Mo uptake by the sediment under extremely euxinic conditions, i.e., the 'basin reservoir effect' of Algeo & Lyons (2006). Alternatively, the 'global drawdown model' (Thibault et al., 2018; Kemp et al., 2022) invokes Mo drawdown throughout the world's oceans owing to widespread deposition of anoxic black shales, generating low-Mo seawater globally (cf. Algeo, 2004). Evaluation of these models has been hampered by the fact that most research on the T-OAE has been undertaken in the NW European region, focused on a few basins in which local watermass euxinia prevailed during the Early Toarcian.

One testable aspect of this debate is whether sea levels were stable (or fell) during the T-OAE, favoring the local restriction hypothesis (because of increased watermass restriction in marginal-marine basins), or whether they rose during this event, favoring the global drawdown hypothesis (because of reduced restriction in such basins). Remírez & Algeo (2020b) tested this for the Early Toarcian Cleveland Basin (U.K.) by analyzing B/Ga as a palaeosalinity proxy (cf. Wei & Algeo, 2020), demonstrating a shift from high-brackish or marine conditions prior to the T-OAE to low-brackish conditions during that event. The sharp reduction in the salinity of the Cleveland Basin watermass during the T-OAE could have been achieved only through either sea-level fall (reducing overspill from adjacent marine areas) or increased humidity and freshwater runoff (e.g., combined with minimal sea-level change), thus providing strong support for the development of local watermass restriction, at least in the Cleveland Basin (Remírez & Algeo, 2020b). However, the validity of the 'local restriction model' in a regional context does not preclude the possibility of drawdown of seawater Mo concentrations at a global scale during the T-OAE.

The key test of global seawater Mo drawdown would be application of the Mo/TOC proxy (Section 2) to evaluate watermass restriction in basins outside the NW European region. This test has been difficult to conduct due to the paucity of anoxic facies in other regions globally, but a recent study of a Japanese deep-ocean section has yielded new evidence supporting global seawater Mo drawdown in non-Tethyan regions (Kemp
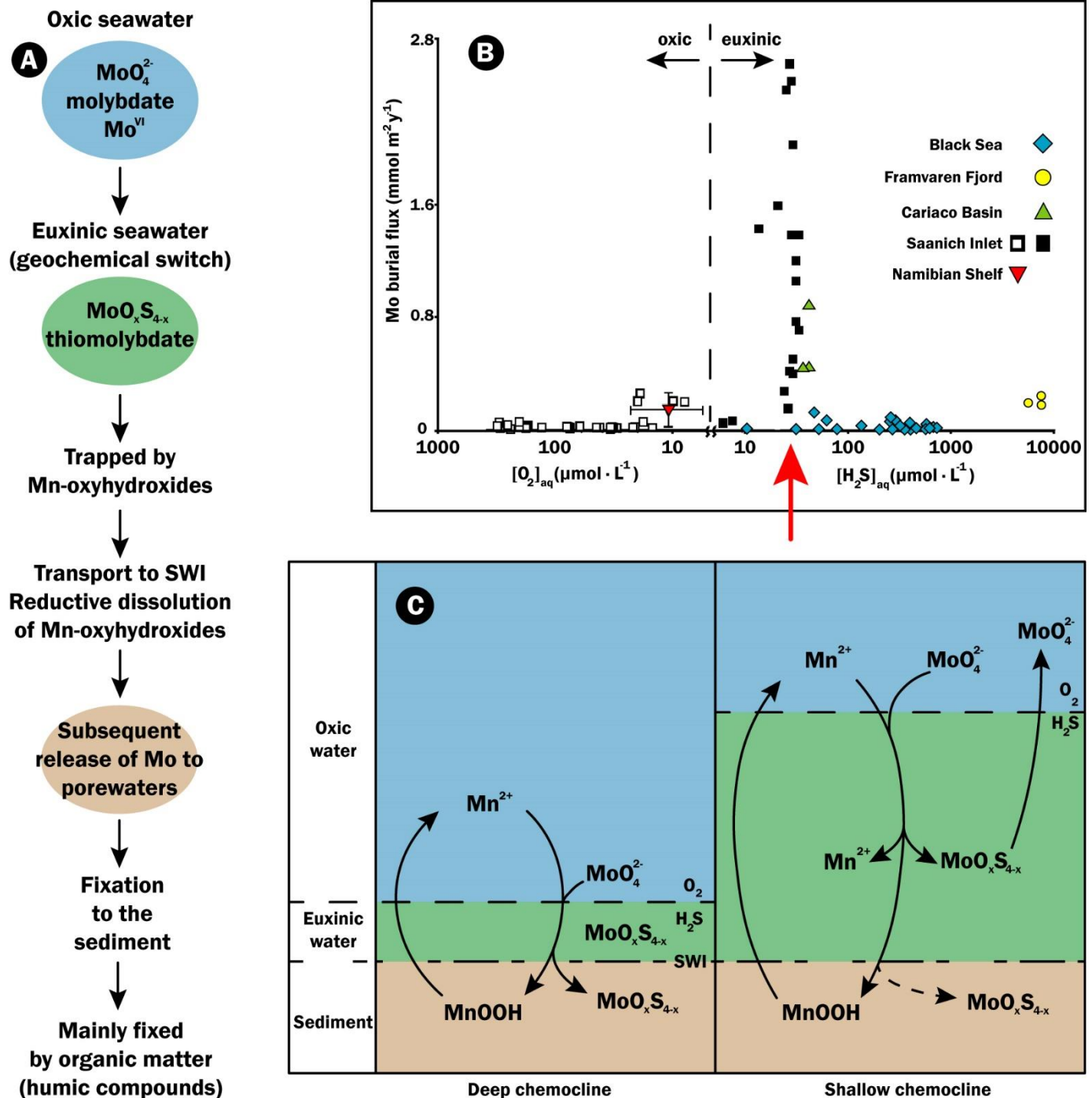
Figure IV.1. (A) Molybdenum ideal path from oxic seawater to its fixation in the sediment. (B) Diagram showing the O_2/H_2S concentration in relation with Mo burial flux. Red arrow indicates the geochemical switch (euxinia increments to the right). (C) Scheme showing the influence of the chemocline depth in the Mo transport from the column water to the sediment (modified from Algeo and Tribovillard, 2009). Note that deeper chemoclines, even providing smaller reactive-Mo reservoirs, facilitate the Mo sequestration from the seawater to the sediment via Mn redox cycle. A shallow chemocline, on the contrary, eases the return of sequestrated Mo to the water column. SWI: sediment/water interface.

et al., 2022). In this context, we generated new Mo/TOC and auxiliary geochemical data for two sections (Lastres and Rodiles) in the Asturian Basin of northern Spain, which was located on the southern perimeter of the NW European Sea and, thus, affords a window into marine environmental changes in the open Tethys Ocean (Section 3). In addition, we compiled Mo/TOC and auxiliary geochemical data from 16 other basins (20 sections) with a wide palaeogeographic distribution, located both around the margins of the

Tethys Ocean (Northwestern, Southwestern, and Eastern Tethyan regions) and in the Panthalassic Ocean (Northern, Central, and Southern Panthalassic regions) (Section 4), and we evaluated the full Mo/TOC dataset for evidence of regional (i.e., watermass restriction) versus global (i.e., seawater Mo concentration) controls on sediment Mo/TOC (Section 5). This meta-analysis provides new insights into Mo patterns during the T-OAE and permits a test of the 'global drawdown hypothesis'.

2. THE Mo/TOC PROXY FOR WATERMASS RESTRICTION

Black shales and other organic-rich sediments are commonly characterized by high concentrations of molybdenum, a well-studied trace metal that is authigenically enriched in the sediment under sulfidic (i.e., euxinic) conditions (Helz et al., 1996). In oxic facies, molybdenum is present mainly as the stable, behaviorally conservative molybdate ion (MoO_4^{2-}), which is relatively abundant ($\sim$105 nmol·kg^{-1}) and has a long residence time in seawater (estimates range from 440 kyr to 870 kyr) (Algeo & Lyons, 2006; Miller et al., 2011; Algeo & Rowe, 2012). The transformation from stable molybdate to highly-reactive, scavenging-prone thiomolybdates (MoO_xS_{4-x}; $x = 0$-3) begins when there is sufficient free hydrogen sulfide in the water column, at a threshold termed a 'geochemical switch' (Helz et al., 1996). This transformation, which preserves the hexavalent form of Mo, occurs only if HS$^-$ or H$_2$S is present; alternatively, Mo(VI) can be reduced to Mo(IV) in the presence of polysulfide ions (S_n^{2-}) or molecular sulfur (S_8) (Vorlicek et al., 2004). These reactions lead to fixation of Mo in the sediment, at or just below the sediment/water interface (SWI), by diverse pathways controlled by sulfide, which renders molybdenum concentrations a valuable proxy for euxinic conditions (Fig. IV.1A). In modern restricted basins with euxinic bottomwaters, the geochemical switch is commonly activated under weakly euxinic conditions ($\sim$10-50 µmol H$_2$S·L^{-1}) (Algeo & Lyons, 2006) (Fig. IV.1B).

Organic matter is the main host of sedimentary Mo, but other compounds can play a complementary role in Mo uptake by the sediment. The manganese redox cycle can help to transfer Mo to the sediment (Fig. IV.1C) through oxidation of Mn^{II} to Mn^{IV}-oxyhydroxides (MnOOH) at the chemocline; Mo is then readily transported to the sediment/water interface via a particulate shuttle (Algeo & Tribovillard, 2009; Scholz et al., 2013). As aqueous Mo fixation requires sulfidic waters, the chemocline position also acts as an important control on Mo uptake by the sediment, with reductive dissolution of Mn-particulates and release of adsorbed Mo to the water column more likely as chemocline height above the seafloor increases (Fig. IV.1C). Particulate shuttles tend to lead to greater enrichment of Mo in relation to other trace metals, and its effect is inhibited in persistently sulfidic bottomwaters but enhanced when basinal euxinia is seasonal and chemocline depth fluctuates (Anderson & Devol, 1973; Algeo & Lyons, 2006).

Because authigenic Mo is taken up primarily by the organic fraction of the sediment (although uptake by sulfides is also possible; Vorlicek et al., 2004), sediment Mo concentrations are generally normalized to total organic carbon (i.e., Mo/TOC) in order to evaluate changes in seawater Mo removal to the sediment (Algeo & Lyons, 2006; Algeo & Rowe, 2012). Changes in Mo removal rates to the sediment in anoxic facies, in which uptake of aqueous Mo is quantitative or nearly so, generally reflect changes in watermass Mo concentrations. However, a change in Mo/TOC at a single site might be due either to local/regional changes in watermass chemistry within a restricted basin (e.g., Algeo et al., 2007; Rowe et al., 2008; Zhang et al., 2017) or to global changes in seawater Mo concentrations (e.g., Algeo, 2004; Scott et al., 2008; Hetzel et al., 2009; Goldberg et al., 2016), with effective demonstration of the latter (global) mechanism requiring identification of similar coeval declines in sediment Mo/TOC in multiple basins.

The study of black shale deposits associated with the T-OAE using well-established proxies such as the relationship between Mo and TOC (i.e., Mo/TOC, which is reported in units of ppm/%·10^{-4}; Algeo & Lyons, 2006; Algeo & Rowe, 2012) has the potential to provide insight into the causes of low-Mo facies of Early

Toarcian age. Mo drawdown at a local scale is generally linked to the 'basin reservoir effect' described by Algeo and Lyons (2006), which is modulated by watermass renewal time (n.b., the same effect can operate at a global scale if Mo removal rates to euxinic facies are sufficiently high; Algeo, 2004). When a basinal connection with the open ocean (the main source of aqueous Mo) is inhibited, the rate of Mo sequestration in the sediment can exceed its replenishment in the water column, causing a long-term decrease in both aqueous and authigenic sedimentary Mo concentrations. In a restricted basin, the onset of euxinia in bottomwaters will transiently enhance the Mo flux to the sediment but lead to depletion of the aqueous Mo reservoir, causing a long-term decline of sedimentary Mo concentrations (cf. figure 9 of Algeo and Lyons, 2006). In a Mo versus TOC crossplot, the regression-line slope ($m_{Mo/TOC}$) can be used to estimate the degree of hydrographic restriction of a palaeo-depositional basin (Algeo & Lyons, 2006; Algeo & Rowe, 2012). Calibration to modern euxinic settings yields $m_{Mo/TOC}$ of ~4.5 for strongly restricted basins (e.g., Black Sea), ~9-25 for moderately restricted basins (e.g., Framvaren Fjord and Cariaco Basin), and ~45 for minimally restricted basins (e.g., Saanich Inlet). In modern settings, $m_{Mo/TOC}$ is also correlated with both deepwater Mo concentrations ($[Mo]_{aq}$) and renewal time ($\square$). As $m_{Mo/TOC}$ becomes smaller, deepwater $[Mo]_{aq}$ decreases linearly from ~100 nmol/L to <5 nmol/L and $\square$ increases log-linearly from <10 yr to >500 yr.

The parameter $m_{Mo/TOC}$ is subject to some limitations in its application as a watermass restriction proxy. In open settings such as continental margins subject to upwelling (e.g., the Namibian Shelf), anoxic bottomwaters may lead to high TOC combined with low Mo contents, resulting in low $m_{Mo/TOC}$ (Algeo & Lyons, 2006). In these environments, the lack of a marginal sill prevents formation of a stable redoxcline, allowing only limited enrichments of authigenic sedimentary Mo as a result of highly fluctuating redox conditions at the SWI. Thus, low $m_{Mo/TOC}$ in such settings is not indicative of strong watermass restriction. This consideration underscores the need to combine Mo-TOC restriction analysis with auxiliary geochemical and sedimentological data that assess the redox conditions of a palaeodepositional system in order to properly constrain the hydrodynamics of the basin under investigation.

3. CASE STUDY OF ASTURIAN BASIN T-OAE SECTIONS

3.1. Geological background

As a case study of the Toarcian OAE, two sections were selected, Lastres and Rodiles, in the Jurassic Asturian Basin (AB in Fig. IV.2A). Both sections are located in cliffs along the Asturian coast of northern Spain (Fig. IV.2C): one on the northern part of Lastres beach (43°30'41.2"N 5°16'06.2"W) and the other on the eastern part of Rodiles beach (43°32'19.7"N 5°22'25.5"W), ~9.5 km ESE of Lastres. Both sections are composed largely of alternating limestone and marl beds, but they contain two black shale beds at the *Tenuicostatum/Serpentinum* zonal boundary (Fig. IV.3), and the negative C isotope excursion associated with the T-OAE has been identified in this interval at Rodiles (Figs. IV.4 and S1) (Gómez et al., 2008; García Joral & Goy, 2009).

In the Early Jurassic, the Asturian Basin was on the northern Iberian Palaeomargin and formed an epeiric, homoclinal carbonate ramp grading proximally into more terrestrial facies yielding abundant reptile footprints, known as the 'Dinosaur Coast' (García-Ramos et al., 2006). Upper Sinemurian to Toarcian strata consist of mixed limestone and marl containing abundant invertebrate fossils such as ammonoids, belemnites, bivalves and brachiopods as well as marine reptiles such as plesiosaurs and ichthyosaurs, along with intercalated black shales (García-Ramos et al., 2006; Bardet et al., 2008). Located at ~35ºN palaeolatitude (Osete et al., 2011), the climatic conditions of the study area remain uncertain, with proposals ranging from warm-humid to semi-arid (e.g., van de Schootbrugge et al., 2005; Dera et al., 2009). The study sections belong to the Rodiles Formation, which is divided into two members: the Buerres Member, representing shallow subtidal facies, and the overlying Santa Mera Member, representing a more distal, deeper setting (Fernández-Martínez et al., 2021a, and references therein).
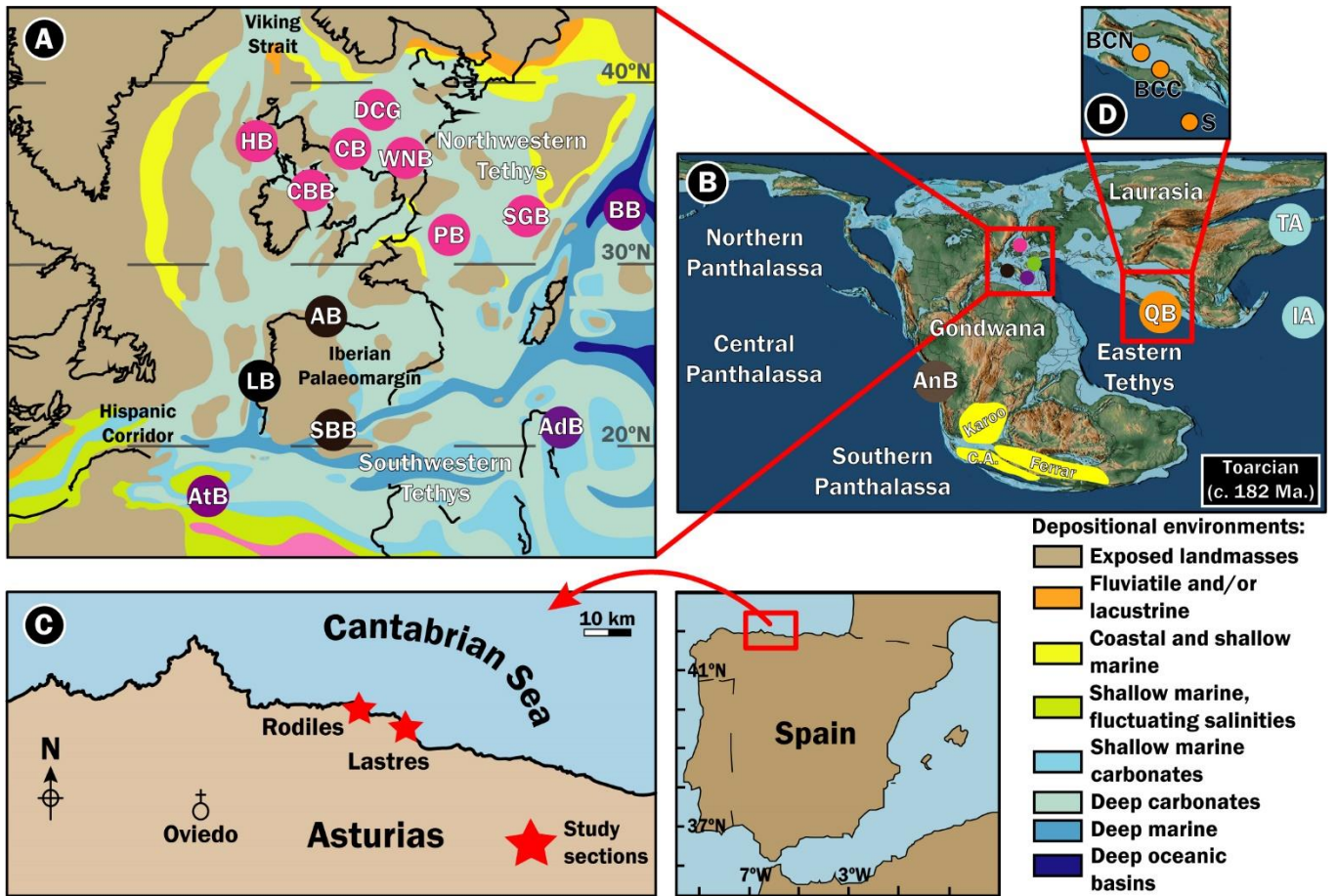
Figure IV.2. (A) Western Tethys map showing all the studied basins in the region (modified from Thierry et al., 2000). (B) Toarcian paleogeography indicating the area represented in (A), the situation of the basins in Panthalassic and east Tethys oceans, and the approximate extension of the Karoo, Ferrar, and Chon Aike Large Igneous Provinces (modified from Scotese et al., 2013; Percival et al., 2015). (C) Location of the study sections in the Asturian Basin, over the Iberian Peninsula (right) and the Asturian coast (left). (D) Map showing the distribution of the study sections in the Qiangtang Basin. C. A.: Chon Aike LIP; BCN: Bilong Co North; BCC: Bilong Co Central; S: Sewa.

Changes in ecological and depositional environmental conditions in the Asturian Basin during the T-OAE were investigated in recent sedimentological and ichnological studies (Fernández-Martínez et al., 2021a, b). Prior to this event (i.e., in the lower *Tenuicostatum* Zone, Fig. IV.4), abundant and diverse trace fossil associations in the limestone-marl succession indicate the existence of oxic conditions at both study sites (Bioturbation Index, BI = 3-6) (Taylor & Goldring, 1993). At the *Tenuicostatum/Serpentinum* zonal boundary (onset of T-OAE), an abrupt shift to anoxic conditions is recorded by two laminated (i.e., apparently unbioturbated, BI = 0) black shale beds. Between these beds, alternating light, bioturbated marls (BI = 5) and dark, mostly laminated marls (BI = 0-1) were deposited, reflecting fluctuations between oxic/dysoxic and euxinic conditions, being associated with sparse and absent

bioturbation, respectively. The overlying limestones and marls (i.e., upper *Serpentinum* Zone) show a recovery of diverse and abundant ichnoassociations (BI = 5-6), similar to those in the lower *Tenuicostatum* Zone, indicating a rapid recovery of habitable conditions for the endobenthic fauna. Therefore, in the Asturian Basin, the T-OAE is expressed as two black shale beds recording anoxia, separated by variably bioturbated marls indicating fluctuations between oxic/dysoxic and euxinic conditions (figure 12 in Fernández-Martínez et al., 2021a).

3.2. Methods

The Rodiles and Lastres sections were analysed and sampled bed-by-bed, yielding 51 samples (28 from Rodiles, and 23 from Lastres) of ~5 g each, collected at intervals of 4 to 6 cm in each section. The rock samples

	Mediterranean	Submediterranean	Subboreal	Japan	Chile	
Middle Toarcian	*Bifrons* (B)	*Bifrons* (B)	*Bifrons* (B)		*Largaense* (La)	
Lower Toarcian	*Levisoni* (Le)	*Serpentinum* (Se)	*Falciferum* (F)	*Inouyei* (I)	*Hoelderi* (Ho)	NCIE
	Polymorphum (Po)	*Tenuicostatum* (T)	*Tenuicostatum* (T)	*Helianthoides* (He)	*Tenuicostatum* (T)	
				Paltus (Pa)		
Upper Pliensb.	*Emaciatum* (E)	*Emaciatum* (E)	*Spinatum* (Sp)	*Japonica* (J)	*Spinatum* (Sp)	

Figure IV.3. Biostratigraphic framework illustrating the equivalences of ammonite zonations among the different domains covering the studied basins. Note the approximate extension of the negative C-isotopic excursion (NCIE) in blue. The Mediterranean and Submediterranean domains include the Atlassic, Adriatic, Subbetic, Asturian, Lusitanian and Paris basins; the Subboreal domain includes the Cleveland, West Netherlands, Hebrides, Cardigan Bay and Belluno basins and the Dutch Central Graben; the Chilean domain consists of the Andean Basin; and the Japanese domain consists of the Toyora Area. Pliensb.: Pliensbachian.

were trimmed to remove the exposed surfaces and pulverized in an agate mortar for geochemical analysis.

Molybdenum concentrations were measured with an ICP-MS (NexION 300D) using certified standards (BR-N, GH, DR-N, UB-N, AGV-N, MAG-1, GS-N, and GA) for calibration. The sample powder was digested with HNO_3 and HF in a Teflon vessel for 30 minutes, under high pressure and temperature (~200 psi, ~180°C) until complete dissolution. Subsequently, the solution was evaporated to dryness and the residue redissolved in 100 mL of HNO_3 (4 vol. %), and then measured in triplicate at the Analytical Facilities of the University of Granada (Centro de Instrumentación Científica, CIC). Precision was ±2 % and ±5 % rel. for analyte concentrations of 50 ppm and 5 ppm, respectively.

Organic matter content was measured by RockEval pyrolysis at the Institute of Earth Sciences at the University of Lausanne, Switzerland. The process consists in measuring hydrocarbons, CO, and CO_2 during the decomposition of organic matter and carbonate minerals (Ordoñez et al., 2019). Samples are freeze-dried and homogenized in a mortar, introduced in Incoloy crucibles, and analysed in a Vinci Technologies pyrolyser model Rock-Eval 6. The first pyrolysis step (to 200 °C) yielded the bulk of TOC content (S1). Subsequent stepwise heating of the samples to 650 °C yielded additional free and complex hydrocarbons and

kerogen through cracking (S2), along with concurrent release of CO and CO_2 (S3). Finally, the samples were heated again from 300 °C to 850 °C in order to calculate the residual amount of TOC (S4).

The enrichment factor (EF) of Mo was calculated as $Mo_{EF} = [(Mo/Al)_{sample} / (Mo/Al)_{PAAS}]$, using Post-Archean Australian Shale (PAAS) from Taylor and McLennan (1985). The geochemical data for the non-Asturian sections utilized in this study were obtained from the literature (Table IV.1) and are available in the supplementary material of this study (Table S1). For $m_{Mo/TOC}$ values, confidence intervals (*p* values) were calculated by "t tests for equal means", using the PAST software, and standard errors were calculated in Excel.

3.3. Results

The TOC and Mo profiles of the two study sections are similar, with the highest values in the black shale beds. TOC ranges from 0.32% to 2.05% (median 0.67%) at Rodiles and from 0.40% to 2.34% (median 1.09%) at Lastres (*n.b.*, all ranges represent the 16th to 84th percentiles of a distribution in order to avoid the influence of outliers). Mo concentrations before and after the T-OAE are <1 ppm (i.e., near PAAS), but rise to 3-5 ppm (maximum 18 ppm) in the event-linked black shale beds (Table IV.2).

Mo/TOC differs between the TOC-impoverished light marls and limestones versus the organic-rich dark marls and black shales (Fig. IV.4). In
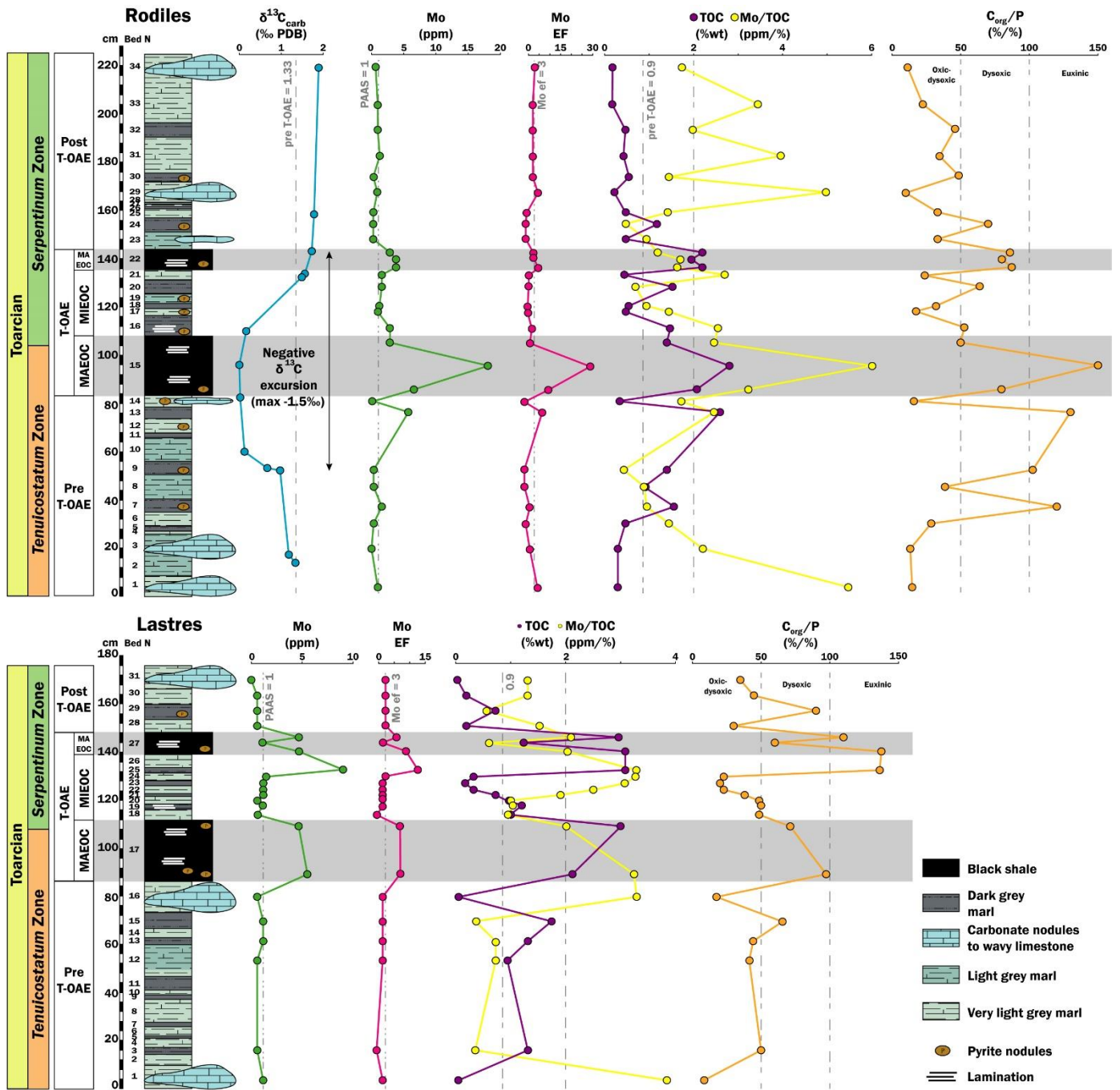
Figure IV.4. Stratigraphic columns of the Rodiles and Lastres sections, in the Asturian Basin, indicating pre-, post-, and T-OAE stages regarding its biological and sedimentological effects (Fernández-Martínez et al., 2021a), showing lithology, and ammonite zonations. TOC, Mo, MoEF, Mo/TOC and Corg/P values are from this work and Rodiles isotopic ^{13}C values from Gómez et al. (2008). Note dashed lines, indicating background values or redox thresholds. Bed N: Bed number; MAEOC: Major episode of oxygenation crisis; MIEOC: Minor episodes of oxygenation crisis.

Rodiles, Mo/TOC ratios range from 2.38 to 5.31 (median 3.87) in limestones and from 1.22 to 3.83 (median 1.68) in light grey marls, while dark marls and black shales show lower ranges of 0.89 to 2.36 (median 1.29) and 1.51 to 3.86 (median 2.06) respectively. Similar results are obtained in the Lastres section, where limestones exhibit a range of 1.81 to 3.32 (median 2.87)

and light grey marls from 0.73 to 2.03 (median 1.19), while dark grey marls and black shales yield values even lower than in the Rodiles section, ranging from 0.62 to 2.38 (median 0.89) and from 1.28 to 2.17 (median 1.69) respectively.

The regression slopes ($m_{Mo/TOC}$) show differences between the pre-, syn- and post-event intervals (Fig.
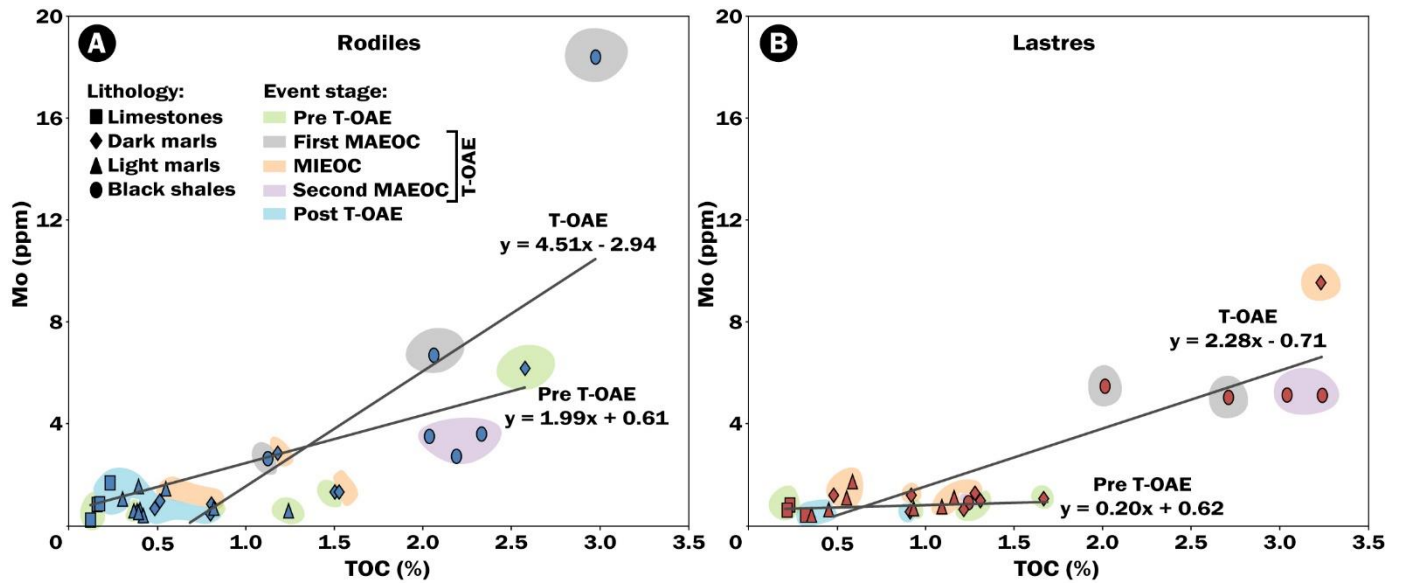
Figure IV.5. Mo (ppm) versus TOC (%) crossplots for the Asturian Basin, showing its regression slopes for pre- and syn-T-OAE stages: Rodiles (A) and Lastres (B). Different event-linked stages are colored after Fernández-Martínez et al., 2021a. MAEOC: Major episode of oxygenation crisis; MIEOC: Minor episodes of oxygenation crisis.

IV.5, Table IV.2). For the T-OAE event interval, $m_{Mo/TOC}$ values are 4.5 ± 1.4 ($r = +0.73$; $p < 0.01$; $n = 11$) at Rodiles and 2.3 ± 0.4 ($r = +0.88$; $p < 0.01$; $n = 13$) at Lastres. The pre-event strata show lower $m_{Mo/TOC}$ values: 2.0 ± 0.5 ($r = +0.85$; $p < 0.01$; $n = 8$) at Rodiles, and 0.20 ± 0.13 ($r = +0.62$; $p \sim0.32$; $n = 6$) at Lastres. The post-T-OAE strata exhibit non-significant Mo-TOC correlations (Table IV.3). During the pre- and post-event stages, low TOC contents led to variable but frequently high Mo/TOC ratios. During the T-OAE, black shales also show high Mo/TOC ratios, but in this case linked to higher Mo and TOC contents. Profiles for Mo and TOC at Rodiles and Lastres exhibit a distinctive pattern (Fig. IV.5) associated with the 'basin reservoir effect' (cf. figure 9 in Algeo & Lyons, 2006). Note that, at Rodiles, Mo enrichment begins just before black shale deposition, in a dark marl bed (Fig. IV.4).

In order to interpret the significance of Mo/TOC ratios, the redox conditions of each lithology must be determined. C_{org}/P (%/%) was used as a redox proxy, with established ranges for oxic (<50), dysoxic (50-100), and euxinic facies (>100) (Algeo & Ingall, 2007; Algeo & Li, 2020). This proxy shows similar profiles for the two study sections (Fig. IV.4). Below the T-OAE, light-coloured marls and limestones yield values <50 whereas dark-coloured marls yield values between 50 and 100, implying fluctuations between oxic and

dysoxic conditions. Within the T-OAE interval, the two black shale beds yield the highest C_{org}/P values (~80-150), and marls yield variable values depending on TOC content (dark marls >50 and light marls <50). Above the T-OAE, nearly all beds yield low C_{org}/P values (< 50).

3.4. Interpretation

The two organic-rich black shale beds of the T-OAE interval accumulated under relatively reducing conditions, whereas the light grey marl between them was associated with oxic conditions. This pattern demonstrates the intermittent nature of euxinia within the Asturian Basin during the T-OAE. This interpretation is supported by the ichnoassemblage present in the marls, which is dominated by the ichnogenus *Chondrites*, reflecting an opportunistic endobenthic fauna (Fernández-Martínez et al., 2021a, b). Similar 'brief intervals of oxygenation', attributed to tropical storms, were noted by McArthur et al. (2008) and Röhl et al. (2001) in the Cleveland Basin (Yorkshire coast) and the South German Basin (Dotternhausen section), respectively.

T-OAE strata of the Asturian Basin show moderate authigenic Mo enrichment and variable $m_{Mo/TOC}$, i.e., 4.5 ± 1.4 at Rodiles ($r = +0.73$; $p < 0.01$; $n = 11$) and 2.3 ± 0.4 at Lastres ($r = +0.88$; $p < 0.01$; $n = 13$). These low values nominally imply either strong basinal watermass restriction, approximately equivalent

Palaeoregion	Basin	Abbreviation	Section	Black shale deposits?	Euxinic conditions?	References
Northwestern Tethys	Cleveland Basin	CB	Yorkshire coast	Yes	Yes	McArthur *et al.*, 2008
	West Netherlands Basin	WNB	Well Rijswijk-1	Yes	Yes	Dickson *et al.*, 2017; Houben *et al.*, 2021
	Dutch Central Graben	DCG	Well F11-01	Yes	Yes	
	South German Basin	SGB	Dotternhausen	Yes	Yes	Dickson *et al.*, 2017
	Paris Basin	PB	ANDRA EST433 borehole	Yes	Yes	Lézin *et al.*, 2013
	Cardigan Bay Basin	CBB	Mochras borehole	No	No	Percival *et al.*, 2016
	Hebrides Basin	HB	Raasay	Yes	Yes	Chen *et al.*, 2021
Southwestern Tethys	Atlassic Basin	AtB	Ratnek El Kahla	No	Yes	Ruebsan *et al.*, 2020b
	Adriatic Basin	AdB	Kovk	No	Yes	Ettinger *et al.*, 2021
	Belluno Basin	BB	Dogna core	Yes	Yes	Bellanca *et al.*, 1999 Dickson *et al.*, 2017
Southwestern Tethys (Iberian Palaeomargin)	Subbetic Basin	SBB	Fuente de la Vidriera	No	No	Rodríguez-Tovar and Reolid, 2013
	Lusitanian Basin	LB	Peniche	No	Yes	Fantasia *et al.*, 2019
	Asturian Basin	AB	Lastres, Rodiles	Yes	Yes	This work; Fernández-Martínez *et al.*, 2021a, b
Eastern Tethys	Qiangtang Basin	QB	Bilong Co North	Yes	Yes	Xia and Mansour, 2022
			Bilong Co Central	Yes	Yes	Fu *et al.*, 2017
			Sewa	No	No	Fu *et al.*, 2021
Southern Panthalassa	Andean Basin	AnB	El Peñón	No	No	Fantasia *et al.*, 2018a
Northern Panthalassa	Toyora Area	TA	Sakuraguchi-dani succession	No	No	Kemp and Izumi, 2014
Central Panthalassa	Inuyama Area	IA	Sakahogi section	Black chert	Yes	Kemp *et al.*, 2022

Table IV.1. Data of analyzed sections, their abbreviations, and references.

to that of the modern Black Sea (Algeo & Lyons, 2006; Algeo & Rowe, 2012), or severe global seawater Mo drawdown (cf. Algeo, 2004; Hetzel et al., 2009). However, the Mo contents of the event-related black shales are modest (3-18 ppm) and not consistent with completely euxinic bottomwater conditions but, rather, only with euxinia in sediment porewaters. During the T-OAE, bottomwaters in the Asturian Basin are likely to have been dysoxic or intermittently euxinic, based on the Mo concentration thresholds of Scott & Lyons (2012). This redox interpretation agrees with the C_{org}/P proxy data (Fig. IV.4). Because watermass redox conditions were insufficiently reducing (cf. Algeo & Lyons, 2006; Algeo & Rowe, 2012), the Mo/TOC proxy is unlikely to offer a reliable assessment of hydrographic restriction of the Early Toarcian Asturian Basin.

4. META-ANALYSIS OF Mo/TOC IN GLOBAL T-OAE SECTIONS

In order to more robustly evaluate the hydrographic significance of Mo/TOC ratios in multiple basins with a wide palaeogeographic distribution, it is first necessary to understand their depositional environments and redox characteristics. Here, we provide geological background to the 16 other (i.e., non-Asturian) basins examined in this study (Section 4.1), and we summarize their redox characteristics (Section 4.2) and sediment Mo/TOC patterns (Sections 4.3.1 to 4.3.3). We then evaluate redox versus hydrographic controls on the Mo/TOC records of each basin (Section 4.4).

4.1. Geological background

4.1.1. Palaeogeography and palaeo-environments

Our global Lower Toarcian database includes basins located within both the Tethyan and Panthalassic oceans. The majority of them are in the western Tethys, where we differentiate between the Northwestern Tethyan ($n = 7$) and Southwestern Tethyan ($n = 6$) regions, with smaller numbers of basins in the Eastern Tethyan ($n = 1$) and Panthalassic ($n = 3$) regions.

The western Tethyan sections (Table IV.1, Fig. IV.2A) cover a wide variety of depositional environments. The Northwestern Tethyan region was a broad epicontinental sea located between the Laurasian and Gondwanan landmasses dotted by several massifs. In this study, it is represented by five intrashelf troughs that are characterized by organic-rich black shale deposition (the Cleveland, West Netherlands, South German and Paris basins, and the Dutch Central Graben), and two other basins sited between present-day Ireland and Great Britain islands, close to the former Viking Strait, that were characterized by shallow, low-energy, open-marine settings in which black shale deposition was scarce or absent (Cardigan Bay and Hebrides basins; pink circles in Fig. IV.2). The Southwestern Tethyan region, which was located on the northern Gondwanan palaeomargin, is dominated by carbonate platform/ramp and slope/basinal settings but generally lacks black shale deposits (Atlassic and Adriatic basins) (purple circles). Three basins are located on the Iberian Palaeomargin (Asturian, Lusitanian and Subbetic basins) (black circles), whose northern margin comprises a carbonate ramp with black shales, and whose western and southern margins consist of hemipelagic and shallow carbonates lacking black shales. A third basin (Belluno Basin) with black shales interbedded within pelagic to hemipelagic carbonates deposited in a trough (purple circle, note that this section is located further north).

The Eastern Tethyan region is represented by three sections from a single basin (Qiangtang Basin) but deposited in different palaeoenvironments (Fig. IV.2D). Two sections contain an alternation of limestones and marls with interbedded black shales, deposited in a fluvio-deltaic or inner-shelf setting (Bilong Co North) and a barrier-lagoonal environment (Bilong Co Central).

The southern section (Sewa) represents an open-marine setting that accumulated silty and calcareous mudstone beds.

The Panthalassic Ocean is represented by shallow-marine sections that lack black shale, including one in the Southern Panthalassic region that consists mainly of limestone and marl (Andean Basin, Chile), and one in the Northern Panthalassic region that consists of mixed sand and mudstone deposits (Toyora Area, Japan). Finally, a deep-marine section in the Central Panthalassic region (Inuyama Area, Japan) is dominated by black chert (see Table IV.1 for summary).

4.1.2. Biostratigraphy, carbon isotopes, and global correlations

The biostratigraphic framework for the Late Pliensbachian to Middle Toarcian is based largely on regional ammonoid zonations (Fig. IV.3). The Subboreal domain, herein adopted as the key ammonoid reference area, contains the Late Pliensbachian *Spinatum* Zone, the Early Toarcian *Tenuicostatum* and *Falciferum* zones, and the Middle Toarcian *Bifrons* Zone. Ammonoid zonation schemes have also been developed for the Mediterranean, Submediterranean, Southern Panthalassic (Andean Basin), and Northern Panthalassic domains (Toyora Area), with zones based on different taxa but that can be readily correlated with their Subboreal domain equivalents (Fig. IV.3). The average duration of individual ammonoid biozones within the study interval is 1 to 3 Myr (Ogg, 2012). The T-OAE corresponds to the lower part of the *Falciferum* Zone. Its duration remains in debate, with estimates ranging from as low as 120 kyr to as high as 1200 kyr, with a median of 930 kyr (Remírez & Algeo, 2020b).

The T-OAE negative carbon isotopic excursion (NCIE) is regarded as commencing at the *Tenuicostatum/Falciferum* zonal boundary and terminating within the *Falciferum* Zone (Fig. IV.6, Fig. S1). The NCIE shows regional variation in magnitude, being larger in the Northwestern Tethyan (~7‰) and Northern Panthalassic (~6‰) regions relative to the other regions considered here. In most sections, the NCIE shows a symmetric pattern (i.e., the two limbs of the excursion are of subequal thickness) with smaller-magnitude
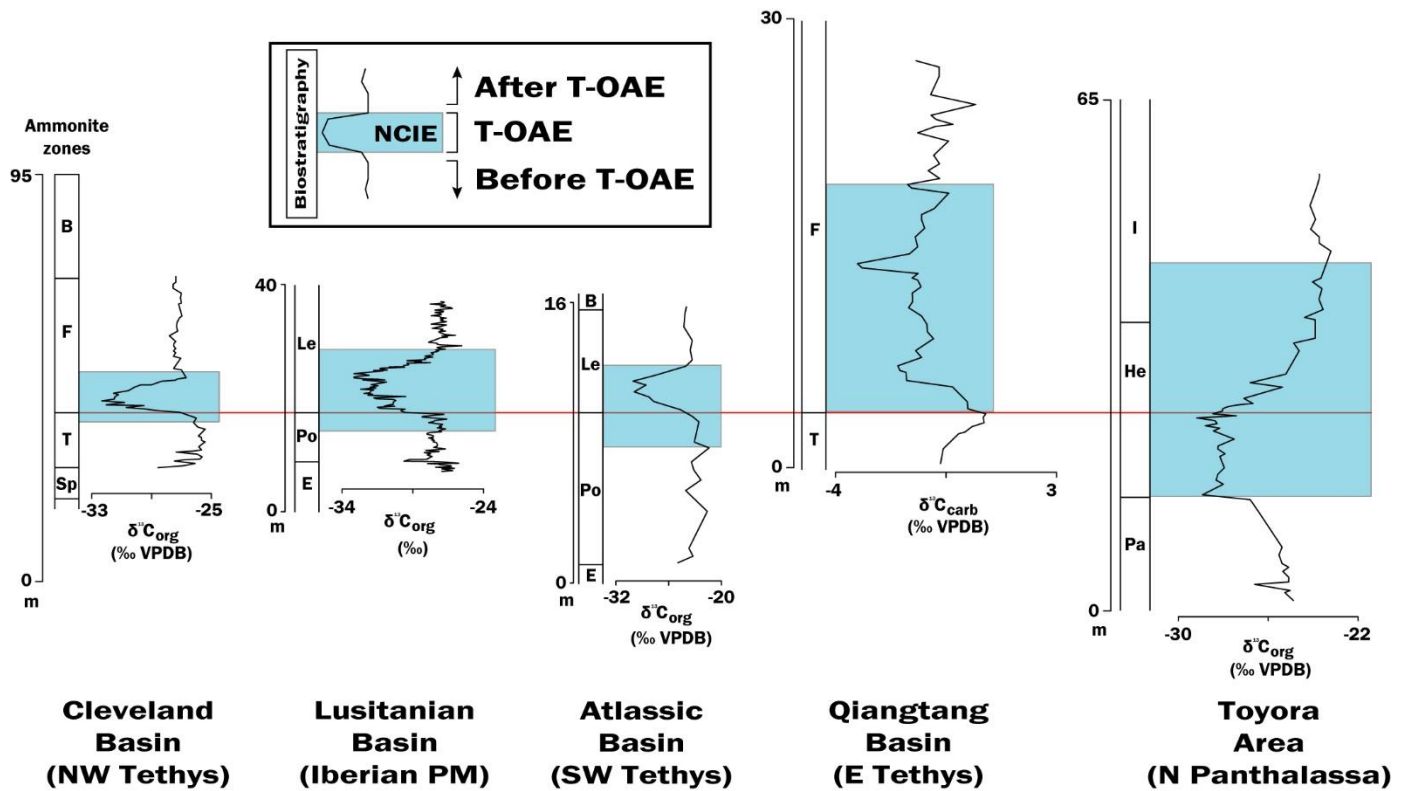
Figure IV.6. Correlation, on top of the Tenuicostatum or Polymorphum zones (red line), of the negative isotopic C excursion (NCIE) in selected basins, grouped by paleoregion. Note the variable duration of the NCIE regarding ammonite biozonation. As a response to a global effect, the NCIE probably evidences the asynchronicity of ammonoid biozonation in each basin. Abbreviations for ammonite zones are in Fig. IV.3, data obtained from references in Table IV.1. Pre-, syn- and post- T-OAE (i.e., NCIE) stages are indicated. PM: Paleomargin.

perturbations overprinting the main excursion (Fig. S1). However, some sections show thinning or truncation of either the falling (lower) or rising (upper) limb of the NCIE: (1) the West Netherlands Basin lacks the falling limb, indicating non-deposition during the early T-OAE interval, (2) the Dutch Central Graben lacks the rising limb, indicating non-deposition during the late T-OAE interval, (3) the Belluno and Qiangtang (Central) basins and the Toyora Area exhibit a thinner falling limb and thicker rising limb, reflecting slowed sedimentation prior to the excursion minimum, and (4) the Paris, Hebrides and Andean basins as well as the Central Panthalassa (Inuyama) exhibit a thicker falling limb and thinner rising limb, reflecting slowed sedimentation after the excursion minimum.

Lower Toarcian global correlations are facilitated by $\delta^{13}C_{carb}$ and $\delta^{13}C_{org}$ records (e.g., Dickson et al., 2017; Fu et al., 2017; 2021; Houben et al., 2021). Existing biostratigraphic data are insufficiently high-resolution to conclusively demonstrate the synchronicity

of the T-OAE at a global scale, but given that this event represents a single large perturbation to the global carbon cycle, small differences in the timing of its onset and termination among different regions (e.g., Fig. S1) are likely due to errors in the ammonoid zonation of individual sections, or in the global correlation of regional biostratigraphic schemes. For example, the NCIE occurs within the upper *Tenuicostatum* and lower *Falciferum* zones in the Cleveland Basin (NW Tethys), while in the Inuyama Area (Central Panthalassa) it occurs within the upper *Falciferum* Zone (Fig. S1). Thus, sections in which such discrepancies exist need to be restudied with regard to their ammonoid biostratigraphy.

4.2. Redox evaluation of study basins

For some of the studied basins, several redox proxies available in the literature were selected to assess the extent of euxinic conditions and thus test whether the Mo/TOC proxy is valid for hydrographic reconstruction. Pre-established thresholds were used and plotted for TOC (Fig. S2): C_{org}/P, adopting values

<50 for oxic conditions, 50-100 for dysoxic, and >100 for euxinic conditions (Algeo & Ingall, 2007); and, for two basins in which the other redox proxies were not available, Mo_{EF} vs U_{EF} covariation (Algeo & Tribovillard, 2009; Tribovillard et al., 2012).

In the Northwestern Tethyan region, euxinic conditions existed during the T-OAE in almost every basin. In the Cleveland Basin, most samples from the T-OAE interval yield high TOC (>2 %) and C_{org}/P values (72-389) indicative of euxinic conditions (McArthur et al., 2008) (Fig. S2), in agreement with DOP (degree of pyritization) values of 0.8-0.9 and small pyrite framboid sizes (Raiswell & Berner, 1985; Wignall et al., 2005; Pearce et al., 2008). [Note that the analysis below makes use of DOP_T, not true DOP, and that the DOP redox thresholds of Raiswell et al., 1988, are therefore inapplicable; see Algeo & Li, 2020, for discussion of this issue.] In the West Netherlands Basin, C_{org}/P in most samples from sediments deposited before the T-OAE and all of them from sediments linked to the event fall in the euxinic field, while sediments from after the T-OAE were deposited under oxic to dysoxic conditions. Similar results (C_{org}/P > 100) were obtained from the nearby Dutch Central Graben, where euxinic conditions existed during most of the T-OAE (Dickson et al., 2017; Houben et al., 2021). In the South German Basin (Dotternhausen section), mostly euxinic conditions prevailed during Toarcian but were interrupted by several oxic intervals, as shown by sedimentological and palaeontological evidence (Röhl et al., 2001; Röhl & Schmid-Röhl, 2005) as well as biomarker data (Schouten et al., 2000; Schwark & Frimmel, 2004). The Paris Basin shows similar results to the Cleveland Basin, with consistently euxinic conditions during the T-OAE and post-event intervals (C_{org}/P > 100), and oxic environments before the event (C_{org}/P < 50) (Lézin et al., 2013). Finally, contrary to the tendency toward euxinia in this region, the Hebrides and the Cardigan Bay basins experienced only oxic to dysoxic conditions throughout the Toarcian, as indicated by U_{EF} vs Mo_{EF} (Fig. S2), although Mo and TOC indicates that slight euxinic conditions were reached during the *Falciferum* Zone in the Hebrides Basin (Percival et al., 2016; Chen et al., 2021).

Focusing on some of these basins NW Tethyan basins, interesting results appear when comparing the profiles of the selected proxies (Fig. IV.7). In the Cleveland Basin, TOC positive peak coincides with those for the C_{org}/P, and were developed at the same time as the NCIE (i.e., during the T-OAE *sensu stricto*), while Mo and Mo/TOC peaks are observed just below and above the NCIE. The Paris and South German basins show similar profiles, in which maximum peaks of TOC and C_{org}/P within the NCIE and Mo risings after it, although also a lower positive peak in Mo is present in coincidence with the TOC maximum. The West Netherlands Basin continues the tendency showing positive peaks of TOC and C_{org}/P coeval to the NCIE and an increase in Mo and Mo/TOC values after it; while the incomplete profile of the Dutch Central Graben inhibits a proper interpretation, although in this case Mo, TOC and C_{org}/P seem to exhibit coeval positive peaks. Thus, is remarkable that increased values of C_{org}/P and TOC occur coeval with the NCIE development (i.e., during the T-OAE *sensu stricto*), while Mo and Mo/TOC increases mainly appeared after the NCIE (i.e., after the T-OAE).

In the Iberian Palaeomargin (Southwestern Tethyan region), sediments in the southern Subbetic Basin were deposited under oxic to dysoxic conditions, although showing a large difference between those deposited during the T-OAE (one sample) vs deposits from after and before the event (C_{org}/P of 85 vs <50) (Rodríguez-Tovar & Reolid, 2013). The western Lusitanian Basin does not exhibit enrichments of redox-sensitive proxies and thus experienced only oxic to dysoxic conditions during the T-OAE (Fantasia et al., 2019). In the northern Asturian Basin, two black shale beds accumulated under dysoxic to euxinic conditions, whereas marls associated with the T-OAE indicate oxic to dysoxic conditions (see Section 3.3).

The Belluno Basin, in the northern part of the Southwestern Tethyan region, developed anoxic to slightly euxinic conditions during the T-OAE, as indicated by TOC and Mo values and several black shale beds (Dickson et al., 2017), although these modest enrichments do not indicate persistent euxinia. In the southern area of this region, sediments in the Atlassic

Hydrographic restriction in Northwestern Tethys
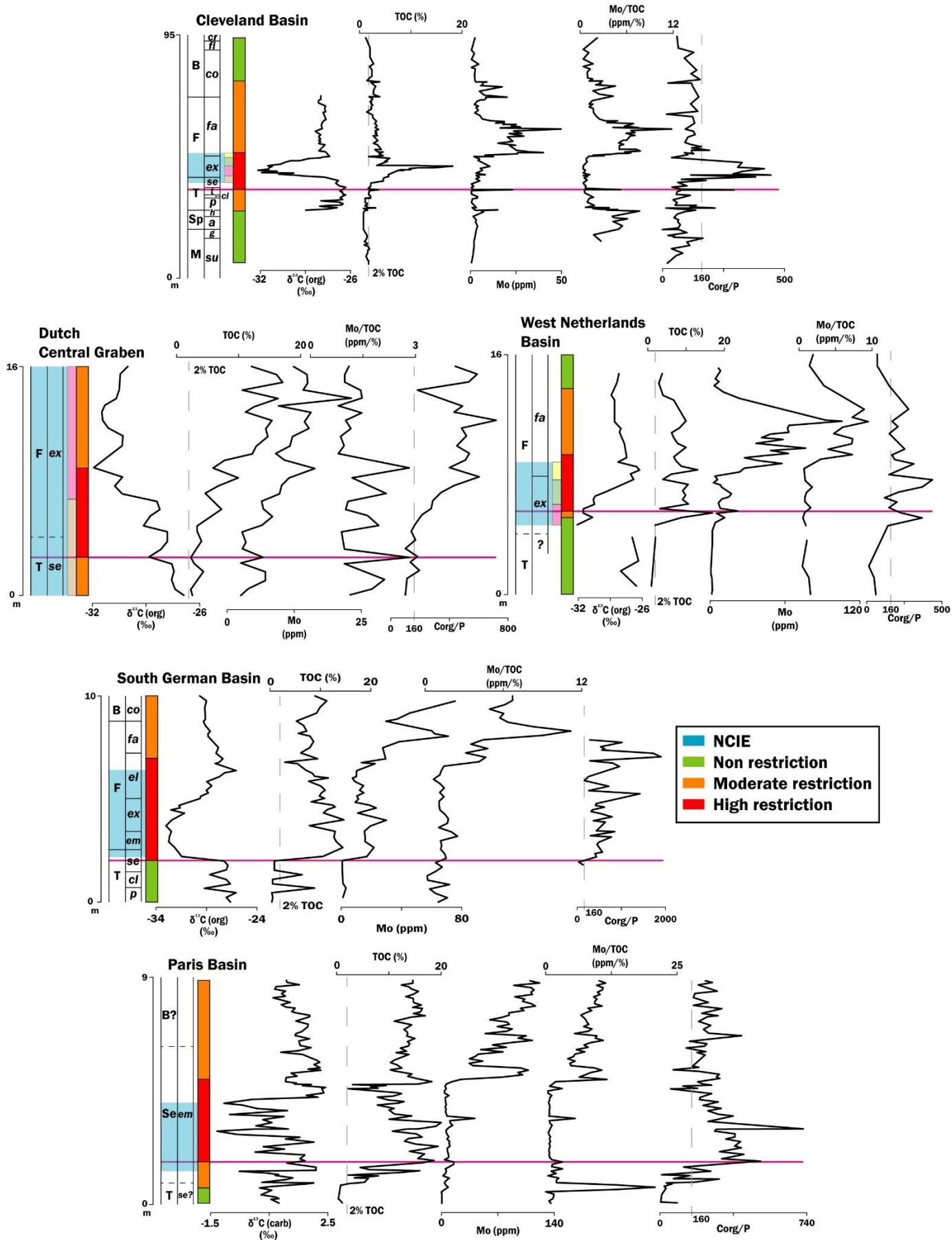
Basin were deposited under oxic conditions throughout the Toarcian (C_{org}/P <30) (Ruebsam et al., 2020b), while in the Adriatic Basin, geochemical and palaeontological data indicate persistently anoxic conditions in the photic zone and episodically dysoxic/anoxic conditions in the bottomwaters during the T-OAE, although TOC values remain distinctly low (<1%) throughout the Toarcian (Ettinger et al., 2021).

In the Eastern Tethyan region (Qiangtang Basin), all sediments in the Bilong Co Central section show high C_{org}/P values (>175) indicating generally euxinic conditions during the Toarcian, with black shales exhibiting higher TOC contents than the calcareous shales (8-14% vs 3-7%) and the sediments from before and after the T-OAE (1.5-4%) (Fu et al., 2017). In the northern section (Bilong Co North), most sediments exhibit low C_{org}/P (<50) and TOC (<2%) values indicating oxic to dysoxic conditions before and after the T-OAE, while black shale beds linked to the event show higher TOC (5-21%) and C_{org}/P (245-500) contents indicating euxinic conditions (Xian & Mansour, 2022) (Fig. S2). Finally, the southern section (Sewa) is characterized by pervasive oxic conditions during the Toarcian, as indicated by very low TOC (<1%) and C_{org}/P (10-20) contents (Fu et al., 2021).

In Northern Panthalassa, sediments in the Toyora Area show C_{org}/P values indicative of mostly oxic-dysoxic conditions before and during the T-OAE, and, although euxinia developed both during and after the event, organic matter and authigenic Mo enrichments remained low (Kemp & Izumi, 2014). The black chert beds in the Central Panthalassa (Inuyama) exhibit high C_{org}/P (210-770) and TOC (6-34%) values, indicating euxinic conditions during the T-OAE, while oxic-dysoxic conditions prevailed before and after the event, as indicated by lower C_{org}/P (<50) and TOC (<2%)

contents (Kemp et al., 2022). Finally, in the Southern Panthalassic region (Andean Basin), C_{org}/P values and ichnological data indicate that oxic to dysoxic conditions prevailed during the entire Early Toarcian (Fantasia et al., 2018a).

4.3. Regional Mo/TOC patterns
4.3.1. Mo/TOC in Northwestern Tethyan region

In most Northwestern Tethyan basins (i.e., the Cleveland, West Netherlands, South German, and Paris basins and the Dutch Central Graben), black shales associated with the T-OAE yield high values of both TOC and Mo, ranging from 4.0% to 12.6% of TOC (median 8.6%) and 4.5 ppm to 14.7 ppm Mo (median 8.1 ppm) (Table IV.2). In these basins, post-event deposits show lower TOC contents and higher Mo values (e.g., up to 120 ppm in the Paris Basin), a relationship yielding consistently low $m_{Mo/TOC}$ during the T-OAE and high $m_{Mo/TOC}$ after it. For example, the Cleveland Basin has a $m_{Mo/TOC}$ of 0.41±0.09 ($r = +0.78$; $p < 0.001$; $n = 17$) during the T-OAE but 10.0±1.1 ($r = +0.75$; $p < 0.001$; $n = 71$) after this event. $m_{Mo/TOC}$ values from all the studied basins are given in Table IV.3 and illustrated in Figures IV.8 and S3; note that the lower the slope during the T-OAE (blue lines), the higher it is after the event (green lines). Before the T-OAE, sediments deposited in these basins exhibit little to no enrichment of Mo and low TOC content (Table IV.2), which leads to poor correlations between these parameters ($p > 0.32$; Table IV.3, red lines in Figs. IV.8 and S3). The abrupt onset of black shale deposition in these basins represents a rapid transition from oxic to euxinic bottomwaters during the Early Toarcian. The extremely low $m_{Mo/TOC}$ recognized in these basins (Figs. IV.9A, IV.10B) is evidence that the degree of watermass restriction in these basins at that time was significantly greater than that of the modern Black Sea ($m_{Mo/TOC}$ of 4.5; Algeo & Lyons, 2006). The highly variable Mo and TOC concentrations of these

Figure IV.7. Diagram showing the correlation between the negative 13C isotopic excursions (NCIE) in Northwestern Tethyan basins presenting highly restricted conditions and euxinic bottomwaters. In addition, hydrographic restriction intensity is also recorded based on Mo, TOC, and Mo/TOC profiles, differentiating between unrestricted (green rectangles), moderately restricted (orange rectangles) and strongly restricted (red rectangles) conditions. Ammonite zones abbreviations are in Fig. IV.3, and references in Table IV.1. Dashed lines for TOC and Corg/P profiles indicate the euxinic threshold (note: see Algeo and Ingall, 2007, for description of Corg/P). Subzones abbreviations: su: Subnodosus, g: Gibbosus, a: Apyrenum, h: Hawkserense, p: Paltum, cl: Clevelandicum, t: Tenuicostatum, se: Semicelatum, ex: Exaratum, fa: Falciferum, co: Commune, fi: Fibulatum, cr: Crassum, em: Elegantulum, el: Elegans.

Table 1

Palaeoregion	Basin		Pre						T-OAE						Post					
		Mo (ppm)	TOC (%)	Mo/TOC *	Mo EF	m ± σ	n	Mo (ppm)	TOC (%)	Mo/TOC *	Mo EF	m ± σ	n	Mo (ppm)	TOC (%)	Mo/TOC *	Mo EF	m ± σ	n
Northwestern Tethys	Cleveland Basin	2.56 (21.1)	1.65 (3.7)	1.55 (5.70)	4.98 (26.28)	4.94±1.19	19	4.74 (10.5)	5.62 (18.2)	0.84 (1.37)	9.98 (27.01)	0.41±0.09	17	8.18 (45)	2.74 (4.6)	2.99 (12.5)	12.86 (41.99)	9.95±1.07	71
	West Netherlands Basin	1.19 (1.96)	1.29 (2)	0.93 (1.51)	1.00 (1.67)		4	5.93 (15.66)	7.04 (10.67)	0.84 (1.72)	12.28 (40.22)	0.65±0.25	10	25.56 (88.26)	6.77 (12.9)	3.78 (9.52)	29.75 (141.67)	5.69±2.27	16
	Dutch Central Graben						0	5.84 (23.05)	4.23 (17.18)	1.38 (2.75)	10.15 (38.17)	0.81±0.11	30						0
	South German Basin	0.97 (3.09)	1.28 (8.81)	0.76 (1.86)		0.21±0.06	7	13.95 (29.67)	10.53 (14.66)	1.33 (2.47)		1.70±0.41	22	38.81 (75.64)	6.94 (11.28)	5.59 (11.16)		5.07±1.93	15
	Paris Basin	1.32 (8.31)	0.45 (1.8)	2.90 (20.77)	4.55 (30.24)		9	7.16 (41.37)	7.50 (14.8)	0.96 (5.59)	15.53 (148.53)	0.32±0.26	44	80.49 (121.8)	10.13 (13.4)	7.95 (11.38)	175.47 (562.22)	14.02±2.02	43
	Hebrides Basin	0.16 (0.23)	1.12 (2.08)	0.14 (0.29)	0.22 (0.30)		12	0.47 (1.83)	2.72 (8.01)	0.17 (0.38)	0.78 (4.21)	0.19±0.04	17	0.78 (1.73)	1.32 (4.07)	0.59 (2.83)	3.62 (9.52)		6
Southwestern Tethys	Atlassic Basin	0.40 (1.18)	0.27 (0.36)	1.49 (3.81)	0.55 (1.61)		12	1.97 (6.42)	0.39 (0.49)	5.01 (15.06)	2.67 (11.01)	18.63±14.39	9	1.29 (3.61)	0.28 (0.35)	4.62 (10.32)	1.63 (4.39)	17.58±11.81	5
	Adriatic Basin	1.58 (4)	>0.01 (0.01)	200.75 (500)	313.25 (1500)		13	3.72 (8)	0.01 (0.02)	385.22 (1000)	231.11 (2000)		6	2.31 (5)	0.01 (0.02)	259.40 (1000)	349.66 (1667)		20
	Belluno Basin	0.14 (0.18)	0.15 (0.19)	0.97 (1)			2	4.17 (15.09)	1.81 (3.34)	2.31 (12)		2.1±0.42	14						0
Southwestern Tethys (Iberian Palaeomargin)	Lusitanian Basin	1.18 (1.7)	0.16 (0.94)	7.38 (13.09)	4.45 (7.41)		8	0.36 (14.6)	0.61 (10.03)	0.59 (51.55)	0.52 (44.58)	0.78±0.15	64	36.8	0.645049534	57.04988228	55.52		1
Asturian Basin	Lastres	0.79 (1.08)	0.71 (1.66)	1.19 (3.54)	1.28 (1.97)	0.20±0.13	6	2.14 (9.58)	1.35 (3.24)	1.58 (2.96)	2.69 (13.17)	2.28±0.38	13	0.50 (0.64)	0.46 (0.91)	1.08 (1.42)	1.00 (1.42)		4
	Rodiles	0.86 (6.22)	0.57 (2.57)	2.08 (9.44)	2.05 (8.83)	1.99±0.50	8	2.63 (18.45)	1.33 (2.97)	1.98 (6.21)	3.30 (27.28)	4.51±1.40	11	0.76 (1.58)	0.38 (0.79)	2.01 (5.16)	1.43 (3.10)		9
Eastern Tethys / Qiangtang Basin	Bilong Co Central	0.58 (1.07)	1.76 (2.53)	0.33 (0.45)	5.10 (8.19)	0.69±0.09	8	27.84 (42.3)	10.16 (14.1)	2.74 (3.88)	52.66 (72.68)	1.99±1.04	18	1.06 (3.86)	3.06 (4.45)	0.35 (0.87)	5.39 (14.33)	1.27±0.27	17
	Calc. Shales (BiLCo C)							2.59 (3.66)	4.42 (6.91)	0.59 (1.10)	6.21 (13.20)	-0.34±0.19	11						
	Bilong Co North	1.19 (7.68)	0.58 (2.52)	4.29 (45)	0.36 (1.76)	1.87±0.47	21	34.64 (83.10)	7.54 (21.50)	4.84 (9.55)	4.82 (14.49)	2.82±0.25	18	7.65 (11.1)	1.69 (3.86)	10.7 (22.88)	1.59 (1.96)	1.55±0.19	3
Central Panthalassa	Inuyama Area	93.8 (615)	0.63 (4.41)	253 (831)	241 (1010)	-4.87±40.91	15	56.19 (184)	11.76 (34.2)	4.96 (17.29)	156 (463)	5.05±0.48	22	2.62 (5.94)	0.28 (0.60)	12.16 (34.94)	2.78 (6.16)	-5.38±5.47	7

Table 2

Palaeoregion	Basin		Pre					T-OAE					Post				
		m ± σ	r	r2	p	n	m ± σ	r	r2	p	n	m ± σ	r	r2	p	n
Northwestern Tethys	Cleveland Basin	4.94±1.19	0.71	0.50	0.00068309	19	0.41±0.09	0.78	0.61	0.00020856	17	9.95±1.07	0.75	0.56	7.7801E-14	71
	West Netherlands Basin	0.47±0.81	0.38	0.14	0.62219	4	0.65±0.25	0.68	0.46	0.032299	10	5.69±2.27	0.56	0.31	0.025221	16
	Dutch Central Graben					0	0.81±0.11	0.81	0.66	5.4121E-08	30					0
	South German Basin	0.21±0.06	0.83	0.69	0.020639	7	1.70±0.41	0.68	0.46	0.0005138	22	5.07±1.93	0.58	0.35	0.021035	15
	Paris Basin	0.98±2.10	0.16	0.027	0.65	9	0.32±0.26	0.19	0.04	0.22	44	14.02±2.02	0.73	0.54	2.09E-08	43
	Hebrides Basin	-0.03±0.04	-0.21	0.04	0.4988	12	0.19±0.04	0.77	0.59	0.0028717	17	0.12±0.16	0.36	0.13	0.48582	6
Southwestern Tethys	Atlassic Basin	1.45±1.79	0.25	0.06	0.38759	12	18.63±14.39	0.44	0.19	0.23487	9	17.58±11.81	0.65	0.43	0.24496	5
	Adriatic Basin	133.04±110	0.32	0.10	0.37544	13	33.16±306	0.05	0.01	0.97499	13	62.64±78.98	0.16	0.03	0.36139	20
	Belluno Basin	0.88±0	1	1		2	2.1±0.42	0.12	0.02	0.0006801	14					0
Southwestern Tethys (Iberian Palaeomargin)	Lusitanian Basin	0.07±0.38	0.08	0.01	0.8567	8	0.78±0.15	0.56	0.32	1.2794E-06	64	0.19±0.25	0.49	0.24	0.51202	1
Asturian Basin	Lastres	0.20±0.13	0.62	0.38	0.19439	6	2.28±0.38	0.88	0.77	0.000086854	13	-0.50±0.73	-0.25	0.06	0.50863	4
	Rodiles	1.99±0.50	0.85	0.73	0.0072737	8	4.51±1.40	0.73	0.54	0.010416	11	1.27±0.27	0.78	0.60	0.00024908	9
Eastern Tethys / Qiangtang Basin	Bilong Co Central	0.69±0.09	0.95	0.91	0.00027717	8	1.99±1.04	0.43	0.19	0.074311	18	1.27±0.27	0.78	0.60	0.00024908	17
	Calc. Shales (BiLCo C)					0	-0.34±0.19	-0.51	0.26	0.10974	11					0
	Bilong Co North	1.87±0.47	0.67	0.45	0.11255	21	2.82±0.25	0.87	0.75	8.19E-06	18	1.55±0.19	0.99	0.99	0.043779	3
Central Panthalassa	Inuyama Area	-4.87±40.91	-0.032983413	0.001	0.030937	15	5.05±0.48	0.92	0.85	0.00037214	22	-5.38±5.47	-0.40	0.16	0.012131	7

basins, despite their relative proximity to each other (Fig. IV.7), highlights the local nature of watermass restriction in this region.

Contrary to general patterns in the Northwestern Tethyan region, the Cardigan Bay Basin and Hebrides Basin exhibit, respectively, an absence and a scarcity of black shales within the T-OAE interval (Percival et al., 2016; Chen et al., 2021). Mo contents are uniformly low (< 2 ppm), and TOC is also low in most samples, although the Hebrides Basin shows moderate TOC (2-8%) in some samples of the T-OAE interval (Table IV.2). Moreover, both basins exhibit a poor Mo-TOC correlation (non-significant r) for the full section, although the Hebrides Basin yields a highly significant relationship ($r = +0.77$; $p < 0.001$; $n = 17$) within the T-OAE interval, with a very low $m_{Mo/TOC}$ of 0.19 ± 0.04 (blue line in Fig. S4). Sediments in these basins were deposited in open-marine settings rather than in restricted troughs or embayments, as for other sections of the Northwestern Tethyan region. In the Cardigan Bay and Hebrides basins, low TOC and Mo contents are evidence that neither restricted nor euxinic conditions were reached in bottomwaters or porewaters (Fig. IV.9B, Table IV.2), in agreement with U_{EF} vs Mo_{EF} values, and, therefore, restricted conditions are discounted for these sections.

4.3.2. Mo/TOC in Southwestern Tethyan region

In contrast to the Northwestern Tethyan basins, black shales are absent in several sections of the Southwestern Tethys, i.e., the Atlassic and Adriatic basins, which exhibit very low TOC contents (< 0.5%) with low to moderate Mo values (< 8 ppm) during the T-OAE. In the Atlassic Basin, the $m_{Mo/TOC}$ for T-OAE deposits is 19 ± 14 ($r = +0.44$; non-significant; $n = 9$), and for sediments deposited after the event is 18 ± 12 ($r = +0.65$; non-significant; $n = 5$) (blue and green lines in Fig. IV.8, respectively), while $m_{Mo/TOC}$ in the Adriatic Basin is high (33 to 133) and with high p values (Table

IV.3, dashed lines in Fig. S5). In these settings, moderate concentrations of Mo may reflect the presence of euxinic bottomwaters. However, as in the Cardigan Bay Basin, the absence of organic matter supports the sparse and sporadic character of euxinia in these basins. However, the $m_{Mo/TOC}$ values are high (Fig. IV.10B), indicating that restriction was similar to that of the Cariaco Basin ($m_{Mo/TOC}$ of 25). Therefore, the Early Toarcian in these settings was characterized by well-connected and oxic environments, sometimes showing weak or sporadic euxinia, but not related to hydrographic restriction (green circles in Fig. IV.10A).

The Belluno Basin, located at the northern margin of the Southwestern Tethyan region, contains black shales exhibiting small increases in Mo and TOC relative to pre-T-OAE beds (from < 0.2 to 1-3 % TOC and from < 0.2 up to 15 ppm Mo) (Table IV.2). Scarcity of samples for pre- and post-event deposits inhibits the correlation among Mo and TOC (Table IV.3), and T-OAE black shales show a $m_{Mo/TOC}$ of 0.5 ± 1.2 (non-significant r; $n = 14$), similar to that of Northwestern Tethyan sites such as the Cleveland and West Netherlands basins (blue line in Fig. S4 cf. Fig. S3). Despite the low $m_{Mo/TOC}$, the open setting of the Belluno Basin (Bellanca et al., 1999) would not have limited watermass exchange but would only have favoured slightly anoxic/euxinic conditions in bottomwaters near/at the sediment-water interface, which resulted in limited Mo and TOC enrichment (as supported by isotopic Mo data from Dickson et al., 2017).

On the western Iberian Palaeomargin (Lusitanian Basin), the T-OAE interval consists of dark marls with low Mo and TOC contents (Table IV.2), although some levels deposited during the event show episodic, non-coeval, positive excursions of TOC (2 to 10%) and Mo (< 2 up to 15 ppm). Notably, the relative TOC enrichment causes an extremely low $m_{Mo/TOC}$ slope of 0.79 ± 0.15 ($r = +0.56$; $p < 0.001$; $n = 64$) during the

---

*(Left) Table IV.2. Geochemical data of the analyzed sections where euxinic conditions were reached, indicating mean values and the maximum between parentheses. Only statistically significant mMo/TOC values are indicated (i.e., p < 0.32). *: ppm/%.*

(Right) Table IV.3. Regression slopes (mMo/TOC) data of analyzed sections for pre-, syn- and post-event stages. Only those basins which presented euxinic conditions are represented. Slopes with p > 0.32 are not considered statistically significant.
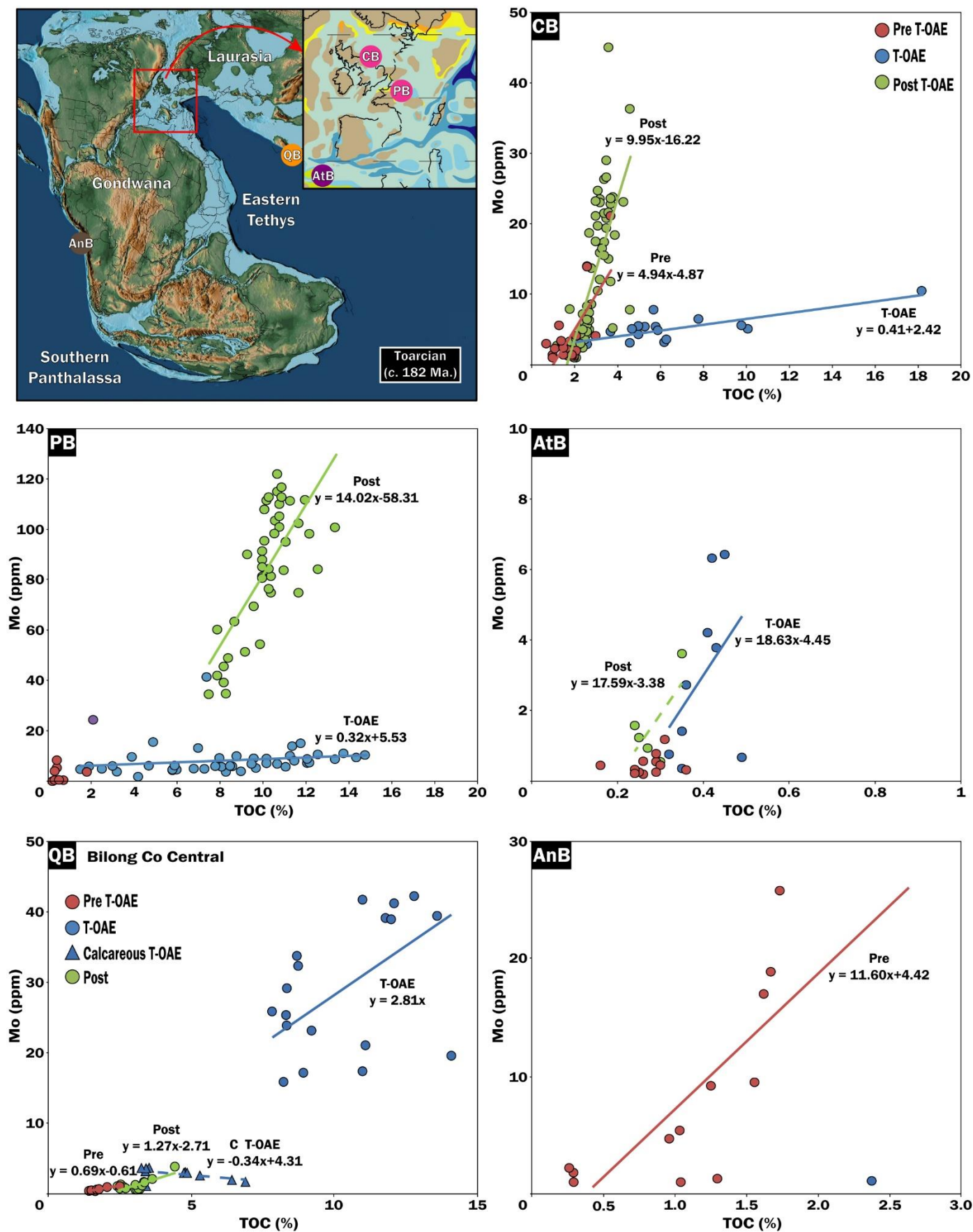
Figure IV. 8. Mo vs TOC crossplots for several of the analyzed basins and their situation in the map. mMo/TOC are indicated for each stage: before the event (red), during the T-OAE (blue) and after it (green). Dashed lines are mMo/TOC statistically non-significant.

T-OAE, similar to that of Northwestern Tethyan basins such as the West Netherlands Basin (blue line in Fig. S5 cf. Fig. S3, Table IV.3). In southern Iberia, sediments in the Subbetic Basin show extremely low Mo and TOC values (Table IV.2), which are poorly correlated (negative $m_{Mo/TOC}$ and/or $p > 0.32$, dashed lines in Fig. S5). As mentioned above (Section 3.3), the Asturian Basin, in northern Iberia, shows slight Mo and TOC enrichments in its event-linked black shales, resulting in low $m_{Mo/TOC}$ (Fig. IV.5, Fig. S5).

Therefore, in the shallow-marine carbonate deposits of the Subbetic Basin (southern Iberia), the T-OAE is scarcely recognizable, with neither black shales nor enrichments in TOC and Mo, which points to continuously oxic, unrestricted bottomwaters during the Early Toarcian (in agreement with ichnological data from Rodríguez-Tovar & Reolid, 2013). In the nearby hemipelagic deposits of the Lusitanian Basin (western Iberia), the absence of general authigenic Mo enrichment and black shales, notwithstanding relatively high TOC content and low $m_{Mo/TOC}$ (Fig. IV.10B), points not to persistent hydrographic restriction but only to euxinia in porewaters before and during the T-OAE, and to intermittently euxinic conditions in bottomwaters after the event. Finally, the Mo/TOC and $m_{Mo/TOC}$ variations among the pelagic black shales in the Asturian Basin (northern Iberia) reveal the onset of two pulses of slightly euxinic bottomwaters during the Early Toarcian interrupted by well-connected, non-euxinic bottomwaters represented by marl deposits between the black shales (Figs. IV.4, IV.5) (Section 3.4). Thus, hydrographic restriction is unlikely to have existed in any sections of the Southwestern Tethyan region.

4.3.3. Mo/TOC in Eastern Tethyan and Panthalassic regions

In the Eastern Tethyan region, the Qiangtang Basin exhibits variation in Mo/TOC records betwee n settings: Bilong Co North (Xia & Mansour, 2022), deposited in a deltaic/shelf setting, Bilong Co Central (Fu et al., 2017), representing a barrier/lagoon palaeoenvironment, and the southern Sewa section (Fu et al., 2021), an open-marine setting (see map in Fig. 2D to the precise situation of each section). The Bilong Co Central section (barrier-lagoon) contains T-OAE

deposits enriched in Mo and TOC, although they show different concentrations depending on lithology (Fu et al., 2017): the lower calcareous shales (3.4% to 5.8%% TOC, median 4.8%; 1.8 ppm to 3.6 ppm Mo, median 3.0 ppm) versus the upper black shales (8.3% to 12.3% TOC, median 10.1%; 19.0 ppm to 40.0 ppm Mo, median 27.6 ppm) (Table IV.2). Mo and TOC are well correlated among all samples of this section, showing variations from low $m_{Mo/TOC}$ for sediments deposited before the T-OAE (0.69±0.09; $r = +0.95$; $p < 0.001$; $n = 8$) to higher values during (2.0±1.0; $r = +0.43$; $p \sim 0.32$; $n = 18$) and after the event (1.3±0.3; $r = +0.78$; $p < 0.001$; $n = 17$) (Fig. IV.7), while the calcareous shales deposited during the T-OAE show a negative slope (dashed line in Fig. IV.8, Table IV.3). In the Bilong Co Central section, calcareous shales represent the onset of anoxic to sporadic, slightly euxinic conditions during the lower part of the T-OAE, but not under restricted environments as evidenced by the poor Mo-TOC correlation. Upwards, black shales with high Mo-TOC and low $m_{Mo/TOC}$ represent the onset of restricted conditions during the upper part of the T-OAE in this barrier-lagoon, which abruptly ended with a return to oxic, unrestricted environments.

The Bilong Co North section (deltaic to inner-shelf) contains T-OAE black shales capped by a unconformity separating them from overlying Bathonian-age sediments (Xia & Mansour, 2022). These black shales are enriched in both Mo (11 ppm to 61 ppm, median 26 ppm) and TOC (1.4% to 14%, median 7%), while sediments from before the event are impoverished in Mo (< 2 ppm) and TOC (<1 %) and those from after the event exhibit intermediate values (6-9 ppm Mo, 0.5-3% TOC) (Table IV.2). Mo and TOC are well correlated in all intervals, showing low $m_{Mo/TOC}$ before (1.87±0.47; $r = +0.67$; $p = < 0.32$; $n = 21$) and after the T-OAE (1.55±0.19; $r = 0.99$; $p = < 0.32$; $n = 3$), while the black shales linked to the event exhibit a higher slope (2.82±0.25; $r = 0.87$; $p = < 0.001$; $n = 18$) (Fig. S6, Table IV.3). In this northern section, black shales accumulated in a deltaic/inner-shelf setting with euxinic porewaters and intermittently euxinic bottomwaters. Despite the low $m_{Mo/TOC}$ exhibited by these shales, restricted conditions are unlikely in a deltaic/shelf
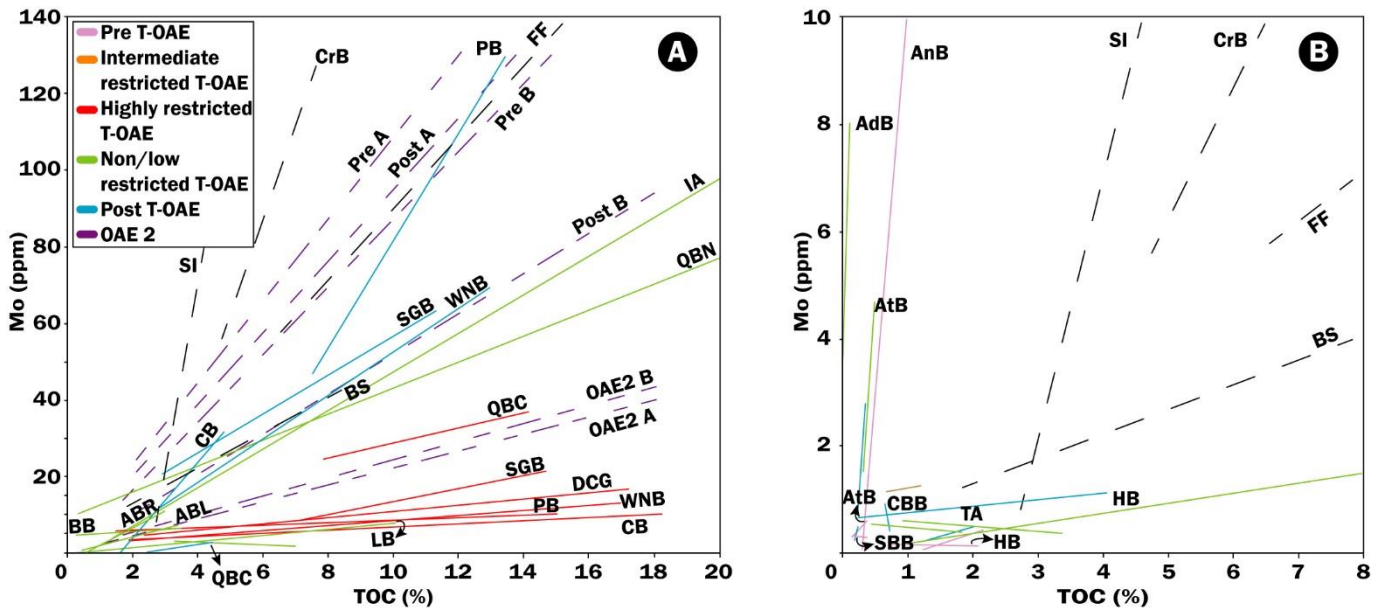
Figure IV.9. Mo-TOC regression slopes for restricted (A) and unrestricted (B) basins. Dashed lines are mMo / TOC from modern analogs: SI: Saanich Inlet (45), CrB: Cariaco Basin (25), FF: Framvaren Fjord (9), BS: Black Sea (4.5) (Algeo and Lyons, 2006). Abbreviations are in Table IV.1.

setting, and, thus, the anoxic conditions were probably related to high productivity and/or watermass stratification, as indicated by a high P/TOC correlation and P remobilization (Xia & Mansour, 2022).

For the southern Sewa section, Fu et al. (2021) reported very low TOC (< 1%), Mo (EF < 1), U and V (EF 1-1.5), and C_{org}/P (10-20) values for the mudstones deposited in this open-marine setting. Therefore, the Sewa section represents a well-ventilated, oxic environment during all the Toarcian. However, a slight reduction in Mo, U and V enrichment factors during the NCIE linked to the T-OAE is evident (figure 7 in Fu et al., 2021).

Outside of the Tethyan regions, the Toyora Area (Northern Panthalassa) exhibits low Mo (< 1 ppm) and a small TOC increase in some T-OAE deposits (ΔTOC = 0.3%), showing a poor Mo-TOC correlation during and after the T-OAE (negative $m_{Mo/TOC}$ and p > 0.32) and a very low $m_{Mo/TOC}$ for pre-event deposits of 0.40$\pm$0.22 (r = +0.73; p ~0.32; n = 5) (Fig. S6, Table IV.3). T-OAE strata at Inuyama (Central Panthalassa) consist of black cherts enriched in Mo (13 ppm to 112 ppm, median 36 ppm) and TOC (2.44% to 18.37%, median 10.93%), while sediments from before and after the event exhibit lower values of both Mo and TOC (Table IV.2). T-OAE deposits exhibit a moderate $m_{Mo/TOC}$ of 5.05$\pm$0.48 (r =

0.92; p = < 0.001; n = 22), while Mo and TOC are poorly correlated (negative $m_{Mo/TOC}$) in sediments from before and after the event (Fig. S6). The Andean Basin (Southern Panthalassa) offers an incomplete profile (only a single sample from the T-OAE interval), with pre-event sediments yielding low Mo (< 1 ppm) and TOC (< 2%) with intercalated, notably Mo-enriched levels (5-26 ppm) (Table IV.2) yielding a high pre-event $m_{Mo/TOC}$ of 12$\pm$3 (r = 0.77; p < 0.01; n = 12) (red line in Fig. IV.8).

Therefore, similar to Southwestern Tethyan basins, those in the Panthalassic Ocean were characterized by well-ventilated bottomwaters. In the Toyora Area (Northern Panthalassa), the absence of authigenic Mo combined with a slight increase in organic matter (thus, negative $m_{Mo/TOC}$) (Fig. IV.9B) provides evidence of sporadically dysoxic to anoxic conditions in bottomwaters, in which organic matter was partly preserved but euxinic, restricted conditions, were not developed, thus inhibiting Mo uptake by the sediment. In the abyssal setting at Inuyama (Central Panthalassa), black cherts were deposited under anoxic to intermittently euxinic but unrestricted bottomwaters, given that watermass restriction is unlikely to have developed in the deep ocean. Finally, in the Andean Basin (Southern Panthalassa), the absence of black shales and

Figure IV.10. (A) Tethys map (modified from Thierry et al., 2000) and Panthalassic Ocean (modified from Scotese et al., 2013) showing the location of the basins analyzed in this study, indicating unrestricted (green) and highly restricted (red) basins during the T-OAE. (B) Diagrams showing the relation among mMo/TOC slopes for each basin before, during, and after the T-OAE, and its correspondent bottomwater renewal time (modified from Algeo et al., 2007). Note that the chemocline depth might be indicated by the amount of sedimentary Mo in the basin: the higher is the Mo content, the higher was the aqueous Mo reservoir prone to fixation, i.e., the euxinic water column (cf. figure 7 in McArthur 2008).

organic matter and the relatively strong bioturbation in Toarcian strata (Fantasia et al., 2018a) point to well-oxygenated bottomwaters. However, high $m_{Mo/TOC}$ and authigenic Mo enrichment before the T-OAE (Fig. IV.9B, Table IV.2, Fig. S6) suggest intermittent hydrographic restriction (cf. Framvaren Fjord), causing euxinia to develop in porewaters or bottomwaters.

4.4. Control of sediment Mo/TOC by redox versus watermass restriction

Covariation between Mo/TOC and redox proxies can be used to assess redox versus hydrographic control of sediment Mo concentrations, as this element is sensible to both controls (Algeo & Lyons, 2006; Algeo & Rowe, 2012). For each study unit, Mo/TOC was plotted against available auxiliary redox proxies, yielding

three distinct patterns that provide insights into controls on Mo accumulation: (1) when Mo/TOC is constant despite variable redox conditions through a stratigraphic section, then Mo accumulation was likely controlled by hydrographic restriction; (2) when Mo/TOC is positively correlated with the redox proxies, then Mo accumulation was likely controlled by redox conditions; and (3) when Mo/TOC varies but is not correlated with the redox proxies, then Mo accumulation may have been controlled by changes in the aqueous Mo content of seawater (Fig. S7).

In the Northwestern Tethyan region, Mo/TOC in the Cleveland Basin is significantly correlated with both DOP_T and C_{org}/P: both before and after the T-OAE, these redox proxies exhibit strong correlations, indicating a redox control on Mo accumulation, but during the T-OAE, a narrow range of Mo/TOC values in conjunction with wide variation of DOP_T and C_{org}/P values is consistent with hydrographic control of Mo accumulation. Similar to the Cleveland Basin, in the West Netherlands Basin Mo/TOC and C_{org}/P proxies show large ranges and a weakly positive correlation during the pre-event stage, indicating redox control of Mo accumulation, but during the T-OAE, the range of Mo/TOC becomes narrow while that of C_{org}/P is broadened, implying a hydrographic control. The Dutch Central Graben also shows a similar relationship although with a weak negative correlation between Mo/TOC and C_{org}/P. In the Paris Basin, the T-OAE interval shows a narrow Mo/TOC range and broad C_{org}/P range, whereas the post-event interval is characterized by more variable Mo/TOC and less variable C_{org}/P, thus indicating a shift from a hydrographic control during the T-OAE to greater redox influence following it. Contrary to the general pattern in the NW Tethyan region, the Cardigan Bay Basin shows a tight correlation between Mo/TOC values and U_{EF}, thus indicating redox control throughout the Early Toarcian, and the Hebrides Basin shows a poor correlation among all proxies, obviating interpretation of controls on Mo accumulation.

On the Iberian Palaeomargin, Mo/TOC and redox proxies show a poor correlation in the Subbetic Basin, which, combined with low Mo/TOC values, inhibits interpretation as a redox-controlled

environment. The same pertains to the Asturian Basin, where Mo/TOC and redox proxies show poor correlations in both sections. In the Southwestern Tethys, the Atlassic Basin exhibits a poor correlation between Mo/TOC and C_{org}/P for sediments deposited during and after the T-OAE, which may indicate redox-controlled Mo accumulation, although the Mo content in this basin is low (<7 ppm) (Table IV.2).

In the Qiangtang Basin (Eastern Tethys), the Bilong Co Central section exhibits similarities with T-OAE sections in the Northwestern Tethyan region, showing a tight correlation between Mo/TOC and C_{org}/P for sediments deposited before and after the T-OAE, implying a dominant redox control. On the contrary, black shale deposits of the T-OAE interval show high variation in Mo/TOC content, indicating a transient hydrographic control on Mo drawdown, which is in agreement with a barrier-lagoon setting for this section (Fu et al., 2017). On the other hand, correlations between Mo/TOC and C_{org}/P are low in the Bilong Co Central section, showing negative regression slopes, thus precluding an accurate interpretation.

Both the Andean Basin in Southern Panthalassa and the Toyora Area in Northern Panthalassa show a poor correlation between Mo/TOC and redox proxies, and their low C_{org}/P and Mo/TOC values inhibit a confident interpretation. Finally, Inuyama (Central Panthalassa) shows a poor correlation between Mo/TOC and C_{org}/P (negative regression slope) and wide Mo/TOC variation during continuously oxic conditions before the T-OAE, thus indicating that Mo uptake by the sediment was probably controlled by the aqueous Mo content of global seawater.

5. DISCUSSION

We now discuss the implications of the Mo/TOC interpretations in Section 4, including the roles of local basinal restriction versus a general drawdown of global seawater Mo content during the T-OAE. This discussion is organized into subsections that address Mo/TOC variation in Mesozoic and modern analog environments (Section 5.1), local hydrographic controls on Mo/TOC during the T-OAE (Section 5.2),
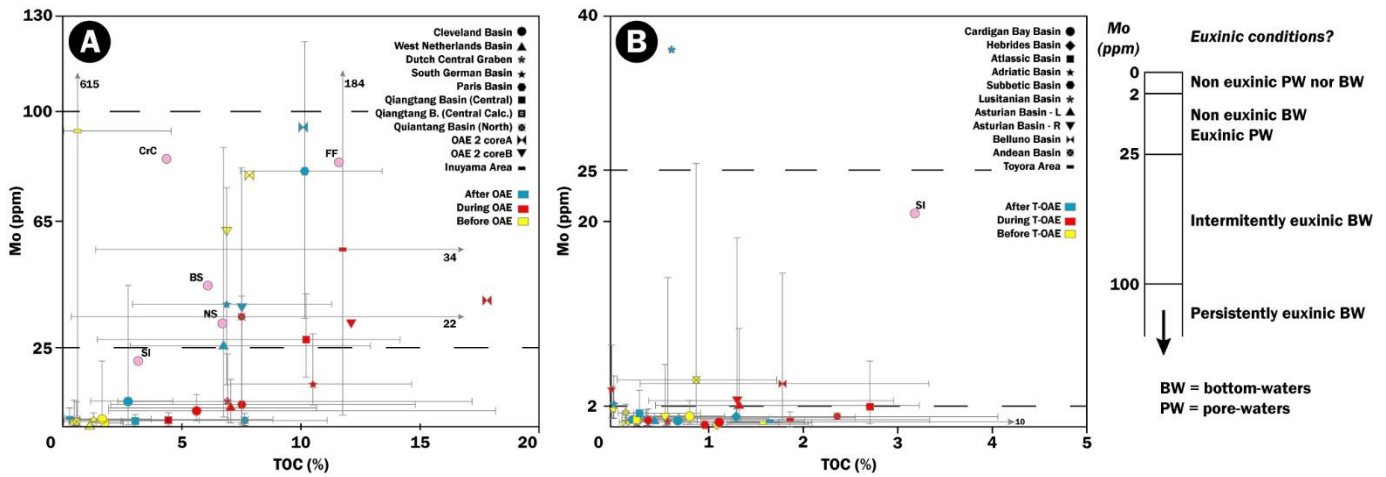
Figure IV.11. Mean Mo (ppm) versus TOC (%) crossplots for all the analyzed basins, showing higher (A) or lower (B) Mo contents, and compared with two sections from the OAE-2 (Hetzel et al., 2009) and modern analogs (Algeo and Lyons, 2006). Bar-and-whisker plots indicate maximum and minimum values. Note that maximum Mo values are >130 ppm for modern basins (A) and that most of them show higher Mo and TOC values than the illustrated basins (B).

the relationship between Mo/TOC and sea-level changes in the Northwestern Tethyan basins (Section 5.3), and, finally, global seawater controls on Mo/TOC during the T-OAE (Section 5.4).

5.1. Comparison with Mo/TOC of modern and Mesozoic analog environments

To calibrate Mo drawdown in the black shale deposits associated with the T-OAE, we compare them with modern and Mesozoic analog environments. Most basins in the Northwestern Tethys (i.e., the Cleveland, West Netherlands, South German, and Paris basins, and Dutch Central Graben) and Eastern Tethys (Qiangtang Basin), in which Mo contents were relatively high (Table IV.2), exhibit notably lower Mo values than modern euxinic basins (e.g., the Black Sea, Framvaren Fjord, Cariaco Basin, and Saanich Inlet) (Fig. IV.11A; Algeo & Lyons, 2006). In these basins, average Mo in the T-OAE interval is mostly <25 ppm, with the exception of Inuyama (56 ppm) and the Qiangtang Basin North and Central sections (35 ppm and 28 ppm, respectively). In contrast, the Mo concentrations of sediments in modern euxinic basins range from 33 to 84 ppm, with only Saanich Inlet having a lower value (21 ppm). The modern basins also exhibit much higher maximum Mo values (126-265 ppm) than the Toarcian sections (0.9-38 ppm, median 3.9 ppm). Furthermore, after the T-OAE, when Mo contents generally rose, only the South German, West Netherlands and Paris basins show maximum values that are as high as those of modern settings (76-

121 ppm). The remaining Toarcian basins, even those that contain black shales such as the Asturian and Belluno basins, show lower average (<10 ppm) and maximum Mo contents (mostly <20 ppm) (Fig. IV.11B). Other Mesozoic oceanic anoxic events, e.g., OAE-2 (Cenomanian/Turonian boundary; Hetzel et al., 2009), also tend to show higher Mo contents (mean ~30-100 ppm, maximum >> 100 ppm) than the Toarcian (Fig. IV.11A).

Values for $m_{Mo/TOC}$ are also much lower in most T-OAE sections than in modern and Mesozoic analogs (Figs. IV.9A-B, IV.10). Saanich Inlet shows $m_{Mo/TOC}$ of 45±5, much higher than other basins, while the $m_{Mo/TOC}$ of the Cariaco Basin (25±5) and Framvaren Fjord (9±2) are comparable to those of post-T-OAE sediments. The Black Sea (4.5±1), which is the paradigm of euxinic and hydrographically restricted modern environments, exhibits $m_{Mo/TOC}$ (~4.5) similar to those of T-OAE deposits in the Asturian Basin (Rodiles section) and the Central Panthalassa (Inuyama), and to post-T-OAE deposits from the South German and West Netherlands basins (NW Tethys, Fig. IV.10B). The rest of the basins containing T-OAE black shales show lower $m_{Mo/TOC}$ than any modern euxinic environment, ranging from 0.3 to 2.3 (Figs. IV.9A, IV.10). On the other hand, OAE-2 sections show similar $m_{Mo/TOC}$ (2.3-2.4) to several Northwestern and Eastern Tethyan basins (South German, Qiangtang and Asturian-Lastres section). Thus,

during both OAEs similarly low $m_{Mo/TOC}$ are observed despite large differences in Mo content.

5.2. Controls on development of local hydrographic restriction

Sedimentological analysis shows that local geographic features in each basin acted as important controls on the development of euxinia and hydrographic restriction during the T-OAE. Our analysis allows differentiation between: a) silled, shallow settings in the Northwestern (epicontinental intrashelf troughs) and Eastern (barrier-lagoon) Tethys, where global Mo drawdown was overprinted by the onset of several episodes of hydrographic restriction and euxinia; and b) basins having well-ventilated bottomwaters and an absence or minimal euxinic conditions, represented mainly by hemipelagic, pelagic settings and carbonate platforms/ramps lacking a sill. This interpretation is supported also by strong Mo/TOC covariation with redox proxies in open settings such as the Cardigan Bay Basin, reflecting a redox control, and weak covariation in more restricted settings such as the Cleveland and Qiangtang basins, reflecting a hydrographic control (Fig. S7).

The Qiangtang Basin, in the Eastern Tethyan region, shows how local topography heavily influenced the onset of watermass restriction and euxinic conditions even in the same region. In the barrier-lagoon (Bilong Co Central section), local topography and connectivity with the open ocean strongly controlled the onset of restriction. Moreover, watermass stratification was enhanced by the input of continental freshwater to the system (Fu et al., 2017). In the nearby deltaic/shelf setting of the Bilong Co North section, anoxic conditions were related to high productivity and/or watermass stratification, also enhanced by increased precipitation and river runoff (Xia & Mansour, 2022). Therefore, hydrological cycle intensification triggered development of restricted and euxinic conditions in some shallow-marine settings, but its final effect was heavily conditioned by local topography and distance to landmasses (cf. McArthur et al., 2008; Fantasia et al., 2018b). Finally, the southern Sewa section represents a continuously oxic, well-ventilated open-marine setting

throughout the Toarcian, which was not influenced by hydrological cycle intensification.

In the Southwestern Tethys, euxinia developed only sporadically and was heavily influenced by topography. Hemipelagic and shallow carbonate settings (Atlassic, Adriatic and Belluno basins) are considered to represent open-marine conditions, allowing at most only weak euxinic conditions in porewaters. On the Iberian Palaeomargin, the open setting of the Subbetic Basin (south) makes almost unrecognisable the effects of the T-OAE (cf. Cardigan Bay Basin), while sporadically euxinic conditions are recorded in the hemipelagic to pelagic facies of the Lusitanian (west) and the Asturian (north) basins. Therefore, local topography played a major role in the onset of intermittent euxinia in the Southwestern Tethyan region. Similarly, two Panthalassic basins are represented by shallow settings without sills, precluding watermass restriction.

The deep, open-marine Inuyama section (Central Panthalassa) was characterized by anoxic/euxinic conditions during the T-OAE that are unlikely to have been linked to hydrographic restriction, although they may have been influenced by general watermass warming and stratification, while its low $m_{Mo/TOC}$ can be attributed to low aqueous Mo availability due to general seawater Mo drawdown (Kemp et al,. 2022). Furthermore, a global depletion of the seawater Mo inventory was also inferred from open-marine settings of the Eastern Tethys (Sewa section, Qiangtang Basin), where Mo (and U) values decreased during the onset of the NCIE under persistently oxic conditions (figure 7 in Fu et al., 2021).

5.3. Relationship of Mo enrichment to sea-level change in NWES

Sea-level changes, via their influence on hydrographic restriction in marginal-marine settings, are regarded as one of the main controls on sedimentary Mo accumulation. Here, we compare the Mo profiles of several of the study basins with their sea-level records in order to evaluate such influences. The Late Pliensbachian experienced a eustatic regression, which ended at the top of the *Serpentinum* Zone and was followed by an Early Toarcian transgression that commenced at the base or
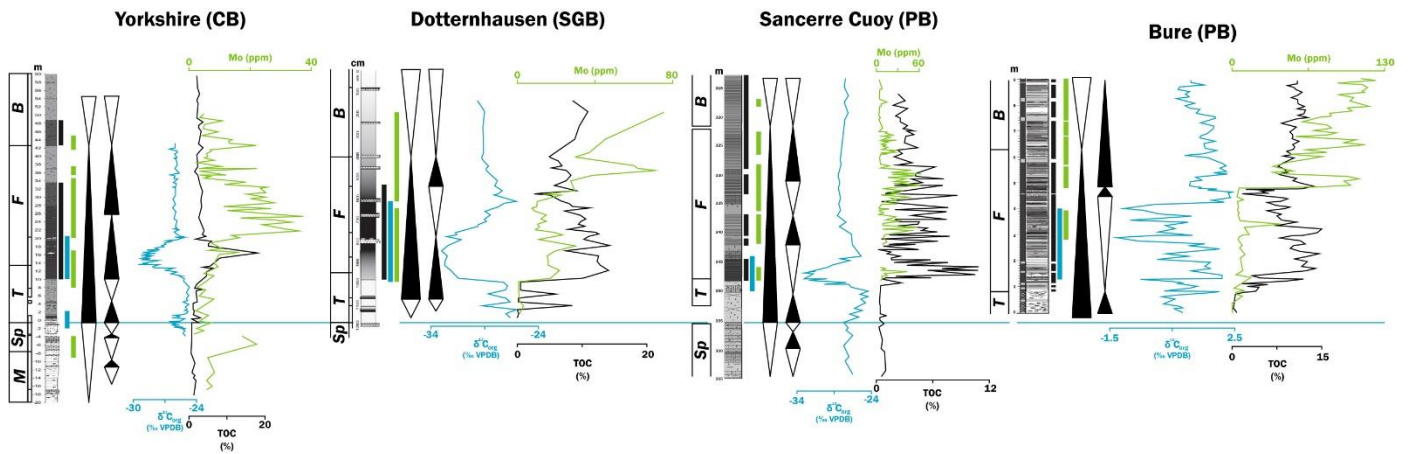
Figure IV.12. Correlation of the transgressive-regressive cycles in several Northwestern Tethyan basins with their profiles of the NCIE, Mo and TOC. Lithology and ammonite zones are indicated. Black rectangles indicate black shale deposits, blue rectangles indicate negative C isotopic excursions, and green rectangles indicate Mo enriched intervals.

within the *Tenuicostatum* Zone. This transgression continued to the *Falciferum/Bifrons* zonal boundary, after which a global regression commenced that continued through the *Bifrons* Zone. Superimposed on this broad global pattern is considerable regional variation, however (Fig. IV.12).

The focus of this analysis is the Northwestern Tethyan region, where most basins are sited among shallow epicontinental seas in which sea-level changes may have had a larger impact on sedimentological dynamics than in other settings due to the abundance of arches and sills serving to isolate various watermasses. Sedimentary Mo concentrations in the Cleveland Basin peaked during transgressions of the *Tenuicostatum* and *Falciferum* zones, but its onset are not coeval with their base: the lower Mo peak coeval with the NCIE begins at the top of a short regression continuing upwards during the subsequent transgression, and the upper peak encompasses two different transgressions; notably, a third Mo enrichment occurs during the regression of the *Bifrons* Zone. In the South German Basin, Mo enriched intervals occur both during transgressions and regressions ranging from the *Tenuicostatum* to the *Bifrons* zones, showing no relation in their onsets. In the Paris Basin, two sections are analysed, showing notably differences among them evidencing the wide variability in these epicontinental settings: the Sancerre Cuoy section exhibits a lower Mo enrichment coeval with the NCIE during a regression in the *Tenuicostatum* to lower *Falciferum* zones, while subsequent enrichments occur

both during transgressions and regressions upwards in the *Falciferum* and *Bifrons* zones; on the other hand, the Bure Area is marked by an enrichment during a regression in the *Falciferum* Zone, coeval with the NCIE and correlated with its analogue in the Sancerre section, followed by several episodes of Mo enrichment during two transgressions upwards the *Falciferum* and *Bifrons* zones.

Therefore, it is very remarkable that sea-level changes show no correlation with Mo-enriched intervals in these settings (in any case the onset of Mo enrichment coincided with the onset of transgressive nor regressive dynamics) (Fig. IV.12). This fact can be explained by several factors (e.g., inaccuracy in determining the boundaries between transgressive and regressive trends, different sequential stratigraphy stages), and evidences that sea-level changes must be interpreted cautiously when regarding hydrographic restriction, and other local factors as an enhanced hydrological cycle, sea currents, sill depth or seawater salinity must have played a major role in the stratification/restriction of the watermass (e.g., Remírez & Algeo, 2020b).

5.4. Global seawater influences on expression of the T-OAE

The present study provides evidence that sedimentary Mo in Toarcian basins was notably lower than Mesozoic and modern environmental analogs, which necessarily implies that the concentration of aqueous Mo in the Toarcian oceans was lower than during other epochs. Therefore, it is likely that the T-
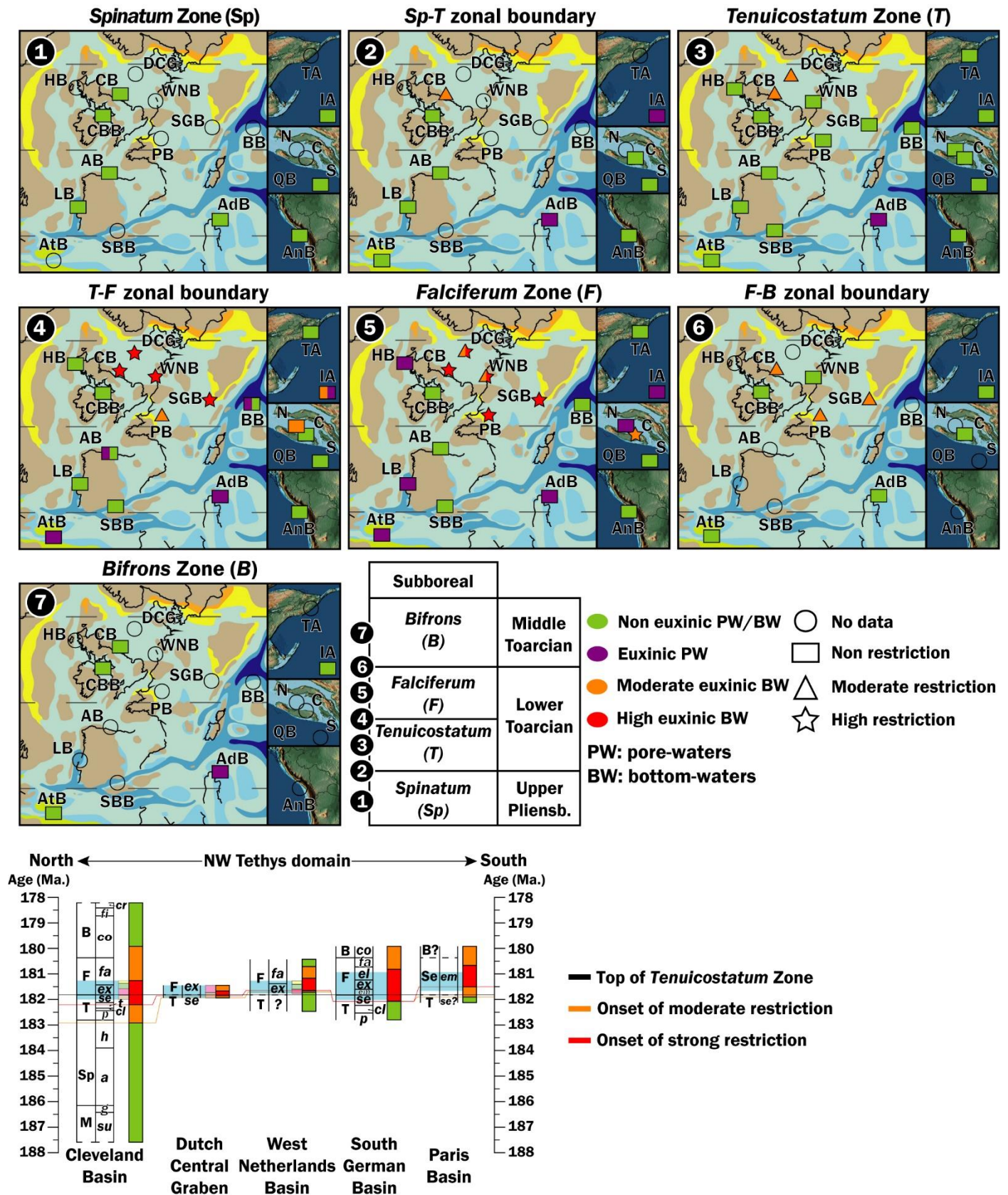
Figure IV.13. Maps illustrating the temporal dynamics of euxinia and hydrographic restriction in bottomwaters from upper Pliensbachian (1) to Middle Toarcian (7). Divided symbols in Tenuicostatum/Falciferum zonal boundary (4) and in Falciferum Zone (5) indicate changes in the intensity of conditions. For basins located in the Northwestern Tethyan region, a detailed biostratigraphy framework is provided based on Figure IV.7, with dates given in Ma (millions of years ago) (Ogg, 2012).

OAE caused depletion of Mo in global seawater, contributing to low sediment Mo/TOC at a global scale. This conclusion was also reached by Thibault et al. (2018), although their analysis considered only two Toarcian sections (in the Cleveland and South German basins) and, therefore, was not sufficient to establish a conclusion of global import. In the present study, this deficiency was addressed by analyzing all Mo data available for Toarcian basins (a total of twenty sections from seventeen basins) and considering multiple features that can affect Mo enrichment in black shales associated with the T-OAE, evidencing the minor role played by sea-level changes as controls in the development of restricted conditions during the T-OAE. More recently, a general depletion of Mo in Toarcian seawater was also inferred by Kemp et al. (2022) based on analysis of an open, deep-marine Panthalassic section, and is supported by the Mo depletion in another Eastern Tethyan, open-marine section (Sewa; Fu et al., 2021). The drawdown of seawater Mo during the T-OAE appears to have been greater than that during other Mesozoic OAEs, including the Cenomanian-Turonian OAE-2 (Hetzel et al., 2009). Therefore, the T-OAE may have been one of the most severe anoxic events of the whole Mesozoic, triggering major changes in seawater chemistry linked to widespread development of bottomwater euxinia and black shale deposition.

At the same time, our results also provide support for the hypothesis that regional/local factors were important controls on regional differences in hydrographic restriction and bottomwater euxinia during the Early Toarcian (Fig. IV.13). Although the T-OAE was triggered by a global-scale phenomenon, i.e., greenhouse gas emissions from the Karoo-Ferrar-Chon Aike Large Igneous Provinces, its final expression in depositional systems was geenerally controlled by local factors, e.g., basinal topography and size, sill depth, hydrological cycle, sea-currents, and connectivity with the open ocean, all of which played an influential role in the final expression of the global T-OAE. Therefore, the global effects of this event, e.g., widespread development of bottomwater anoxia and deposition of black shales, were significantly overprinted by local influences.

6. CONCLUSIONS

The present work supports a drawdown of Mo in global seawater during the Toarcian OAE, leading to low sedimentary Mo/TOC values in euxinic marine facies of many basins. The effects of this global drawdown of aqueous Mo were locally overprinted by local hydrographic factors, especially watermass restriction within some basins of the Northwestern and Eastern Tethys regions. Therefore, this research proposes a model in which the T-OAE caused global effects that were heavily conditioned by local/regional features in each basin, such as regional palaeoenvironment, local palaeogeography, topography, and ocean currents.

The use of sedimentological proxies, combined with Mo and TOC covariations, evidences the onset of asynchronous episodes of high hydrographic restriction with euxinic bottomwaters during the Early Toarcian, mainly at the *Falciferum* Zone. These restricted environments were characterized by high Mo and TOC contents and low regression slope of Mo and TOC ($m_{Mo/TOC}$) associated with black shale deposits in the Northwestern and Eastern Tethys, deposited in shallow silled settings (intrashelf troughs and barrier-lagoons).

In contrast, well-connected bottomwaters are recognized in the rest of the study sections, mostly showing low Mo and TOC values in combination with higher $m_{Mo/TOC}$. These basins were mainly pelagic to hemipelagic settings and carbonate platforms/ramps where water exchange was continuous during all the Toarcian, with minimal Mo enrichments related to sporadic euxinic porewaters in some basins. Notably, open-marine Panthalassic settings can exhibit high Mo and TOC contents accumulated under unrestricted and intermittent euxinic bottomwaters. The Asturian Basin, in the northern Iberian Palaeomargin, represents a special case characterized by local factors, with two major episodes of euxinic porewaters, interrupted by fluctuations between oxic to anoxic/weakly euxinic conditions.

CHAPTER V

The Pennsylvanian cyclothems: sea-level changes, transgressive black shales, and the response of benthic fauna

Tracemaker response to glacio-eustatic cyclic changes: The Late Pennsylvanian Midcontinent Sea

Javier Fernández-Martínez[1*], Francisco J. Rodríguez-Tovar[1], Francisca Martínez Ruíz[2], Thomas J. Algeo [3, 4, 5]

[1] *Departamento de Estratigrafía y Paleontología, Universidad de Granada, Avenida de Fuente Nueva, s/n, Granada 18071, Spain*

[2] *Instituto Andaluz de Ciencias de la Tierra (CSIC-UGR), Av. de las Palmeras, 4, Armilla 18100, Granada, Spain*

[3] *State Key Laboratory of Biogeology and Environmental Geology, China University of Geosciences, Wuhan 430074, China*

[4] *State Key Laboratory of Geological Processes and Mineral Resources, China University of Geosciences, Wuhan 430074, China*

[5] *Department of Geosciences, University of Cincinnati, Cincinnati, OH 45221-0013, U.S.A.*

ABSTRACT

The ichnoassemblages of Upper Pennsylvanian cyclothems in the North American Midcontinent region and their relationship to long-term sea-level changes remain poorly understood. In this study, we conducted a comprehensive ichnological and sedimentological analysis of three complete cyclothemic transgressive-regressive sequences. These sequences include limestone deposits formed during marine transgressions and regressions, black shale deposits under highstand conditions, and sandstone/siltstone alternations and paleosols formed during lowstands. The study focused on three consecutive cyclothems (Hertha, Swope, and Dennis) containing the Mound City, Hushpuckney, and Stark black shales, respectively. These cyclothems were analyzed at sites in the Illinois Basin and the Midcontinent Shelf, representing more proximal (nearshore) and distal (offshore) environments within the Late Pennsylvanian Midcontinent Sea, respectively.

Biogenic structures exhibit a distinct distribution among lithofacies, with *Planolites*, *Palaeophycus*, *Chondrites*, and *?Conichnus* found in nearshore gray shales and siltstones (deposited during lowstands), and *Zoophycos* and *Chondrites* characterizing the offshore black shales (deposited during highstants). The integration of ichnological and sedimentological data permit identification of several depositional paleoenvironments, ranging from open-marine to tidal settings and defined by 12 lithofacies. While lithologies exhibit significant lateral variation across the study basins (carbonate units dominating on the Midcontinent Shelf, and sandstone and shale alternations prevailing in the Illinois Basin), the ichnoassemblages are similar for each facies. The recovery of oxic conditions after highstand anoxic pulses is documented by deep-tier ichnotaxa, with their development strongly influenced by the basin's connection to the open ocean.

KEY WORDS

1. INTRODUCTION

During the final phase of the Late Paleozoic Ice Age, the inner region of the North American continent was predominantly occupied by the Late Pennsylvanian Midcontinent Sea (LPMS) (Heckel, 2023). This shallow, broad epicontinental sea underwent cyclic sedimentation during the Middle Pennsylvanian and Early Permian periods (approximately 315-270 million years ago), associated with subsequent transgressions and regressions of the sea (Heckel, 1977, 1980; see a review in Algeo and Heckel, 2008). These cyclic sedimentary deposits, referred to as cyclothems, were linked to the growth and melting cycles of Gondwanan ice sheets and significant eustatic rises, defining Pennsylvanian sedimentology in the North American region (e.g., Soreghan, 1994; Soreghan and Giles, 1999). A complete cyclothem consists of transgressive and regressive limestone units (sometimes with interbedded shale and sandstone), sandwiching a central organic-rich black "core shale" deposited under anoxic conditions during the sea-level highstand, and topped by a paleosol (massive claystone and coal beds) representing the sea-level lowstand (Heckel, 1980).

In the context of substantial sea-level changes and sediment deposition under anoxic/euxinic conditions, ichnology emerges as a well-established tool for paleoenvironmental characterization. Since the late 20th century, ichnology has been widely employed in sequence stratigraphic research to identify genetically related sedimentary packages such as depositional sequences, system tracts, and transgressive-regressive sequences. The recognition of substrate-controlled ichnoassemblages and the description of vertical distribution of trace fossils enable geologists to identify discontinuities between different packages and interpret their paleoenvironmental significance in both marine and continental settings (e.g., Pemberton and MacEachern, 1995; Olóriz and Rodríguez-Tovar, 2000; Buatois and Mángano, 2004, 2009; Pearson et al., 2012; Bayet-Goll et al., 2017; see Rodríguez-Tovar, 2010 for a review). Ichnology has also been utilized to characterize not only the "Big Five" mass extinctions (e.g., Nichols, 2018; Luo et al., 2020; Rodríguez-Tovar et al., 2022) but also

minor events related to abrupt changes in bottomwater oxygenation, leading to the deposition of organic-rich sediments in most cases. Examples include the Toarcian Oceanic Anoxic Event (early Toarcian, Lower Jurassic) (e.g., Fernández-Martínez et al., 2021a, b; Rodríguez-Tovar, 2021) or the Bonarelli Event (Cenomanian-Turonian boundary, Upper Cretaceous) (e.g., Uchman et al., 2013). In the case of the LPMS, shifts between oxic and anoxic conditions during sea-level highstands led to the deposition of black shale facies (e.g., Heckel, 1977; Algeo et al., 1997, 2004), and the study of their ichnology and sedimentary structures allows for an assessment of the response of benthic communities to changes in bottomwater conditions.

Previous ichnological works in the LPMS allowed a detailed characterization of marginal-marine depositional settings (see section *Ichnology of the LPMS*), analyzing both vertical and lateral distribution of trace fossils (e.g., Martino, 1989; Mángano et al., 2002). However, the study of black shale facies is still poorly developed. Thus, in this work we have studied three successive cyclothems (Hertha, Swope, and Dennis) of the Missourian Stage (lower Upper Pennsylvanian; c. 305 Ma), characterized by the record of their respective black "core shale" facies (Mound City, Hushpuckney, and Stark, respectively) (Fig. V.1A). An integrated sedimentological and ichnological analysis has been conducted, aiming to assess the influence of long-term sea-level changes on seafloor paleoenvironmental conditions affecting macrobenthic tracemaker communities.

Our analyses included five cores from Illinois and Kansas (U.S.A.), representing sedimentation in two different basins of the Late Pennsylvanian Midcontinent Sea, i.e., the Illinois Basin and the Midcontinent Shelf (Fig. V.1B). This study is focused on characterizing trace fossil assemblages present in each cyclothemic facies association, with special attention to the black shale facies, which represents changes from anoxic/euxinic to dysoxic/oxic bottom- and porewaters, thus representing the recovery of the macrobenthic community after an interval of inhospitable, de-oxygenated seafloor conditions.
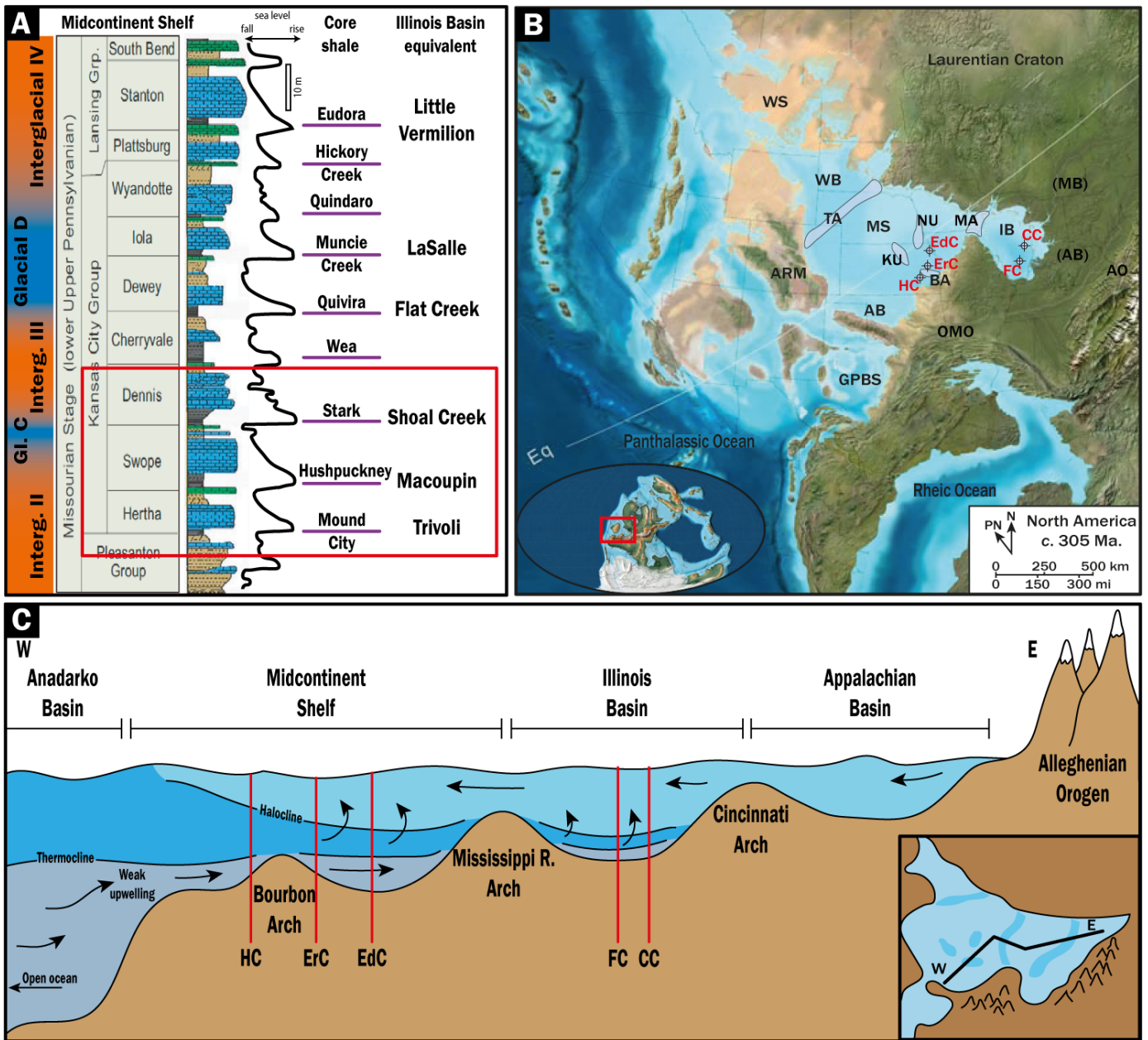
Figure V.1. Biostratigraphy and paleogeography of the study sections. (A) Stratigraphic column of several Missourian cyclothems, indicating names, sea-level changes, glacial-interglacial phases, core shale names, and the correlation between the Midcontinent Shelf and the Illinois Basin (modified from Fig. 1 in Algeo & Heckel, 2008). Red rectangle indicates studied cyclothems; (B) Paleogeographic map of the Late Pennsylvanian Midcontient Sea, indicating the location of the studied cores, and the names of the main basins, orogens, and submerged arches. Gray-shadowed lines indicates actual frontiers between U.S.A. states. Map of the Earth during Late Pennsylvanian at bottom-left corner; (C) Cross-section of the Late Pennsylvanian Midcontinent Sea, indicating the position of the studied cores and the submerged arches, and showing the watermass circulation patterns and the position of the halo- and thermocline (modified from Fig. 2 in Algeo & Heckel, 2008). AB: Anadarko Basin, (AB): Appalachian Basin, AO: Alleghenian Orogen, ARM: Ancestral Rocky Mountains, BA: Bourbon Arch, CC: Charleston core, EdC: Edmonds core, ErC: Ermal core, FC: Fritschle core, GPBS: Greater Permian Basin Seaway, HC: Heilman core, IB: Illinois Basin, KU: Central Kansas Uplift, (MB): Michigan Basin; MS: Midcontinent Shelf, NU: Nemaha Uplift, OMO: Ouachita-Marathon Orogen, PN: paleo-north, TA: Transcontinental Arch, WB: Williston Basin, WS: Wyoming Shelf.
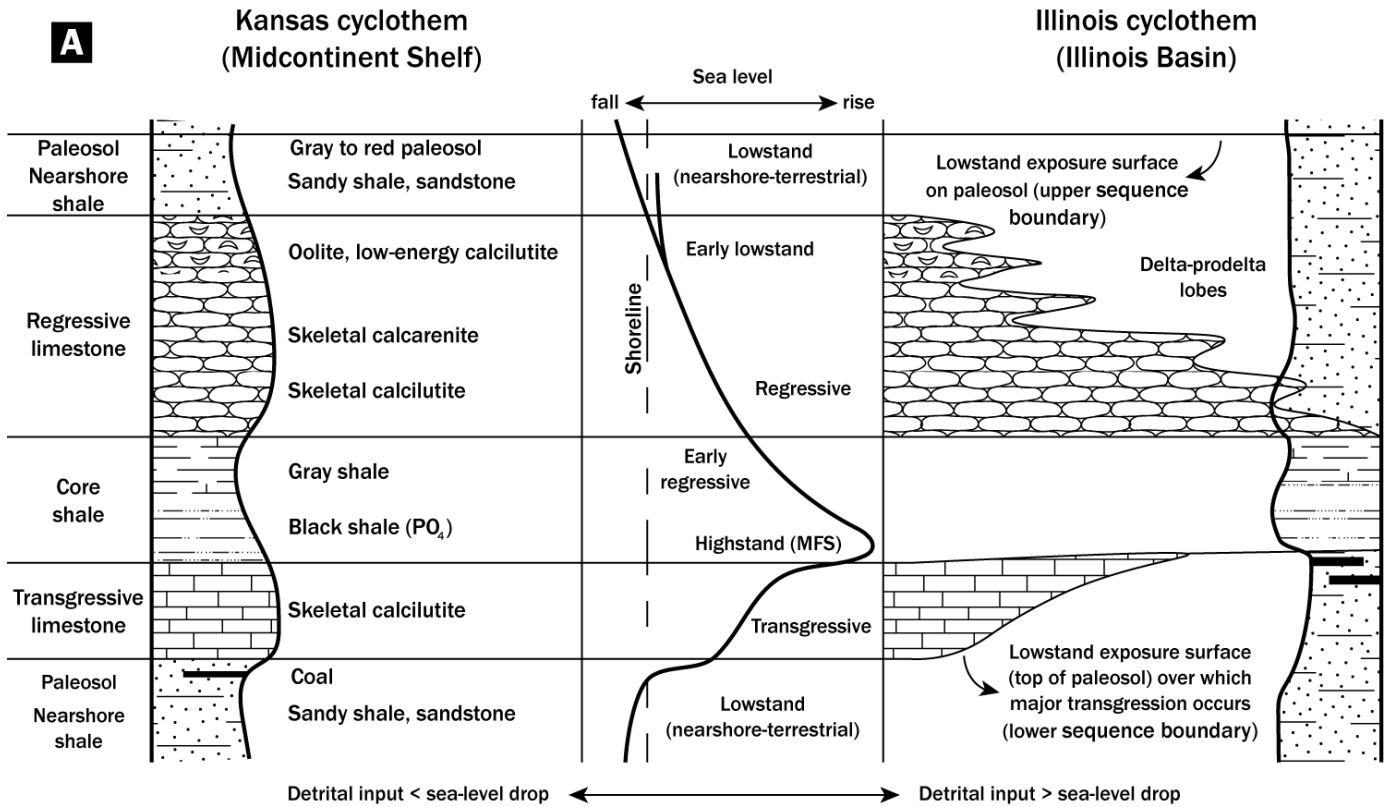
Figure V.2. Schematic ideal cyclothem for the Midcontinent Shelf and its correlation with the Illinois Basin, indicating the cyclothemic facies associations, sea-level changes, sequential stages and lithologies (modified from Figs. 2 and 7 in Heckel, 1977). Note the reduction in thickness of limestones from the Midcontinent Shelf through the Illinois Basin, and the prevalence of sandstones and shales in the latter. MFS: maximum flooding surface.

2. GEOLOGIC BACKGROUND

2.1 Geography, tectonics, and climate of Late Pennsylvanian North America

The Late Pennsylvanian Midcontinent Sea (LPMS) comprises several basins (Fig. V.1B-C), arranged from east to west: Appalachian Basin, Illinois Basin, Michigan Basin, Midcontinent Shelf, and Williston Basin. To the southwest, the LPMS connects with the Panthalassic Ocean through a lengthy, winding strait passing through the Anadarko Basin and the Great Permian Basin region. Despite this connection, the LPMS is mostly surrounded by landmasses, influenced by various active orogens during the Pennsylvanian and Permian periods (see review of Algeo and Heckel, 2008). The Ancestral Rocky Mountains in the west separated the LPMS from the open Panthalassic Ocean, while the eastern and southern margins of North America were affected by the Appalachian and Ouachita-Marathon orogens, separating it from the open Rheic Ocean (e.g., Arbenz, 1989; Yang and Dorobek, 1995;

Ye et al., 1996). The Laurentian Craton forms the lower-altitude northern margin, while the Wyoming Shelf dominates the northwestern margin. The southern Greater Permian Basin Seaway provided the only long-term connection of the LPMS to the open ocean, making the latter almost, but not entirely, landlocked (Fig. V.1B).

The bathymetry of the LPMS increases westwards, featuring several arches in the bottom topography (Fig. V.1C). The shallow Appalachian Basin is separated from the Illinois Basin by the Cincinnati Arch, and the latter is separated from the Midcontinent Shelf by the Mississippi River Arch (Kolata and Nelson, 1990; Algeo and Herrmann, 2018). The Transcontinental Arch detaches the Midcontinent Shelf from the Williston Basin, with uplifts present in the central (Nemaha Uplift) and southern (Central Kansas Uplift and Bourbon Arch) areas. The Bourbon Arch, situated between the distal Midcontinent Shelf and the southern, deep Anadarko Basin, connected with the

Greater Permian Basin Seaway at a paleolatitude approximately 5-8° N (Fig. V.1B). The latter connection facilitated the transfer of shallow pools of oxygen-deficient waters from Panthalassa to the LPMS through the Panhandle Strait, contributing to the development of anoxic bottom-waters during transgressive phases of sea-level cycles (Handford and Dutton, 1980; Algeo and Heckel, 2008).

The Alleghenian-Ouachita-Marathon orogenic belt in the southeast influenced the LPMS with humid Trade Winds from the northeast, resulting in a monsoonal climate (e.g., Soreghan et al., 2002; Cecil et al., 2003a). Coupled with tropical conditions, this climate brought high precipitation and significant continental runoff into the LPMS (Gibling et al., 1992; Archer and Greb, 1995; Cecil et al., 2003b). These climatic factors played a crucial role in the sedimentological dynamics, with proximal settings like the Appalachian and Illinois basins showing thick sandstone and shale deposits indicative of fluvio-deltaic systems, while marine carbonates dominated in the distal Midcontinent Shelf (Fig. V.2) (e.g., Heckel, 1977; Bisnett, 2001).

The paleogeographic boundary conditions of the LPMS resulted in a pattern of watermass circulation referred to as "superestuarine" (Algeo and Heckel, 2008; Algeo et al., 2008). During flooding episodes, widespread anoxic conditions developed due to the westward influx of oxygen-deprived waters from Panthalassa, coupled with humid conditions causing substantial continental freshwater runoff from the east. This interplay of factors in the mostly landlocked basins created a gradient of benthic redox conditions, with stronger anoxic pulses occurring in the inner, shallower regions of the LPMS (Illinois and Appalachian basins). In these basins, regional precipitations and extensive continental runoffs fostered a robust halocline and a deep pycnocline (Fig. V.1C), limiting vertical water-mixing and facilitating the development of anoxic conditions, preconditioned by the oxygen-deprived deep watermass from Panthalassa. Consequently, the development of anoxic conditions in the LPMS was highly susceptible to changes in climatic conditions (Algeo and Heckel, 2008, and references therein).

2.2. Stratigraphy

Each depositional cycle comprises four distinct facies associations, representing a single transgressive-regressive cycle (deposition of a major cyclothem ranges from 235 to 393 kyr, Heckel, 1986) (Fig. V.2). An ideal cyclothem, as outlined by Heckel (1977, 2013, 2023), consists, from bottom to top, of the following: I) Transgressive successions characterized by thin (0.3 – 1.5 m), dark, and dense skeletal calcilutite beds, featuring abundant and diverse marine fossils ("transgressive limestones"). These beds usually overlie paleosols. II) Shale successions, represented by thin (< 1 m), black to gray shale beds with abundant conodonts and phosphatic lenses/layers. These successions signify the maximum flooding episodes and are deposited during highstand conditions under anoxic/euxinic (black) to dysoxic (gray) bottom- and pore-waters ("core shales"). III) Regressive successions characterized by thick limestone beds (up to 9 m), featuring abundant and diverse marine fossil content. This category consists of a lower part (skeletal calcilutite) and an upper part (variable lithology depending on the paleogeographic setting) ("regressive limestones"). IV) Shale and sandstone successions deposited during lowstand conditions, exhibiting variable thickness and sandy content ("nearshore shales"). These successions are characterized by the absence or sparse distribution of marine fossils, and the presence of coal beds and claystone units interpreted as paleosols.

Importantly, these cyclothems exhibit lateral correlation throughout the LPMS, as documented by Heckel (2013). Conodonts, particularly abundant in the core shales, and the correlation of coal beds and their stratigraphic position serve as primary tools of correlation. Despite variations in nomenclature across different basins, most major cyclothems are present and correlated from the Midcontinent Shelf to the Illinois and Appalachian basins.
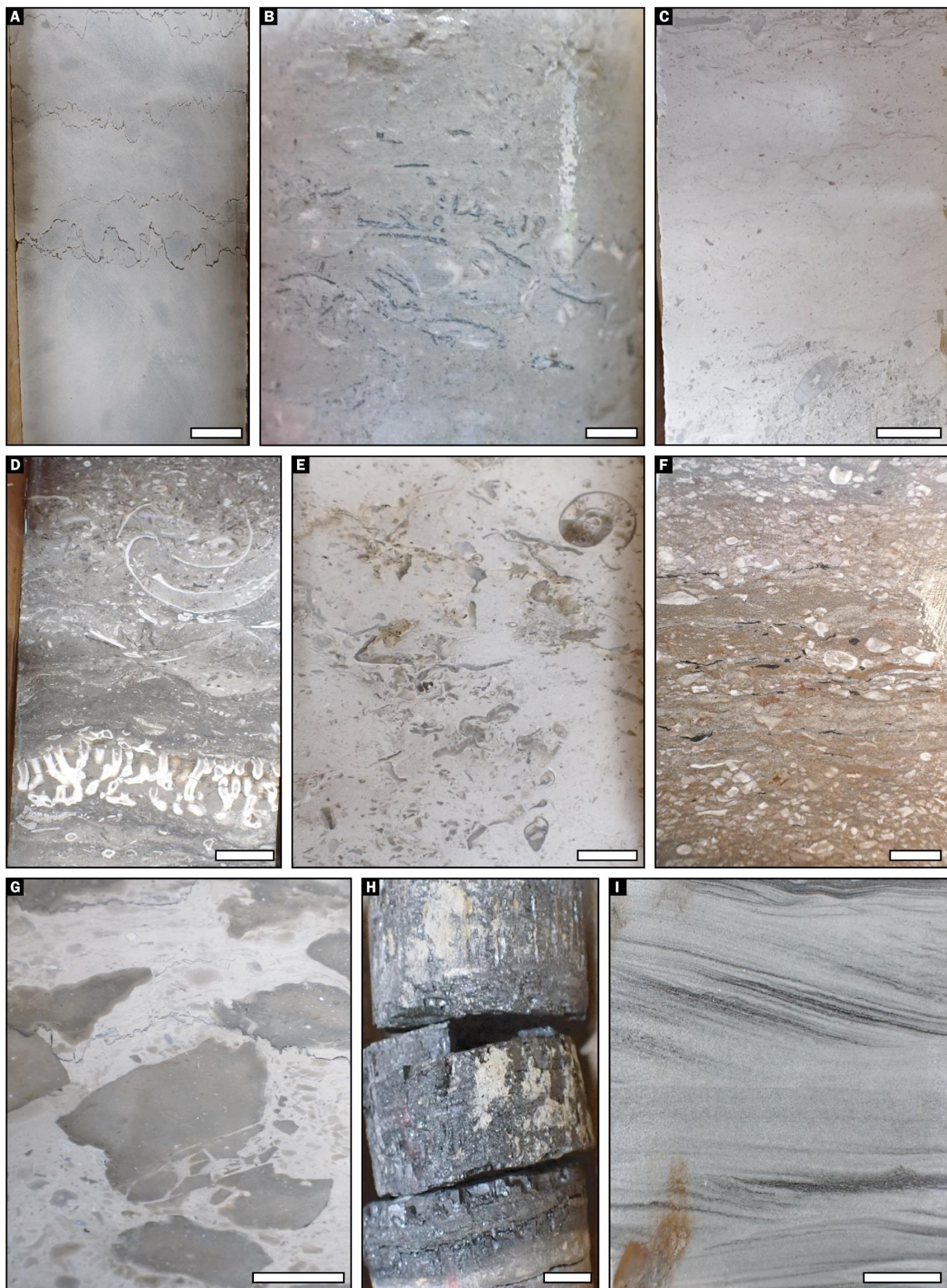
The two study sections in the Illinois Basin are positioned near the center of the basin (Fig. V.1B-C), approximately 60 km apart, showcasing continental influence with evidence of marginal-marine settings through sandstone beds and large-scale interfingering of sandstone and shale. In contrast, the three study sections on the Midcontinent Shelf (Fig. V.1B-C) predominantly exhibit carbonate facies, manifested as thick limestone beds with highly variable fossil content (Fig. V.2). The Midcontinent Shelf, as classified by Heckel (1977), is divided into different facies from north to south: (1) shoreline units consisting of mudflats to coastal shoals, (2) open-marine shelf units characterized by well-developed cyclothems and marine carbonates, (3) shelf-margin algal mound facies, and (4) a basinal terrigenous-detrital belt consisting of thick sandstone beds. In this context, we have studied one core from the open-marine shelf (Edmonds) and two cores from the algal-mound facies, one to the north (Ermal) and the other to the south (Heilman) of the Bourbon Arch (Fig. V.1B-C). Thus, the two study sections in the central Illinois Basin represent similar restricted-shelf settings, but the three from the Midcontinent Shelf represent a spectrum of proximal to distal open-shelf environments.

3. UPDATE ICHNOLOGICAL INFORMATION OF THE LPMS

Numerous studies have delved into trace fossils within cyclothems, with a particular emphasis on siliciclastic units deposited in marginal-marine environments. Conversely, carbonate units, paleosols, and organic-rich shales remain relatively understudied from an ichnological perspective. In brief, siliciclastic units deposited in marginal-marine settings such as estuaries, tidal flats, deltaic areas, or embayments (i.e., nearshore shales) display diverse ichnoassociations. The distribution of these associations is significantly influenced by salinity, showcasing higher diversity under marine and freshwater conditions and lower diversity or monospecific suites in brackish settings. In contrast, carbonate units (i.e., regressive and transgressive limestones) commonly feature a mottled texture indicative of extensive biogenic reworking. Bivalve burrows are prevalent, and in the presence of siltstone interbeds, poorly diverse ichnoassociations with *Rhizocorallium*, *Chondrites*, and *Planolites* may be observed. Notably, *Zoophycos* has been identified in facies deposited in environments characterized by oxygen-deprived bottomwaters.

Fenton and Fenton (1937a, b) present the earliest reports of trace fossils within Pennsylvanian cyclothems, having identified several new ichnogenera such as *Olivellites* and *Aulichnites* in Texas sediments. Decades later, the initial reports of tetrapod tracks emerged, albeit sporadically and infrequently found among Pennsylvanian sediments in Kansas (Moore, 1964). In their study, Moore and Merriam (1965) acknowledged the presence of tracks and burrows in the Rock Lake Shale (Missourian). Bandel (1967a) was the first to exclusively focus on invertebrate trace fossils, specifically in the Rock Lake Shale, comparing it with the Virgilian Vinland Shale. The work described diverse ichnoassemblages unique to each unit, although both were classified within the Seilacherian *Cruziana* ichnofacies. Notable ichnogenera identified included

Figure V.3. Core photos illustrating the different lithofacies present in the study sections (note: core and footage indicated in brackets). (A) Facies D: white calcareous mudstone with stylolite and a homogeneous (mottled) texture (Edmonds ft. 430); (B) Facies F: shell bed of Lingulata brachiopods within a light-gray calcareous wackestone (Edmonds ft. 438); (C) Facies D: white calcareous mudstone with sparse crinoids fossils at the lower part (Heilman ft. 168); (D) Facies F: gray calcareous wackestone with disarticulated gastropod, crinoid, bivalve and coral fossils (Heilman ft. 200); (E) Facies F: gray calcareous wackestone with abundant gastropod and bivalve remains (Heilman ft. 174); (F) Facies F: brownish calcareous grainstone/wackestone with disarticulated crinoid and coral remains, note the presence of dark claystone lenses (Charleston ft. 771); (G) Facies G: calcareous breccia formed by angular clasts embedded within light-gray carbonate mudstone (Ermal ft. 78); (H) Facies K: coal bed (Galesburg paleosol) (Heilman ft. 100.5); (I) Facies C: yellow, fine-grained sandstone bed with thin layers of black claystone/siltstone. Note the alternation between trough crossbedding and planar lamination (Heilman ft. 84). Top is always upwards. Scale bar is 1 cm (0.4 in).
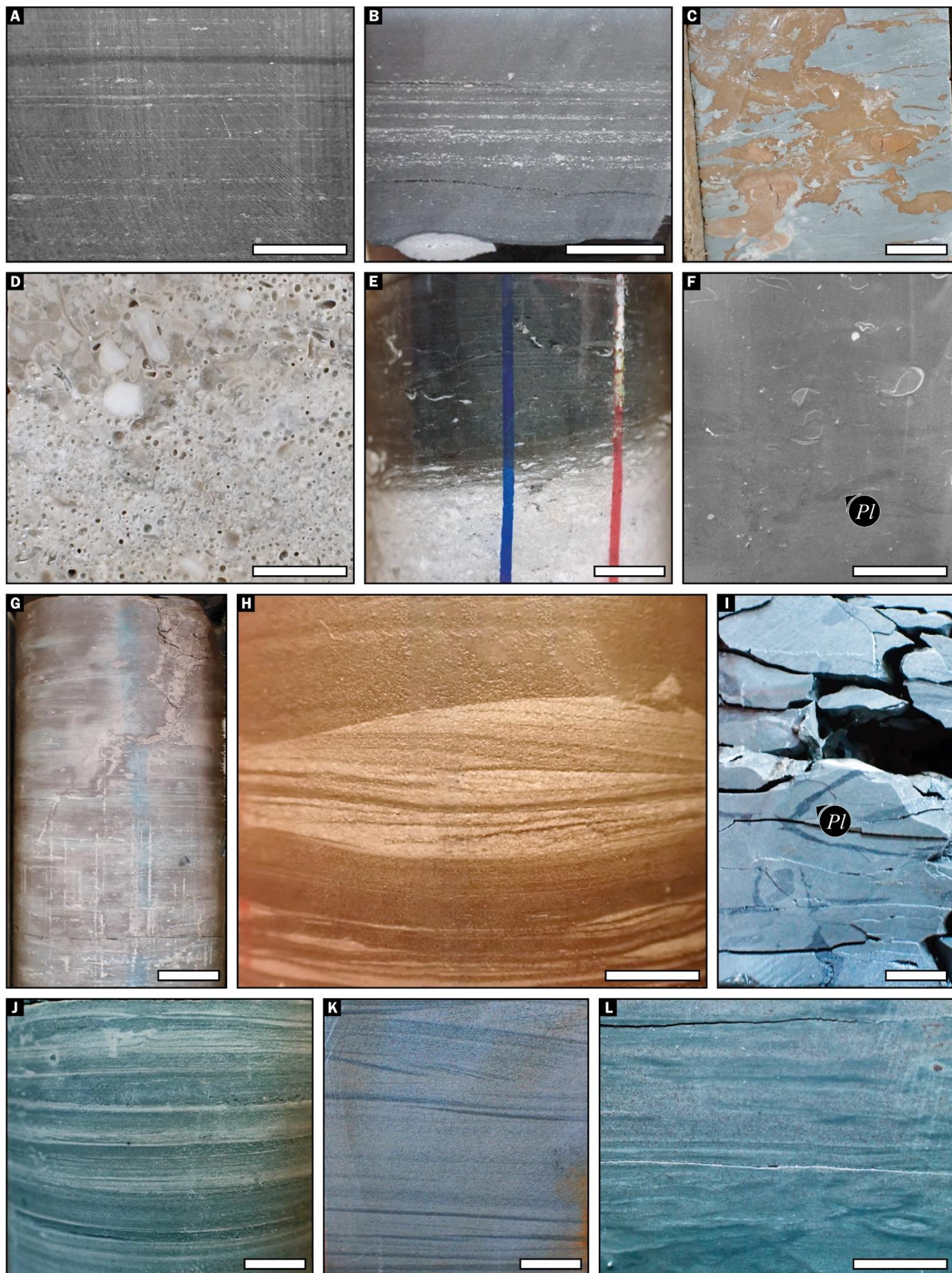
Asterichnus, *Gordia*, *Chondrites*, *Zoophycos*, and *Planolites*. In a subsequent work, the same author (Bandel, 1967b) detailed trails and tracks presumed to be produced by limulids and isopods in the Tonganoxie Sandstone (Virgilian).

3.1. Ichnology of carbonate units

Concerning calcareous rocks, the pioneer publications on this subject were by Harbaugh and Davie (1964) and Imbrie et al. (1964). In these papers, they documented a mottled texture and vertical burrowing attributed to bivalves in limestones from the upper Pennsylvanian and Lower Permian, respectively. Subsequently, Ball (1971) reported trace fossils in the Westphalia Limestone (Virgilian), which overlies the Tonganoxie Sandstone. The study concluded that the activity of bivalves, colonizing benthic settings after storm events, significantly influenced the packing of fusulinid grains in calcareous mud, resulting in grainstone textures at its lower contact with siliciclastic beds.

Following this, Maerz et al. (1976) conducted research on bioturbation in two Virgilian limestones from Kansas. They reported vertical burrows in grainstone beds directly overlying siliciclastic units and introduced a new ichnogenus produced by ophiuroids called *Pentichnus*. Merrill (1983) identified large *Rhizocorallium*, along with *Chondrites* and *Planolites*, in limestones interbedded within siliciclastic units (Oak Grove Member, Desmoinesian). Lastly, Joeckel (2008)

described enigmatic structures in the Stoner Limestone (Missourian) in Nebraska, displaying similarities to *Conichnus* and *Conostichnus*. However, their biogenic origin remains problematic.

3.2. Ichnology of paleosol-bearing units

Miller and Knox (1985) focused on coal-bearing sequences in Tennessee, specifically the Fentress Formation from the Lower Pennsylvanian. They utilized trace fossils to reconstruct the depositional settings of several largely unfossiliferous units. Their study identified three primary ichnoassemblages, with the absence of non-marine trace fossils, leading to the conclusion that coals were deposited in transitional settings such as back-barrier lagoons, tidal flats, or deltaic environments. Subsequently, this paper was incorporated into a comprehensive review of trace fossils in coal-bearing sequences by Pollard (1988).

3.3. Ichnology of siliciclastic units

Siliciclastic rocks, predominantly sandstone and shale units, represent the most extensively studied successions within cyclothems. A series of papers by Hakes (1976, 1977) delved into the Rock Lake Shale and other Virgilian units, identifying diverse ichnoassemblages. Notably, the Rock Lake Shale exhibited a rich variety of trace fossils, including *Asteriacites*, *Bergaueria*, *Chondrites*, *Lockeia*, *Aulichnites*, *Planolites*, and unclassified arthropod trails and burrows.

Figure V.4. Core photos illustrating the different lithofacies present in the study sections (note: core and footage indicated in brackets). (A-B) Facies H: organic-rich, black shale beds with planar parallel lamination formed by thin siltstone layers (A) and phosphate-rich layers and nodule (B) (Charleston ft. 736 and Edmonds ft. 403, respectively); (C) Facies J: light-gray claystone with abundant siderite content, note the faint mottled texture (Charleston ft. 746); (D) Facies E: white, porous carbonate bed in the lower part, and oolitic grainstone in the upper part (Ermal ft. 60); (E) Lower contact of a black shale bed (facies H) with a white limestone bed (facies D), note the erosive nature of the contact and the presence of small calcareous fragments (Edmonds ft. 434.5); (F) Facies I: calcareous gray siltstone with scarce brachiopod shells. Note the mottled texture overprinted by dark-infilled Planolites *(Heilman ft. 215.5); (G) Facies J: red to light gray claystone unit. Red color is due to siderite (iron) content. Upper structure likely represent a root mold (Edmonds ft.. 460); (H) Facies B: dark-gray siltstone with interbedded yellow, fine-grained sandstone beds. The lower part showcase wavy / lenticular bedding, while the center part is characterized by trough crossbbeding (Heilman ft.. 215.5); (I) Facies I: light-gray siltstone with dark-infilled* Planolites *(Ermal ft. 46); (J) Facies B: dark-gray siltstone beds alternating with yellow, fine-grained sandstone layers, forming fining-upward sequences (Heilman ft. 97); (K) Facies C: yellow, fine-grained sandstone bed with interbedded fine dark-gray siltstone layers. Parallel lamination turns upwards to cressbedding (Heilman ft. 70); (L) Facies J: light- and dark-gray claystone with alternating mottled texture and parallel lamination (Fritschle ft. 938). Top is always upwards. Scale bar is 1 cm (0.4 in). Pl: Planolites.*
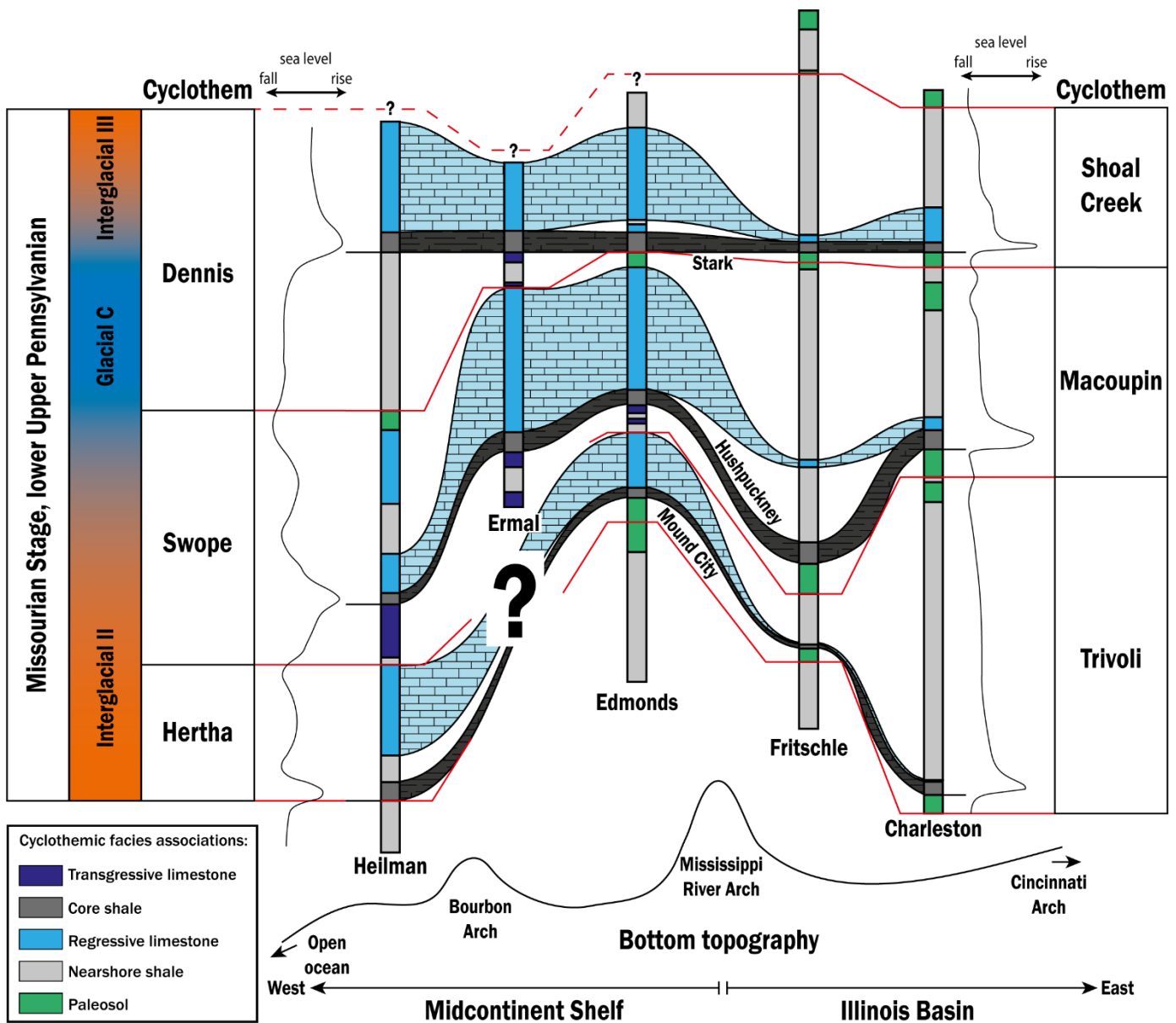
Figure V.5. Correlation of the studied cyclothems through the Midcontinent Shelf and the Illinois Basin (note that the same cyclothem has a different name in each basin). Stratigraphic columns showing the cyclothemic facies associations identified in each core, the correlation of the "core shale" units (Mound City, Hushpuckney and Stark) and the main regressive limestones. Also, sea level curves for the Heilman and Charleston cores. Note that the Hertha cyclothem is not present in the Ermal core. Base of Stark core shale is selected as datum.

This diversity suggested a wide range of depositional settings, ranging from marine to freshwater environments.

In subsequent research, Hakes (1985) focused on these units to describe the characteristics of brackish water ichnoassemblages. This work highlighted relatively abundant and diverse, albeit diminutive, ichnogenera in these environments. Similarly, Archer and Maples (1984) explored various deltaic environments (Morrowan and Desmoinesian), identifying ichnoassemblages for each unit. Their findings indicated lower ichnodiversity in brackish conditions, with an increase towards marine and freshwater settings. Devera (1989) reported brackish conditions in southern Illinois after studying Lower Pennsylvanian sandstone and shale units. Despite high ichnodiversity, the traces were produced by a few distinct tracemakers. Martino (1989) investigated the lateral and vertical distribution of trace fossils in the Kanawha Fm. from West Virginia (Middle

Pennsylvanian). Three ichnoassemblages were identified, strongly influenced by the salinity gradient: annulated vertical burrows in deltaic and fluvial settings under freshwater conditions; *Phycodes-Zoophycos* assemblage in tidal flats and restricted bays under poorly oxygenated bottomwaters; and *Olivellites* ichnoassemblage, described as an impoverished version of the *Cruziana* ichnofacies, developed in tidal flats and distributary mouth bars.

In western North America, several studies have detailed the ichnology of siliciclastic units. Marine to non-marine successions from the Minturn and Fountain formations in Colorado (Desmoinesian and Atokan, respectively) were investigated by Lockley (1987) and Maples and Suttner (1990). They described ichnoassociations dominated by the ichnogenera *Curvolithus* in nearshore settings with high sedimentation rates. Burton and Link (1991) examined carbonate-clastic mixed turbidites from the Pennsylvanian-Permian boundary in Idaho. The work reported *Chondrites* in facies representing dysoxic inter-turbidite settings. After turbidite deposits, oxygen-rich water fluxes led to the establishment of two different ichnocoenoses: one dominated by pascichnia (such as *Phycosiphon* and *Taenidium*), and a second one which substituted the former with fodinichnia (*Zoophycos* and *Lophoctenium*). In Utah, Chamberlain and Clark (1973) investigated the Oquirrh Fm., describing the vertical distribution of trace fossils in the homonymous basin: *Cruziana* ichnofacies from Morrowan to Desmoinesian, *Zoophycos* and *Scalarituba* in fine sandstone units deposited from Atokan to Virgilian, and a high ichnodiversity assemblage within fine-grained turbidite units (*Nereites*, *Scalarituba*, *Neonereites*, *Phycosiphon*, *Spirophycus*, and *Lophoctenium*) deposited during Virgilian and Early Permian.

Eastwards, the Appalachian Basin was explored by Greb and Chesnut (1994). They described units from the Breathitt Fm. (Morrowan) in Kentucky, deposited in shallow-marine to brackish tidal-flats, identifying four different facies: dark shale facies with low-diverse ichnoassemblages (*Conostichnus*, *Planolites*, and *Thalassinoides*) and interbedded siltstone beds exhibiting higher ichnodiversity (*Lockeia*, *Paleophycus*, *Monocraterion*, and *Rhabdoglyphus*); bioturbated sandstone units with

Asterosoma, *Conostichus*, and *Rosselia*, and siltstone and gray shale beds with abundant *Planolites* and *Teichichnus*; ripple-bedded sandstone and shale with variable diversity and abundance of trace fossils, including *Asterosoma*, *Curvolithus*, *Helminthoida*, and *Lockeia*, among others; and two ripple-dominated sandstone units deposited in channel fills where trace fossils are rare (only *Beaconichnus* and arthropod resting tracks).

Moving southwards, the Arkoma Basin and the Ouachita Mountains were examined by Chamberlain (1971a, b), detailing the lateral and vertical distribution of trace fossils in marine settings during the Pennsylvanian. Mud substrates were dominated by *Nereites*, indicating oxygenated bottom waters in Central Ouachita; highly diverse ichnoassemblages dominated by *Chondrites*, *Zoophycos*, or *Cruziana* occurred northwards in the siltstone flysch facies from Frontal Ouachita; and the Anadarko Basin is characterized by the presence of a *Cruziana* ichnoassemblage within shallow open- or marginal-marine settings.

In the late 1990s and early 2000s, a series of papers by Mángano, Buatois, and collaborators focused on describing marginal-marine settings in Kansas. Buatois et al. (1997) revisited the Tonganoxie Sandstone (Virgilian) at Buildex Quarry, examining the ichnology of tidal rhythmites (planar-laminated siltstones) deposited in the proximal zone of an inner estuary. Despite lithofacies being decoupled from salinity, the identification of *Mermia* and *Scoyenia* ichnofacies allowed for the precise delineation of freshwater/terrestrial benthic fauna, outlining the salinity gradient in the estuarine system. In the same units, Buatois et al. (1998a) explored crosscut relationships, concluding that grazing and feeding traces were formed in a soft, submerged substrate. Resting and arthropod tracks are registered in stiffer, subaerial substrates. Isopod traces previously described by Bandel (1967b) were reinterpreted as myriapod (*Diplichnites gouldi*) and limulid tracks (*Kouphichnium* and *Dendroichnites*). Buatois et al. (1998b) emphasized the significance of the Buildex ichnofauna for sequence stratigraphy, detailing the fresh-to-brackish succession during a TST by the replacement of the *Mermia*/*Scoyenia* ichnofacies with the *Cruziana* ichnofacies. Remarkably well-preserved trace fossils

facilitated detailed ichnotaxonomy: the characterization of the ichnogenus *Tonganoxichnus*, representing feeding and resting traces produced by monuran insects (Mángano et al., 1997, described later in Indiana by Mángano et al., 2001); the reassessment of *Beaconichnus* as *Diplichnites* and the description of several myriapod tracks (Buatois et al., 1998c); and the analysis of the ichnogenus *Asteriacites*, interpreted as the work of ophiuroids (not asteroids) in brackish environments (Mángano et al., 1999), a topic previously studied by West and Ward (1990).

Buatois et al. (1999, 2002) study estuary and open-marine settings recorded in cores drilled from the Morrow Sandstone (Morrowan). They found that ichnodiversity was low in estuarine facies due to harsh conditions (brackish bottomwaters), resulting in depauperate *Skolithos* and *Cruziana* ichnofacies and common monospecific suites, whose tracemakers displayed an *r*-strategy (opportunistic). In contrast, open-marine facies exhibited higher ichnodiversity produced by climax benthic organisms (*K*-strategy) under full-marine salinities.

Mángano et al. (1998, 2002) conducted a study of the Stull Shale Member (Virgilian) at Waverly, detailing several subfacies in a microtidal shoreline (tidal flat) connected with the open sea. Despite harsh conditions, including desiccation, salinity, high-energy, and high temperatures, these settings led to highly diverse ichnoassociations (41 ichnotaxa). The distribution of trace fossils varied from rich benthic communities in sand-flat facies to poorly diverse benthos in mud- and mixed-flat units, indicating more stressful conditions. A detailed analysis of crosscutting relationships allowed the identification of two different groups of *Lockeia*, such as large specimens with associated vertical burrows, suggesting permanent residence and filter-feeding, and small specimens associated with locomotion traces, indicating the movement of deposit-feeders.

Works conducted from 2000 to 2020 further showcased the diversity of trace fossils in Pennsylvanian siliciclastic units. McIlroy and Falcon-Lang (2006) identified *Zoophycos*-group trace fossils in the Maritimes

Basin (Stephanian of Nova Scotia, Canada). Smith et al. (2011) described *Cochlichnus* and *Diplichnites* in siltstones from the Llewellyn Fm. (Bashkirian-Gzhelian) at Pennsylvania, deposited in swamp settings under freshwater conditions. Getty et al. (2013, 2017) studied the Rhode Island Fm. (Westphalian) from the Narragansett Basin, describing lacustrine settings with trace fossils from the *Mermia* and *Scoyenia* ichnofacies, including *Tonganoxichnus*. Finally, Liebach et al. (2020) described trace fossils produced in an estuary by *Xiphosura* (horseshoe crab), occurring with *Rhizocorallium*, coprolites, and crab body fossils in the Pony Creek Shale (Virgilian).

4. MATERIALS AND METHODS

Five cores from various states in the U.S.A. (Fig. V.1B), have been studied: Edmonds (EdC, API#1510321241), Ermal (ErC, KID#1037995662), and Heilman (HC, KID#1032413173), stored at the warehouse of the Kansas Geological Survey, and Charleston (CC, API#120292279500) and Fritschle (FC, API#120792535400) from the Illinois State Geological Survey. The segments analyzed from each core were selected based on the presence of previously identified core shales (Hushpuckney, Stark, and Mound City) (e.g., Algeo et al., 1997; Bisnett, 2001), aiming to correlate the analyzed intervals through the Illinois Basin (Fritschle and Charleston cores) and the Midcontinent Shelf (Edmonds, Ermal, and Heilman cores).

An integrative sedimentological/stratigraphical and ichnological analysis was conducted on the studied core intervals. Sedimentological/stratigraphical analyses focused on lithology, texture, and sedimentary structures, especially lamination. Additionally, the fossil content of each unit was assessed. Ichnological analyses focused on ichnofabric characterization, encompassing ichnotaxonomy, size of traces, distribution, abundance, infilling material, cross-cutting relationships, orientation, internal structures, and penetration depth. Abundance is expressed by the bioturbation index (BI) (Reineck, 1963, 1967; slightly modified by Taylor and Goldring, 1993), where 0 indicates the absence of trace

fossils, and 6 designates complete biogenic reworking, usually resulting in a mottled texture.

Detailed photographs were taken to illustrate both the lithological texture and the described ichnofabrics. Some photos were then processed using Adobe Photoshop CS6 to enhance the visibility of several ichnological features, following the methodology proposed by Dorador and Rodríguez-Tovar (2018).

5. RESULTS

5.1. Sedimentological and stratigraphical analysis

5.1.1. Lithological characterization

The study intervals comprise 12 sedimentary facies (designated A to L), encompassing limestone units exhibiting diverse textures; shale units with varying sand content, black to gray shale beds, and various claystone and coal units interpreted as paleosols (Figs. V.3 and V.4). These facies manifest as cyclic patterns, allowing for correlation across different cores. However, the only beds showcasing lateral continuity across the Midcontinent Shelf and the Illinois Basin are the black shales (Mound City, Hushpuckney, and Stark) and some limestone units (Fig. V.5, Table V.1).

These facies are equivalent to classical cyclothemic facies associations (Heckel, 1986), providing a more detailed characterization of depositional settings: facies A, B, and C correspond to nearshore shales deposited during lowstands in shallow open- to marginal-marine settings; facies D, E, F, and G represent limestone units equivalent to both regressive and transgressive limestones deposited in shallow marine environments; facies H and I are characterized by gray and organic-rich black shale beds, equivalent to core shales deposited during highstands under dysoxic to anoxic bottomwaters; and facies J, K, and L encompass coal beds and siltstone/claystone units, interpreted as paleosols formed during lowstands, typically in subaqueous environments.

Facies A: mottled gray mudstone. Facies A consists of light-gray mudstone (siltstone/claystone) beds (0.5 to 3 m thick), usually with high carbonate content, and occurring mostly interbedded within limestone units. Scarce, thin, fine-grained sandstone layers can appear interbedded within mudstone beds. Lenticular to wavy bedding is common when the rippled sand layers are present. Fossil content is recorded as sparse, small brachiopod and bivalve shells, usually fragmented/disarticulated. Small *Planolites* and *?Palaeophycus* occur sparsely distributed, and mottled texture is common.

Facies B: fine-grained sandstone and mudstone interbeds. Facies B is formed by light-yellow, fine-gained sandstone beds alternating with dark- to light-gray mudstone (siltstone/claystone) layers, resulting in thick units (1 to 15 m, usually c. 10 m) (Fig. V.4H, J). Flaser to wavy lamination is usually recorded (along with ripples), although planar parallel bedding is also common. Notably, trough cross-lamination occurs sometimes showing opposite directions, thus evidencing tidal influence. Fossil content is very scarce, consisting of disarticulated and/or fragmented bivalve shells. Ichnology is represented by sand-infilled *Planolites*, small *Chondrites*, and sparse *Palaeophycus* and *?Conichnus*.

Facies C: fine-grained sandstone. Facies C consists of light-yellow, fine-grained sandstone beds, usually 0.5 to 3 m-thick (although one bed reaches 10 m) (Figs. V.3I, V.4K). It occurs mostly between facies B units, and usually contains very thin, dark-gray mudstone (siltstone/claystone) layers. Sedimentary structures include planar parallel lamination, ripples, and trough cross-lamination. Body fossils are absent, and trace fossils are represented by sparse, sand-infilled *Planolites* linked to the mudstone layers.

Facies D: mottled calcareous mudstone. Facies D is formed by white limestone beds (mudstone texture) exhibiting absent or sparse marine fossils (Figs. V.3A, C, V.4E). Thickness ranges from 2 to 10 m, usually *c.* 5 m. Sometimes, thin, dark-gray shale (siltstone/claystone) layers occur interbedded within the carbonate units. Sedimentary structures are scarce, exhibiting abundant stylolites. Fossil content is absent or less than 10% of the grains, consisting of disarticulated crinoids and corals. Discrete burrows are absent,

although the sediment is apparently totally reworked (mottled texture).

Facies E: porous calcareous grainstone. Facies E consists of white, calcareous 2 to 4 m-thick beds. These limestone units exhibit high porosity (always rounded porous) (Fig. V.4D), formed after oolite dissolution (therefore formerly a calcareous oolitic grainstone) (Heckel, 1978). Facies E is present only in the Midcontinent Shelf, and neither body nor trace fossils are recorded.

Facies F: gray to brown calcareous wackestone/grainstone. Facies F consists of light-gray to light-brown, fossil-rich calcareous beds, forming wackestone to grainstone textures (Fig. V.3B, D, E, F). Fossil content is disarticulated and/or fragmented, and consist of marine components (i.e., brachiopods, bivalves, algae, corals, gastropods, and bryozoans) sometimes forming shell-beds. Although trace fossils are absent in the study units, previous works have identified several bivalve burrows, *Rhizocorallium*, *Chondrites*, and *Planolites* (see section *Ichnology of calcareous units*).

Facies G: brecciated limestone. Facies G is formed by light-gray to brownish, calcareous, mud-supported breccias, which consist of angular fragments of carbonate rocks embedded within calcareous mud (Fig. V.3G). Facies G occurs linked to other calcareous facies, and neither body nor trace fossils are observed.

Facies H: laminated black shale. Facies H consists of black, organic-rich, laminated shale beds. Phosphatic nodules/layers are common, along with silt layers forming planar parallel lamination (Fig. V.4A, B, E). Bed thickness ranges from 0.1 to 1.8 m, usually *c.* 0.3 m. Upper and lower contacts are usually erosive, albeit an upwards gradual transition to facies I (bioturbated gray shales) is common. Body fossils consist of conodonts, which permits precise dating and lateral correlation of these units. Common trace fossils are light-infilled *Zoophycos*, *Chondrites* and subhorizontal burrows, penetrating downwards from overlying light-shale beds (facies I).

Facies I: bioturbated gray shale. Facies I is formed by dark- to light-gray shale beds, sometimes with carbonate content (Fig. V.4F, I). Beds are 0.1 to 0.6 m-thick, and are recorded always overlying facies H. This unit can exhibit erosive upper and lower contacts, although gradations from underlying black shale beds and upwards to facies D and F are common. Fossil content consists of sparse bivalve and brachiopod shell fragments, mostly in the upper and lower parts of the beds. Trace fossils are represented by dark- and light-infilled *Planolites* commonly overprinting a mottled texture.

Facies J: light-gray shale with siderite. Facies J consists of light-gray, siltstone to claystone beds with abundant red siderite nodules (Fig. V.4C, G, L). Sometimes, these units can occur completely dyed in red. Bed thickness ranges from 0.5 to 3 m. These units are usually massive, albeit sometimes faintly parallel planar lamination is recorded. Body fossils and discrete burrows are absent, while mottled texture is common.

Facies K: coal beds. Facies K consists of thin coal beds ranging from 5 to 10 cm in thickness (Fig. V.3H). These units are primarily found in the Illinois Basin, displaying a distinctive high brightness and black color. Given their abundance in organic matter, these beds should be classified as paleohistosols (DiMichele, 2014). The upper contact of the coal beds is consistently erosive, transitioning upward to black shale beds in the Illinois Basin. This transition represents ravinement surfaces, providing evidence that they were deposited prior to marine transgression.

Figure V.6. Stratigraphic columns for the Heilman, Ermal and Edmonds cores (Midcontinent Shelf), indicating trace fossil distribution through the studied facies. Box color for trace fossils indicates infill type: light-gray, dark-gray, or sandy. Note that the scale in the imperial system indicates the depth from the core head. Labels in red represent the stratigraphic position of core photos in Figs. V.3, V.4, V.8 and V.9. CFA: cyclothemic facies associationa, F: described facies.

Heilman

Ermal

Edmonds
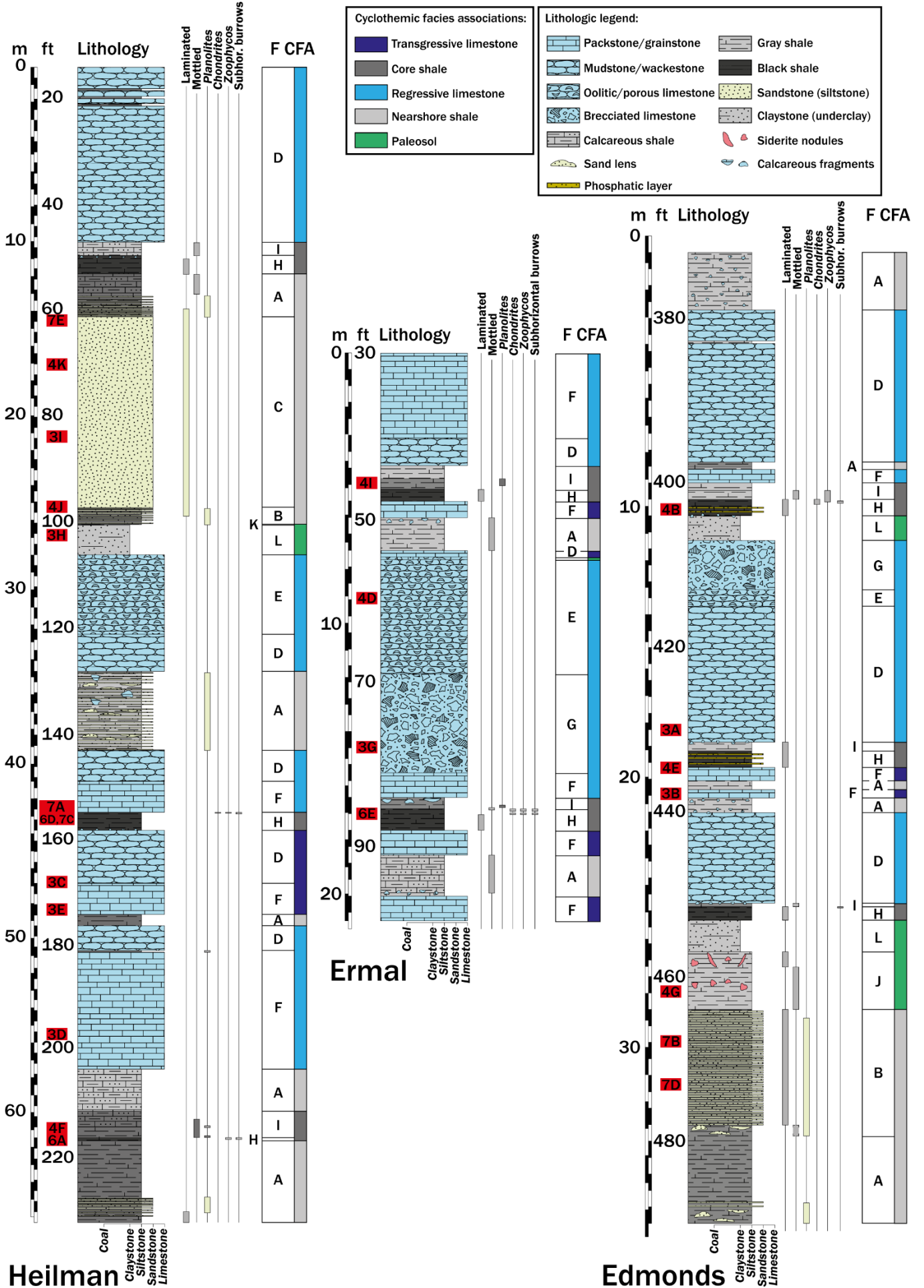
Facies L: massive gray claystone. Facies L consists of light-gray, massive claystone beds. Thickness ranges from 0.2 to 1.5 m, and are usually disintegrated due to drilling. These beds are genetically linked to coal beds (Huddle and Patterson, 1961; DiMichele, 2014), therefore associated with the development of coastal swamps, and are considered as paleosols units called "underclays". In the Illinois Basin, Facies L is usually recorded underlying Facies K (coal beds); while underlying Facies H (black shales) in the Midcontinent Shelf, where they indicate an obliterated or not developed coal bed. Body and trace fossils are absent in these units.

5.1.2. Lithological distribution and cyclicity

The distribution of the described facies exhibits variations between the two studied basins (Figs. V.5, V.6, and V.7). In the Midcontinent Shelf, calcareous facies (D-G) dominate, and paleosols are predominantly represented by massive claystones (facies L). Conversely, in the Illinois Basin, sandstone and shale beds prevail (facies A-C), and coal beds are common (facies K). Despite these differences, a shared characteristic is the cyclical pattern of these facies, representing the three subsequent cyclothems studied in this work. These sequences are correlated through the study sections based on the presence of the Mound City, Hushpuckney, and Stark "core" shale units (facies H), which were identified and dated in previous works (e.g., Heckel & Pope, 1992; Bisnett, 2001; Heckel, 2013) (Figs. V.1A and V.5).
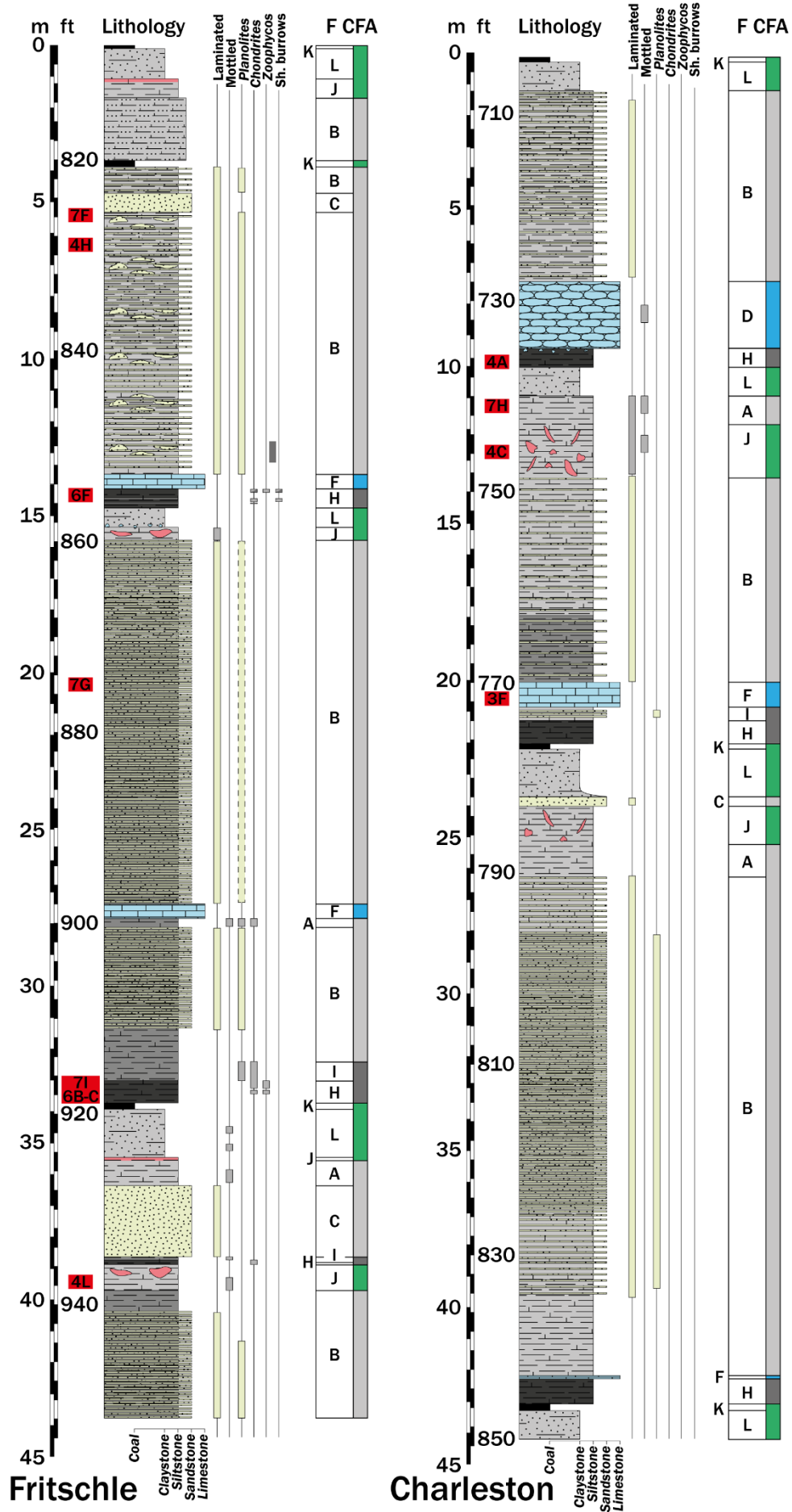
Facies and cyclicity in the Midcontinent Shelf. The three cores from the Midcontinent Shelf correspond to different settings within the basin: the Heilman (south) and the Ermal (central) cores are located in the phylloid algal mound belt, while the northern Edmonds core is situated in the open-marine facies association belt (Fig. V.1B). This distribution leads to sedimentological differences, despite the prevalence of carbonate deposits throughout the entire basin. The distribution of facies in these cores, along with their equivalence with the cyclothemic facies, is summarized in Table V.1 and Fig. V.6. The studied cores from the Midcontinent Shelf are characterized by cyclothems dominated by carbonates, primarily facies D and F, alternating with facies A. All cores display interbeddings of facies H-I, and the southernmost core (Heilman) exhibits a thick sandstone unit (facies C). Remarkably, there is a limestone/shale alternation (F-D-F) with *Lingulata* brachiopods (Fig. V.3B) correlated through the central and northern areas (Ermal and Edmonds cores). Finally, paleosols are primarily represented by underclay beds (facies L), and locally, by coal units (facies K).

Facies and cyclicity in the Illinois Basin. In the Illinois Basin, sedimentation is primarily characterized by siliciclastic units, in contrast to the prevalent carbonate deposits in the Midcontinent Shelf. The study cores are located in the basin's depocenter: the Fritschle core in the south and the Charleston core in the north (Fig. V.1B). The facies successions in these cores exhibit greater similarity to each other compared to those in the Midcontinent Shelf. The distribution of facies in these cores, along with their equivalence with the cyclothemic facies, is summarized in Table V.1 and Fig. V.7.

The sedimentary record in the Illinois Basin is characterized by layers of sand and shale interbedding, along with common sandstone beds (facies B and C). Carbonate deposits, mainly represented by facies F, are confined to thin beds overlying facies H-I successions (Fig. V.7). Paleohistosols are primarily identified as underclay-coal successions, a notable difference from the Midcontinent Shelf where coal units are virtually absent. Notably, gray shales (facies I) are often missing in the "core shales", and the black shale beds (facies H) in the

Figure V.7. Stratigraphic columns for the Fritschle and Charleston cores (Illinois Basin), indicating trace fossil distribution through the studied cyclothems and facies. Box color for trace fossils indicates infill type: light-gray, dark-gray, or sandy. Lithologic legend in Fig. V.6. Note that the scale in the imperial system indicates the depth from the core head. Labels in red represent the stratigraphic position of core photos in Figs. V.3, V.4, V.8 and V.9. CFA: cyclothemic facies associationa, F: described facies, Sh. burrows: subhorizontal burrows.

Fritschle

Charleston

Cyclothem	Cyclothemic facies associations	Midcontinent Shelf						Illinois Basin			
		Heilman Core		Ermal Core		Edmonds Core		Fritschle Core		Charleston Core	
		Name	Facies	Name	Facies	Name	Facies	Name	Facies	Name	Facies
Dennis - Shoal Creek	Nearshore shale		A, B, C						B, C		B
	Regressive limestone	Winterset Ls.	D	Winterset Ls.	D, F	Winterset Ls.	A, D, F	Carthage Ls.	F	Carthage Ls.	D
	Core shale	Stark	H, I	Stark	H, I	Stark	H, I	Stark	H, I	Stark	H
	Transgressive limestone			Canville Ls.	A, D, F						
	Paleosol	Galesburg	K, L	Galesburg	J	Galesburg	L	Un-named	L	Un-named	L
Swope - Macoupin	Nearshore shale	Ladore Shale	B						A, B, J		A, B, J
	Regressive limestone	Bethany Falls Ls., Mound Valley Ls.	D, F	Bethany Falls Ls.	E, F, G	Bethany Falls Ls.	D, E, G	Macoupin Ls.	F	Macoupin Ls.	D
	Core shale	Hushpuckney	H, I	Hushpuckney	H, I	Hushpuckney	H, I	Hushpuckney	H, I	Hushpuckney	H
	Transgressive limestone	Middle Creek Ls.	A, D, F	Middle Creek Ls., Elm Branch Shale	A, F	Middle Creek Ls., Elm Branch Shale	A, D				
	Paleosol							Womac coal	K, L	Womac coal	K, L
Hertha - Trivoli	Nearshore shale										A, B, C, K
	Regressive limestone	Sniabar Ls.	A, D, F			Sniabar Ls.	D			Cramer Ls.	F
	Core shale	Mound City	H, I			Mound City	H, I	Mound City	H, I	Mound City	H
	Transgressive limestone										
	Paleosol					Ovid Coal	L	Chapel Coal	J	Chapel Coal	L

Charleston core are significantly thicker than those in other cores (> 1 m).

5.1.3. Cyclothem characterization

The studied cyclothems, identified as Hertha, Swope, and Dennis from bottom to top, were characterized through sedimentological analysis and the prior identification of their "core shale" members (Mound City, Hushpuckney, and Stark, respectively) (e.g., Heckel & Pope, 1992; Bisnett, 2001; Heckel, 2013) (Fig. V.5). Each cyclothem represents the transgressive-regressive cycle associated with the flooding and withdrawal of the Late Pennsylvanian Midcontinent Sea. They consistently feature a paleohistosol (facies J, K, and L) formed during lowstand stages, and a "core shale" (facies H and I) deposited during highstand stages (Fig. V.2). Furthermore, the correlation of cyclothems across the Midcontinent Shelf, the Illinois Basin, and the Appalachian Basin is based on laterally continuous coal and black shale beds, along with the abundant conodont fauna found in the latter (n.b., cyclothem nomenclature in the Illinois Basin differs from the Midcontinent Shelf) (Fig. V.5). The names, lithology, thickness of the study units, and their equivalence with the cyclothemic facies associations are summarized in Table V.1 and Figures V.6 and V.7.

Based on prior conodont and sedimentological analyses, a Missourian age (lower upper Pennsylvanian) is proposed for the study sections, with lower cyclothems (Hertha and Swope) developing during interglacial II. The upper Dennis cyclothem occurred just after the end of glacial C at the beginning of the subsequent interglacial III (Fig. V.5, cf. figure 7 in Heckel, 2013).

Facies forming the cyclothems exhibit marked lateral variations across the studied basins (Figs. V.2 and V.5). Highstand deposits consistently appear as laterally continuous "core shale" units (facies H and I). Regressive and transgressive deposits are primarily composed of carbonate units in the Midcontinent Shelf (facies D, E, F, and G), which are scarce in the Illinois Basin. In the latter, limestone beds are thin, and siliciclastic units (facies D and C) prevail due to extensive continental input during sea-level regressions. Lowstand deposits mainly consist of sandstone and mudstone interbeddings (facies A in the Midcontinent Shelf and facies B in the Illinois Basin) and paleosols/paleohistosols (facies J, K, and L).

5.2. Ichnological analysis

5.2.1. Trace fossil characterization and distribution

The Illinois Basin and Midcontinent Shelf exhibit very similar, poorly diverse trace fossil composition, consisting of *Chondrites*, *Planolites*, *Zoophycos*, *Palaeophycus*, ?*Conichnus*, and subhorizontal burrows (Figs. V.8 and V.9).

The most abundant trace fossil is *Planolites*, appearing as flattened circles (diameter 2-5 mm) in facies A, B, and C (Fig. V.9B, D, E, F, G) and occasionally in facies I (Figs. V.4I and V.8A). It exhibits sand infill in facies A, B, and C and light/dark-gray shale infill in facies I. In sandstone and shale facies (A and B), it can occur in association with ?*Conichnus* and sand-infilled *Palaeophycus* and *Chondrites* (Fig. V.9B, D), while in the gray beds of the "core shale" units (facies I) occurs as a monospecific suite usually overprinting a mottled texture (Fig. V.8A).

Zoophycos is exclusive to the "core shale" units (Figs. V.8, V.9A, C, I), always occurring with light-gray shale infill, and penetrating black shale units (facies H) from the overlying gray shale (facies I). *Zoophycos* is usually present as laminae or tubes with dark meniscate infill, displaying variable morphologies like horizontal parallel *spreiten* structures, subvertical tubes, or convoluted/spiral forms (note: commonly, part of the meniscate infill has been erased). It usually occurs in association with *Chondrites*, which appear as flattened, small dots or branching burrows, both grouped in patches (diameter ≤1 mm) (Fig. V.9A) and scattered in

Table V.1. Table illustrating the facies distribution within each cyclothem in each core, including names of cyclothems in the Midcontinent Shelf and the Illinois Basins, classical cyclothemic facies associations, names of Formations and described facies.

the substrate (diameter 1-3 mm) (Figs. V.8D, E, F, V.9C); sometimes exhibiting pyritized infill (Fig. V.9I). Subhorizontal burrows are recorded with *Chondrites* and *Zoophycos* in several units of facies H (Figs. V.8A, D, E, F, V.9C). These burrows occur as flattened dots and horizontal to subvertical tubes, with variable diameter (1-5 mm). Notably, the lower part of black shale beds (facies H) lacks trace fossils but usually showcases planar parallel lamination. The upper parts show light-filled burrows penetrating < 1 to 30 cm from the overlying bed (Fig. V.10).

Finally, shale and claystone units (facies A, I, and J) as well as carbonate beds (facies D) can exhibit a mottled texture (BI=6), indicating intense bioturbation that homogenized the substratum around the sediment-water interface (Figs. V.4F, L, V.9H).

5.2.2. Ichnology of the "core shale" units

Mound City shale. The Mound City shale displays infrequent and small burrows filled with light material in the uppermost section of the black beds, predominantly ?*Chondrites*, occasionally accompanied by *Zoophycos*. The overlying gray shale consistently exhibits mottling and may display small, dark-infilled *Planolites*. Within the Midcontinent Shelf, bioturbation in facies H is less abundant and penetrative northward, while in the Illinois Basin, it is solely present in the Fritschle core (Fig. V.10).

In the Midcontinent Shelf, the Mound City core shale is only found in the Heilman and Edmonds cores (Fig. V.5). Light-infilled burrows are found in the uppermost part of the black beds (Fig. V.10). In the southern Heilman core, it is characterized by facies H (30 cm) and I (60 cm). The gray shale exhibits a mottled texture, occasionally overprinted by sparse, dark-filled *Planolites* (diameter ~2-4 mm). *Zoophycos* is present in

the black bed, penetrating 5 cm, alongside small burrows resembling *Chondrites* (diameter 1-2 mm). Conversely, bioturbation is scarce in the northern Edmonds core: while facies I is mottled, facies H (black units) displays planar parallel lamination throughout most of the bed, with only sporadic light-filled small (diameter < 2 mm) burrows (?*Chondrites*) recorded in the uppermost part, penetrating less than 1 cm.

In the Illinois Basin, the Mound City shale is found in both cores. In Fritschle, the black bed exhibits light-filled burrows resembling *Chondrites* (diameter < 1 mm), penetrating from the overlying facies I. In contrast, Mound City in the Charleston core displays black shale without bioturbation, overlain by facies D (carbonate mudstone), featuring an erosive/sharp contact.

Hushpuckney shale. The Hushpuckney shale is identified in all study cores. When bioturbated, it showcases similar ichnoassemblages (*Chondrites*, *Zoophycos*, and subhorizontal burrows), but the intensity of bioturbation varies between the two basins (Fig. V.10). In the Midcontinent Shelf, trace fossils in Hushpuckney black beds are smaller and less penetrative towards the north (cf. Mound City shale). In the Illinois Basin, bioturbation is observed solely in the Fritschle core, with *Zoophycos* displaying notably greater penetration and development compared to other black beds.

Within the Midcontinent Shelf, bioturbation is evident in the Heilman (south) and Ermal (central) cores but absent in the northern Edmonds core. In the Heilman core, it is exclusively represented as facies H without lamination. The upper 16 cm of this black bed features light-infilled unclassified burrows, along with *Zoophycos* and *Chondrites* in the uppermost 10 cm. Notably, *Zoophycos* intersect several unclassified burrows. In the

---

Figure V.8. Core photos illustrating the different ichnoassemblages present in the study sections (note: core and footage indicated in brackets). (A) Sharp contact between facies H and I (Mound City, Heilman ft. 216). Facies I exhibit dark-infilled Planolites *overprinting a mottled texture. Facies H is characterized by* Zoophycos *and subhorizontal burrows; (B-C)* Zoophycos *penetrating downwards within the Hushpuckney black shale (facies H) (Fritschle core ft 918-919), note the faint meniscate infill; (D-E)* Zoophycos, Chondrites *and subhorizontal burrows from the Hushpuckney black bed (facies H) (Heilman ft. 154.7 and Ermal ft. 86, respectively); (F) top of Stark black bed (facies H) (Fritschle ft. 856), showcasing light- and dark-infilled structures from the* Zoophycos *ichnoassemblage. Top is always upwards. Scale bar is 1 cm (0.4 in). Ch: Chondrites, Pl: Planolites, Zo: Zoophycos, SB: subhorizontal burrows.*
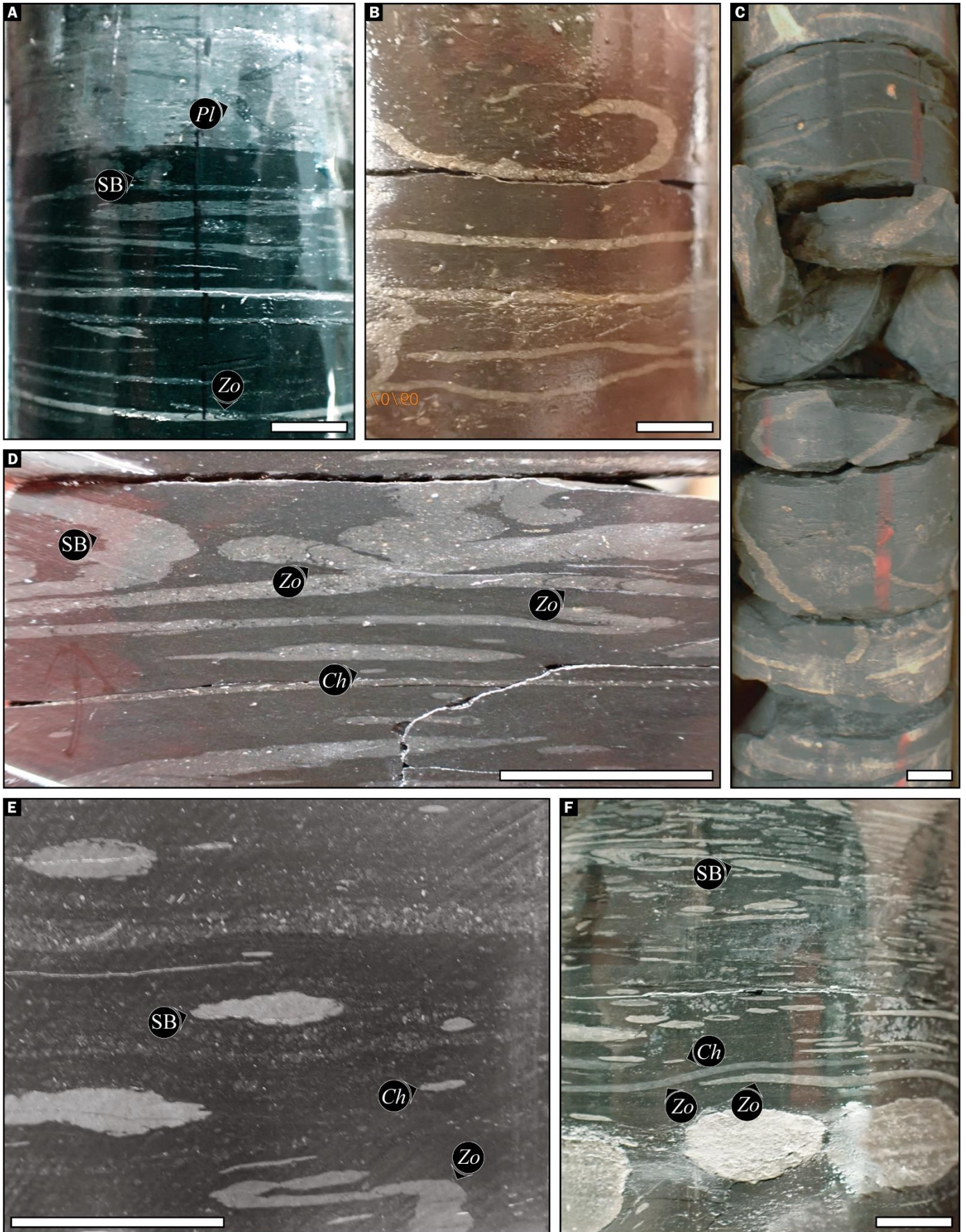
Ermal core, penetration depth and bioturbation index are lower than in the Heilman core. The lower 40 cm of the black bed exhibits planar parallel lamination, and two bioturbated horizons occur upwards. The lower one consists of a thin (2-3 cm) bed of light gray shale, with light-infilled *Zoophycos* and subhorizontal burrows penetrating 5 cm. The second bioturbated horizon occurs in the uppermost 5 cm of the black bed, featuring light-infilled burrows, patches of small *Chondrites* (circles, diameter < 1 mm), and *Zoophycos*. In the northern Edmonds core, the "core shale" comprises 50 cm of laminated black shale (facies H), with abundant phosphatic layers and lenses, transitioning gradually into 10 cm of dark-gray shale, followed by 20 cm of calcareous light shale (facies I). Previous studies have identified meio-bioturbation at the H-I facies boundary using X-ray scanning, together with the presence of *Trichichnus* penetrating 4 cm downwards in the black bed, and *Planolites*, *Schaubcylindrichnus*, *Zoophycos*, *Phycosiphon*, *Helminthopsis*, and *Trichichnus* in the gray shale (Figure 3 in Algeo et al., 2004).

In the Illinois Basin, the ichnoassemblage in the Fritschle core resembles that of the Midcontinent Shelf cores, while trace fossils are absent in the Charleston core. In the Fritschle core, facies H transitions sharply to a mottled facies I, with a 5 cm-thick shell-bed at the boundary. The uppermost 20 cm of the black bed features abundant light-infilled *Zoophycos* in variable morphologies, along with subhorizontal burrows and sparse *Chondrites* showing light or pyritized infill. The Charleston core comprises a thick black bed overlaid by light-gray sandy shale. The boundary is recorded as a sharp/erosive contact formed by a fossil lag, mainly consisting of shell fragments, in the bottom part of the light bed.

Stark shale. The ichnoassemblages found in the Stark "core shale" exhibit considerable variability among the studied basins and predominantly display sparse bioturbation. In the Midcontinent Shelf, black beds are primarily laminated, with variations northward from unbioturbated to sparsely bioturbated. Conversely, in the Illinois Basin, the Frischle core reveals a densely and diversely bioturbated top, while the Charleston core remains unbioturbated (Fig. V.10).

Within the Midcontinent Shelf, the Stark core shale consistently comprises facies H-I successions. In the southern Heilman core, the black bed lacks any burrows but exhibits planar parallel lamination in the lower 35 cm. The Ermal core shows sparse, light-infilled subhorizontal burrows (diameter 2-5 mm) penetrating 5 cm into the black shale bed (with the lower 60 cm being laminated). Light beds display dark-infilled *Planolites* overprinting a mottled texture. In the northern Edmonds core, the lower 30 cm of the black bed displays parallel lamination, which disappears with the presence of sparse, light-infilled burrows (diameter ~2 mm). Upwards, bioturbation becomes gradually more abundant, characterized by the appearance of small, light-infilled *Chondrites* (diameter < 1 mm) and *Zoophycos* (width 1-3 mm). The overlaying gray shale bed presents a mottled texture and light-infilled subhorizontal burrows in the lower 10 cm, sometimes with meniscate infill.

In the Illinois Basin, the Stark core shale is exclusively formed by facies H in both cores. In Fritschle, the upper contact of the black bed is disrupted in the core

Figure V.9. Core photos illustrating the different ichnoassemblages present in the study sections (note: core and footage indicated in brackets). (A) Contact between facies H (Hushpuckney black bed) and F (white wackestone) (Heilman ft. 154.5). Black bed is characterized by Zoophycos *and small, grouped* Chondrites*; (B) Lenticular bedding within facies B (sandstone/siltstone interbeddings) with scattered, sand-infilled* Planolites*,* Chondrites *and* Palaeophycus *(Edmonds ft. 468); (C) ?*Chondrites *and subhorizontal burrows in the Hushpuckney core shale (facies H) (Heilman ft. 154.9); (D) Lenticular bedding within facies B (sandstone/siltstone interbeddings) with ?*Conichnus *and scattered, sand-infilled* Planolites*,* Chondrites *and* Palaeophycus *(Edmonds ft. 473); (E) Facies C, formed by fine-grained sandstone with intercalated dark siltstone layers. Sand-infilled* Planolites *appear linked to a siltstone layer (Heilman ft. 61); (F-G)* Planolites *in wavy bedding from facies B (Fritschle ft. 825 and 875); (H) Mottled texture in a light-gray claystone paleosol (facies J) (Charleston ft. 741); (I) Vertical view of* Zoophycos *from the Hushpuckney black shale (facies H) (Fritschle ft. 919), note the meniscate infill of* Zoophycos *and pyritized* Chondrites*. Top is always upwards, except for (I). Scale bar is 1 cm (0.4 in). Ch: Chondrites, ?Co: ?Conichnus, Pa: Palaeophycus, Pl: Planolites, Zo: Zoophycos, SB: subhorizontal burrows.*
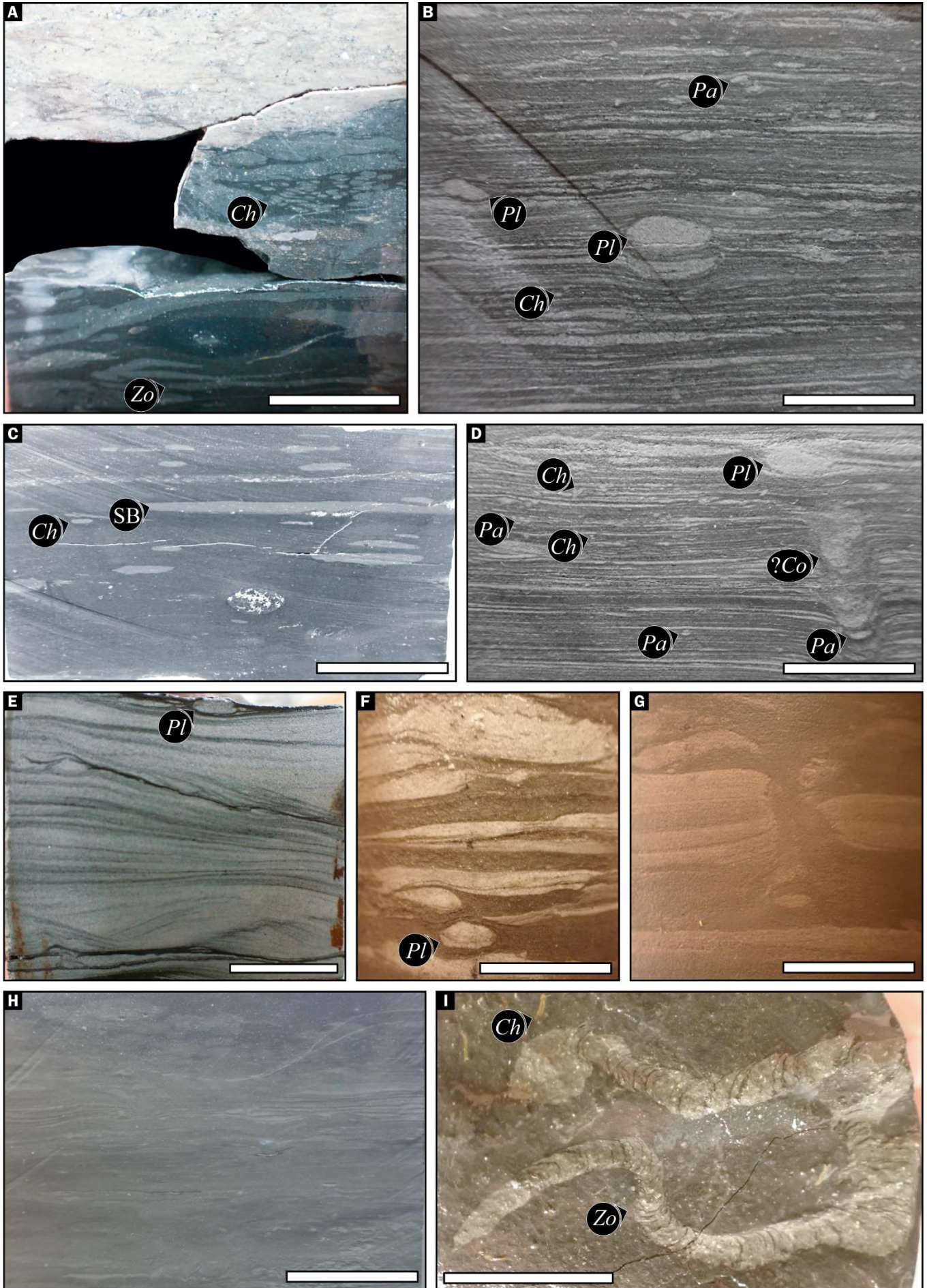
and transitions directly to brownish packstone (facies F). This black bed reveals two distinct bioturbated horizons: the first, 18 cm below the top, consists of a thin layer (1-2 cm) of light gray shale with sparse, light-infilled *Chondrites* (diameter < 2 mm), and the second, in the upper 10 cm, is highly bioturbated (BI 4-5), with abundant *Chondrites* and subhorizontal burrows, and sparse *Zoophycos*. All three ichnogenera exhibit both dark- or light-gray shale infill, showing no crosscut relationships. The Stark core shale in the Charleston core lacks bioturbation and consists of a black bed with an upper erosive contact, displaying calcareous clasts and transitioning upwards to white limestone (facies D).

6. DISCUSSION

6.1. Ichnoassemblages and paleoenvironmental reconstruction

Trace fossils have played a crucial role, improving lithological facies analysis for paleoenvironmental reconstructions (e.g., Frey, 1975; Frey et al., 1990; Goldring, 1993; Pemberton et al., 2004; Buatois & Mángano, 2011; Knaust & Bromley, 2012; Fernández-Martínez et al., 2021a). In this particular context, the recorded trace fossils within the Late Pennsylvanian Midcontinent Sea sediments facilitate the reconstruction of the macrobenthic tracemaker community that inhabited the benthic settings of the LPMS, and the interpretation of dominant paleoenvironmental (i.e., ecological and depositional) conditions.

6.1.1. Zoophycos *ichnoassemblage*

Black shale units (facies H) are characterized by the record of the *Zoophycos* ichnoassemblage, consisting of *Zoophycos* accompanied by *Chondrites* and subhorizontal burrows. Both *Chondrites* and *Zoophycos* are well-known deep-tier structures, classically linked to deposit-feeding of organisms specialized in optimizing resources within the substratum. They are also usually associated to oxygen-deficient settings. Thus, can be considered trace fossils recording the opportunistic occupation of a nearly-inhospitable benthic habitat. On the other hand,

the *Chondrites* producer is also interpreted as a chemosymbiont (after Seilacher, 1990), the same as the *Zoophycos* tracemaker (e.g., Bromley, 1996, Buatois & Mangano, 2011), therefore making them steady, lifetime structures made by highly-specialized organisms. In this case, both ichnogenera, but specially *Zoophycos*, can be considered trace fossils produced by climax tracemaker communities, used to leverage the resources of sulfide-rich sediments by gardening bacteria or accumulating nutrient-particles ("cache strategy") (e.g., Bromley, 1991; Lowemark et al., 2004).

Organic-rich black beds of the facies H were deposited under anoxic/euxinic bottomwaters (e.g., Algeo et al., 2004; Algeo & Maynard, 2008), leading to inhospitable settings for macrobentich tracemakers, as supported by common planar parallel lamination. The presence of trace fossils from the *Zoophycos* ichnoassemblage in the upper part of the black beds records the recovery of oxic/disoxic conditions during the deposition of the overlying light shale beds. *Zoophycos* producers colonized a deep setting, just after the maximum flooding of the LPMS (Fig. V.10, identification of maximum flooding surfaces is based on unpublished geochemical data), at depths around 100 m, below the storm-wave base level where sedimentation was dominated by mud decantation.

Ethology of this ichnoassemblage is doubtful, although associated with organic-matter consumption and chemosymbiosis (note the high Sulphur content in the black shale beds, which exhibit abundant phosphate-rich layers). Geochemical analyses have shown that deposition of gray shale beds (facies I) occurred mostly under dysoxic bottom-waters (Algeo et al., 2004; Algeo and Maynard, 2008), therefore, tracemakers responsible of the *Zoophycos* ichnoassemblage inhabited oxygen-deficient settings and burrowed an anoxic/euxinic substratum. Considering the complexity of *Zoophycos* and *Chondrites* morphology, these structures were permanently inhabited, probably during the whole lifespan of the tracemaker (e.g., Baucon et al., 2020).

Therefore, the tracemakes responsible of the *Zoophycos* ichnoassemblage were highly-specialized organisms which colonized an oxygen-deprived setting

(facies I) and burrowed anoxic/euxinic sediments (facies H) to consume organic matter or sulfate-reducing microorganisms.

6.1.2. Planolites *ichnoassemblage*

The *Planolites* ichnoassemblage consists primarily of *Planolites*, accompanied locally by sparse *Palaeophycus*, *Chondrites* and ?*Conichnus* in facies A and B. *Planolites* are produced by vagile organisms at shallow tiers. The ethological assignation of *Planolites* is problematic, as they can be considered as grazing traces (pascichnia), deposit-feeding structures (fodinichnia), or even domiciles (domichnia). However, all these behaviors are heavily linked to well-ventilated conditions at or just below the sediment-water interface (i.e., shallow tier).

Planolites ichnoassemblage can occur in gray "core shale" beds (facies I) or in "nearshore shale" units (facies A, B and C). In facies I, considered to be deposited in relatively deep, open marine settings (such as facies H), this ichnoassemblage is recorded as monospecific *Planolites* suites commonly overprinting mottled texture, indicating reworking of the substrate when the mottled sediment was stiffer. Burrows are infilled of both light- and dark-gray shale, therefore evidencing similar oxyc/disoxic conditions during deposition of facies I, disregarding different depositional redox conditions for lighter and darker parts within the shale beds.

In the siltstone and sandstone alternations interpreted as "nearshore shales" (facies A, B and C), ichnodiversity is locally slightly higher than in facies I (locally 4 ichnotaxa). Sedimentary structures of these facies indicate deposition in shallow to marginal marine settings, where salinity variations, high-energy, and high sedimentation rates are major limiting factors for the development of benthic communities. Sand beds (facies C) were deposited in sub-tidal to lower inter-tidal settings with large wave influence, as indicated by abundant ripples, trough crossbedding and parallel lamination; on the contrary, facies B interbeddings corresponds to a middle-intertidal (mixed) flat, characterized by heterolithic deposits exhibiting flaser to wavy lamination and small ripples. Facies B are usually capped by massive light-gray claystone units and coal

beds (facies J, K, and L), interpreted to be deposited in mudflat or coastal swamp settings.

In these settings, previous works have described highly diverse ichnoassociations classified within the *Scoyenia*, *Mermia*, *Skolithos* and *Cruziana* ichnofacies (see section Ichnology of siliciclastic units). Ichnodiversity is strongly controlled by the salinity gradient, leading to highly diverse mixed *Scoyenia* and *Mermia* ichnoassemblages developed under freshwater bottomwaters, highly diverse *Cruziana* ichnoassemblages in settings with full-marine salinity, and low diverse, depauperate ichnoassemblages from the *Skolithos* and *Cruziana* ichnofacies developed under brackish bottomwaters. However, in the study section ichnodiversity is very low (from monospecific *Planolites* suites to ichnoassemblages formed by 4 ichnotaxa); therefore, large differences in ichnodiversity and trace fossil abundance are apparent between the study units and their counterparts analyzed in previous works. This fact is partially due to differences between outcrop vs core analysis, as horizontal structures (such as *Cruziana*, *Asteriacites*, *Psammichnites*, or *Curvolithus*) are unlikely to be recognized in vertical sections, i.e., in cores ("the lost ichnogenera" from Bromley, 1996). However, absence of vertical structures, which have high preservation potential in the heterolithic sediments of facies A and B, disregard the classification of the *Planolites* ichnoassemblage as *Skolithos* ichnofacies. Low ichnodiversity of the studied ichnoassemblages can be related to strong brackish conditions (indicated by monospecific suites, e.g., Buatois & Mángano, 2011) or fast shifts to marine or freshwater salinity conditions.

6.2. Response of tracemaker community to sea-level changes

Conducted ichnological analysis allows approach the response of tracemaker communities to the long-term sea-level changes determining the sedimentological dynamics of the Late Pennsylvanian Midcontinent Sea (Fig. V.11). As exposed above, the studied sections correspond to three subsequent transgressive-regressive sequences (Hertha/Trivioli, Swope/Macoupin, and Dennis/Shoal Creek cyclothems) linked to successive melting and growth cycles of the Gondwanan icesheets

(Fig. V.5). In this context, contrary to the large variability of facies distribution among the Midcontinent Shelf and the Illinois Basin, trace fossils distribution shows a clear and very similar pattern within each stage of the transgressive-regressive cycles in both basins.

"Core shale" organic-rich black beds (facies H) were deposited during the final transgressive phase and the highstand stage (Figs. V.2, V.10 and V.11), under anoxic/euxinic (i.e., inhospitable) conditions at bottom- and pore-waters as revealed by geochemistry, parallel lamination and absent ichnofossils. Immediately over the black facies occur the deposit of gray shale beds (facies I), recording the improvement to oxic/dysoxic conditions evidenced by mottled texture, the presence of *Planolites* and geochemical proxies (e.g., Algeo et al., 2004). At the boundary between the black and gray beds, the *Zoophycos* ichnoassemblage is usually recorded (Fig. V.10) penetrating downwards into the upper part of black shale bed, revealing the activity of the first endobenthic communities which occupied the benthic habitat after the highstand anoxic conditions. Previous works (Algeo et al., 2004) have identified minor transgressive-regressive cycles within the core shale deposits, demonstrating that the maximum flooding surface is usually recorded within the black bed, and the upwards deposits of the core shale (top of facies H and the entire facies I) are deposited during the early phases of sea-level fall (Fig. V.10). Thus, when recorded, bioturbation in the core shales is produced only during the early phases of the regressive stage (upwards the maximum flooding surface), not during transgressive/highstand phases.

Limestone units (facies D, E, F and G), dominant at the regressive stages in the Midcontinent Shelf, but also early transgressive phases within the Swope cyclothem, exhibit absent or scarce trace fossils. Absence

of trace fossils in the packstone/grainstone limestones (facies F) is interpreted as due to high reworking of the sediment, as indicated by the highly remobilized fossil remains (Fig. V.3F), which erased the present biogenic structures. On the contrary, white mudstones represented a soupy benthic habitat which inhibited the preservation of discrete trace fossils, recording only a mottled texture (Fig. V.3A). Thus, substrate consistency and setting energy played a major role determining the preservation of trace fossils in carbonate facies deposited during regressive and transgressive stages. In the Midcontinent shelf, facies A (gray claystone/siltstone beds) usually occur interbedded within carbonate units, exhibiting mottled texture. This facies must correspond to moments of $CaCO_3$ starvation, probably linked to shallower conditions and/or rise in continental input, when a shallow-tier benthic community densely burrowed a soupy substrate.

Facies A, B and C, regarded as "nearshore shales", are late regressive and lowstand deposits conformed mainly by sandstone/siltstone interbeddings and sandstone beds. These deposits exhibit the *Planolites* ichnoassemblage. Lowstand settings (ranging from subtidal to intertidal) are characterized by temporary-occupied, shallow-tier structures linked to deposit feeders (Fig. V.11).

Finally, lowstand and late regressive deposits are also recorded as facies J, which are massive claystone units interpreted as paleosols, sometimes showcasting a mottled texture. This ichnofabric evidences a completely homogenized sediment, indicating soupy substratum and well-oxygenated bottom- and pore-waters, where shallow-tier tracemakers densely colonized the sediment near/at the sediment-water interface in swamp settings.

Figure V.10. In-detail schematic illustration of all the studied "core shale" units, indicating the bioturbated intervals and their core-view. When possible, differentiation between lower and upper "core shale" is made (LH and UH, respectively), based on geochemical data both from Algeo et al. (1997), Algeo et al. (2004) and Algeo and Maynard (2008). Bioturbation occurs always upwards the maximum flooding surface (mfs). In the Stark core shale, note the presence of the Iowa IRC core (see Fig. V.2B for location), with salinity proxy (B/Ga ratio) and sea-level curve for the latter and the Charleston core (modified from Fig. 2 in Wei et al., 2022). Redox and sea-level curve for the Edmonds core modified from Fig. 8 in Algeo et al. (2004). Letters within columns indicate the facies.
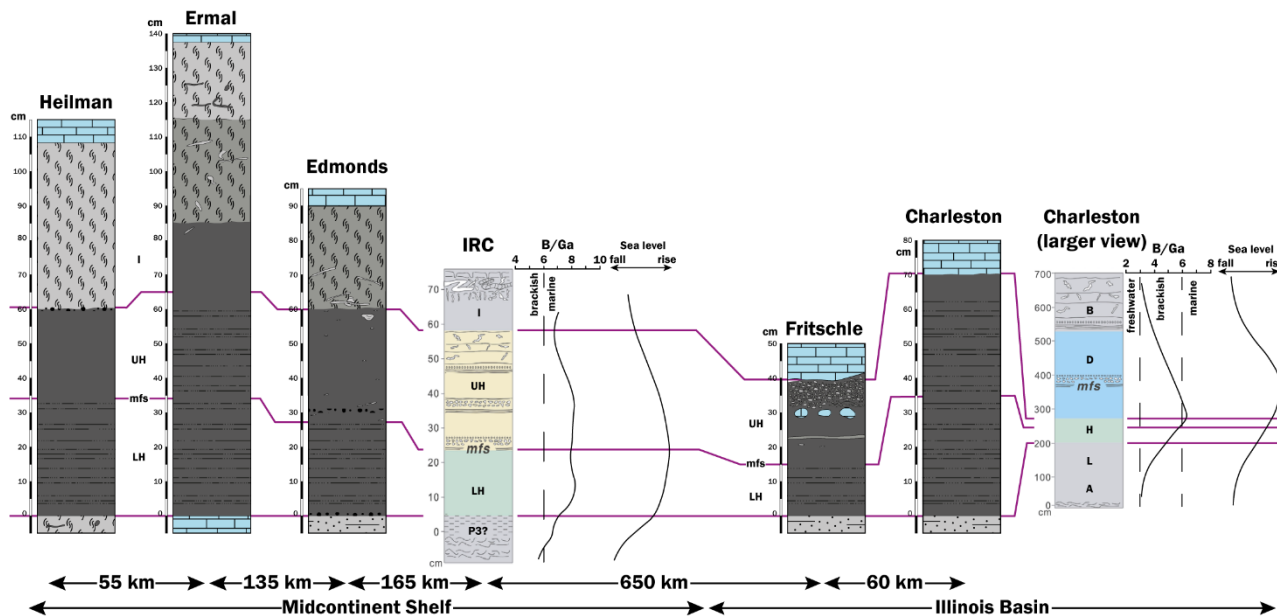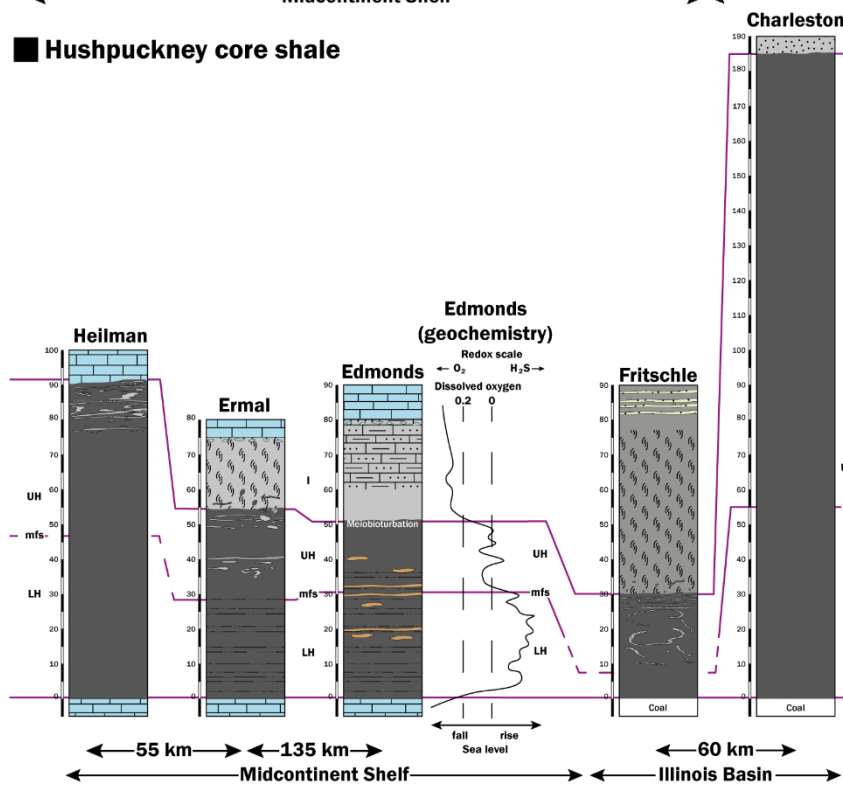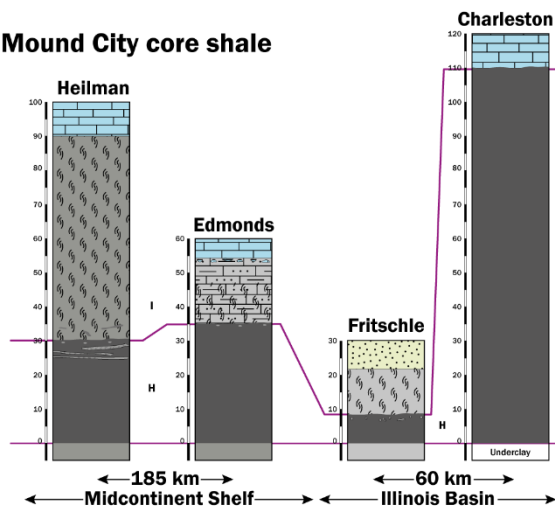
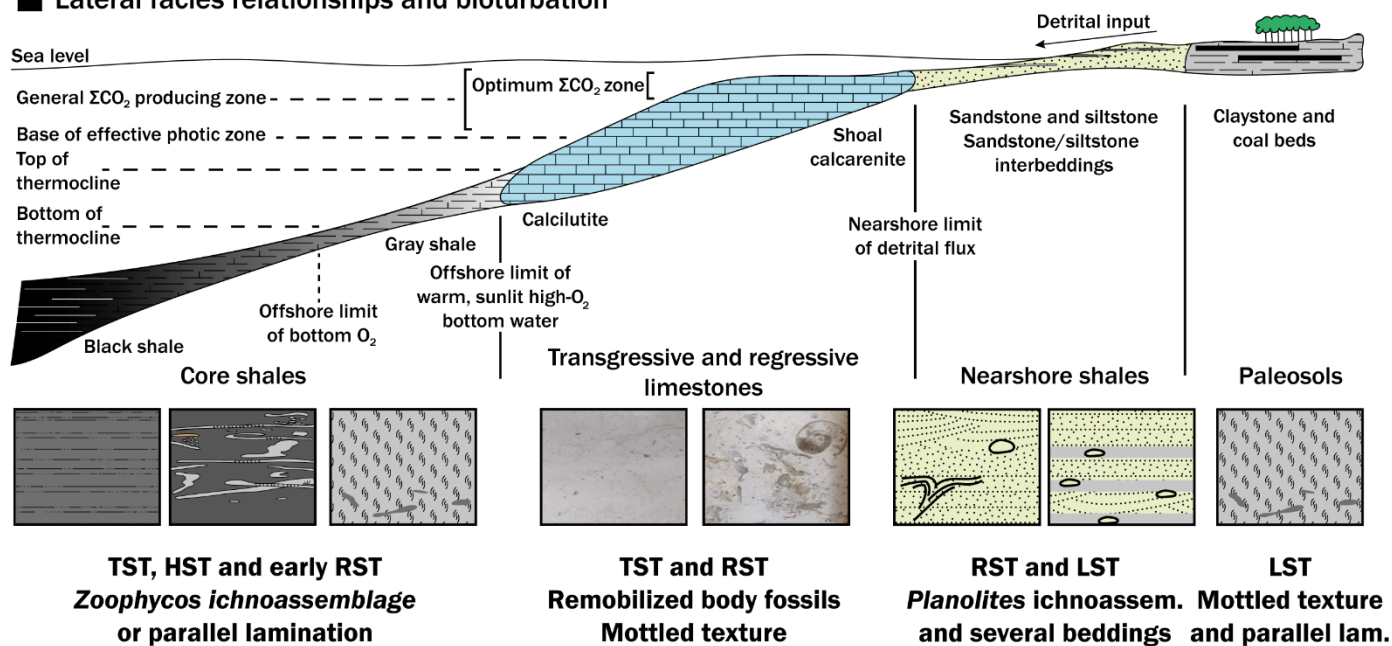■ **Lateral facies relationships and bioturbation**

Figure V.11. Lateral facies relationships (modified from Fig. 1 in Heckel, 1986) and present bioturbation. Scheme illustrating the main ichnological features for each sequential stage and cyclothemic facies associations. Note that, although lithology varies among the studied basins, ichnoassemblages are very similar in both basins within each lithology.

6.3. Recovery of the macrobenthic tracemaker community: ichnology of "core shales" in the Midcontinent shelf

Shifts from anoxic to oxic/disoxic bottomwaters are recorded in the boundary between black and gray shale beds (facies H and I) of the "core shale" units. In these deposits, the *Zoophycos* ichnoassemblage is recorded during the early phases of the regressive stage. However, there are several differences in the trace fossils distribution between the "core shale" units in the study area depending on the age and depositional setting.

The Mound City and Hushpuckney units exhibit the same pattern in trace fossil distribution. In the southern, distal area of the Midcontinent Shelf (Heilman core, southwards the Bourbon Arch), trace fossils are more abundant and penetrative than in the central and northern areas (more proximal, Ermal and Edmonds cores), characterized by less penetrative *Zoophycos* and dominated by scarce subhorizontal burrows with shallow penetration (Fig. V.10).

This ichnological distribution evidences that the recovery of the benthic community after anoxic conditions was slower in proximal areas of the

Midcontinent Shelf (between the Bourbon Arch and the Laurentian shore) than in distal settings (between the Bourbon Arch and the deeper Anadarko Basin) (Fig. V.5). This fact is linked to the good connection of the southern Midcontinent Shelf with Panthalassa, compared with the partially-isolated central and northern areas (Fig. V.1B). Watermass input from the open-ocean (via the Greater Permian Basin Seaway), although poorly-oxygenated, favored the presence of upwelling and well-ventilated conditions (Algeo and Heckel, 2008) (Fig. V.1C), allowing the occurrence of a more diverse, deep-tier tracemaker community in the southern area, in contrast with proximal, more-restricted settings. This pattern, where the basinal connectivity with the open-sea favors distal colonization relative to proximal, is similar for that recorded in the Cenomanian-Turonian OAE at southern Spain (Rodríguez-Tovar et al., 2009), where the upwelling nutrient-flux from the open ocean favored the presence of highly diverse ichnoassemblages after anoxic pulses.

The poorly-developed *Zoophycos* ichnoassemblage recorded in Mound City, in contrast with the well-developed *Zoophycos* recorded in Hushpuckney shale (penetrating even 20 cm) (Fig.

V.10), indicate that disoxic conditions were stronger during deposition of the gray shales (facies I) from the Mound City "core shale".

The Stark shale in the Midcontinent Shelf exhibits the opposite pattern than the other "core shale" units, with diversity and abundance of trace fossils increasing northwards (*i.e.*, towards proximal settings). This trend is confirmed by ichnological data from a northern core (IRC, Fig. V.10) (Wei et al., 2022). This pattern may be related with the melting and growth cycles of Gondwanan icesheets. The Dennis cyclothem occurred at the beginning of an interglacial episode, in contrast with the lower Swope and Hertha cyclothems, which occurred during the middle and terminal phase of interglacial II (Fig. V.5). Therefore, paleoenvironmental conditions in southern/distal areas of the Midcontinent Shelf were likely heavily influenced by the input of cold, poorly-oxygenated, and relatively-brackish watermasses from the recently melted icesheets in Panthalassa. In this context, contrary to the favoring conditions during Hertha and Swope cyclothems, connectivity with the open-ocean led to more inhospitable benthic settings in the southern area of the Midcontinent Shelf. This agrees with the fact that abundance and penetration depth of the burrows are markedly lower in the Stark than in the Hushpuckney core shale, therefore indicating more stressful conditions during the Dennis cyclothem "core shale" units.

7. CONCLUSIONS

An integrated ichnological and sedimentological analysis has been conducted in five cores representative of the sedimentation in two basins from the Late Pennsylvanian Midcontinent Sea (Midcontinent Shelf and Illinois Basin). Comparison of sedimentary and biological features among both settings evidence that paleogeography heavily influenced the sedimentary dynamics among the LPMS, where carbonate units domain in the Midcontinent Shelf and sandstone and shale beds prevail in the Illinois Basin (analysis of sedimentological features permit the identification of various depositional paleoenvironments, from shallow marine to subtidal and intertidal settings). Similar ichnoassemblages are recorded in both basins for each sequential stage, therefore paleogeography scarcely influenced macrobenthic tracemakers. "Core shale" units deposited during sea-level highstands, are characterized by *Zoophycos*, *Chondrites* and subhorizontal burrows, while shale beds deposited in marginal marine settings exhibit *Planolites* and scarce *Palaeophcus, Chondrites,* and *?Conichnus*.

Recovery of oxic conditions after highstand anoxic pulses (i.e., during black shale deposition) was recorded by the *Zoophycos* ichnoassemblage, produced by organisms which steadily occupied the benthos. On the contrary, shale and sandstone units deposited in subtidal to intertidal settings during regressions and lowstands, are characterized by the *Planolites* ichnoassemblage, developed by tracemakers which shortly occupied the substrate.

A detailed analysis of the bioturbation in black shale units reveal a pattern in benthic settings occupation. In the Midcontinent Shelf, bioturbation in "core shale" units is characterized by deeper and well-developed structures in the southern (distal) area regarding more proximal settings. Thus, recovery after anoxic pulses was faster in distal areas of the Midcontinent Shelf, due to upwelling fluxes favored by the southwards connection of the basin to the open ocean.

CHAPTER VI

CYCLIC SEDIMENTATION IN PENNSYLVANIAN BLACK SHALES

Integrating geochemical and ichnological analyses to assess depositional conditions of Pennsylvanian black shales: cyclic sedimentation in an epeiric sea from North America

Javier Fernández-Martínez[1*], Francisco J. Rodríguez-Tovar[1], Francisca Martínez Ruíz[2], Thomas J. Algeo [3, 4, 5]

[1] *Departamento de Estratigrafía y Paleontología, Universidad de Granada, Avenida de Fuente Nueva, s/n, Granada 18071, Spain*

[2] *Instituto Andaluz de Ciencias de la Tierra (CSIC-UGR), Av. de las Palmeras, 4, Armilla 18100, Granada, Spain*

[3] *State Key Laboratory of Biogeology and Environmental Geology, China University of Geosciences, Wuhan 430074, China*

[4] *State Key Laboratory of Geological Processes and Mineral Resources, China University of Geosciences, Wuhan 430074, China*
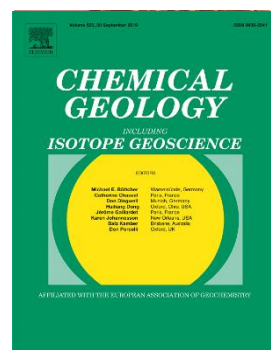
[5] *Department of Geosciences, University of Cincinnati, Cincinnati, OH 45221-0013, U.S.A.*

To be submitted to *Chemical Geology*.

Editor

Available at:

ABSTRACT

The integration of geochemical and ichnological analyses has provided a precise characterization of redox conditions during the deposition of the Stark and Hushpuckney shales, offering insights into the palaeoenvironmental factors influencing redox conditions at time of deposition. Each black shale deposit corresponds to the transgressive phase of a "cyclothem": transgressive-regressive sequences linked to glacio-eustatic sea-level changes, which characterize the sedimentological record during the North American Pennsylvanian. The black shale beds exhibit a distinct pattern with a prominent euxinic pulse in their lower part, coinciding with periods of sea level transgression. Following the maximum flooding surface, a secondary, weaker euxinic pulse occurs during the early regressive phase. The uppermost part of the black beds shows abrupt transitions to suboxic redox conditions, progressing to dysoxic facies during the deposition of the upper grey shale bed. Geochemical analyses reveal diverse redox trends correlated with changes in sea level influenced by glacio-eustatic processes and punctuated by high-frequency climatic fluctuations (TE-cycles). The development of a robust pycnocline during transgressive, highstand, and early regressive stages correlates with the euxinic pulses observed in the lower black beds. Conversely, decreased sea levels and continental input weaken the pycnocline, facilitating increased water mass mixing, resulting in suboxic conditions in the uppermost black beds and dysoxic conditions in the grey shale bed. Detailed examination of Mo and TOC patterns disregards hydrographic restriction as a factor influencing euxinia development. Low ichnodiversity further support predominantly dysoxic conditions during grey shale deposition. The abundance and distribution of ichnotaxa highlight a regional recovery pattern following euxinic pulses in the Midcontinent Shelf. In the Dennis cyclothem, weaker pycnoclines northwards facilitate rapid and efficient benthic colonization during the regressive stage in the inner regions of the shelf. Conversely, during the Swope cyclothem, trace fossils indicate enhanced benthic colonization following reductive pulses, despite sparse bioturbation in the inner region, likely due to stronger pycnoclines towards the craton influenced by moderate freshwater input, leading to oxygen-depleted bottom waters nearshore.

KEY WORDS

1. INTRODUCTION

The depositional conditions of black shales have been discussed and subjected to an extensive debate since the early 20th century (e.g., Woolnough, 1937). Despite they have been widely studied, the mechanisms leading to the accumulation of organic-rich facies remain poorly understood (e.g., Wignall, 1994). Anoxia and productivity are often cited as key factors in the deposition of these facies (see preservation and productivity models in Chapter I). Additionally, sea-level changes play a significant role, as black shales are typically associated with transgressive periods (e.g., Hallam, 1967; Hudson & Martill, 1991).

Black shale facies deposited during the Upper Pennsylvanian (Upper Carboniferous) in North America represent a well-studied example of facies that still present several uncertainties regarding their deposition. Traditionally, these facies have been regarded as transgressive black shales (Heckel, 1977; Algeo et al., 2004), though the proposed depositional model has varied from a productivity-triggered accumulation of organic carbon (Heckel, 1977) to an anoxic/euxinic water masses with low salinity (Wei et al., 2022). However, several features remain untested for these facies, such as importance of the bottom-water hydrographic circulation and the impact of oxygen conditions.

In this work, we have studied two black shale units within two subsequent transgressive-regressive sequences, known as cyclothems, deposited during the Upper Pennsylvanian in an epeiric sea that covered most of the North American continent, known as the Late Pennsylvanian Midcontinent Sea (LPMS) (Fig. VI.1). The integration of ichnological and geochemical data have been used to assess redox conditions during black shale deposition, and estimate the roles played by productivity, hydrographic restriction, and salinity. Moreover, the influence of these palaeoenvironmental conditions on the macrobenthic tracemaker community has also been approached.

2. GEOLOGICAL SETTING

The Late Pennsylvanian Midcontinent Sea (LPMS) encompasses the Appalachian, Illinois, Michigan, Midcontinent Shelf, and Williston Basins, which are separated by several submerged arches (Fig. VI.1). LPMS was connected to the Panthalassic Ocean through a narrow strait via the Anadarko and Great Permian basins, though it was predominantly landlocked and surrounded by orogens such as the ancestral Rocky Mountains and the Appalachian and Ouachita-Marathon ranges (Fig. VI.1). The Laurentian Craton forms the northern margin, while the Wyoming Channel permitted shallow, intermittent water exchange with Eastern Panthalassa. Sedimentation throughout the LPMS, particularly in the Midcontinent Shelf, was characterised by the presence of transgressive-regressive sequences linked to the growth and melting cycles of the Gondwanan ice sheets.

An ideal depositional sequence, known as a cyclothem, consists of a black shale bed ("core" shale) deposited during the late transgressive/early regressive stage (Algeo et al., 2004), flanked by limestone beds deposited during the the transgressive and regressive stages ("transgressive" and "regressive" limestones, respectively). Finally, the sequence may be capped by interbedded shale and sandstone layers deposited during lowstands, commonly bearing thin coal beds and other palaeosols (Fig. VI.1).

The LPMS is characterised by a distinctive water mass circulation pattern, described as the "superestuarine model" by Algeo and Heckel (2008). During flooding episodes, widespread anoxic conditions arose from the westward influx of oxygen-deprived waters from Panthalassa, coupled with humid conditions causing significant continental freshwater runoff from the east. This combination of factors in the predominantly landlocked basins created a gradient of benthic redox conditions, with more intense anoxic pulses in the inner, shallower regions of the LPMS. In these basins, regional precipitation and extensive runoff established a strong halocline and a deep pycnocline, limiting vertical water mixing and promoting the development of anoxic conditions, initially influenced by the oxygen-deprived
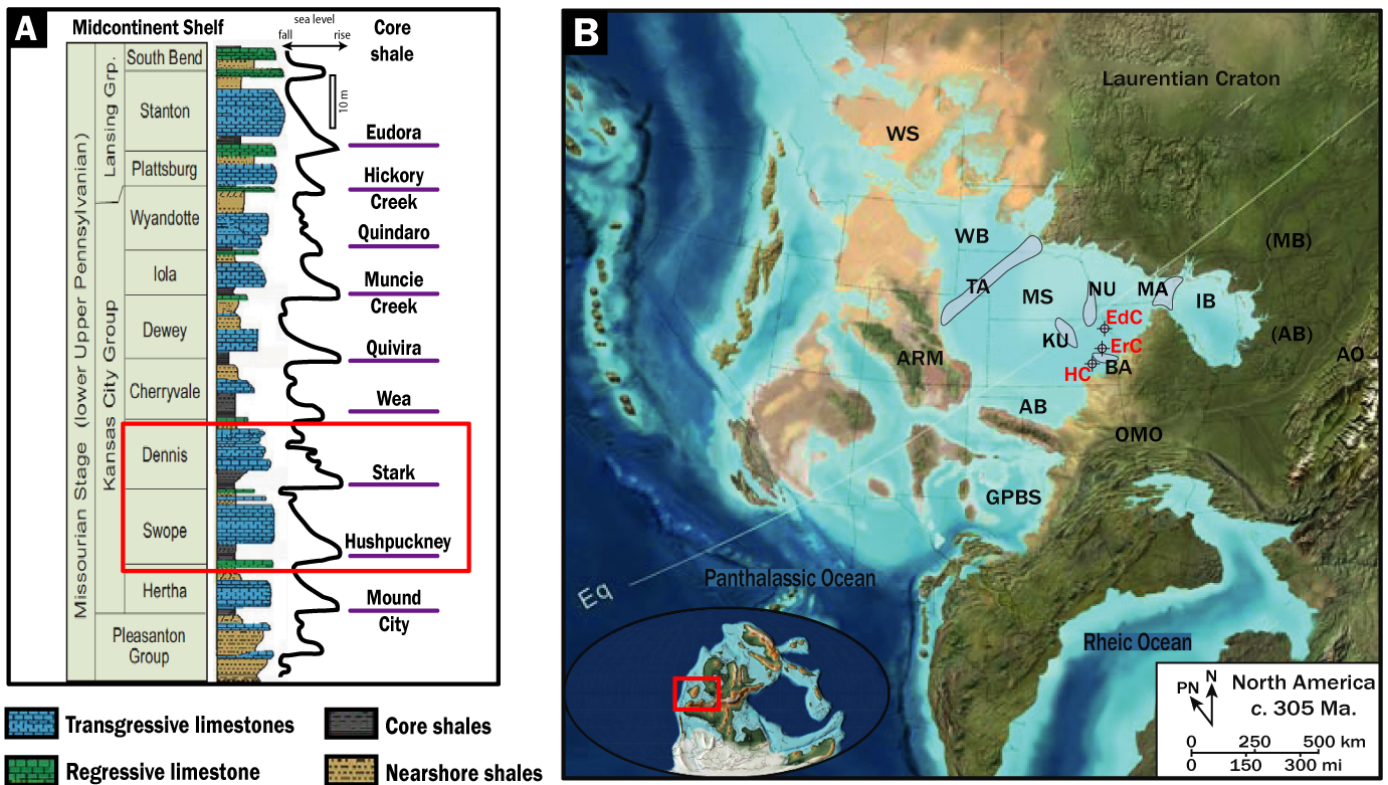
Figure VI.1. Biostratigraphy and palaeogeography of the study sections. (A) Stratigraphic column of several Missourian cyclothems, indicating names, sea-level changes, and core shale names (modified from Fig. 1 in Algeo & Heckel, 2008). Red rectangle indicates studied cyclothems; (B) Palaeogeographic map of the Late Pennsylvanian Midcontient Sea, indicating the location of the studied cores, (black crosshairs) and the names of the main basins, orogens, and submerged arches. Gray-shadowed lines indicate actual frontiers between U.S.A. states. Map of the Earth during Late Pennsylvanian at bottom-left corner; AB: Anadarko Basin, (AB): Appalachian Basin, AO: Alleghenian Orogen, ARM: Ancestral Rocky Mountains, BA: Bourbon Arch, EdC: Edmonds core, ErC: Ermal core, GPBS: Greater Permian Basin Seaway, HC: Heilman core, IB: Illinois Basin, KU: Central Kansas Uplift, (MB): Michigan Basin; MS: Midcontinent Shelf, NU: Nemaha Uplift, OMO: Ouachita-Marathon Orogen, PN: palaeo-north, TA: Transcontinental Arch, WB: Williston Basin, WS: Wyoming Shelf. Parenthesis in the Michigan and Appalachian basins indicates that those areas were not completely flooded during low sea level phases.

deep water mass from Panthalassa. Consequently, the occurrence of anoxic conditions in the LPMS was highly sensitive to climatic variations (Algeo & Heckel, 2008).

The study sections are located in the Midcontinent Shelf; the Edmonds core (EdC) in the north, the Ermal core (ErC) in the centre, and the Heilman core (HC) southwards of the Bourbon Arch, forming a deepened sequence from north to south (Fig. VI.1). It is separated from the Illinois Basin by the Mississippi River Arch, and from the Williston Basin by the Transcontinental Arch. Additionally, the Bourbon Arch and the Central Kansas Uplift are situated within the southern parts of the basin. The LPMS deepens westwards; thus, the Appalachian and Illinois Basins are characterised by shallower depositional settings (deltaic),

while the Midcontinent Shelf is dominated by shallow marine carbonates.

3. MATERIAL AND METHODS

This study focuses on the Hushpuckney and Stark black shale units, which are part of the Swope and Dennis cyclothems, respectively (Missourian Stage, lower Upper Pennsylvanian, c. 305 Ma) from the studied sections. These facies consist of black, organic-rich, laminated shale (mudrock) beds and were studied in three selected cores (stored at the Kansas Geological Survey).

Black shale beds were studied in the selected cores and a detailed ichnological analysis was performed, mainly focused on the shape, infill, and depth of the trace

fossils, along with their distribution, abundance, and diversity. Stratigraphic columns were created, with special attention to lithological variations and primary sedimentary structures. Photographs were taken and analysed using Adobe Photoshop CS6, following the methodology of Dorador & Rodríguez-Tovar (2018), to improve visibility of sedimentary and biogenic structures.

For geochemical analyses, black facies were sampled approximately every 2 cm (see detailed methodology in Chapter IV). Organic carbon content was determined via Rock-Eval pyrolysis, using a Vinci Technologies pyrolyser model Rock-Eval 6 at the Institute of Earth Sciences at the University of Lausanne, Switzerland. Trace elements were measured with an ICP-MS (NexION 300D) using certified standards (BR-N, GH, DR-N, UB-N, AGV-N, MAG-1, GS-N, and GA) for calibration, at the Analytical Facilities of the University of Granada (Centro de Instrumentación Científica, CIC). Major elements were obtained by Wavelength Dispersive X-Ray Fluorescence (WDXRF) using a BRUKER S4 Pioneer spectrometer and a PERKIN-ELMER ICP-OES spectrometer OPTIMA 830, both at the Andalusian Institute for Earth Sciences (IACT) in Granada.

4. GEOCHEMICAL PROXIES FOR PALAEOREDOX RECONSTRUCTIONS

Plaeoredox conditions in marine basins can be reconstructed by using diverse geochemical proxies, particularly variations in the concentration of redox-sensitive elements such as U, Mo, Fe, Th, V, Cr, Cd, Co, and Cu, along with other proxies like the degree of pyritization (DOP), TOC, or Corg/P (e.g., Jones and Manning, 1994; Algeo and Ingall, 2007; Li et al., 2010; Poulton and Canfield, 2011). These studies have led to the definition of redox "boundaries" based on the concentration of these elements. However, recent works by Algeo and Li (2020) and Algeo and Liu (2020) have highlighted the importance of calibrating the redox boundaries for each basin, based on elemental concentration covariations and the use of elemental enrichment factors (EF) instead of elemental ratios.

Covariation between pairs of proxies can be classified as either "simple" or "compound". Simple covariation results in an approximately linear relationship with a positive slope, indicating concurrent co-enrichment of the proxies. This concurrent enrichment may have initiated simultaneously at the same redox threshold or at different thresholds, with subsequent enrichment obscuring the sequential onset. Conversely, compound covariation is characterised by two line segments connected by a sharp bend, indicating the sequential enrichment of proxies. Here, the proxy showing earlier enrichment (X axis) began increasing at a higher redox threshold (less reducing conditions) than the later-enriched proxy (Y axis). The sharp bend marks a specific threshold in the redox ladder where the enrichment of the second proxy (Y) commences (Algeo & Li, 2020). Additionally, Algeo and Maynard (2008) presented several methods for representing trace element concentrations to facilitate the interpretation and identification of trends.

4.1. Palaeoredox and palaeoenvironmental proxies

Several redox-sensitive trace metals have been analysed to assess suboxic to euxinic conditions (V, U, and Mo), along with the DOP-T, Corg/P, and FeT/Al ratios. The best way to represent variations in the concentration of trace elements in the sediment is through enrichment factors (EFs), calculated as $XEF = [(X/Al)sample / (X/Al)PAAS]$, where X corresponds to the selected element and PAAS refers to values from the standard (Post-Archean Average Shales, from Taylor and McLennan, 1985).

As mentioned in Chapter I, trace elements like V, U, and Mo are commonly used as redox proxies and their abundances relate to suboxidized, subreduced, and euxinic conditions, respectively.

Vanadium (V) is intricately linked to the manganese (Mn) redox cycle. In the water column, it exists predominantly as V(V) in the form of vanadate oxyanions, which can be adsorbed by Mn and iron (Fe) oxyhydroxides. Two reduced forms of vanadium can occur: V(IV), which can be deposited in sediments via organometallic ligands, and V(III), which forms under

euxinic conditions in the presence of H_2S and can precipitate in sediments as oxides or hydroxides. Due to its close association with Mn and Fe oxyhydroxides, V can be removed from pore waters upon reaching its reduced state. Thus, it is considered an indicator of the suboxidized-subreduced redox boundary.

Uranium (U) is closely associated with the presence of organic matter. In the water column, under normal oxic conditions, it primarily exists as uranyl ions (U(VI)), which can complex with carbonate ions to form uranyl tricarbonate $(UO_2(CO_3)_3^{4-})$ by binding with $CaCO_3$ particles. This process plays a crucial role in the authigenic enrichment of U in sediment, where it can precipitate or reduce to U(IV) in various oxide forms such as uraninite (UO_2), influenced by bacterial activity and reactions with hydrogen sulfide (H_2S). However, U can be depleted under oxic conditions, showing a significant correlation with organic matter primarily under anoxic conditions. Therefore, is considered a proxy for well-developed suboxic subreduced conditions.

Molybdenum (Mo) is also tied to organic matter and a reliable proxy for euxinic conditions (see details in Chapter IV). In oxic seawater, it exists predominantly as Mo(VI) in the form of molybdate ions (MoO_4^{2-}). Unlike uranium, its enrichment in sediment is strongly associated with Mn-oxyhydroxides. The exact fixation process of Mo in sediment is unclear, but diverse observations support it occurs at the water-sediment interface in the presence of free hydrogen sulfide (H_2S), with Mn playing a crucial role in bonding Mo particles to organic (macromolecular detritus) and/or metallic (pyrite) sulfur-rich particles. Thus, Mo is a key proxy for identifying euxinic bottom and pore waters. Scott and Lyons (2012) studied modern basins with euxinic bottom waters and identified threshold values of Mo concentration for different euxinic conditions: Mo values below 2 ppm (crustal average) indicate non-euxinic conditions; Mo ranging from 2 to 25 ppm indicates euxinic pore waters but free sulfide did not reach the water column; Mo enrichments between 25 and 100 ppm are associated to euxinic pore waters and intermittent euxinic conditions in bottom waters; and Mo concentrations exceeding 100 ppm indicate persistent euxinic conditions in both pore and bottom waters.

Regarding Fe species, these are used as a palaeoredox proxy based on the accumulation of highly reactive Fe in authigenic minerals (e.g., pyrite) during anoxic pulses. These enrichments are commonly represented by the Degree of Pyritization (DOP) and the Fe/Al ratio. DOP is typically calculated using Fe speciation measures. However, when detailed Fe speciation analyses are not available, DOP can be approximated by total DOP (DOP-T) (Algeo & Liu, 2020), calculated as DOP-T $= 55.85/64.12 \times S/FeT$, using total sulfur (S) and iron (Fe) from XRF or ICP-OES analyses. The FeT/Al ratio is also widely used (e.g., Taylor & McLennan, 1985; Lyons et al., 2003; Raiswell et al., 2008, 2018; Algeo & Liu, 2020) to indicate euxinic conditions when FeT/Al > 0.5-0.6.

The Corg/P ratio has also been considered a redox proxy due to its relationship with benthic redox conditions (Algeo & Ingall, 2007). In oxygen-rich environments, C oxidation and sedimentary phosphorus (P) preservation occur, whereas under anoxic conditions, P is released to the water column while organic carbon (Corg) preservation in the sediment is enhanced, resulting in high Corg/P ratios for anoxic conditions and lower values for oxic environments. It is calculated by dividing TOC and P values by their respective molar weights, following the equation Corg/P $= (TOC/12) / (P/30.97)$.

According to the reservoir effect (Algeo & Lyons, 2006), the Mo/TOC ratio serves as a useful tool for assessing hydrographic circulation in bottom waters (see Chapter IV). Molybdenum (Mo) concentrations in sediments, especially when normalized to total organic carbon (TOC), can reveal changes in seawater Mo removal rates, and permits to estimate the degree of basin restriction, with different regression-line slopes (mMo/TOC) corresponding to various levels of restriction. Strongly restricted basins have lower slopes, indicating limited Mo replenishment and higher watermass renewal times, while non-restricted basins exhibit higher slopes.

The utility of the Mo/TOC proxy, however, has limitations. In open marine settings such as upwelling continental margins, anoxic conditions can lead to high TOC but low Mo contents, resulting in misleadingly low mMo/TOC values. This scenario occurs due to the absence of a marginal sill, preventing stable redoxcline formation and leading to fluctuating redox conditions. Consequently, it is crucial to supplement Mo/TOC analysis with additional geochemical and sedimentological data to accurately interpret the hydrodynamics of the paleoenvironment under study.

5. RESULTS

5.1. Ichnological and sedimentological characterization

5.1.1. Hushpuckney black shale

The Hushpuckney shale is typically distinguished by planar parallel lamination in its lower half and consistently exhibits bioturbation in its upper part, characterized by *Chondrites*, *Zoophycos*, and subhorizontal burrows (for detailed description, refer to Chapter V) (Fig. VI.2). In the southern Heilman core, the Hushpuckney shale measures 90 cm in thickness, whereas it measures 50 cm in the Ermal (central) and Edmonds (northern) sections.

Bioturbation in the Heilman (south) and Ermal (central) cores penetrates 15 to 20 cm into the black shale, whereas in the northern Edmonds core, bioturbation was not identified in our analyses. However, previous works (Algeo et al., 2004) have identified small trace fossils using X-radiograph, including *Planolites*, *Schaubcylindrichnus*, *Zoophycos*, *Phycosiphon*, *Helminthopsis*, and *Trichichnus* (see Figure 3 in Algeo et al., 2004). Particularly noteworthy, the Ermal core displays a thin, light shale bed in its upper part (15 cm below the top), indicating redox fluctuations during the deposition of the black bed.

In all three sections, black beds overly limestone deposits with erosive/sharp contacts. Upward in the Ermal and Edmonds cores, black facies transition into light-grey shale beds, which are subsequently overlaid by limestone deposits (typically showing small carbonate fragments at contacts). The grey shales also exhibit bioturbation: common mottled texture, with dark-filled burrows in the Ermal core and the mentioned ichnoassociation defined by Algeo et al. (2004) in the Edmonds core.

5.1.2. Stark black shale

Stark shale predominantly exhibits sparse bioturbation. In the Midcontinent Shelf, the thickness of black beds varies from 60 cm in the northern (Edmonds) and southern (Heilman) cores to 80 cm in the central Ermal core. The black facies typically display planar parallel lamination in their lower 30 cm (extending up to 60 cm in the Ermal core) and transition upwards into grey shale beds (30-50 cm thick) that exhibit a mottled texture (Fig. VI.2).

Bioturbation is absent in the southern Heilman core, sparse in the central Ermal section, and slightly more abundant in the northern Edmonds core. Additionally, the depth of burrow penetration increases from south to north (5 cm in Ermal, 30 cm in Edmonds). The prevalent ichnogenera include *Zoophycos*, *Chondrites*, and *Planolites*. In the black beds, small *Chondrites* dominate. *Planolites* are found primarily in the grey shale deposits (both with light and dark infill). *Zoophycos* is rare and occurs only in the lower grey bed of the northern Edmonds core. Trace fossils observed in the grey deposits overlay a mottled texture.

5.2. Geochemical variations and palaeoredox conditions

5.2.1. Calibration of redox thresholds and trace element scales

In recent decades, seminar papers have established widely used measures of geochemical redox proxies as thresholds for different redox stages, particularly in reductive facies (suboxic to euxinic) (e.g., Raiswell et al., 1998; Wignall & Newton, 1998; Poulton & Canfield, 2005; Tribovillard et al., 2006; Algeo & Ingall, 2007; Algeo & Tribovillard, 2009). However, it is highly recommended to calibrate these thresholds for the specific study basin based on proxy covariation (Algeo & Li, 2020).
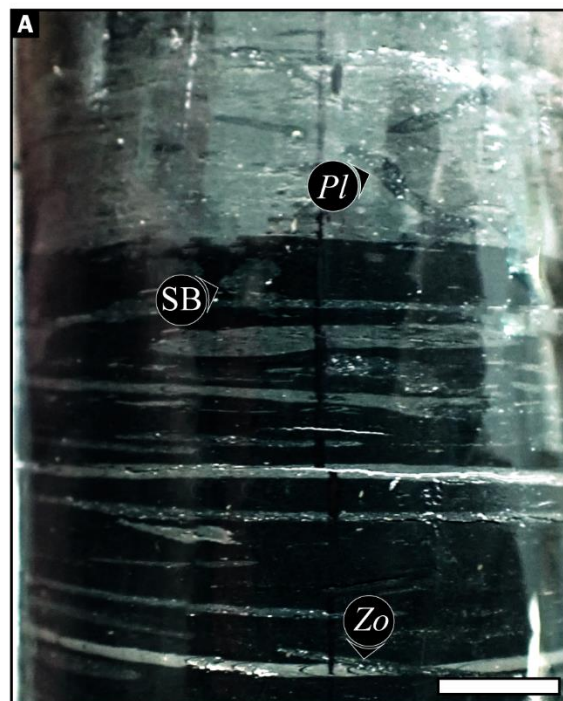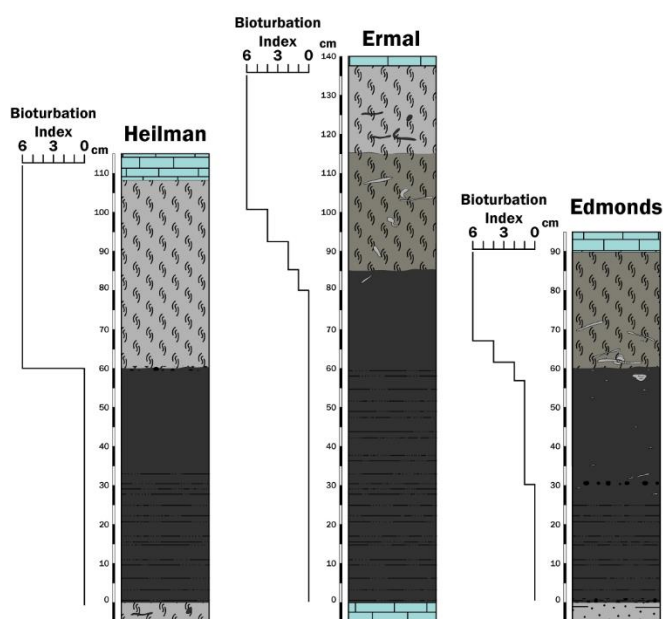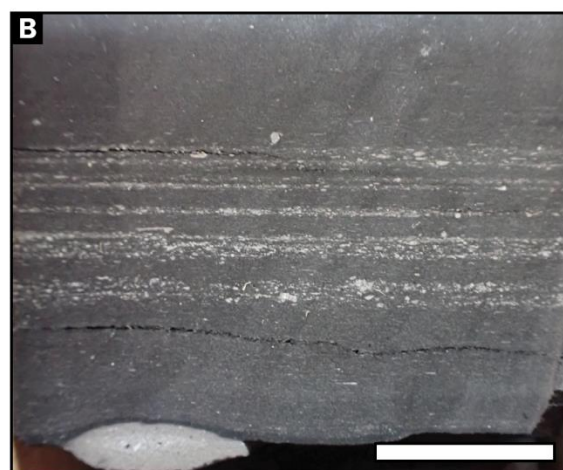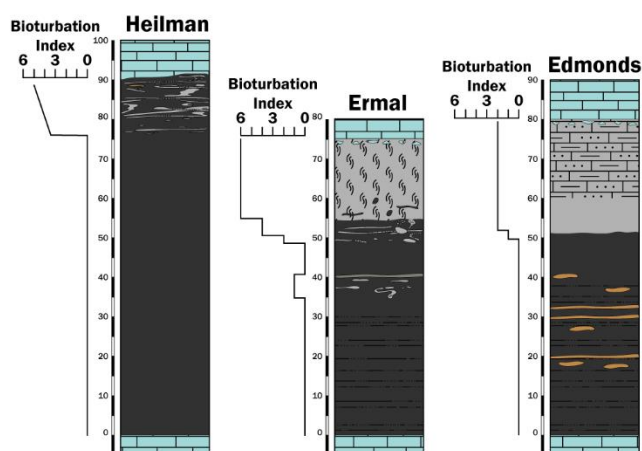
Figure VI.2. In-detail schematic illustration of all the studied "core shale" units, indicating the bioturbated intervals, and Bioturbation index, and their core-view. A) Contact between the black and grey beds, showing some light-infilled burrows in the black facies and dark Planolites *(Pl) in the grey bed. B) Planar parallel lamination and phosphate nodules, characteristic of the lower part of the black beds. SB: sub-horizontal burrow,* Zo: *Zoophycos. Scale bar is 1 cm.*

For the study units, several redox-sensitive metals (V, U, and Mo) and ratios (DOP-T, DOP est, $Corg/P$, and Fe/Al) have been calibrated to identify redox thresholds (see Supplementary Material Figs. 1-6). Generally, all proxies yield similar values for the T1, T2, and T3 redox thresholds (suboxidised-subreduced, subreduced, and euxinic, respectively) in both the Hushpuckney and Stark shales (Table VI.1). Similar values for the suboxidised to euxinic stages indicate

rapid, sharp shifts from dysoxic to euxinic conditions (Algeo & Li, 2020). In one particular case (DOP-T in Stark Shale, Heilman core), T3 values (0.4) are slightly higher than T1 and T2 (0.3), indicating a slower transition from dysoxic-suboxic to euxinic stages.

Previous studies on Pennsylvanian black shales (Algeo et al., 2004; Algeo & Maynard, 2008) identified high-frequency variations in trace elements. To facilitate the identification of secular trends in trace elements, the

		V EF	U EF	Mo EF	DOP-T	DOPest	Corg/P	Fe/Al
T1	Black Sea				0.3		160	
	Hushpuckney - Edmonds				0.4	0.2	15	0.41
	Hushpuckney - Ermal				0.61	0.45	20	0.35
	Hushpuckney - Heilman				0.52	0.35		0.8
	Stark - Edmonds				0.42	0.25	20	0.45
	Stark - Ermal				0.4	0.22	55	0.5
	Stark - Heilman				0.5	0.3	15	0.4
T2	Black Sea				0.27		160	
	Hushpuckney - Edmonds	1.8	10		0.4	0.2	15	0.41
	Hushpuckney - Ermal	2	10		0.61	0.45	20	0.35
	Hushpuckney - Heilman	4	10		0.52	0.35		0.8
	Stark - Edmonds	2	5		0.42	0.25	20	0.45
	Stark - Ermal	1	1		0.4	0.22	55	0.5
	Stark - Heilman	3.5	7		0.5	0.3	15	0.4
T3	Black Sea		1		0.3		160	
	Hushpuckney - Edmonds	1.8	10	50	0.4	0.2	15	0.41
	Hushpuckney - Ermal	2	10	40	0.61	0.45	20	0.35
	Hushpuckney - Heilman	4	10	100	0.52	0.35		0.8
	Stark - Edmonds	2	5	8	0.42	0.25	20	0.45
	Stark - Ermal	1	1	1	0.4	0.22	55	0.5
	Stark - Heilman	3.5	7	50	0.55	0.4	15	0.4

Table VI.1. Calibrated values of selected proxies (VEF, UEF, MoEF, DOP-T, DOP est, Corg/P, and Fe/Al) for the T1, T2 and T3 thresholds (suboxic to euxinic facies).

present research has represented trace elemental concentrations using different scales (logarithmic, estimated, and Z-scale). This approach aims to standardize trace metals to a narrow range of values and facilitate comparison of trends among them.

The Z-scale is calculated by normalizing the elemental concentration to a mean of 0 and standard deviation of 1, while the estimated (est) scale normalizes the elemental measure using the mean of the central interval of the black shale (Algeo & Maynard, 2008). Additionally, DOP est is calculated following the equation developed by Cruse & Lyons (2004): DOP est = $0.65 \cdot DOP\text{-}T^2 + 0.29 \cdot DOP\text{-}T + 0.016$. The representation of trace elements in different scales allows for detailed identification of sample-to-sample variations and cyclic patterns.

5.2.2. Redox proxies and trace elements

For the Hushpuckney shale (Fig. VI.3), TOC values range from 10 to 40% in the black bed and below 5% in the upper grey shale. DOP-T varies between 0.4 and 1 in the black shale and remains below 0.5 in the grey shale, while DOP est ranges from 0.2 to 1 in the black beds and is consistently below 0.2 in the grey shale. The FeT/Al ratio in the black units is between 0.35 and 1.

VEF ranges from 2 to 80 in the black units, decreasing sharply to below 2 in the grey shale. UEF and MoEF exhibit similar patterns, ranging from 10 to 600 and 50 to 9000, respectively, in the black beds, and dropping below 10 and 50 in the grey shale.

In the Stark shale (Fig. VI.4), TOC values are slightly lower than in the Hushpuckney shale, with 5 to 35% in the black units and below 2% in the grey units. DOP-T ranges from 0.4 to 1 in the black unit and is always below 0.5 in the grey beds, while DOP est varies from 0.25 to 1 in the black beds and remains under 0.25 in the upper grey shale. The FeT/Al ratio ranges from 0.25 to 0.8 in the black shale and is below 0.35 in the grey shale. VEF is between 3 and 11 in the black facies, decreasing to below 2 in the grey shale. UEF and MoEF trends follow a similar pattern, with values between 5 and 300 and 8 and 900, respectively, in the black shale, and below 5 and 8, respectively, in the grey shale.

Several trace elements (TE) were selected as redox-sensitive proxies (Zn, Cu, Ni, Cr, Mo, U, and V). Representing these elements on different scales (estimated, logarithmic, and Z-scale) stretches raw values to a discrete range, enabling the identification of
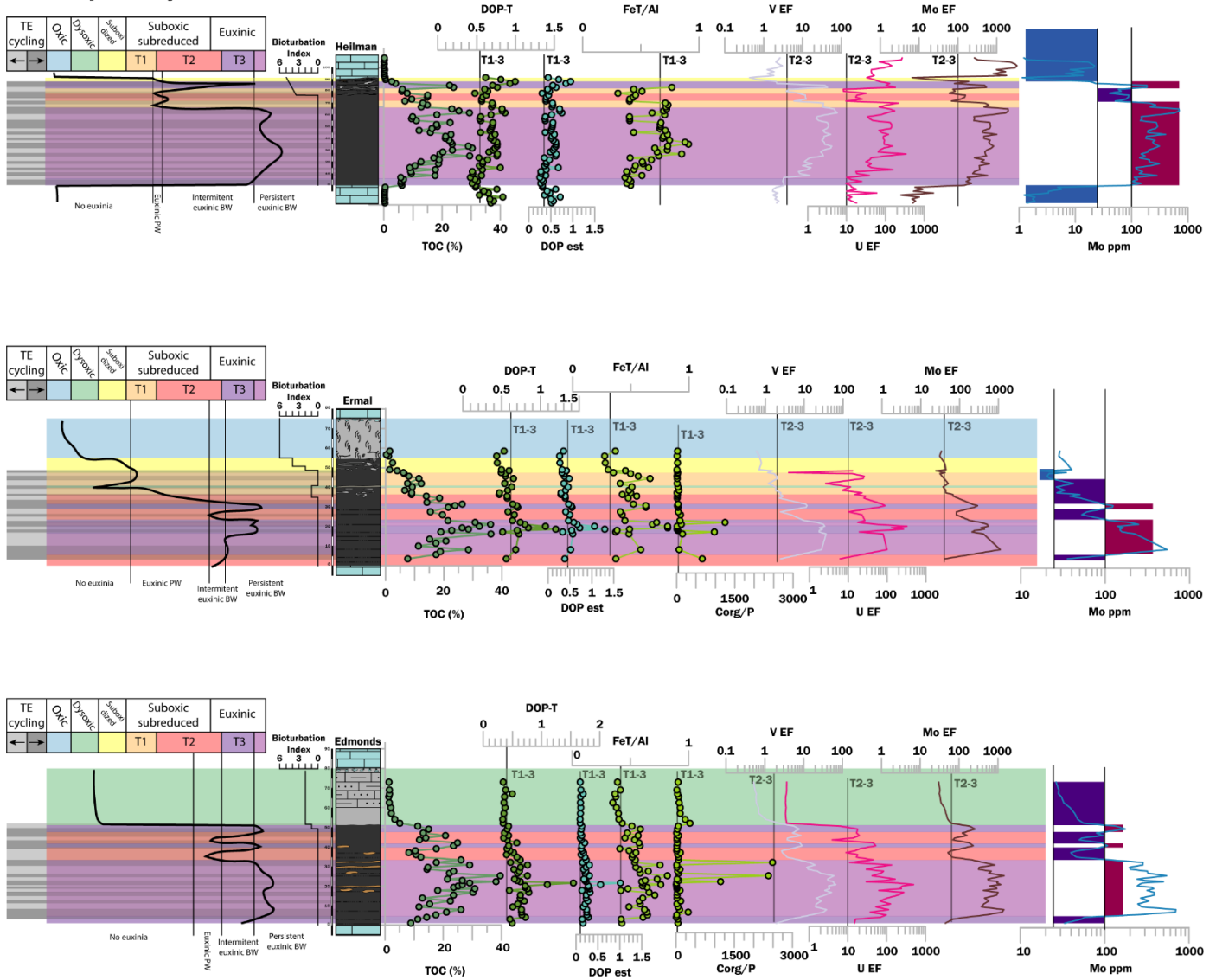
Figure VI.3. Redox proxies for the Hushpuckney Shale in the study sections (TOC; DOP-T, DOP est, FeT/Al, Corg/P, VEF, UEF, MoEF, and Mo ppm). A general, integrated trend is illustrated in the left diagram. Note the presence of H2S (euxinia) in the bottom- and/or pore-water.

small-scale shifts during the deposition of the black facies.

In the Hushpuckney shale (Fig. VI.5), nearly 15 cycles, ranging from 2 to 10 cm, were identified within the 50 cm-thick black bed at the northern Edmonds and central Ermal cores. In contrast, the thicker (90 cm) black bed in the southern Heilman core contains 25 cycles, ranging from 5 to 15 cm.

In the Stark shale black units (Fig. VI.6), cycles are similar in thickness, ranging from 2 to 10 cm. Nearly 18 cycles were identified in the 60-70 cm black beds of the Edmonds and Ermal cores, while in the Heilman

core, only the lower 35 cm of the black shale displayed TE-cycles, with 16 identified.

5.2.3. Redox trends

By analysing the profiles of the selected proxies, several positive and negative peaks are identified (Fig. VI.7), forming multiple cycles that can be subdivided into major and minor redox trends. Therefore, high-frequency cycles (2-10 cm) exhibited by TEs, are overprinted by major (10-40 cm) and minor (5-15 cm) redox trends.

Major redox trends are similar for the Hushpuckney and Stark shales across the three study
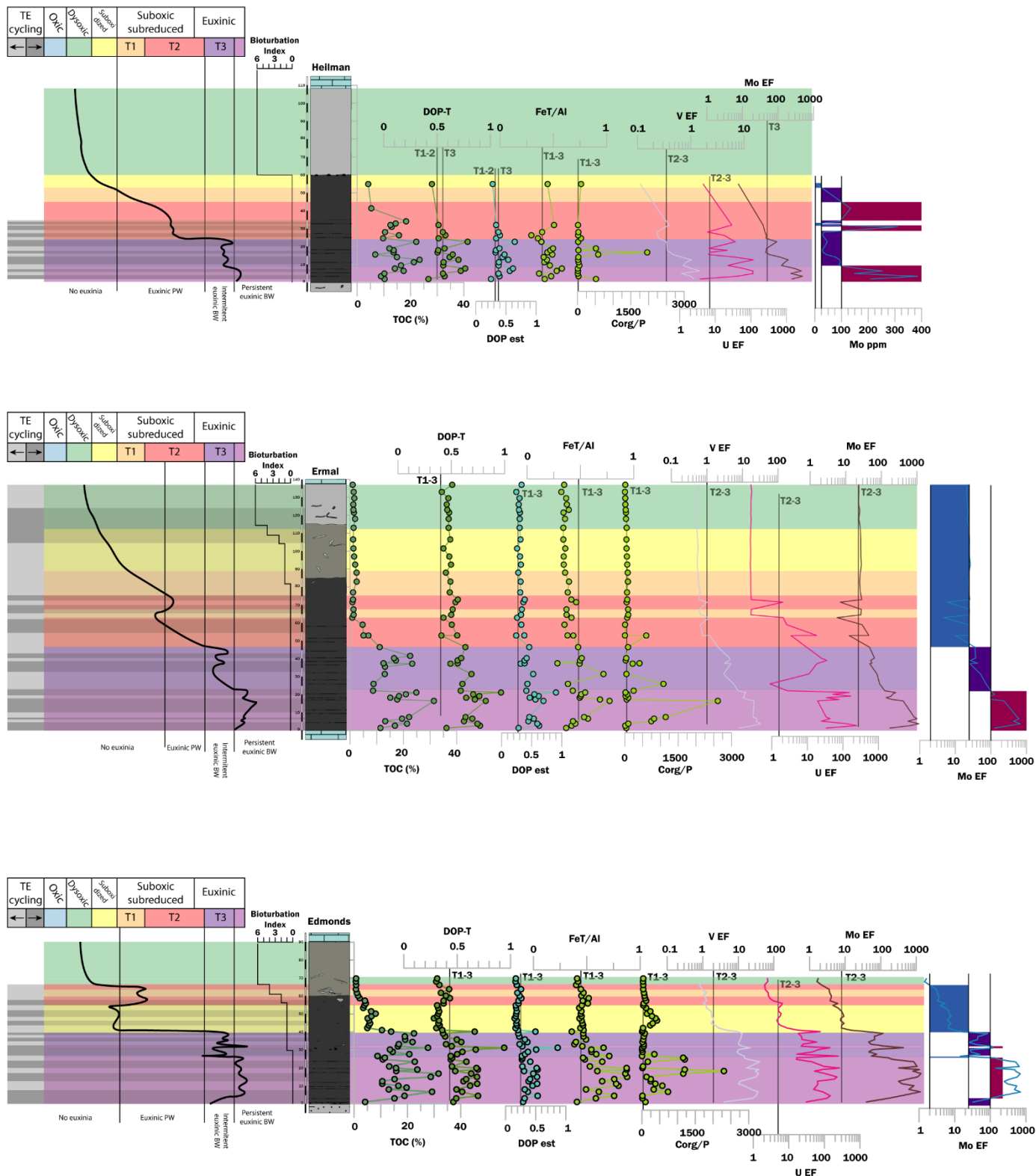
Figure VI.4. Redox proxies for the Stark Shale in the study sections (TOC; DOP-T, DOP est, FeT/Al, Corg/P, VEF, UEF, MoEF, and Mo ppm). A general, integrated trend is illustrated in the left diagram. Note the presence of H2S (euxinia) in the bottom- and/or pore-water.
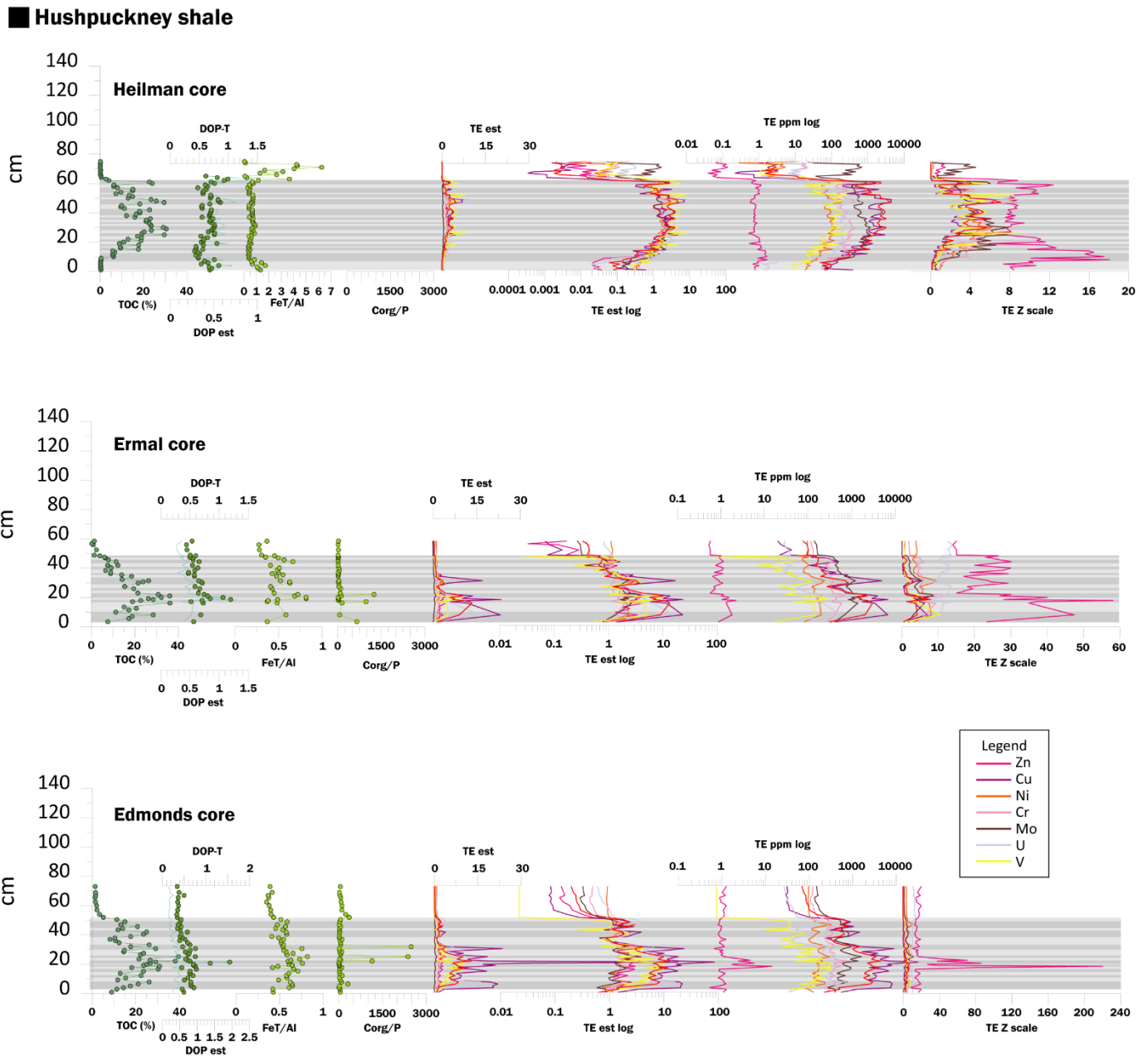
Figure VI.5. Trace element measures for the Hushpuckney Shale, showcasing Zn, Cu, Ni, Cr, Mo, U, and V in different scales (estimated, logarithmic and Z-scale). Dark bands indicate positive trends, while light bands indicate negative peaks (TE-cycles).

sections (Fig. VI.7). An initial trend towards more reductive (euxinic) facies (lowermost 20-35 cm) is indicated by a positive peak in all the redox-sensitive proxies. The maximum accumulation of trace elements marks the maximum flooding surface (MFS) of the highstand stage, during which black shales are deposited (Algeo et al., 2004; Algeo & Maynard, 2008). Following this first euxinic pulse, proxy values sharply decline, and a second euxinic pulse begins, continuing until the middle-upper part of the black facies (subsequent 10-25 cm) (Fig. VI.7). Finally, redox conditions shift towards oxic/dysoxic facies, typically indicated by a sharp

reduction in the concentration of redox-sensitive elements through the uppermost part of the black beds and into the overlying grey shale (Fig. VI.7).

Minor trends exhibit greater variability among the study sections, reflecting subtle variations in redox conditions within the same redox stage (5-15 cm). In the Stark Shale, the first euxinic pulse is subdivided into 1 to 4 reductive minor trends, with an increasing number of minor trends towards the northern Edmonds core (Fig. VI.7). The second euxinic pulse is divided into three minor pulses, generally trending towards more reductive conditions, except for a negative peak just above the MFS
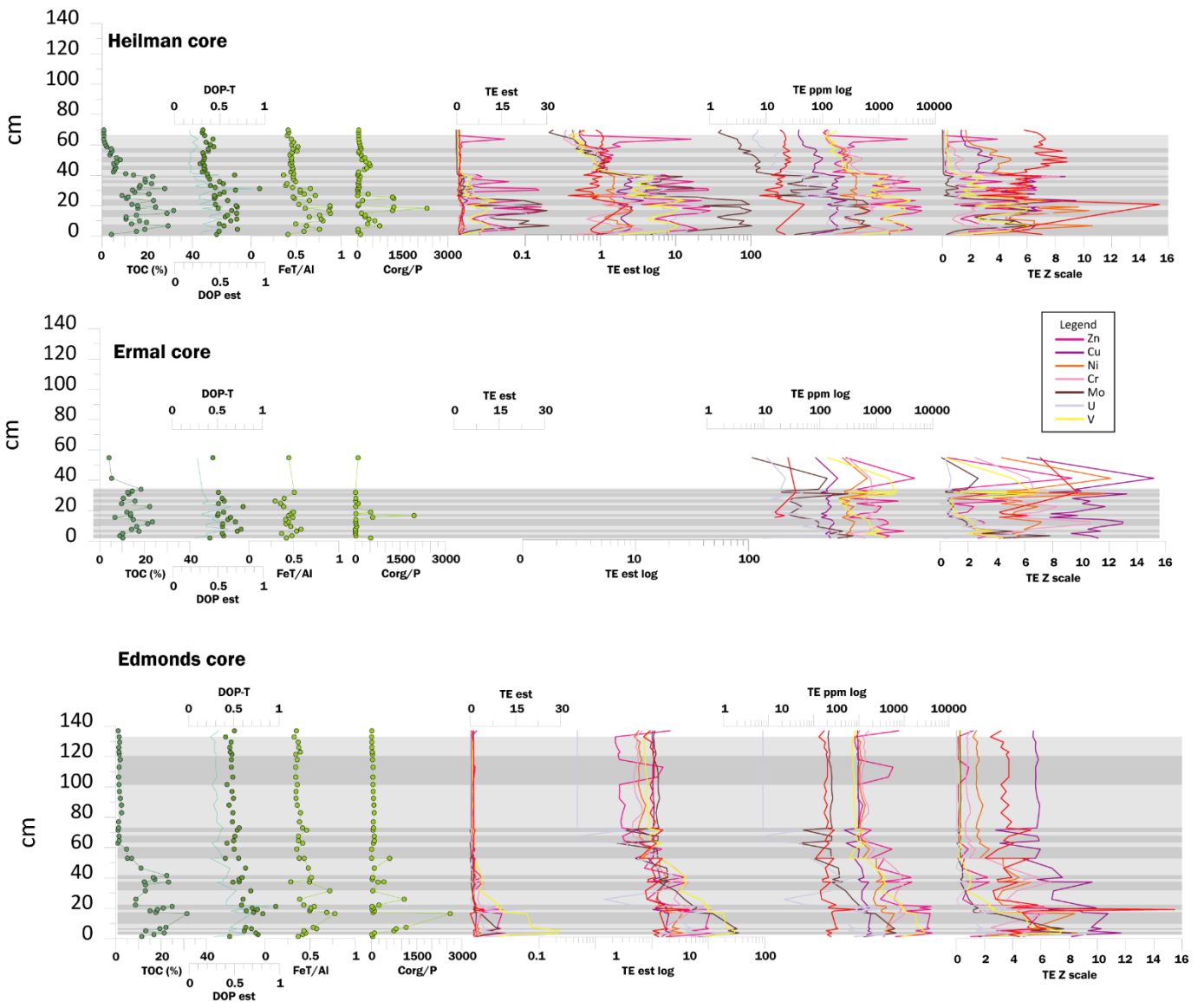
Figure VI.6. Trace element measures for the Stark Shale, showcasing Zn, Cu, Ni, Cr, Mo, U, and V in different scales (estimated, logarithmic and Z-scale). Dark bands indicate positive trends, while light bands indicate negative peaks (TE-cycles).

in the Ermal core (Fig. VI.7). In the Hushpuckney Shale, the initial euxinic pulse is divided into three minor trends in the central and northern sections, showing an initial shift towards euxinic conditions, followed by a negative peak in geochemical measures, and a subsequent trend towards more euxinic conditions (Fig. VI.7). After the MFS, 2 to 3 minor trends are identified within the second euxinic pulse, indicating high variability between subreduced and euxinic facies (Fig. VI.7).

5.2.4. Hydrographic restriction proxies

Mo, TOC, and Mo/TOC trends were analysed to assess hydrographic circulation patterns during the deposition of the Hushpuckney and Stark shales. As

indicated in previous sections, two main parts can be identified within the black beds: a lower black shale below the MFS, roughly corresponding to the first euxinic pulse; and an upper black shale above the MFS, associated with the second euxinic pulse and sometimes extending into the lower part of the dysoxic/suboxic trend.

When plotting TOC versus Mo values (Fig. VI.8), the slopes (mMo/TOC) are typically lower for the upper than for the lower parts of the black beds (Table VI.2). In the Stark Shale, slopes for the lower black shale are similar to those from the Framvaren Fjord and the Cariaco Basin (11-21), while descending to

slopes lower than those of the Black Sea (0.8-3.8). A similar pattern is observed in the Hushpuckney Shale, with slopes for the lower black beds (6-13) comparable to the Framvaren Fjord, but similar to the Black Sea (0.8-3.8) for the upper black beds. Notably, the Mo and TOC show a poor correlation in the Heilman core for the Stark Shale, and yield a higher slope for the upper black bed in the Hushpuckney Shale, contrary to the other sections.

The Mo/TOC profiles (Fig. VI.9) align with the trends outlined earlier, exhibiting a positive excursion in the lower black bed followed by a negative excursion in the upper black bed. These variations in the Mo/TOC ratio reflect a concurrent increase (lower black bed) and decrease (upper black bed) in both Mo and TOC concentrations. Occasionally, a third positive peak in the Mo/TOC ratio is observed in the uppermost part of the upper black shale, correlating with a simultaneous increase in Mo and TOC, akin to the first euxinic pulse.

6. DISCUSION

### 6.1. Redox conditions during black shale deposition

As discussed in the previous section, distinct redox trends are identified during the deposition of the Hushpuckney and Stark shales (Fig. VI.7). The major trends are similar for both shales across all the study sections, starting with the initial euxinic pulse in the lower black beds, which reaches its maximum intensity towards the MFS. Subsequently, a sharp negative peak is observed in all proxy values, corresponding with the onset of regressive sea-level trends. A second euxinic pulse occurred in the middle part of the black beds during the regressive stage, although its intensity is consistently lower than that of the first euxinic pulse. Finally, the uppermost part of the black beds was deposited under suboxic conditions, exhibiting variable shifts from suboxidised to strongly subreduced bottom waters, the latter in combination with euxinic pore waters.

Similar trends are observed for Hushpuckney and Stark black shale members suggesting analogous redox patterns for the Dennis (Stark Shale) and Swope (Hushpuckney Shale) cyclothems, whose redox conditions can be identified for each sea-level stage. The onset of transition is marked by the lowermost contact of the black units, which commonly overlie limestones, and end at the MFS when the shoreline reaches its maximum extension cratonwards. The first euxinic pulse corresponds with this transgressive stage, characterised by a strong pycnocline. Just below and above the MFS, TE-cycles are thicker than those registered in the lower and upper parts of the black beds, indicating higher sedimentation rates during the maximum sea-level. Following the MFS, the regressive stage begins, marked by the second euxinic pulse. In this stage, sea-level fall, along with reduced continental input, led to a deeper pycnocline, evidenced by lower concentrations of redox-sensitive proxies. The upper regressive stage is characterised by less reductive conditions (suboxic), exhibiting abrupt shifts from suboxidised to strongly subreduced conditions (T1 to T3). This is consistent with the similar values identified in the calibration of the proxies for the T1-T3 redox stages and indicates a weak pycnocline. This suggests that water mixing began to recover after the two euxinic pulses, transitioning to stable oxic-dysoxic conditions during the deposition of the upper grey shale member at the end of the regressive stage.

Notably, a regional pattern is observed in both cyclothems though the Midcontinent Shelf (Fig. VI.7, cf. Figs. VI.3-6). In the Dennis cyclothem (Stark Shale), the MFS is recorded higher towards the north (10 to 25 cm), and TE-cycles are slightly thicker. This indicates higher sedimentation rates in the inner regions of the Midcontinent Shelf (Edmonds and Ermal cores) during the transgressive stage, with stronger reductive pulses in these inner sections. Conversely, in the Swope cyclothem (Hushpuckney Shale), the MFS is recorded at nearly the same position (30 cm), and reductive conditions are similarly strong in both the southern and northern sections (Heilman and Edmonds cores, respectively). In contrast, the middle Ermal section exhibits intermittent euxinic conditions during the early transgressive stage, with dysoxic to suboxic conditions occurring earlier than in the other sections.

Based on previous estimations of sedimentation rates for the studied black facies (Heckel, 1986; Algeo & Wilkinson, 1988; Watney et al., 1991; Saller et al., 1994; Rasbury et al., 1998; Algeo et al., 2004), we adopt
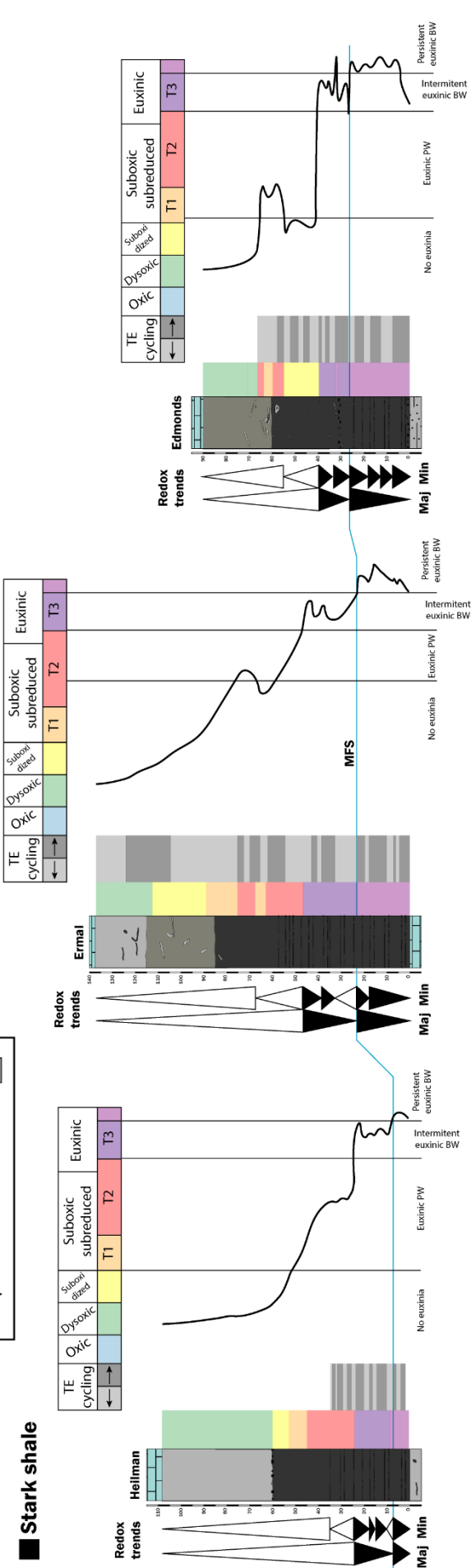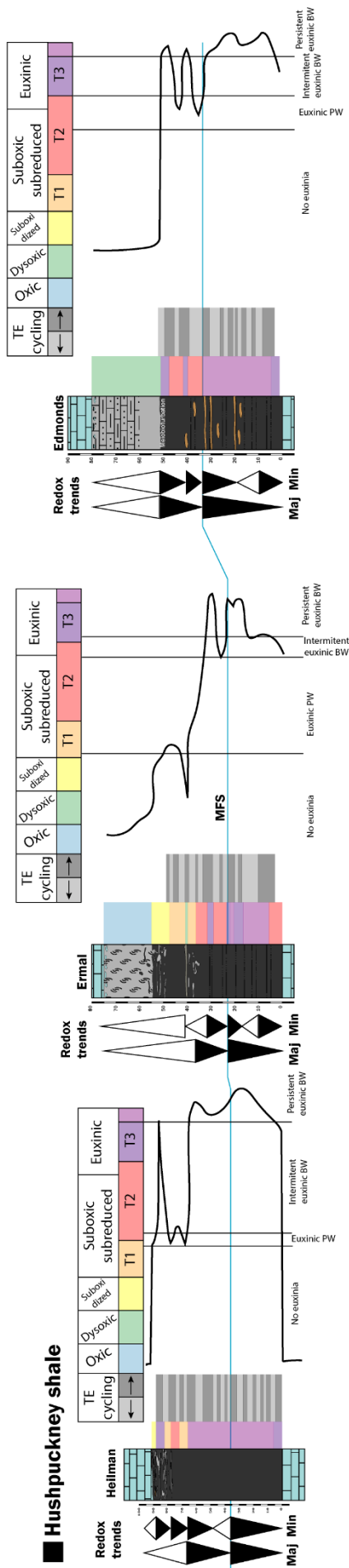
a tentative sedimentation rate of 0.5-2 cm/kyr for the Hushpuckney and Stark black shale units to evaluate the triggers of the redox trends. The Hushpuckney Shale was deposited over a period of 25-100 kyr, similar to the 30-120 kyr estimation for the Stark Shale. TE-cycles (2-10 cm) are estimated to span 2-10 kyr, suggesting they correspond to sub- Milankovitch climatic fluctuations. In contrast, major and minor (decimetric) redox trends exhibit a wide range of durations, commonly exceeding 30 kyr, indicating a combination of major glacio-eustatic cycles (>50 kyr) (e.g., Heckel, 1986) superimposed on high-frequency climatic fluctuations.

Hydrographic restriction during black shale deposition can be tentatively inferred based on Mo/TOC patterns and low mMo/TOC. However, a detailed study of the TOC and Mo trends indicates that Mo/TOC variations correspond to shifts in redox conditions rather than the reservoir effect (Algeo & Lyons, 2006). Sluggish bottom-water circulation during euxinic conditions would lead to higher TOC values along with variable Mo concentrations. However, the Hushpuckney and Stark black shales exhibit similar patterns for Mo and TOC, thereby discounting the role of hydrographic restriction during euxinic conditions. Similarly, low values of productivity-related proxies (barium and phosphorous) indicate that a) primary productivity played a minor role during black shale deposition, and/or b) diagenesis erased or remobilised Ba content from the black shale facies.

The cause of the euxinic pulses can be likely associated with a combination of climatic and sea-level variations. The lower part of the studied black beds (i.e., the first euxinic pulse) corresponds to a period when the melting of the Gondwanan ice sheets caused a sea-level transgression associated with a humid climate (e.g., Algeo et al., 2004). Increased continental detrital and freshwater input led to a strong pycnocline, reducing water mass mixing during the transgressive and highstand stages. During this period, high-frequency climatic fluctuations are recorded as TE-cycles, associated with

shifts between higher and lower continental input (e.g., more or less humid climate and coastal swamp development). Following the MFS, the growth of ice sheets produced a sea-level regression, which can be subdivided into two subsequent parts linked to the weakening of the pycnocline. The early regressive stage is characterised by euxinic conditions, weaker than during the highstand stage, corresponding to the early movement of the shoreline basinwards. The formation of the Gondwanan ice sheets also led to a more arid climate, reducing the continental input to the basin. With the decrease in freshwater input, the pycnocline subsequently destabilised upwards during the regressive stage, leading to higher water mass mixing and thus less reductive conditions. Finally, an abrupt shift to dysoxic/sparsely oxic conditions is recorded during the deposition of the upper grey member of the Stark and Hushpuckney shales.

6.2. The role of bioturbation

In the study cores, trace fossils are mostly present in the upper grey shale beds and the uppermost part of the black facies (Fig. VI.2). All of them showcase grey shale infill, indicating that they were produced during the deposition of the upper grey shale member, regardless of whether the burrows are observed in the light or dark facies. Geochemical proxies indicate oxic to dysoxic conditions during the deposition of the grey shales; however, stable low values do not allow differentiation within the oxic-dysoxic range. In this context, the ichnological analysis of the present ichnotaxa will enable us to a) precisely determine the redox conditions during the deposition of the grey shale bed (i.e., late regressive stage), and b) study the recovery of benthic communities after the suboxic/euxinic pulses.

Low ichnodiversity (1-3) of the ichnoassemblages present in the grey shales, well-ventilated (i.e., completely oxic) conditions must be ruled out. Instead, dysoxic conditions are likely, supported by the fact that common ichnogenera in the study units (*Zoophycos* and *Chondrites*) are typically

Figure VI.7. Major and minor redox trends for the Hushpuckney and Stark shales in all the study sections. MFS: maximum flooding surface, Maj: major redox trends, Min: minor redox trends. T1, T2 and T3 indicates the calibrated redox thresholds.
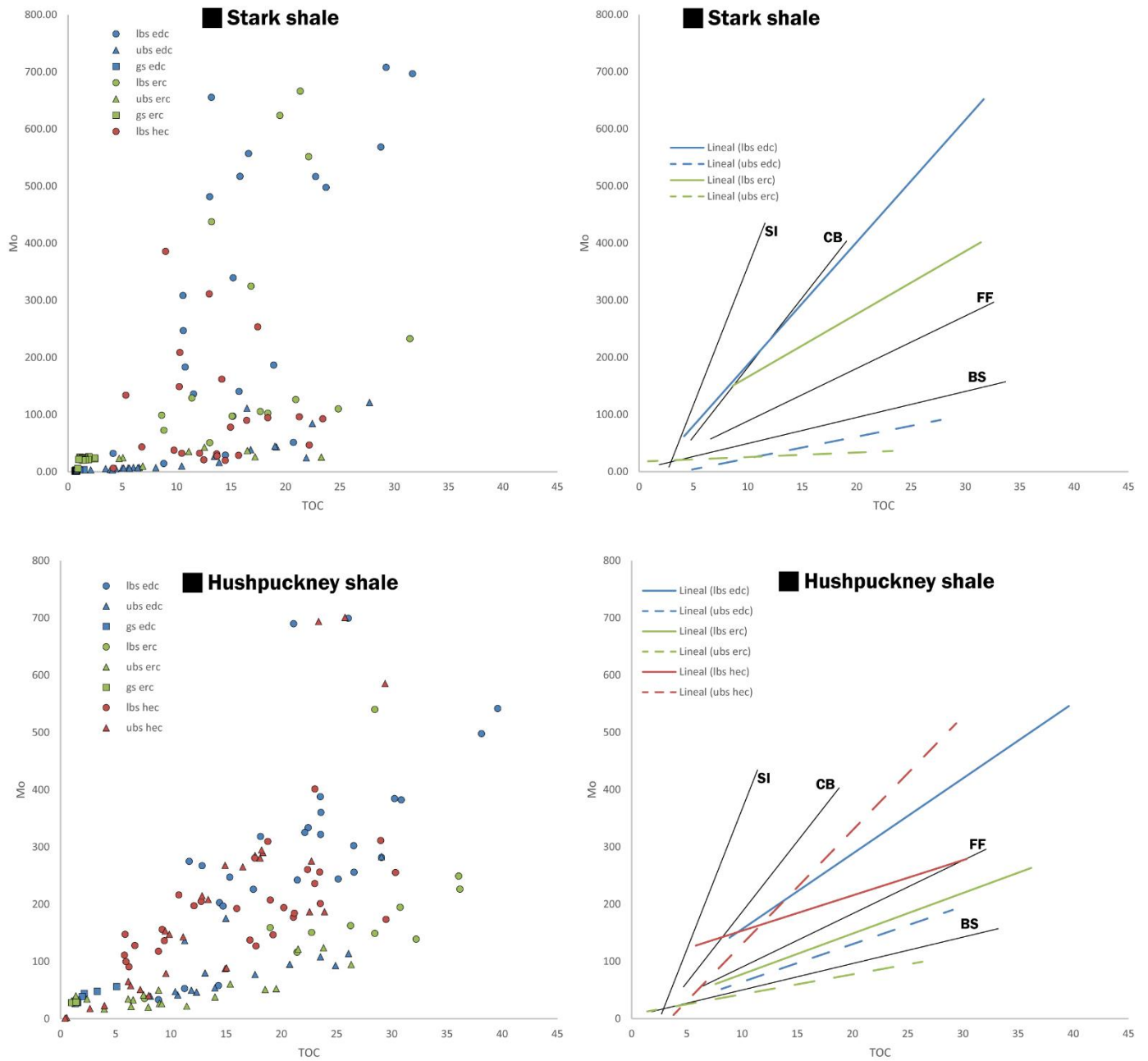
Figure VI.8. Mo vs TOC plots for the Hushpuckney and Stark shales, indicating the mMo/TOC slopes for the lower and upper black shales of each study section. Lbs: lower black shale, UBS: upper black shale, Gs: grey shale, Edc: Edmonds core, erc: Ermal core, Hec: Heilman core. Note the moder analogues as references: BS: Black Sea, FF: Framvaren Fjord, CB: Cariaco Basin, SI: Saanich Inlet.

Black shale unit	Core	Lower Black Shale					Upper Black Shale				
		m	r	r²	p	n	m	r	r²	p	n
Hushpuckney	Edmonds	13.16	0.64	0.41	0.0004	26	6.6	0.54	0.29	0.0308	16
	Ermal	7.1	0.46	0.21	0.1525	11	3.48	0.81	0.64	3.76E-05	19
	Heilman	6.16	0.64	0.41	0.0002	29	19.89	0.82	0.67	1.67E-07	27
Stark	Edmonds	21.43	0.64	0.41	0.0017	22	3.79	0.82	0.67	1.85E-06	23
	Ermal	11	0.32	0.1	0.2522	15	0.8	0.51	0.26	0.1298	12
	Heilman	-1.04	-0.05	0.003	0.8154	23					

Legend: p < 0.05 (2σ) | p < 0.32 (1σ) | p > 0.32

Table VI.2. Mo/TOC slopes for the Hushpuckney and Stark shales, with differentiation of lower and upper black shales.
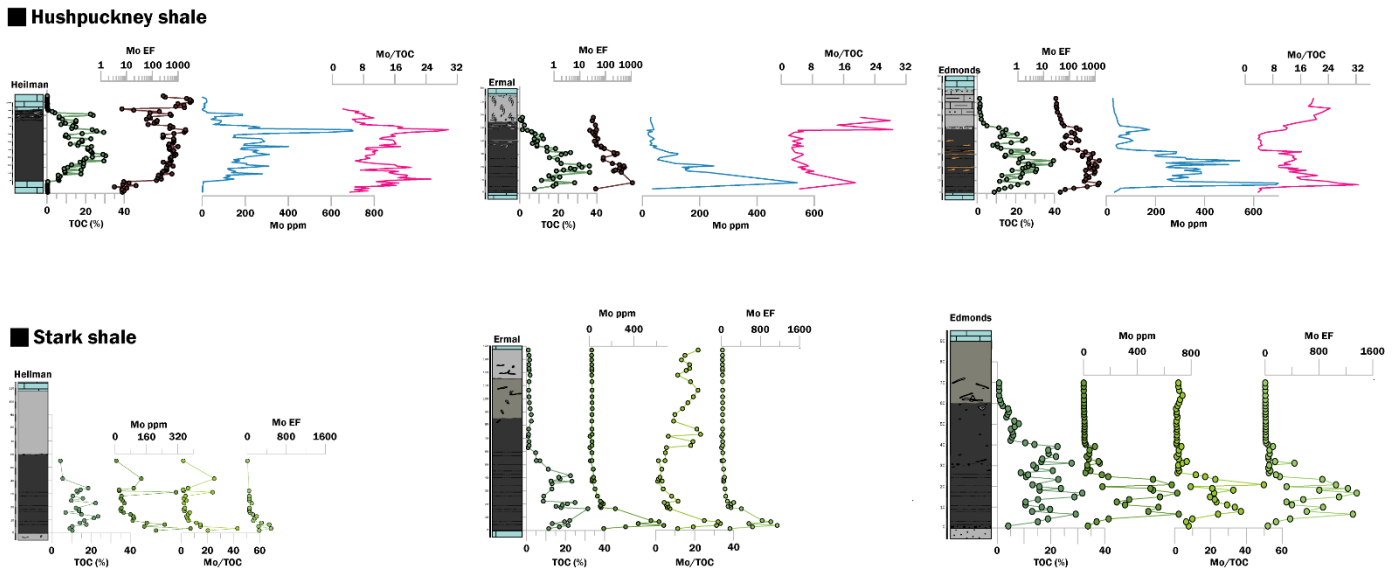
Figure VI.9. Selected proxies for hydrographic restriction (TOC, Mo, MoEF, and Mo/TOC) for the Hushpuckney and Stark shales in the studied cores. Note the similar trends for Mo and TOC.

associated with the leverage of organic matter under poorly oxygenated conditions. It is noteworthy that the development of simple burrows such as *Planolites* and a mottling texture can occur a few weeks after sedimentation, whereas the development of more complex structures (*Zoophycos*, *Chondrites*) can span months to years. Therefore, the presence of simpler structures more accurately reflects the redox conditions during sedimentation.

During the Dennis cyclothem (Stark Shale), bioturbation is more abundant in the central (Ermal) and northern (Edmonds) sections, while only sparse mottling is recorded in the southern Heilman core (Fig. VI.2). This trend aligns with the pycnocline trend evidenced by geochemical proxies, as a weaker pycnocline northwards facilitates bottom-water mixing and oxygenation, allowing faster and more efficient colonisation of the benthos after the highstand euxinic pulse. In contrast, the Swope cyclothem (Hushpuckney Shale) is characterised by scarce bioturbation in the northern (Edmonds) section (only *Trichichnus* penetrates within the black shale, see figure 4 in Algeo *et al.*, 2004), while the central and southern regions exhibit well-developed burrows penetrating the black beds. This scarce bioturbation coincides with an extremely abrupt redox shift from euxinic to dysoxic conditions at the boundary between the black and grey facies. This could be interpreted as revealing faster recovery of macrobenthic tracemaker

communities from the euxinic/suboxic conditions during the Swope cyclothem (south-central sections) compared with the Dennis cyclothem, associated to weaker pycnoclines and higher water mass mixing for the Swope cyclothem. However, moderate freshwater input during the early regressive stage could have strengthened the pycnocline near the shoreline (northern Edmonds core) without affecting basinwards regions, unlike during the transgressive and highstand stages.

7. CONCLUSIONS

The integration of geochemical and ichnological analyses has enabled the precise characterization of redox conditions during the deposition of the Stark and Hushpuckney shales at the Upper Pennsylvanian (Upper Carboniferous) in North America, along with the evaluation of the palaeoenvironmental factors controlling redox trends.

The black shale beds are characterised by a strong euxinic pulse in the lowermost part of the bed, corresponding to periods of sea level transgression. After the maximum flooding surface, a second, weaker euxinic pulse is recorded during the early regressive phase. The uppermost part of the black beds is marked by abrupt shifts towards suboxic redox conditions, transitioning to dysoxic facies during the deposition of the upper grey shale.

Geochemical composition has allowed to identify major and minor redox trends, linked to changes in sea level (glacio-eustatic influence), overlaid by high-frequency climatic fluctuations (TE-cycles). The development of a strong pycnocline during the transgressive, highstand, and early regressive stages is associated with the euxinic pulses characterising the deposition of the lower black beds. Conversely, lower sea levels and continental input weaken the pycnocline, allowing easier mixing of the water mass, resulting in suboxic conditions during the deposition of the uppermost part of the black beds and dysoxic conditions during the deposition of the grey shale bed. Detailed study of Mo and TOC patterns has ruled out the influence of hydrographic restriction on the development of euxinia.

Low ichnodiversity suggests predominantly dysoxic conditions during the deposition of the grey shale. The abundance and distribution of ichnotaxa have identified a regional pattern of recovery after the euxinic pulses in the Midcontinent Shelf. During the Dennis cyclothem, weaker pycnoclines towards the north facilitated faster macrobenthic tracemaker colonisation during the regressive stage in the inner regions of the Midcontinent Shelf. In contrast, during the Swope cyclothem, trace fossils indicate higher rates of macrobenthic tracemaker colonisation after the reductive pulses, although the inner region exhibits sparse bioturbation. This variability can be attributed to stronger pycnoclines towards the craton due to moderate freshwater input, resulting in oxygen-deprived bottom waters nearshore.

CHAPTER VII

FINAL REMARKS AND CONCLUSIONS

1. FINAL REMARKS AND HIGHLIGHTS

The multiproxy approach used in this dissertation, based on an integrative geochemical and ichnological analysis, has provided insights into several questions surrounding the interpretation of black shale facies. Thus, four main questions of significant interest have emerged from our research: i) Are black shales exclusively related to anoxic conditions? ii) How does the macrobenthic tracemaker community respond to inhospitable conditions associated with black shales? iii) Can black shales be considered the record of global phenomena? And iv) Are reductive conditions persistent during black shale deposition? The conducted research has provided answers to these relevant questions:

i) Although it is well established that organic matter can be preserved in sediments under both oxic and anoxic conditions (see Chapter I), black shales have traditionally been perceived as forming exclusively under severe and widespread anoxic conditions (e.g., Wignall, 2005). However, as demonstrated by the obtained results, even slightly reductive conditions (suboxic) can lead to organic carbon preservation and black shale formation as seen in the Asturian and Belluno basins during the T-OAE, and some parts of black shale beds deposited in the Late Pennsylvanian Midcontinent Sea. Moreover, reductive conditions typically appear abruptly in the geological record, as supported by geochemical data, indicating that these abrupt redox shifts are widespread and recurrent, occurring not only at the onset of black shale deposition but also intermittently during and after the reductive phases (see Chapter VI). In this regard, calibration of redox thresholds has helped demonstrate that slightly suboxic to strongly euxinic conditions are evidenced by similar trace element values or ratios (see Chapters IV and VI, and Appendices I and II). Therefore, while black shales are characterized by reductive conditions during deposition, strict anoxia/euxinia is not a prerequisite; instead, the common factor is the occurrence of rapid and pronounced redox fluctuations.

ii) It has been widely demonstrated that black shales represent short intervals in the geological record —for instance, the T-OAE lasted no more than 500 kyr (e.g., Boulila et al., 2014, 2019; Boulila & Hinnov, 2017), and Pennsylvanian black shales are estimated to span 25 to 120 kyr. In this context of abrupt onset and development of black shales, especially interesting is the rapid reappearance of macrobenthic tracemaker communities following the inhospitable (reductive) conditions governing black shale deposition. The conducted research reveals that this fast recovery varies depending on dominant redox conditions after black shale deposition. For example, the macrobenthic tracemaker community registered in the aftermath of the T-OAE in the Asturian Basin is similar, in terms of composition and abundance, to that observed prior to the event, suggesting a swift return of well-ventilated benthic habitats. Conversely, after the deposition of Pennsylvanian black shales, dysaerobic conditions are dominant, in agreement with the record of low diversity in poorly abundant ichnoassemblages. Therefore, the macrobenthic tracemaker community recolonizes the seafloor shortly after reductive pulses, sometimes within periods as brief as weeks (Barret & Schieber, 1999; see details in Chapter I), regardless of the total reestablishment of oxic conditions.

iii) Another important point in the interpretation of black shales is the role of global phenomena. The obtained results support the significant impact of local triggers over global factors. This is exemplified in both case studies, with the T-OAE serving as a prime example of a palimpsest involving local, regional, and global mechanisms, as detailed in Chapter IV. Analysis of the global T-OAE record indicates that black shale deposits are predominantly associated with sluggish bottom-water circulation, induced by local basin features such as seabed topography (e.g., sills) or broader regional settings like the shallow, epeiric northwestern Tethyan Sea. Furthermore, in Pennsylvanian black shales deposited within an epeiric sea influenced by glacio-eustatic sea-level changes, detailed geochemical analyses highlight the significant impacts of short-term climatic fluctuations, unique water mass circulation patterns, and variations in continental freshwater input on sedimentological dynamics. Thus, across all case studies, global processes do not uniformly lead to extensive black shale deposits; instead, their effects tend to be localized, as observed in the NW Tethys during the T-OAE, therefore highlighting the importance of local factors for the deposit of black shale facies.

iv) Given that extremely reductive conditions are not always a requirement for black shale deposition,

it is important to highlight that a reductive benthic environment may or may not persist throughout the entire intervals enriched in organic matter. In some cases, such as in the Asturian Basin during the Toarcian, black shales are intermittently interrupted by sediments indicative of more oxic conditions (light marls). There are more extreme cases, such as the Posidonia Shale, deposited under stronger anoxic conditions than the Asturian shales, where layers containing abundant bivalves (Wignall's paper pectens) are found within the black shale beds. These layers indicate brief oxic intervals that interrupt the prevailing anoxic conditions. In contrast, Pennsylvanian black shales lack these brief oxic pulses, and reductive benthic conditions appear to have been more continuous. Thus, while pervasive and strong anoxia is not a prerequisite for black shale accumulation, brief oxic intervals are not universally recorded during organic carbon burial. When present, however, these intervals are independent of the overall redox stage, occurring across a spectrum from suboxic to euxinic conditions. This observation aligns with previous points, providing further evidence of rapid and abrupt redox shifts during black shale deposition.

The expounded results reveal the usefulness of a multiproxy approach involving complementary tools. As discussed in the introductory chapters, geochemical proxies are valuable tools for assessing reductive redox stages, while ichnological proxies also serve to reconstruct oxic to dysoxic conditions. Both procedures, in an integrative perspective, are therefore essential for comprehensive black shale studies. Recent works have highlighted the utility of meioturbation in black shale analysis, providing insights into brief oxygenation pulses during periods presumed to be strongly anoxic. Future research will likely identify intervals of increasing oxygenation within allegedly anoxic conditions through the recognition of these small biogenic structures (see notable examples in Devonian black shales in Wilson et al., 2021). Furthermore, ichnology and geochemistry operate on different temporal scales, allowing exploration of the temporal dynamics of these redox shifts. Further studies dedicated to improving the calibration of these proxies will increase their reliability and enhance their complementary value.

2. CONCLUSIONS

The conducted PhD research has made it possible to highlight some general conclusions on global and regional factors controlling black shale deposition:

I. Black shales can form under a wide range of reductive redox conditions, contrary to the classical assumption that strong anoxia is commonly necessary. Our findings from both study cases demonstrate that organic-rich sediments can form not only under euxinic conditions but also under slightly suboxic conditions. Moreover, transitions between euxinic and suboxic stages during black shale deposition are frequently observed.

II. Redox shifts associated with black shale deposition are typically sharp and abrupt. Calibration of various geochemical proxies consistently shows overlapping values across less to more reductive redox stages, suggesting rapid transitions from oxic/dysoxic to euxinic conditions in benthic environments. Intermediate redox conditions, such as suboxic or ferruginous, are often confined to few cm in the benthic setting, making them nearly imperceptible on a geological scale.

III. Macrobenthic tracemaker recovery following reductive conditions is consistently rapid. Ichnological analysis has demonstrated that shortly after the cessation of reductive pulses associated with organic carbon burial, macrobenthic tracemaker communities swiftly reoccupy the seafloor, regardless of whether oxygen levels were predominantly oxic or slightly dysoxic (distinct ichnoassemblages indicate each redox stage).

IV. Local triggers consistently exert a significant influence on black shale deposition compared to global phenomena. Our findings from both study cases underscore the critical role played by local and regional factors such as seabed topography and paleogeographic conditions in shaping the black shale record. While global causes are key in creating the conditions conducive to black shale deposition, their effect

is confined to specific settings, emphasizing the primacy of local and regional factors.

V. Brief oxic pulses are frequently observed during black shale deposition, although they are not consistently identified. Given that black shales can accumulate under varying degrees of reductive conditions, these brief oxic intervals can often be discerned regardless of the specific redox stage in which black shales are deposited.

VI. The integration of geochemical and ichnological proxies involves complementary tools for reconstructing black shale depositional conditions. Future research in this field to refine the calibration of these proxies will enhance their reliability and complementary usefulness.

1. CONSIDERACIONES FINALES Y CONCLUSIONES

El enfoque multidisciplinar empleado en esta tesis, basado en la integración de análisis icnológicos y geoquímicos, ha supuesto un avance de gran importancia para abordar las numerosas cuestiones que surgen en torno a la formación de "black shales". Han sido cuatro las principales preguntas planteadas: i) ¿Están las "black shales" relacionadas exclusivamente con condiciones anóxicas?, ii) ¿Cómo responden las comunidades macrobentónicas bioturbadoras a las condiciones desfavorables asociadas al depósito de "black shales"?, iii) ¿Responden las "black shales" únicamente a fenómenos globales?, y iv) ¿Son las condiciones reductoras persistentes y continuas durante el depósito de "black shales"? La investigación realizada ha dado respuesta a estas cuestiones:

i) Aunque está demostrado que la materia orgánica puede acumularse y preservarse en sedimentos marinos tanto en condiciones anóxicas como óxicas (ver Capítulo I), tradicionalmente se ha considerado que las "black shales" se depositaron exclusivamente bajo condiciones anóxicas persistentes (e.g., Wignall, 2005). Aun así, como demuestran los resultados obtenidos, incluso condiciones ligeramente reductoras (subóxicas) pueden dar lugar a la preservación de carbono orgánico y a la formación de "black shales", como se observa en las cuencas de Asturias y Belluno durante el T-OAE, y en partes de las "black shales" depositadas en el Mar Epicontinental del Pensilvaniense Tardío. Además, las condiciones reductoras aparecen habitualmente de forma abrupta en el registro geológico, como ponen de manifiesto los resultados geoquímicos, si bien de manera recurrente y ampliamente extendida, ocurriendo no exclusivamente al inicio del depósito de "black sales" sino también de forma intermitente durante y tras los pulsos reductores (ver capítulos IV y VI). Por lo tanto, aunque las "black shales" están caracterizadas por condiciones reductoras durante su depósito, la anoxia/euxinia no es estrictamente necesaria, sino que el factor común es el desarrollo de fluctuaciones redox rápidas y pronunciadas.

ii) Se ha demostrado que las "black shales" representan intervalos de tiempo cortos en el registro geológico —por ejemplo, el T-OAE no duró más de 500.000 años (e.g., Boulila et al., 2014, 2019; Boulila & Hinnov, 2017) — y se estima que las "black shales" del Pensilvaniense tienen una duración de 25.000 a 120.000 años. En este contexto de aparición abrupta y desarrollo de "black shales", es especialmente interesante la rápida recuperación de las comunidades macrobentónicas bioturbadoras tras los pulsos de condiciones desfavorables (reductoras) habituales durante el depósito de "black shales". La investigación realizada también pone de manifiesto que esta recuperación faunística varía dependiendo de las condiciones redox tras el depósito de las "black shales". Por ejemplo, la comunidad macrobentónica registrada tras el T-OAE en la Cuenca de Asturias es similar, en abundancia y diversidad, a la existente previamente al evento, lo que sugiere un cambio rápido a hábitats bentónicos bien oxigenados. Por el contrario, tras el depósito de las "black shales" del Pensilvaniense, las condiciones dominantes eran disaeróbicas, como sugiere el registro de icnoasociaciones de baja diversidad y escasa abundancia de pistas fósiles. Por lo tanto, se demuestra que las comunidades macrobentónicas bioturbadoras recolonizan el substrato marino rápidamente tras los pulsos de condiciones reductoras, a veces en periodos tan breves como semanas (Barret & Schieber, 1999; ver detalles en Capítulo I) e independientemente de si se han restablecido plenamente o no las condiciones de oxigenación.

iii) Otro aspecto importante en la formación de las "black shales" es el papel que juegan los fenómenos globales. Los resultados obtenidos apoyan un impacto más significativo de los factores locales respecto a los globales. Esto puede observarse en ambos casos de estudio, siendo el T-OAE un ejemplo excelente del depósito controlado por mecanismos tanto locales como regionales y globales (como se detalla en el Capítulo IV). El análisis del registro global del T-OAE indica que los depósitos de "black shales" están predominantemente asociados con una circulación lenta de las aguas de fondo (i.e., baja tasa de renovación de las aguas del fondo marino), que está siempre asociada a las características locales de cada cuenca, como la topografía del lecho marino (por ejemplo, barreras) o a contextos regionales más amplios, como el mar epicontinental somero del noroeste del Mar de Tetis. Además, en el caso de las "black shales" del Pensilvaniense, depositadas en un mar epicontinental bajo la influencia de cambios glacio-

eustáticos, los indicadores geoquímicos ponen de manifiesto que fluctuaciones climáticas jugaron un papel muy significativo en la dinámica sedimentaria, junto con la circulación de las masas de agua y las variaciones en el aporte continental de agua dulce. Así, en todos los casos de estudio, los procesos globales no han conducido siempre al depósito de "black shales" sino que, por el contrario, sus efectos tienden a ser localizados, como demuestra la importancia de los factores locales en el depósito de facies de "black shales" en el noroeste del Tetis durante el T-OAE.

iv) Dado que condiciones extremadamente reductoras no son siempre un requisito para el depósito de "black shales", es importante destacar también que dichas condiciones no son necesariamente constantes en los ambientes bentónicos durante los intervalos de acumulación de materia orgánica. En algunos casos, como en la Cuenca de Asturias durante el Toarciense, las "black shales" alternan con sedimentos (margas claras) depositados en condiciones más oxigenadas. Existen casos más extremos, como las "Posidonia Shale", depositadas bajo condiciones anóxicas, mucho más que las análogas de la Cuenca de Asturias, donde se han identificado capas que contienen abundantes bivalvos (los "paper pectens" de Wignall) en los depósitos de "black shales". Estas capas indican breves intervalos de oxigenación interrumpiendo las condiciones anóxicas. Por el contrario, en las "black shales" del Pensilvaniense no se reconocen estos breves pulsos de oxigenación y las condiciones reductoras parecen haber sido más persistentes. Todo ello demuestra que una anoxia persistente no es siempre un requisito para la acumulación de "black shales", del mismo modo que los breves intervalos de oxigenación no se registran globalmente durante la acumulación de materia orgánica. Sin embargo, cuando están presentes, estos intervalos son independientes de las condiciones redox predominantes, ocurriendo en un espectro que va desde condiciones subóxicas hasta euxínicas. Esta observación se alinea con los puntos anteriores, apoyando las evidencias que indican la existencia de cambios rápidos y abruptos en las condiciones redox durante la formación de "black shales".

Los resultados obtenidos demuestran asimismo la utilidad de un enfoque multidisciplinar empleando herramientas complementarias. Como se discutió en los capítulos introductorios, los indicadores geoquímicos son excelentes herramientas para evaluar las condiciones redox, en particular, condiciones reductoras, mientras que los indicadores icnológicos son especialmente útiles para reconstruir condiciones óxicas a disóxicas. Ambos tipos de herramientas, desde una perspectiva integradora, son, por tanto, esenciales para el estudio de "black shales". Además, diversos trabajos recientes han demostrado la utilidad de la meioturbación en el análisis de "black shales", proporcionando información sobre breves pulsos de oxigenación durante períodos que se presumían fuertemente anóxicos. De hecho, es esperable que investigaciones futuras en este campo sirvan para identifica intervalos de oxigenación durante periodos supuestamente anóxicos gracias al reconocimiento de estas pequeñas estructuras biogénicas (véanse buenos ejemplos en las "black shales" del Devónico en Wilson et al., 2021). Además, la icnología y la geoquímica operan en diferentes escalas temporales, permitiendo explorar la dinámica temporal de estos cambios redox desde varias perspectivas. Finalmente, los estudios para la calibración de estos indicadores aumentarán su fiabilidad y potenciarán su valor complementario.

2. CONCLUSIONES

La investigación realizada durante esta tesis doctoral ha permitido alcanzar diversas conclusiones generales sobre los factores globales y regionales que controlan la formación de "black shales":

I. Las "black shales" pueden formarse bajo una amplia gama de condiciones redox reductoras, en contraste con la asunción clásica de que se requerían condiciones extremadamente anóxicas. Los resultados obtenidos de ambos casos de estudio demuestran que los sedimentos ricos en materia orgánica pueden formarse no sólo bajo condiciones euxínicas, sino también bajo condiciones ligeramente subóxicas. Además, frecuentemente se observan transiciones entre etapas euxínicas y subóxicas durante la formación de las "black shales".

II. Los cambios redox asociados al depósito de "black shales" son comúnmente abruptos y rápidos. La calibración de varios indicadores geoquímicos muestra de manera sistemática valores superpuestos para condiciones redox reductoras de menor a mayor intensidad, lo que sugiere transiciones rápidas de condiciones óxicas/disóxicas a euxínicas. Las condiciones redox intermedias, como las subóxicas o ferruginosas, a menudo se restringen a pocos centímetros en el ambiente bentónico, lo que las hace casi imperceptibles a escala geológica.

III. La recuperación de las comunidades macrobentónicas bioturbadoras tras condiciones reductoras es rápida. El análisis icnológico ha demostrado que poco después del fin de los pulsos reductores asociados con la acumulación de carbono orgánico, las comunidades macrobentónicas bioturbadoras recolonizan rápidamente el substratoo marino, independientemente de si los niveles de oxígeno eran predominantemente óxicos o ligeramente disóxicos (diferentes icnoasociaciones indican las condiciones redox).

IV. Los factores locales ejercen una influencia significativa en el depósito de "black shales", en comparación con los fenómenos globales. Los resultados obtenidos en ambos casos de estudio subrayan el papel jugado por los factores locales y regionales, como la topografía del lecho marino y las condiciones paleogeográficas, los cuales son esenciales en la formación de "black shales". Aunque las causas globales son clave para crear las condiciones propicias para el depósito, su efecto se limita a entornos específicos, enfatizando así la importancia de los factores locales y regionales.

V. Durante el depósito de "black shales" se observan frecuentemente breves pulsos de oxigenación, aunque no siempre se identifican. Dado que las "black shales" pueden acumularse bajo diversos grados de condiciones reductoras, estos breves intervalos de oxigenación a menudo pueden identificarse independientemente de las condiciones redox específicas en el que se depositan las "black shales".

VI. La integración de indicadores geoquímicos e icnológicos implica el uso de herramientas complementarias para reconstruir las condiciones de depósito de "black shales". Futuras investigaciones en este campo pueden ayudar a refinar la calibración de estos indicadores, mejorando así su fiabilidad y utilidad complementaria.

Agradecimientos

Quiero agradecer a todos aquellos que han hecho posible este trabajo.

En primer lugar, a mis padres, Tere y Miguel, que desde que tengo uso de razón han estimulado mi pasión por la paleontología: desde llevarme a cualquier sitio que ofreciera ver un fósil hasta apoyarme cuando decidí mudarme a la otra punta de España para seguir con mi carrera. Y por supuesto también a mi hermano Diego, siempre a mi lado.

A Belén, el amor de mi vida, que siempre estuvo ahí en los buenos momentos, pero sobre todo en los malos. No tengo palabras para expresar el apoyo que has supuesto estos años. La distancia no pudo con nosotros, no podrá ahora el tiempo. Esto no habría sido posible sin ti.

A Laura y a José Carlos, porque con ellos comenzó todo en una charla cuando era niño. Luego llegó el mover estanterías en la litoteca del MUJA, y las salidas de campo en los acantilados de Asturias. Gracias por vuestro cariño y por todo lo que aprendí de vosotros en todos los aspectos de la vida.

A Mateo y a Elvis, mis sempiternos compañeros en este viaje. La casualidad nos juntó en aquella aula hace ya diez años; nadie daba un duro por nosotros, y ahora estamos a punto de cumplir nuestro sueño.

A Alberto Marcos. Con él hice mis primeros pinitos en la investigación, echando horas clasificando sus muestras en el Museo de Geología de la Universidad de Oviedo. Gracias por tus dibujos y tu lucidez, José Carlos me regaló el Seilacher y tú le diste vida. Gracias por confiar en nosotros para cuidar tu amada colección. Descansa en paz.

A todos mis compañeros de la becaría en la Universidad de Granada: Pablo, Christian, Sergio, Carlos, Sarah, Santi, y Willy. Sin vosotros esto no habría sido lo mismo.

I also want to thank Thomas for hosting me during my stay in Cincinnati. It was an extremely enriching experience in every aspect, both scientifically and personally. Thank you for showing me your country and for opening the doors to your home and family: you taught me how to use chopsticks, but in exchange, you let your 7-year-old children humiliate me at chess.

Y por último, pero no menos importante, a mis directores, Francis y Paqui. Gracias por confiar en mí desde el principio y por vuestra *infinita paciencia*. Ninguna tesis doctoral sería posible sin un buen director, pero no hay nadie en el mundo que haya conseguido encontrar el tipo de maestro que vosotros habéis supuesto para mí: siempre complementarios entre vosotros, pero sobre todo siempre sabiendo cómo guiarme en cada momento. Vosotros sois los que verdaderamente habéis permitido que cumpla mi sueño desde niño, y nunca podré estar los suficientemente agradecido.

LIST OF REFERENCES

Algeo, T.J., 2004. Can marine anoxic events draw down the trace element inventory of seawater? Geology, 32, 1057-1060. https://doi.org/10.1130/G20896.1

Algeo, T.J., Ingall, E., 2007. Sedimentary Corg:P ratios, paleocean ventilation, and Phanerozoic atmospheric pO2. Palaeogeography, Palaeoclimatology, Palaeoecology, 256, 130-155. https://doi.org/10.1016/j.palaeo.2007.02.02 9

Algeo, T. J., Heckel, P. H., 2008. The late Pennsylvanian midcontinent sea of north America: A review. Palaeogeography, Palaeoclimatology, Palaeoecology, 268(3-4), 205-221. https://doi.org/10.1016/j.palaeo.2008.03.04 9

Algeo, T. J., Herrmann, A. D., 2018. An ancient estuarine-circulation nutrient trap: The Late Pennsylvanian Midcontinent Sea of North America. Geology, 46(2), 143-146. https://doi.org/10.1130/g39804.1

Algeo, T. J., Maynard, J. B., 2008. Trace-metal covariation as a guide to water-mass conditions in ancient anoxic marine environments. Geosphere, 4(5), 872. https://doi.org/10.1130/ges00174.1

Algeo, T.J., Li, C., 2020. Redox classification and calibration of redox thresholds in sedimentary systems. Geochimica et Cosmochimica Acta, 287, 8-26. https://doi.org/10.1016/j.gca.2020.01.055

Algeo, T.J., Liu, J., 2020. A re-assessment of elemental proxies for paleoredox analysis. Chemical Geology, 540, 119549. https://doi.org/10.1016/j.chemgeo.2020.119 549

Algeo, T.J., Lyons, T.W., 2006. Mo–total organic carbon covariation in modern anoxic marine environments: Implications for analysis of paleoredox and paleohydrographic conditions. Paleoceanography, 21, PA1016. https://doi.org/10.1029/2004PA001112

Algeo, T.J., Rowe, H., 2012. Paleoceanographic applications of trace-metal concentration data. Chemical Geology, 324, 6-18. https://doi.org/10.1016/j.chemgeo.2011.09. 002

Algeo, T.J., Tribovillard, N., 2009. Environmental analysis of paleoceanographic systems based on molybdenum–uranium covariation. Chemical Geology, 268, 211-225. https://doi.org/10.1016/j.chemgeo.2009.09. 001

Algeo, T. J., Hoffman, D. L., Maynard, J. B., Joachimski, M. M., Hower, J. C., Watney, W. L., 1997. Environmental reconstruction of anoxic marine systems: core black shales of Upper Pennsylvanian Midcontinent cyclothems. In Cyclic Sedimentation of Appalachian Devonian and Midcontinent Pennsylvanian Black Shales: Analysis of Ancient Anoxic Marine Systems—A Combined Core and Field Workshop. Joint Meeting of Eastern Section AAPG and The Society for Organic Petrography (TSOP), Lexington, Kentucky (pp. 103-147).

Algeo, T. J., Schwark, L., Hower, J. C., 2004. High-resolution geochemistry and sequence stratigraphy of the Hushpuckney Shale (Swope Formation, eastern Kansas): implications for climato-environmental dynamics of the Late Pennsylvanian Midcontinent Seaway. Chemical Geology, 206(3-4), 259-288. https://doi.org/10.1016/j.chemgeo.2003.12. 028

Algeo, T.J., Lyons, T.W., Blakey, R.C., Over, D.J., 2007. Hydrographic conditions of the Devono-Carboniferous North American Seaway inferred from sedimentary Mo–TOC relationships.

Palaeogeography, Palaeoclimatology, Palaeoecology, 256, 204–230. https://doi.org/10.1016/j.palaeo.2007.02.03 5

Anderson, J.J., Devol, A.H., 1973. Deep water renewal in Saanich Inlet, an intermittently anoxic basin. Estuarine and Coastal Marine Scisciences, 1, 1–10. https://doi.org/10.1016/0302-3524(73)90052-2

Archer, A. W., Maples, C. G., 1984. Trace-fossil distribution across a marine-to-nonmarine gradient in the Pennsylvanian of southwestern Indiana. Journal of Paleontology, 448-466.

Armendáriz, M., Rosales, I., Bádenas, B., Aurell, M., García-Ramos, J.C., Piñuela, L., 2012. High-resolution chemostratigraphic records from Lower Pliensbachian belemnites: Palaeoclimatic perturbations, organic facies and water mass exchange (Asturian basin, northern Spain). Palaeogeography, Palaeoclimatology, Palaeoecology 333-334, 178-191.

Aurell, M., Robles, S., Bádenas, B., Rosales, I., Quesada, S., Meléndez, G., García-Ramos, J.C., 2003. Transgressive–regressive cycles and Jurassic palaeogeography of northeast Iberia. Sedimentary Geology 162, 239-271.

Bádenas, B., Armendáriz, M., Rosales, I., Aurell, M., 2013. Origen de los black shales del Pliensbachiense Inferior de la Cuenca Asturiana (España). Revista de la Sociedad Geológica de España, 26, 41-54.

Ball, S. M., 1971. The Westphalia limestone of the northern midcontinent; a possible ancient storm deposit. Journal of Sedimentary Research, 41(1), 217-232.

Bandel, K., 1967a. Trace fossils from two Upper Pennsylvanian sandstones in Kansas. The University of Kansas Paleontological Contributions, 18, 1-19.

Bandel, K., 1967b. Isopod and limulid marks and trails in Tonganoxie Sandstone (Upper Pennsylvanian) of Kansas. The University of Kansas Paleontological Contributions, 19, 1-10.

Bardet, N., Fernández, M., Garciáa-Ramos, J.C., Suberbiola, X.P., Piñuela, L., Ruiz-Omeñaca, J.I., Vincent, P., 2008. A juvenile plesiosaur from the Pliensbachian (Lower Jurassic) of Asturias, Spain. Journal of Vertebrate Paleontolology, 28, 258-263. https://doi.org/10.1671/0272-4634(2008)28[258:AJPFTP]2.0.CO;2

Baucon, A., Bednarz, M., Dufour, S., Felletti, F., Malgesini, G., Neto de Carvalho, C., Niklas, K.J., Wehrmann, A., Batstone, R., Bernardini, F., Briguglio, A., Cabella, R., Cavalazzi, B., Ferretti, A., Zanzerl, H., McIlroy, D., 2020. Ethology of the trace fossil Chondrites: Form, function and environment. Earth-Science Reviews, 202, 192989. doi. 10.1016/j.earscirev.2019.102989

Bayet-Goll, A., Samani, P. N., Neto de Carvalho, C., Monaco, P., Khodaie, N., Pour, M. M., Kazemeini, H., Zareiyan, M. H.,2017. Sequence stratigraphy and ichnology of Early Cretaceous reservoirs, Gadvan Formation in southwestern Iran. Marine and Petroleum Geology, 81, 294-319. https://doi.org/10.1016/j.marpetgeo.2016.1 1.008

Bellanca, A., Masetti, D., Neri, R., Venezia, F., 1999. Geochemical and sedimentological evidence of productivity cycles recorded in Toarcian black shales from the Belluno Basin, Southern Alps, northern Italy. Journal of Sedimentary Research, 69, 466-476. https://doi.org/10.2110/jsr.69.466

Bertling, M., Braddy, S. J., Bromley, R. G., Demathieu, G. R., Genise, J., Mikuláš, R., Nielsen, J. K., Nielsen, K. S. S., Rindsberg, A. K., Schlirf, M., Uchman, A., 2006. Names for trace fossils: a uniform approach. Lethaia, 39(3), 265-286. https://doi.org/10.1080/0024116060078789 0

Berner, R.A., 1989. Biogeochemical cycles of carbon and sulfur and their effect on atmospheric oxygen over Phanerozoic time. Global and Planetary Change, 1(1-2), 97-122.

Bertling, M., Buatois, L. A., Knaust, D., Laing, B., Mángano, M. G., Meyer, N., Mikuláš, R., Minter, N. J., Neumann, C., Rindsberg, A. K., Uchman, A., Wisshak, M., 2022. Names for trace fossils 2.0: theory and practice in ichnotaxonomy. Lethaia, 55(3), 1-19. https://doi.org/10.18261/let.55.3.3

Bilotta, M., Venturi, F., Sassaroli, S., 2010. Ammonite faunas, OAE and the Pliensbachian-Toarcian boundary (Early Jurassic) in the Apennines. Lethaia 43, 357-380.

Bisnett, A. J., 2001. Petrography and geochemistry of Pennsylvanian black shales in offshore and nearshore stratigraphic settings in Midcontinent and Illinois Basins. The University of Iowa.

Brenner, K., Seilacher, A., 1978. New aspects about the origin of the Toarcian Posidonia Shales. Neues Jahrbuch für Geologie und Paläontologie, 157, 11-18.

Bromley, R. G., 1991. *Zoophycos*: strip mine, refuse dump, cache or sewage farm? Lethaia, 24(4), 460-462. https://doi.org/10.1111/j.1502-3931.1991.tb01501.x

Bromley, R. G., 1996. Trace Fossils: Biology, Taphonomy and Applications. Chapman and Hall.

Bromley, R.G., Ekdale, A.A., 1984. *Chondrites*: a trace fossil indicator of anoxia in sediments. Science, 224, 872-874.

Bromley, R.G., Ekdale, A.A., Asgaard, U., 1999. *Zoophycos* in the Upper Cretaceous chalk of Denmark and Sweden. Greifswalder Geowissenschaftliche Beiträge, 6, 133-142.

Buatois, L.A., Mángano, M.G., 2011. Ichnology. Organism-Substrate Interactions in Space and Time. Cambridge University Press, New York, 358 pp.

Buatois, L.A., Mángano, M.G., 2013. Ichnodiversity and ichnodisparity: significance and caveats. Lethaia, 46, 281-292.

Buatois, L.A., Mángano, M.G., 2018. The other biodiversity record: Innovations in animal-substrate interactions through geologic time. GSA Today, 28, 4-10.

Buatois, L.A., Wisshak, M., Wilson, M.A., Mángano, M.G., 2017. Categories of architectural designs in trace fossils: A measure of ichnodisparity. Earth-Science Reviews, 164, 102-181.

Buatois, L. A., Mangano, M. G., Maples, C. G., 1997. The paradox of nonmarine ichnofaunas in tidal rhythmites; integrating sedimentologic and ichnologic data from the Late Cretaceous of eastern Kansas, USA. Palaios, 12(5), 467-481.

Buatois, L. A., Mangano, G. M., Carr, T. R., 1999. Sedimentology and ichnology of Paleozoic estuarine and shoreface reservoirs, Morrow sandstone, lower Pennsylvanian of southwest Kansas, USA. Current research in earth sciences, 1-35. https://doi.org/10.17161/cres.v0i243.11783

Buatois, L. A., Mángano, M. G., Alissa, A., Carr, T. R., 2002. Sequence stratigraphic and sedimentologic significance of biogenic structures from a late Paleozoic marginal- to open-marine reservoir, Morrow Sandstone, subsurface of southwest Kansas, USA. Sedimentary Geology, 152(1-2), 99-132. https://doi.org/10.1016/s0037-0738(01)00287-1

Buatois, L. A., Mangano, M. G., Maples, C. G., Lanier, W. P., 1998a. Ichnology of an Upper Carboniferous fluvio-estuarine paleovalley: The Tonganoxie Sandstone, Buildex Quarry, Eastern Kansas, USA. Journal of Paleontology, 72(1), 152-180.

https://doi.org/10.1017/s002233600002409
4

Buatois, L. A., Mángano, G., Maples, C. G., Lanier, W. P., 1998b. Allostratigraphic and sedimentologic applications of trace fossils to the study of incised estuarine valleys: an example from the Virgilian Tonganoxie Sandstone Member of eastern Kansas. Bulletin (Kansas Geological Survey), (241), 1-27.

Buatois, L. A., Mángano, M. G., Maples, C. G., Lanier, W. P., 1998. Taxonomic reassessment of the ichnogenusbeaconichnusand additional examples from the Carboniferous of Kansas, U.S.A. Ichnos, 5(4), 287-302. https://doi.org/10.1080/1042094980938642 7

Bucefalo Palliani, R., Mattioli, E., Riding, J.B., 2002. The response of marine phytoplankton and sedimentary organic matter to the early Toarcian (Lower Jurassic) oceanic anoxic event in northern England. Marine Micropaleontology, 46, 223-245.

Burton, B. R., Link, P. K., 1991. Ichnology of fine-grained mixed carbonate-siliciclastic turbidites, Wood River formation, Pennsylvanian-Permian, south-central Idaho. Palaios, 6(3), 291. https://doi.org/10.2307/3514909

Catuneanu, O., 2022. Principles of sequence stratigraphy (2.a ed.). Elsevier Science.

Chamberlain, C. K., 1971. Morphology and ethology of Trace fossils from the Ouachita Mountains, southeast Oklahoma. Journal of paleontology, 45(2), 212-246. http://www.jstor.org/stable/1302637

Chamberlain, C. K., Clark, D. L., 1973. Trace fossils and conodonts as evidence for Deep-Water deposits in the Oquirrh Basin of central Utah. Journal of paleontology, 47(4), 663-682. http://www.jstor.org/stable/1303048

Chen, W., Kemp, D.B., He, T., Huang, C., Jin, S., Xiong, Y., Newton, R.J., 2021. First record of

the early Toarcian oceanic anoxic event in the Hebrides Basin (UK) and implications for redox and weathering changes. Global and Planetary Change 207, 103685. https://doi.org/10.1016/j.gloplacha.2021.10 3685

Deconinck, J.F., Gómez, J.J., Baudin, F., Biscay, H., Bruneau, L., Cocquerez, T., Mathieu, O., Pellenard, P., Santoni, A-L., 2020. Diagenetic and environmental control of the clay mineralogy, organic matter and stable isotopes (C, O) of Jurassic (Pliensbachian-lowermost Toarcian) sediments of the Rodiles section (Asturian Basin, Northern Spain). Marine and Petroleum Geology 115, 104286. https://doi.org/10.1016/j.marpetgeo.2020.1 04286O.

Dera, G., Pellenard, P., Neige, P., Deconinck, J. F., Pucéat, E., Dommergues, J. L., 2009. Distribution of clay minerals in Early Jurassic Peritethyan seas: palaeoclimatic significance inferred from multiproxy comparisons. Palaeogeography, Palaeoclimatology, Palaeoecology, 271, 39-51. https://doi.org/10.1016/j.palaeo.2008.09.01 0

Dera, G., Neige, P., Dommergues, J.L., Fara, E., Laffont, R., Pellenard, P., 2010. High-resolution dynamics of Early Jurassic marine extinctions: the case of Pliensbachian–Toarcian ammonites (Cephalopoda). Journal of the Geological Society of London, 167, 21-33. https://doi.org/10.1144/0016-76492009-068

Dera, G., Neige, P., Dommergues, J.L., Brayard, A., 2011. Ammonite paleobiogeography during the Pliensbachian–Toarcian crisis (Early Jurassic) reflecting paleoclimate, eustasy, and extinctions. Global and Planetary Change, 78, 92-105. https://doi.org/10.1016/j.gloplacha.2011.05. 009

Devera, J. A., 1989. Ichnofossil assemblages and associated lithofacies of the Lower Pennsylvanian (Caseyville and Tradewater Formations), southern Illinois. Geology of the Lower Pennsylvanian in Kentucky, Indiana, and Illinois. Illinois Basin Studies, 1, 57-83.

Dickson, A.J., Gill, B.C., Ruhl, M., Jenkyns, H.C., Porcelli, D., Idiz, E., Lyons, T.W., van den Boorn, S.H.J.M., 2017. Molybdenum-isotope chemostratigraphy and paleoceanography of the Toarcian Oceanic Anoxic Event (Early Jurassic). Paleoceanography, 32, 813–829. https://doi.org/10.1002/2016PA003048

Dorador, J., Rodríguez-Tovar, F.J., 2018. High-resolution image treatment in ichnological core analysis: Initial steps, advances and prospects. Earth-Science Reviews 177, 226-237.

Dunham, R.J., 1962. Classification of carbonate rocks according to depositional texture. In: Ham, W.E. (Ed.), Classification of Carbonate Rocks. American Association of Petroleum Geology Memoirs 1, Tulsa, pp. 108–121.

Ekdale, A. A., Bromley, R. G., 1991. Analysis of composite ichnofabrics: An example in uppermost cretaceous chalk of Denmark. Palaios, 6(3), 232. https://doi.org/10.2307/3514904

Ekdale, A.A., Bomley, R.G., 2003. Paleoethologic interpretation of complex Thalassinoides in shallow-marine limestones, Lower Ordovician, southern Sweden. Palaeogeography, Palaeoclimatology, Palaeoecology, 192, 221-227.

Ettinger, N.P., Larson, T.E., Kerans, C., Thibodeau, A.M., Hattori, K.E., Kacur, S.M., Martindale, R.C., 2021. Ocean acidification and photic-zone anoxia at the Toarcian Oceanic Anoxic Event: Insights from the Adriatic Carbonate Platform. Sedimentology, 68, 63-107. https://doi.org/10.1111/sed.12786

Fantasia, A., Föllmi, K.B., Adatte, T., Bernárdez, E., Spangenberg, J.E., Mattioli, E., 2018a. The Toarcian Oceanic Anoxic Event in southwestern Gondwana: an example from the Andean Basin, northern Chile. Journal of the Geological Society of London, 175, 883-902. https://doi.org/10.1144/jgs2018-008

Fantasia, A., Föllmi, K.B., Adatte, T., Spangenberg, J.E., Montero-Serrano, J. C., 2018b. The Early Toarcian oceanic anoxic event: Paleoenvironmental and paleoclimatic change across the Alpine Tethys (Switzerland). Global and Planetary Change, 162, 53-68. https://doi.org/10.1016/j.gloplacha.2018.01.008

Fantasia, A., Adatte, T., Spangenberg, J. E., Font, E., Duarte, L. V., Föllmi, K. B., 2019. Global versus local processes during the Pliensbachian–Toarcian transition at the Peniche GSSP, Portugal: A multi-proxy record. Earth-Sciences Review, 198, 102932. https://doi.org/10.1016/j.earscirev.2019.102932

Fenton, C. L., Fenton, M. A., 1937a. Burrows and trails from Pennsylvanian rocks of Texas. The American midland naturalist, 18(6), 1079. https://doi.org/10.2307/2420606

Fenton, C. L., Fenton, M. A., 1937b. *Olivellites*, a Pennsylvanian snail burrow. The American midland naturalist, 18(3), 452. https://doi.org/10.2307/2420586

Fernández-Martínez, J., Rodríguez-Tovar, F.J., Piñuela, L., Martínez-Ruiz, F., García-Ramos, J.C., 2021a. Bottom- and porewater oxygenation during the early Toarcian Oceanic Anoxic Event (T-OAE) in the Asturian Basin (N Spain): Ichnological information to improve facies analysis. Sedimentary Geology, 419, 105909. https://doi.org/10.1016/j.sedgeo.2021.105909

Fernández-Martínez, J., Rodríguez-Tovar, F.J., Piñuela, L., Martínez-Ruiz, F., García-Ramos, J.C.,

2021b. The Halimedides record in the Asturian Basin (northern Spain): supporting the Toarcian Oceanic Anoxic Event relationship, in: Reolid, M., Duarte, L.V., Mattioli, E. and Ruebsam, W. (Eds.), Carbon Cycle and Ecosystem Response to the Jenkyns Event in the Early Toarcian (Jurassic). Journal of the Geological Society of London , Special Publications, 514, 173-184. https://doi.org/10.1144/SP514-2020-156

Fernández-Martínez, J., Ruíz, F. M., Rodríguez-Tovar, F. J., Piñuela, L., García-Ramos, J. C., Algeo, T. J., 2023. Euxinia and hydrographic restriction in the Tethys Ocean: Reassessing global oceanic anoxia during the early Toarcian. Global and Planetary Change, 221, 104026.

Fraguas, A., Comas-Rengifo, M.J., Gómez, J.J., Goy, A., 2012. The calcareous nannofossil crisis in Northern Spain (Asturias province) linked to the Early Toarcian warming-driven mass extinction. Marine Micropaleontology 94-95, 58-71.

Frey, R. W., Bromley, R. G., 1985. Ichnology of American chalks: the Selma Group (Upper Cretaceous), western Alabama. Canadian Journal of Earth Sciences, 22(6), 801-828. https://doi.org/10.1139/e85-087

Fu, X., Wang, J., Zeng, S., Feng, X., Wang, D., Song, C., 2017. Continental weathering and palaeoclimatic changes through the onset of the Early Toarcian oceanic anoxic event in the Qiangtang Basin, eastern Tethys. Palaeogeography, Palaeoclimatology, Palaeoecology, 487, 241-250. https://doi.org/10.1016/j.palaeo.2017.09.005

Fu, X., Wang, J., Wen, H., Song, C., Wang, Z., Zeng, S., Feng, X., Wei, H., 2021. A Toarcian Ocean Anoxic Event record from an open-ocean setting in the eastern Tethys: Implications for global climatic change and regional environmental perturbation. Science China Earth Sciences, 64,

1860-1872. https://doi.org/10.1007/s11430-020-9753-1

Fürsich, F.T. 1974. On Diplocraterion Torell 1870 and the significance of morphological features in vertical, spreiten-bearing, U-shaped trace fossils. Journal of Paleontology 48, 952-962.

Gaillard, C., Olivero, D., 2009. The ichnofossil Halimedides in Cretaceous pelagic deposits from the Alps: environmental and ethological significance. Palaios, 24, 257-270.

García Joral, F., Goy, A., 2009. Toarcian (Lower Jurassic) brachiopods in Asturias (Northern Spain): Stratigraphic distribution, critical events and palaeobiogeography. Geobios, 42, 255-264. https://doi.org/10.1016/j.geobios.2008.10.007

García Joral, F., Gómez, J.J., Goy, A., 2011. Mass extinction and recovery of the Early Toarcian (Early Jurassic) brachiopods linked to climate change in northern and central Spain. Palaeogeography, Palaeoclimatology, Palaeoecology, 302, 367-380.

García-Ramos, J.C., Valenzuela, M., Suárez de Centi, C., 1992. Guía de campo. Rampa Carbonatada del Jurásico de Asturias. Reunión Monográfica sobre Biosedimentación. Departamento de Geología, Universidad de Oviedo y Sociedad Geológica de España, Oviedo, 92 pp. (In Spanish).

García-Ramos, J.C., Piñuela, L., Lires, J., 2006. Atlas del Jurásico de Asturias. Ediciones Nóbel, Oviedo (in Spanish).

Getty, P. R., Sproule, R., Wagner, D. L., Bush, A. M., 2013. Variation in wingless insect trace fossils: Insights from neoichnology and the Pennsylvanian of massachussetts. Palaios, 28(4), 243-258. https://doi.org/10.2110/palo.2012.p12-108r

Getty, Patrick R., Sproule, R., Stimson, M. R., Lyons, P. C., 2017. Invertebrate trace fossils from the Pennsylvanian Rhode Island Formation of

Massachusetts, USA. Atlantic geology, 53, 185-206. https://doi.org/10.4138/atlgeol.2017.007

Goldberg, T., Poulton, S.W., Wagner, T., Kolonic, S.F., Rehkämper, M., 2016. Molybdenum drawdown during Cretaceous oceanic anoxic event 2. Earth and Planetary Science Letters, 440, 81-91.

Goldring, R., 1962. The trace fossils of the Baggy Beds (Upper Devonian) of North Devon, England. Paläontologische Zeitschrift, 36, 232-251.

Gómez, J.J., Goy, A., Canales, M.L., 2008. Seawater temperature and carbon isotope variations in belemnites linked to mass extinction during the Toarcian (Early Jurassic) in central and northern Spain. Comparison with other European sections. Palaeogeography, Palaeoclimatology, Palaeoecology, 258, 28-58. https://doi.org/10.1016/j.palaeo.2007.11.005

Gómez, J.J., Goy, A., 2011. Warming-driven mass extinction in the Early Toarcian (Early Jurassic) of northern and central Spain. Correlation with other time-equivalent European sections. Palaeogeography, Palaeoclimatology, Palaeoecology, 306, 176-195.

Gómez, J.J., Comas-Rengifo, M.J., Goy, A., 2016a. Palaeoclimatic oscillations in the Pliensbachian (Early Jurassic) of the Asturian Basin (Northern Spain). Climate of the Past, 12, 1199-1214.

Gómez, J.J., Comas-Rengifo, M.J., Goy, A., 2016b. The hydrocarbon source rocks of the Pliensbachian (Early Jurassic) in the Asturian Basin (northern Spain): Their relationship with the palaeoclimatic oscillations and gamma-ray response. Journal of Iberian Geology, 42, 259-273.

Greb, S. F., Chesnut, D. R., Jr., 1994. Paleoecology of an estuarine sequence in the breathitt formation (Pennsylvanian), central Appalachian basin.

Palaios, 9(4), 388. https://doi.org/10.2307/3515057

Hakes, W. G., 1974. Trace fossils and the depositional environment of the Lawrence Shale (Upper Pennsylvanian) of eastern Kansas. Geological Society of America, Abstracts with program, North-central section, p. 319.

Hakes, W. G., 1974. Trace fossil analysis of two Pennsylvanian shales in Kansas--cyclic sedimentation or continual mud flat deposition?: Am. Assoc. Petroleum Geologists and Soc. of Econ. Paleontologists and Mineralogists. Ann. Mtgs. Abstracts, San Antonio, 41-42.

Hakes, W. G., 1976. Trace fossils and depositional environment of four clastic units, Upper Pennsylvanian megacyclothems, northeast Kansas. The University of Kansas Paleontological Contributions, 63, 1-46.

Hakes, W. G., 1977. Trace fossils in Late Pennsylvanian cyclothems, Kansas, in Crimes, T.P. and Harper, J.C., eds., Trace Fossils 2: Geological journal special issue 9, p. 209–226.

Hakes, W. G., 1984. Trace fossils from brackish-marine shales, Upper Pennsylvanian of Kansas, USA, in Curran, H.A., ed., Biogenic Structures: Their Use in Interpreting Depositional Environments: Society of Economic Paleontologists and Mineralogists Special Publication 35, p. 21–35.

Harbaugh, J. W., 1964. Upper Pennsylvanian calcareous rocks cored in two wells in Rawlins and Stafford Counties, Kansas. Bulletin (Kansas Geological Survey), (170), 1-14.

Heckel, P. H., 1977. Origin of phosphatic black shale facies in Pennsylvanian cyclothems of mid-continent north America. AAPG Bulletin, 61. https://doi.org/10.1306/c1ea43c4-16c9-11d7-8645000102c1865d

Heckel, P. H., 1980. Paleogeography of eustatic model for deposition of Midcontinent Upper Pennsylvanian cyclothems, in Fourch, T.D., and Magathan, E.R., eds., Paleozoic Paleogeography

of the West-central United States: SEPM Rocky Mountain Section, v. 1, pp. 197-271.

Heckel, P. H., 1986. Sea-level curve for Pennsylvanian eustatic marine transgressive-regressive depositional cycles along midcontinent outcrop belt, North America. Geology, 14(4), 330. https://doi.org/10.1130/0091-7613(1986)14<330:scfpem>2.0.co;2

Heckel, P. H., 2013. Pennsylvanian stratigraphy of Northern Midcontinent Shelf and biostratigraphic correlation of cyclothems. Stratigraphy, 10(1–2), 3-39.

Heckel, P. H., 1992. Stratigraphy and cyclic sedimentation of Middle and Upper Pennsylvanian strata around Winterset, Iowa (No. 14). Iowa Department of Natural Resources, Energy and Geological Resources Division, Geological Survey Bureau.

Heckel, P.H., Mitchell, J.C., Nelson, D.L., Ravn, R.L., 1978 Upper Pennsylvanian cyclothemic limestone facies in eastern Kansas, in AAPG/SEPM Annual Meeting Field guide Guidebook Series 2: Lawrence, Kansas, Kansas Geological Survey, 62 p.

Hedges, S.B., 2002. The origin and evolution of model organisms. Nature Reviews Genetics, 3(11), 838-849.

Helz, G.R., Miller, C.V., Charnock, J.M., Mosselmans, J.F.W., Pattrick, R.A.D., Garner, C.D., Vaughan, D.J.V., 1996. Mechanism of molybdenum removal from the sea and its concentration in black shales: EXAFS evidence. Geochimica et Cosmochimica Acta, 60, 3631-3642. https://doi.org/10.1016/0016-7037(96)00195-0

Hermoso, M., Minoletti, F., Pellenard, P., 2013. Black shale deposition during Toarcian super-greenhouse driven by sea level. Climate of the Past, 9, 2703-2712.

Hesselbo, S.P., Gröcke, D.R., Jenkyns, H.C., Bjerrum, C.J., Farrimond, P., Morgans Bell, H.S.,

Green, O.R., 2000. Massive dissociation of gas hydrate during a Jurassic oceanic anoxic event. Nature, 406, 392-395.

Hetzel, A., Böttcher, M.E., Wortmann, U.G., Brumsack, H.J., 2009. Paleo-redox conditions during OAE 2 reflected in Demerara Rise sediment geochemistry (ODP Leg 207). Palaeogeography, Palaeoclimatology, Palaeoecology, 273, 302-328. https://doi.org/10.1016/j.palaeo.2008.11.005

Houben, A.J.P., Goldberg, T., Slomp, C.P., 2021. Biogeochemical evolution and organic carbon deposition on the Northwestern European Shelf during the Toarcian Ocean Anoxic Event. Palaeogeography, Palaeoclimatology, Palaeoecology, 565, 110191. https://doi.org/10.1016/j.palaeo.2020.110191

Huddle, J. W., Patterson, S. H., 1961. Origin of Pennsylvanian underclay and related seat rocks. Geological Society of America Bulletin, 72(11), 1643. https://doi.org/10.1130/0016-7606(1961)72[1643:oopuar]2.0.co;2

Imbrie, J., Laporte, L. F., Merriam, D. F., 1964. Beattie Limestone facies (Lower Permian) of the northern midcontinent. Kansas Geological Survey Bulletin, 169(1), 219-238.

Izumi, K., Miyaji, T., Tanabe, B., 2012. Early Toarcian (Early Jurassic) oceanic anoxic event recorded in the shelf deposits in the northwestern Panthalassa: Evidence from the Nishinakayama Formation in the Toyora area, west Japan. Palaeogeography, Palaeoclimatology, Palaeoecology 315-316, 100-108.

Jenkyns, H.C., 1985. The Early Toarcian and Cenomanian-Turonian anoxic events in Europe: comparisons and contrasts. Geologische Rundschau, 74, 505-518. https://doi.org/10.1007/BF01821208

Jenkyns, H.C., 2010. Geochemistry of oceanic anoxic events. Geochemistry, Geophysics, Geosystems, 11, Q03004. https://doi.org/10.1029/2009GC002788

Jenkyns, H.C., Jones, C.E., Gröcke, D.R., Hesselbo, S.P., Parkinson, D.N., 2002. Chemostratigraphy of the Jurassic System: applications, limitations and implications for palaeoceanography. Journal of the Geological Society, 159, 351-378.

Jiang, S., Song, H., Kemp, D.B., Dai, X., Liu, X., 2020. Two pulses of extinction of larger benthic foraminifera during the Pliensbachian-Toarcian and early Toarcian environmental crises. Palaeogeography, Palaeoclimatology, Palaeoecology, 560, 109998. https://doi.org/10.1016/j.palaeo.2020.109998

Joeckel, R. M., 2008. Enigmatic structures in an upper Pennsylvanian (kasimovian) marine limestone. Palaios, 23(12), 833-847. https://doi.org/10.2110/palo.2008.p08-034r

Keighley, D.G., Pickerill, R.K., 1997. Systematic ichnology of the Mabou and Cumberland groups (Carboniferous) of Western Cape Breton Island, eastern Canada, 1: burrows, pits, trails, and coprolites. Atlantic Geology, 33, 181-215.

Kemp, D.B., Coe, A.L., Cohen, A.S., Schwark, L., 2005. Astronomical pacing of methane release in the Early Jurassic period. Nature, 437, 396-399.

Kemp, D.B., Izumi, K., 2014. Multiproxy geochemical analysis of a Panthalassic margin record of the early Toarcian oceanic anoxic event (Toyora area, Japan). Palaeogeography, Palaeoclimatology, Palaeoecology, 414, 332–341. http://dx.doi.org/10.1016/j.palaeo.2014.09.019

Kemp, D.B., Coe, A.L., Cohen, A.S., Schwark, L., 2005. Astronomical pacing of methane release in

the Early Jurassic period. Nature, 437, 396-399. https://doi.org/10.1038/nature04037

Kemp, D.B., Chen, W., Cho, T., Algeo, T.J., Shen, J., Ikeda, M., 2022. Deep-ocean anoxia across the Pliensbachian-Toarcian boundary and the Toarcian Oceanic Anoxic Event in the Panthalassic Ocean. Global and Planetary Change, 212, 103782. https://doi.org/10.1016/j.gloplacha.2022.103782

Knaust, D., 2009. Complex behavioral pattern as an aid to identify the producer of *Zoophycos* from the Middle Permian of Oman. Lethaia, 42, 146–154.

Knaust, D., 2013. The ichnogenus *Rhizocorallium*: Classification, trace makers, palaeoenvironments and evolution. Earth-Sciences Reviews, 126, 1-47.

Knaust, D., 2017. Atlas of Trace Fossils in Well Core: Appearance, Taxonomy and Interpretation. Springer International Publishing, Cham, 207 pp.

Knaust, D., Bromley, R. G. (eds.). 2012. Trace Fossils as Indicators of Sedimentary Environments. Developments in Sedimentology, 64. Elsevier, AmsterdamKrencker, F.N., Lindström, S., Bodin, S., 2019. A major sea-level drop briefly precedes the Toarcian oceanic anoxic event: implication for Early Jurassic climate and carbon cycle. Scientific Reports, 9, 12518. https://doi.org/10.1038/s41598-019-48956-x

Kotlarczyk, J., Uchman, A., 2012. Integrated ichnology and ichthyology of the Oligocene Menilite Formation, Skole and Subsilesian nappes, Polish Carpathians: A proxy to oxygenation history. Palaeogeography, Palaeoclimatology, Palaeoecology, 331-332, 104-118. DOI: 10.1016/j.palaeo.2012.03.002

Krencker, F.N., Lindström, S., Bodin, S., 2019. A major sea-level drop briefly precedes the

Toarcian oceanic anoxic event: implication for Early Jurassic climate and carbon cycle. Scientific Reports, 9, 12518. doi: 10.1038/s41598-019-48956-x

Little, C.T.S., Benton, M.J., 1995. Early Jurassic mass extinction: A global long-term event. Geology, 23, 495-498.

Lehmann, J., Bargen, D., Engelke, J., Claßen, J., 2016. Morphological variability in response to palaeoenvironmental change–a case study on Cretaceous ammonites. Lethaia, 49, 73–86.

Leibach, W. W., Rose, N., Bader, K., Mohr, L. J., Super, K., Kimmig, J., 2021. Horseshoe crab trace fossils and associated ichnofauna of the Pony Creek Shale Lagerstätte, Upper Pennsylvanian, Kansas, USA. Ichnos, 28(1), 34-45. https://doi.org/10.1080/10420940.2020.181 1268

Lézin, C., Andreu, B., Pellenard, P., Bouchez, J.L., Emmanuel, L., Fauré, P., Landrein, P., 2013. Geochemical disturbance and paleoenvironmental changes during the Early Toarcian in NW Europe. Chem. Geol. 341, 1-15. http://dx.doi.org/10.1016/j.chemgeo.2013.0 1.003

Lockley, M. G., Rindsberg, A. K., Zeiler, R. M., 1987. The Paleoenvironmental Significance of the Nearshore Curvolithus Ichnofacies. Palaios, 2(3), 255. https://doi.org/10.2307/3514675

Lorenz von Liburnau, J. R., 1902. Ergänzung zur Beschreibung der fossilen Halimeda Fuggeri. Sitzungsberichte der kaiserlich-königlichen Akademie der Wissenchaften, Mathematiksch-Naturwissenschaftliche Klasse, 111, 685-712.

Lowemark, L., Lin, I.-T., Wang, C.-H., Huh, C.-A., Wei, K.-Y., Chen, C.-W., 2004. Ethology of the zoophycos-producer: Arguments against the gardening model from 13 org C evidences of the spreiten material. Terrestrial Atmospheric and Oceanic Sciences, 15(4), 713. https://doi.org/10.3319/tao.2004.15.4.713(o)

Lukeneder, A., Uchman, A., Gaillard, C. Olivero, D., 2012. The late Barremian Halimedides horizon of the Dolomites (Southern Alps, Italy). Cretaceous Research, 35, 199-207. DOI: 10.1016/j.cretres.2012.01.002

Luo, M., Shi, G. R., Buatois, L. A., Chen, Z.-Q., 2020. Trace fossils as proxy for biotic recovery after the end-Permian mass extinction: A critical review. Earth-Science Reviews, 203(103059), 103059. https://doi.org/10.1016/j.earscirev.2019.103 059

MacEachern, J.A., Bann, K.L., Gingras, M.K., Zonneveld, J.P., Dashtgard, S.E., 2012. The ichnofacies paradigm. In: Knaust, D., Bromley, R.G. (Eds.), Trace Fossils as Indicators of Sedimentary Environments. Developments in Sedimentology, 64. Elsevier, Amsterdam, pp. 103-138.

Maerz Jr, R. H., Kaesler, R. L., Hakes, W. G., 1976. Trace fossils from the Rock Bluff Limestone (Pennsylvanian, Kansas). The University of Kansas Paleontological Contributions, 80, 1-8.

Mángano, M. G., Buatois, L. A., Maples, C. G., Lanier, W. P., 1997. Tonganoxichnus a new insect trace from the Upper Carboniferous of eastern Kansas. Lethaia, 30(2), 113-125.

Mangano, M. G., Buatois, L. A., West, R. R., Maples, C. G., 1998. Contrasting behavioral and feeding strategies recorded by tidal-flat bivalve trace fossils from the Upper Carboniferous of eastern Kansas. Palaios, 13(4), 335-351.

Mángano, M. G., Buatois, L. A., West, R. R., Maples, C. G., 1999. The origin and paleoecologic significance of the trace fossil Asteriacites in the Pennsylvanian of Kansas and Missouri. Lethaia, 32(1), 17-30.

https://doi.org/10.1111/j.1502-3931.1999.tb00577.x

Mángano, M. G., Labandeira, C. C., Kvale, E. P., Buatois, L. A., 2001. The insect trace fossil Tonganoxichnus from the Middle Pennsylvanian of Indiana: paleobiologic and paleoenvironmental implications. Ichnos: An International Journal of Plant & Animal, 8(3-4), 165-175.

Mangano, G. M., Buatois, L. A., West, R. R., Maples, C. G., 2002. Ichnology of a Pennsylvanian equatorial tidal flat--the Stull Shale Member at Waverly, eastern Kansas. Bulletin (Kansas Geological Survey), (245), 1-139.

Maples, C. G., Suttner, L. J., 1990. Trace fossils and marine-nonmarine cyclicity in the Fountain Formation (Pennsylvanian: Morrowan/Atokan) near Manitou springs, Colorado. Journal of Paleontology, 64(6), 859-880.

Martino, R. L., 1989. Trace fossils from marginal marine facies of the Kanawha Formation (Middle Pennsylvanian), West Virginia. Journal of Paleontology, 63(4), 389-403. https://doi.org/10.1017/s0022336000019648

Mattioli, E., Pittet, B., Petitpierre, L., Mailliot, S., 2009. Dramatic decrease of pelagic carbonate production by nannoplankton across the Early Toarcian anoxic event (T-OAE). Global and Planetary Change 65, 134-145.

Merrill, G. K., 1983. Trace Fossils Within Limestone Interbeds, Oak Grove Member, Carbondale Formation (Pennsylvanian, Desmoesian), Northwestern Illinois. AAPG Bulletin, 67(3), 513-513.

McArthur, J.M., 2019. Early Toarcian black shales: a response to an oceanic anoxic event or anoxia in marginal basins? Chemical Geology, 522, 71-83.

McArthur, J.M., Algeo, T.J., van de Schootbrugge, B., Li, Q., Howarth, R.J., 2008. Basinal restriction, black shales, Re-Os dating, and the Early Toarcian (Jurassic) oceanic anoxic event. Paleoceanography, 23, PA4217. https://doi.org/10.1029/2008PA001607

McElwain, J.C., Wade-Murphy, J., Hesselbo, S.P., 2005. Changes in carbon dioxide during an oceanic anoxic event linked to intrusion into Gondwana coals. Nature, 435, 479-482. https://doi.org/10.1038/nature03618

McIlroy, D., Lang, H. F., 2006. Discovery and paleoenvironmental implications of a Zoophycos-group trace fossil (? Echinospira) from the Middle Pennsylvanian Sydney Mines Formation of Nova Scotia. Atlantic Geology, 42(1), 31-35.

Miguez-Salas, O., Rodríguez-Tovar, F.J., Duarte, L.V., 2017. Selective incidence of the toarcian oceanic anoxic event (T-OAE) on macroinvertebrate marine communities: a case from the Lusitanian basin, Portugal. Lethaia, 50, 548–560. DOI: https://doi.org/10.1111/let.12212

Miguez-Salas, O., Rodríguez-Tovar, F.J., Duarte, L.V., 2018. Ichnological analysis at the Fonte Coberta section (Lusitanian Basin, Portugal): Approaching depositional environment during the Toarcian oceanic anoxic event (T-OAE). Spanish Journal of Palaeontology, 33, 261–276.

Miller III, W. (ed). 2007. Trace fossils: Concepts. Problems. Prospects. Elsevier, Amsterdam.

Miller, C.A., Peucker-Ehrenbrink, B., Walker, B.D., Marcantonio, F., 2011. Re-assessing the surface cycling of molybdenum and rhenium. Geochimica et Cosmochimica Acta, 75, 7146-7179. https://doi.org/10.1016/j.gca.2011.09.005

Miller, M. F., Knox, L. W., 1984. Biogenic structures and depositional environments of a Lower Pennsylvanian coal-bearing sequence, northern Cumberland Plateau, Tennessee, USA, in Curran H.A., ed., Biogenic structures: Their use in interpreting depositional environments: SEPM Society for Sedimentary Geology.

Monaco, P., Rodríguez-Tovar, F. J., Uchman, A., 2012. Ichnological analysis of lateral environmental heterogeneity within the Bonarelli Level (uppermost Cenomanian) in the classical localities near Gubbio, Central Apennines, Italy. Palaios, 27, 48–54. DOI: https://doi.org/10.2110/palo.2011.p11-018r

Monaco, P., Rodríguez-Tovar, F. J., Uchman, A., 2016. Environmental fluctuations during the latest Cenomanian (Bonarelli Level) in the Gubbio area (central Italy) based on an ichnofabric approach. In: Menichetti, M., Coccioni, R. & Montanari, A. (eds.), The Stratigraphic Record of Gubbio: Integrated Stratigraphy of the Late Cretaceous-Paleogene Umbria-Marche Pelagic Basin. Geological Society of America Special Paper, 524, 97–103. DOI: https://doi.org/10.1130/2016.2524(07)

Moore, R. C., 1964. Paleoecological aspects of Kansas Pennsylvanian and Permian cyclothems. In Symposium on cyclic sedimentation (Vol. 169, pp. 287-380). Kansas Geological Survey Bulletin.

Moore, R. C., Merriam, D. F., 1965. Upper Pennsylvanian Cyclotherms in the Kansas River Valley: A Field Conference Guidebook for the Annual Meetings, the Geological Society of America and Associated Societies, Kansas City, Missouri, 1965. Geological Society of America.

Nicholls, K. H., 2019. A Geoconservation perspective on the trace fossil record associated with the end–Ordovician mass extinction and glaciation in the Welsh Basin.

Ogg, J.G., 2012. Jurassic, in: Gradstein F.M., Ogg J.G., Schmitz M, Ogg G. (Eds.), The Geologic Time Scale 2012, pp. 731-791. 10.1016/B978-0-444-59425-9.00026-3

Olivero, D., 2007. *Zoophycos* and the role of type specimens in ichnotaxonomy. In: Miller III, W. (Ed.), Trace Fossils, Concepts, Problems, Prospects. Elsevier, Amsterdam, pp. 219-230.

Olivero, D., Gaillard, C., 2007. A constructional model for *Zoophycos*. In: Miller III, W. (Ed.), Trace Fossils, Concepts, Problems, Prospects. Elsevier, Amsterdam, pp. 466-476.

Olóriz, F., Rodriguez-Tovar, F.J., 2000. *Diplocraterion*: A useful marker for sequence stratigraphy and correlation in the Kimmeridgian, Jurassic (Prebetic Zone, Betic Cordillera, Southern Spain). Palaios, 15, 546-552.

Ordoñez, L., Vogel, H., Sebag, D., Ariztegui, D., Adatte, T., Russell, J.M., Kallmeyer, J., Vuillemin, A., Friese, A., Crowe, S.A., Bauer, K.W., Simister, R., Henny, C., Nomosatryo, S., Bijaksana, S., 2019. Empowering conventional Rock-Eval pyrolysis for organic matter characterization of the siderite-rich sediments of Lake Towuti (Indonesia) using End-Member Analysis. Organic Geochemistry, 134, 32-44. https://doi.org/10.1016/j.orggeochem.2019.05.002

Osete, M.L., Gómez, J.J., Pavón-Carrasco, F.J., Villalaín, J.J., Palencia-Ortas, A., Ruiz-Martínez, V.C., Heller, F., 2011. The evolution of Iberia during the Jurassic from palaeomagnetic data. Tectonophysics, 502, 105-120. https://doi.org/10.1016/j.tecto.2010.05.025

Pearce, C.R., Cohen, A.S., Coe, A.L., Burton, K.W., 2008. Molybdenum isotope evidence for global ocean anoxia coupled with perturbations to the carbon cycle during the Early Jurassic. Geology, 36(3), 231-234. https://doi.org/10.1130/G24446A.1

Pearson, N. J., Mángano, M. G., Buatois, L. A., Casadío, S., Rodriguez Raising, M., 2012. Ichnology, sedimentology, and sequence stratigraphy of outer-estuarine and coastal-plain deposits: Implications for the distinction between allogenic and autogenic expressions of the Glossifungites Ichnofacies. Palaeogeography, Palaeoclimatology, Palaeoecology, 333-334, 192-217.

https://doi.org/10.1016/j.palaeo.2012.03.03 1

Pemberton, G.S., Frey, R.W., 1982. Trace fossil nomenclature and the Planolites-Palaeophycus dilemma. Journal of Paleontology, 56, 843-881.

Pemberton, S. G., MacEachern, J. A., 1995. The sequence stratigraphic significance of trace fossils: examples from the Cretaceous foreland basin of Alberta, Canada, in Van Wagoner, J.C., and Bertram, G.T., eds., Sequence stratigraphy of foreland basin deposits — outcrop and subsurface examples from the Cretaceous of North America: Memoir, American Association of Petroleum Geologists, Memoir 64, p. 429-475.

Pemberton, S.G., Gingras, M.K., 2005. Classification and characterizations of biogenically enhanced permeability. AAPG bulletin, 89(11), 1493-1517.

Pemberton, S.G., MacEachern, J.A., Gingras, M.K., Saunders, T.D., 2008. Biogenic chaos: Cryptobioturbation and the work of sedimentologically friendly organisms. Palaeogeography, palaeoclimatology, palaeoecology, 270(3-4), 273-279.

Pemberton, S.G., MacEachern, J.A., Dashtgard, S.E., Bann, K.L., Gingras, M.K., Zonneveld, J.P., 2012. Shorefaces. In Developments in sedimentology (Vol. 64, pp. 563-603). Elsevier.

Percival, L.M.E., Witt, M.L.I., Mather, T.A., Hermoso, M., Jenkyns, H.C., Hesselbo, S.P., Al-Suwaidi, A.H., Storm, M.S., Ruhl, M., 2015. Globally enhanced mercury deposition during the end-Pliensbachian extinction and Toarcian OAE: A link to the Karoo–Ferrar Large Igneous Province. Earth and Planetary Science Letters, 428, 267-280. https://doi.org/10.1016/j.epsl.2015.06.064

Percival, L.M.E., Cohen, A.S., Davies, M.K., Dickson, A.J., Hesselbo, S.P., Jenkyns, H.C., Leng, M.J., Mather, T.A., Storm, M.S., Xu, W., 2016. Osmium isotope evidence for two pulses of increased continental weathering linked to Early Jurassic volcanism and climate change. Geology, 9, 759-762. https://doi.org/10.1130/G37997.1

Pollard, J. E., 1988. Trace fossils in coal-bearing sequences. Journal of the Geological Society, 145(2), 339-350. https://doi.org/10.1144/gsjgs.145.2.0339

Raiswell, R., Berner, R.A., 1985. Pyrite formation in euxinic and semi-euxinic sediments. American Journal of Science, 285(8), 710-724. https://doi.org/10.2475/ajs.285.8.710

Raiswell, R., Buckley, F., Berner, R.A. and Anderson, T.F., 1988. Degree of pyritization of iron as a paleoenvironmental indicator of bottom-water oxygenation. The Journal of Sedimentary Research, 58(5), 812-819.

Raup, D.M., Sepkoski, J.J., Jr., 1984. Periodicity of extinctions in the geologic past. Proceedings of the Geologists' Association, 81, 801-805. https://doi.org/10.1073/pnas.81.3.801

Reineck, H. E., 1963. Sedimentgefüge im Bereich der südlichen Nordsee. Abhandlungen der Senckenbergischen Naturforschenden Gesellschaft, 505.

Reineck, H.E., 1967. Parameter von Schichtung und Bioturbation. Geologische Rundschau, 56(1), 420-438. https://doi.org/10.1007/bf01848734

Remírez, M.N., Algeo, T.J., 2020a. Carbon-cycle changes during the Toarcian (Early Jurassic) and implications for regional versus global drivers of the Toarcian oceanic anoxic event. Earth-Sciences Reviews, 209, 103283. https://doi.org/10.1016/j.earscirev.2020.103 283

Remírez, M.N., Algeo, T.J., 2020b. Paleosalinity determination in ancient epicontinental seas: A case study of the T-OAE in the Cleveland Basin (UK). Earth-Sciences Reviews, 201, 103072.

https://doi.org/10.1016/j.earscirev.2019.103 072

Reolid, M., Mattioli, E., Nieto, L. M., Rodríguez-Tovar, F. J., 2014. The Early Toarcian Oceanic Anoxic Event in the External Subbetic (South Iberian palaeomargin, westernmost Tethys): Geochemistry, nannofossils and ichnology. Palaeogeography, Palaeoclimatology, Palaeoecology, 411, 79–94.

Reolid, M., Molina, J. M., Nieto, L. M., Rodríguez-Tovar, F. J., 2018. The Toarcian Oceanic Anoxic Event in the South Iberian Palaeomargin. Springer Briefs in Earth Sciences, Cham (Switzerland).

Reolid, M., Duarte, L. V. Rita, P., 2019. Changes in foraminiferal assemblages and environmental conditions during the T-OAE (Early Jurassic) in the northern Lusitanian Basin, Portugal. Palaeogeography, Palaeoclimatology, Palaeoecology, 520, 30–43. DOI: https://doi.org/10.1016/j.palaeo.2019.01.02 2

Ricken, W., 1986. Diagenetic Bedding. A Model for Marl-Limestone Alternations. Lecture Notes in Earth Science 6. Springer-Verlag, Berlin, 195 pp.

Rita, P., Reolid, M., Duarte, L. V., 2016. Benthic foraminiferal assemblages record major environmental perturbations during the Late Pliensbachian-Early Toarcian interval in the Peniche GSSP, Portugal. Palaeogeography, Palaeoclimatology, Palaeoecology, 454, 267–281. DOI: https://doi.org/10.1016/j.palaeo.2016.04.03 9

Rindsberg, A.K., Kopaska-Merkel, D.C., 2005. Treptichnus and Arenicolites from the Steven C. Minkin Paleozoic footprint site (Langsettian, Alabama, USA). In: Buta, R.J., Rindsberg, A.K., Kopaska-Merkel, D.C. (Eds.), Pennsylvanian Footprints in the Black Warrior Basin of Alabama. Alabama Paleontological Society Monograph no. 1, Birmingham, pp. 121-141.

Rodrigues, B., Silva, R.L., Mendonça Filho, J.G., Comas-Rengifo, M.J., Goy, A., Duarte, L.V., 2020. Kerogen assemblages and δ13C kerogen of the uppermost Pliensbachian–lower Toarcian succession of the Asturian Basin (northern Spain). International Journal of Coal Geology, 229, 103573. https://doi.org/10.1016/j.coal.2020.103573

Rodríguez-Tovar, F.J., 2021. Ichnology of the Toarcian Oceanic Anoxic Event: An underestimated tool to assess palaeoenvironmental interpretations. Earth-Science Reviews, 216, 103579. https://doi.org/10.1016/j.earscirev.2021.103 579

Rodríguez-Tovar, F.J., Uchman, A., 2010. Ichnofabric evidence for the lack of bottom anoxia during the Lower Toarcian Oceanic Anoxic Event in the Fuente de la Vidriera section, Betic Cordillera, Spain. Palaios, 25, 576-587.

Rodríguez-Tovar, F. J., Uchman, A., 2011. Ichnological data as a useful tool for deep-sea environmental characterization: a brief overview and an application to recognition of small-scale oxygenation changes during the Cenomanian-Turonian anoxic event. Geo-Marine Letters, 31, 525–536.

Rodríguez-Tovar, F. J., Uchman, A., 2017. The Faraoni event (latest Hauterivian) in ichnological record: The Río Argos section of southern Spain. Cretaceous Research, 79, 109–121.

Rodríguez-Tovar, F.J., Reolid, M., 2013. Environmental conditions during the Toarcian Oceanic Anoxic Event (T-OAE) in the westernmost Tethys: influence of the regional context on a global phenomenon. Bulletin of Geosciences 88, 697-712.

Rodríguez-Tovar, F.J., Puga-Bernabéu, Á., Buatois, L.A., 2008. Large burrow systems in marine Miocene deposits of the Betic Cordillera

(Southeast Spain). Palaeogeography, Palaeoclimatology, Palaeoecology 268, 19-25.

Rodríguez-Tovar, F. J., Uchman, A., Martín-Algarra, A., 2009a. Oceanic Anoxic Event at the Cenomanian-Turonian boundary interval (OAE-2): ichnological approach from the Betic Cordillera, southern Spain. Lethaia, 42, 407–417.

Rodríguez-Tovar, F. J., Uchman, A., Martín-Algarra, A., O'Dogherty, L., 2009b. Nutrient spatial variation during intrabasinal upwelling at the Cenomanian-Turonian oceanic anoxic event in the westernmost Tethys: An ichnological and facies approach. Sedimentary Geology, 215, 83–93.

Rodríguez-Tovar, F.J., Miguez-Salas, O., Duarte, L.V., 2017. Toarcian Oceanic Anoxic Event induced unusual behaviour and palaeobiological changes in Thalassinoides trace-makers. Palaeogeography, Palaeoclimatology, Palaeoecology, 485, 46-56.

Rodríguez-Tovar, F.J., Miguez-Salas, O., Dorador, J., Duarte, L.V., 2019. Opportunistic behaviour after the Toarcian Oceanic Anoxic Event: The trace fossil Halimedides. Palaeogeography, Palaeoclimatology, Palaeoecology, 520, 240-250.

Rodríguez-Tovar, F. J., Uchman, A., Reolid, M., Sánchez-Quiñónez, C. A., 2020. Ichnological analysis of the Cenomanian-Turonian boundary interval in a collapsing slope setting: A case from the Rio Fardes section, southern Spain. Cretaceous Research, 106, 104262. DOI: https://doi.org/10.1016/j.cretres.2019.1042 62

Rodríguez-Tovar, F.J., 2010. Ichnological analysis and sequence stratigraphy research: present-day and prospective: Memoir Geological Society of India, 75, 99-114.

Rodríguez-Tovar, F.J., 2021. Ichnology of the Toarcian Oceanic Anoxic Event: An underestimated tool to assess palaeoenvironmental interpretations. Earth-Sciences Reviews, 216, 103579. https://doi.org/10.1016/j.earscirev.2021.103 579

Rodríguez-Tovar, F. J., 2022. Ichnological analysis: A tool to characterize deep-marine processes and sediments. Earth-Science Reviews, 228(104014), 104014. https://doi.org/10.1016/j.earscirev.2022.104 014

Rodríguez-Tovar, F. J., Kaskes, P., Ormö, J., Gulick, S. P. S., Whalen, M. T., Jones, H. L., Lowery, C. M., Bralower, T. J., Smit, J., King, D. T., Jr, Goderis, S., Claeys, P., 2022. Life before impact in the Chicxulub area: unique marine ichnological signatures preserved in crater suevite. Scientific Reports, 12(1). https://doi.org/10.1038/s41598-022-15566-z

Rodríguez-Tovar, F.J., Reolid, M., 2013. Environmental conditions during the Toarcian Oceanic Anoxic Event (T-OAE) in the westernmost Tethys: influence of the regional context on a global phenomenon. Bulletin of Geosciences, 88, 697–712. https://doi.org/10.3140/bull.geosci.1397

Rodríguez-Tovar, F. J., Uchman, A., 2017. The Faraoni event (latest Hauterivian) in ichnological record: The Río Argos section of southern Spain. Cretaceous Research, 79, 109-121. https://doi.org/10.1016/j.cretres.2017.07.01 8

Rodríguez-Tovar, F. J., Uchman, A., Martín-Algarra, A., O'Dogherty, L., 2009. Nutrient spatial variation during intrabasinal upwelling at the Cenomanian–Turonian oceanic anoxic event in the westernmost Tethys: An ichnological and facies approach. Sedimentary Geology, 215(1-4), 83-93. https://doi.org/10.1016/j.sedgeo.2009.01.00 6

Röhl, H.J., Schmid-Röhl, A., 2005. Lower Toarcian (Upper Liassic) black shales of the Central

European epicontinental basin: a sequence stratigraphic case study from the SW German Posidonia Shale, in Harris, N.B. (ed.), The Deposition or Organic-Carbon-Rich Sediments: Models, Mechanisms, and Consequences, SEPM Special Publication 82, pp. 165–189.

Röhl, H-J., Schmid-Röhl, A., Oschmann, W., Frimmel, A., Schwark, L., 2001. The Posidonia Shale (Lower Toarcian) of SW-Germany: an oxygen-depleted ecosystem controlled by sea level and palaeoclimate. Palaeogeography, Palaeoclimatology, Palaeoecology, 165, 27–52. https://doi.org/10.1016/S0031-0182(00)00152-8

Rosales, I., Barnolas, A., Goy, A., Sevillano, A., Armendáriz, M., López-García, J.M., 2018. Isotope records (C-O-Sr) of late Pliensbachian-early Toarcian environmental perturbations in the westernmost Tethys (Majorca Island, Spain). Palaeogeography, Palaeoclimatology, Palaeoecology, 497, 168-185.

Rowe, H.D., Loucks, R.G., Ruppel, S.C., Rimmer, S.M., 2008. Mississippian Barnett Formation, Fort Worth Basin, Texas: Bulk geochemical inferences and Mo–TOC constraints on the severity of hydrographic restriction. Chemical Geology, 257(1-2), 16-25.

Ruebsam, W., Müller, T., Kovács, J., Pálfy, J., Schark, L., 2018. Environmental response to the early Toarcian carbon cycle and climate perturbations in the northeastern part of the West Tethys shelf. Gondwana Research, 59, 144-158.

Ruebsam, W., Mayer, B., Schwark, L., 2019. Cryosphere carbon dynamics control early Toarcian global warming and sea level evolution. Global and Planetary Change, 172, 440-453. https://doi.org/10.1016/j.gloplacha.2018.11.003

Ruebsam, W., Reolid, M., Sabatino, N., Masetti, D., Schwark, L., 2020a. Molecular paleothermometry of the early Toarcian climate perturbation. Global and Planetary Change,

195, 103351. https://doi.org/10.1016/j.gloplacha.2020.103351

Ruebsam, W., Reolid, M., Marok, A., Schwark, L., 2020b. Drivers of benthic extinction during the early Toarcian (Early Jurassic) at the northern Gondwana paleomargin: Implications for paleoceanographic conditions. Earth-Sciences Reviews, 203, 103117. https://doi.org/10.1016/j.earscirev.2020.103117

Savrda, C.E., 2016. Composite ichnofabrics: Categorization based on number of ichnocoenoses and their temporal incongruence. Palaios, 31, 92-96.

Schieber, J., 2003. Simple gifts and buried treasures–implications of finding bioturbation and erosion surfaces in black shales. The Sedimentary Record, 1(2), 4-8.

Schieber, J., Southard, J., Thaisen, K., 2007. Accretion of mudstone beds from migrating flocculle ripples. Science, 318(5857), 1760-1763.

Schieber, J., Wilson, R.D., 2021. Burrows without a trace—How meioturbation affects rock fabrics and leaves a record of meiobenthos activity in shales and mudstones. PalZ, 95(4), 767-791.

Scholz, F., McManus, J., Sommer, S., 2013. The manganese and iron shuttle in a modern euxinic basin and implications for molybdenum cycling at euxinic ocean margins. Chemical Geology, 355, 56–68. https://doi.org/10.1016/j.chemgeo.2013.07.006

Schouten, S., van Kaam-Peters, H.M., Rijpstra, W.I.C., Schoell, M., Damste, J.S.S., 2000. Effects of an oceanic anoxic event on the stable carbon isotopic composition of early Toarcian carbon. American Journal of Science, 300(1), 1-22. https://doi.org/10.2475/ajs.300.1.1

Schwark, L., Frimmel, A., 2004. Chemostratigraphy of the Posidonia Black Shale, SW-Germany: II.

Assessment of extent and persistence of photic-zone anoxia using aryl isoprenoid distributions. Chemical Geology, 206(3-4), 231-248. https://doi.org/10.1016/j.chemgeo.2003.12.008

Scotese, C.R., 2013. Map Folio 39 Early Jurassic Toarcian (179.3 Ma): PALEOMAP PaleoAtlas for ArcGIS. vol. 3. PALEOMAP Project, Evanston, Illinois. https://doi.org/10.13140/2.1.4497.2326

Scott, C., Lyons, T.W., 2012. Contrasting molybdenum cycling and isotopic properties in euxinic versus non-euxinic sediments and sedimentary rocks: Refining the paleoproxies. Chemical Geology, 324, 19-27. https://doi.org/10.1016/j.chemgeo.2012.05.012

Scott, C., Lyons, T.W., Bekker, A., Shen, Y.A., Poulton, S.W., Chu, X.L., Anbar, A.D., 2008. Tracing the stepwise oxygenation of the Proterozoic ocean. Nature, 452(7186), 456-459.

Seilacher, A., 1990. Aberrations in bivalve evolution related to photo- and chemosymbiosis. Historical Biology, 3, 289-311.

Sepkoski, J.J., Jr., 1996. Patterns of Phanerozoic extinction: a perspective from global data bases, in Walliser O.H. (ed.), Global events and event stratigraphy in the Phanerozoic, Springer, Berlin, Heidelberg, pp. 35-51. https://doi.org/10.1007/978-3-642-79634-0_4

Slater, S. M., Twitchett, R. J., Danise, S., Vajda, V., 2019. Substantial vegetation response to Early Jurassic global warming with impacts on oceanic anoxia. Nature Geoscience, 12, 462–467. DOI: https://doi.org/10.1038/s41561-019-0349-z

Smith, C., Fillmore, D., Simpson, E., Lucas, S., 2011 Invertebrate trace fossils from deposits of the Pennsylvanian-age Llewellyn Formation, Eastern Pennsylvania, USA. Fossil Record 3: Bulletin 53, 53, 152

Stanley, D. C. A., Pickerill, R. K., 1993. Fustiglyphus annulatus from the Ordovician of Ontario, Canada, with a systematic review of the ichnogenera Fustiglyphus Vialov 1971 and Rhabdoglyphus Vassoievich 1951. Ichnos, 3, 57–67.

Soulimane, C., Marok, A., Reolid, M., 2020. Similarity analysis of Ostracoda faunas in the Western Tethys during the Late Pliensbachian-Early Toarcian (Early Jurassic). Arabian Journal of Geosciences, 13, 136. DOI: https://doi.org/10.1007/s12517-020-5178-2

Suan, G., Schöllhorn, I., Schlögl, J., Segit, T., Mattioli, E., Lécuyer, C., Fourel, F., 2018. Euxinic conditions and high sulfur burial near the European shelf margin (Pieniny Klippen Belt, Slovakia) during the Toarcian oceanic anoxic event. Global and Planetary Change 170, 246-259.

Taylor, S.R., McLennan, S.M., 1985. The Continental Crust: Its Composition and Evolution. Blackwell Scientific Publications, Oxford, 312 pp.

Taylor, A.M., Goldring, R., 1993. Description and analysis of bioturbation and ichnofabric. Journal of the Geological Society, 150, 141-148.

Taylor, A., Goldring, R., Gowland, S., 2003. Analysis and application of ichnofabrics. Earth-Science Reviews, 60, 227-259.

Them II, T.R., Gill, B.C., Caruthers, A.H., Gröcke, D.R., Tulsky, E.T., Martindale, R. C., Poulton, T.P., Smith, P.L., 2017. High-resolution carbon isotope records of the Toarcian Oceanic Anoxic Event (Early Jurassic) from North America and implications for the global drivers of the Toarcian carbon cycle. Earth and Planetary Science Letters, 459, 118-126.

Thibault, N., Ruhl, M., Ullmann, C.V., Korte, C., Kemp, D.B., Gröcke, D.R., Hesselbo, S.P., 2018. The wider context of the Lower Jurassic

Toarcian oceanic anoxic event in Yorkshire coastal outcrops, UK. Proceedings of the Geologists' Association, 129, 372-391. https://doi.org/10.1016/j.pgeola.2017.10.007

Thierry, J., Barrier, E., Abbate, E., Ait-Ouali, R., Ait-Salem, H., Bouaziz, S., Canerot, J., Elmi, S., Geluk, M., Georgiev, G., Guiraud, R., Hirsch, F., Ivanik, M., Le Metour, J., Le Nindre, Y.M., Medina, F., Nikishin, A.M., Page, K., Panov, D.L., Pique, A., Poisson, A., Sandulescu, M., Sapunov, I.G., Seghedia, A., Soussi, M., Tarkowski, R.A., Tchoumatchenko, P.V., Vaslet, D., Volozh, Y.A., Voznezenski, A., Walley, C.D., Ziegler, M., Ait-Brahim, L., Bergerat, F., Bracener, R., Brunet, M.F., Cadet, J.P., Guezou, J.C., Jabaloy, A., Lepvrier, C., Rimmele, G., 2000. Map 8. Middle Toarcian (180-178 Ma), in: Dercourt, J., Gaetani, M., Vrielynck, B., Barrier, E., Biju-Duval, B., Brunet, M.-F., Cadet, J.P., Crasquin, S., Sandulescu, M. (Eds.), Atlas Peri-Tethys Palaeogeographical Maps, vol. I-XX. CCGM/CGMW, Paris, 9 pp.

Tribovillard, N., Algeo, T.J., Baudin, F., Riboulleau, A., 2012. Analysis of marine environmental conditions based on molybdenum–uranium covariation—Applications to Mesozoic paleoceanography. Chemical Geology, 324, 46-58. https://doi.org/10.1016/j.chemgeo.2011.09.009

Uchman, A., 1999. Ichnology of the Rhenodanubian flysch (Lower Cretaceous-Eocene) in Austria and Germany. Beringeria, 25, 67-173.

Uchman, A., Wetzel, A., 2011. Deep-sea ichnology: the relationships between depositional environment and endobenthic organisms. In: Hüneke, H., Mulder, T. (Eds.), Deep-Sea Sediments. Developments in Sedimentology Vol. 63. Elsevier, Amsterdam, pp. 517-556.

Uchman, A., Wetzel, A., 2012. Deep-sea fans. In: Knaust, D., Bromley, R.G. (Eds.), Trace Fossils as Indicators of Sedimentary Environments. Developments in Sedimentology Vol. 64. Elsevier, Amsterdam, pp. 643-671.

Uchman, A., Bąk, K., Rodríguez-Tovar, F. J., 2008. Ichnological record of deep-sea palaeoenvironmental changes around the Oceanic Anoxic Event 2 (Cenomanian-Turonian boundary): an example from the Barnasiówka section, Polish Outer Carpathians. Palaeogeography, Palaeoclimatology, Palaeoecology, 262, 61–71.

Uchman, A., Caruso, C., Sonnino, M., 2012. Taxonomy review of Chondrites affinis (Stenberg, 1883) from Cretaceous-Neogene offshore-deep-sea Tethyan sediments and recommendation for its further use. Rivista Italiana di Paleontologia e Stratigrafia, 118, 313-324.

Uchman, A., Rodríguez-Tovar, F. J., Oszczypko, N., 2013a. Exceptionally favourable life conditions for macrobenthos during the Late Cenomanian OAE-2 event: Ichnological record from the Bonarelli Level in the Grajcarek Unit, Polish Carpathians. Cretaceous Research, 46, 1–10.

Uchman, A., Rodríguez-Tovar, F. J., Machaniec, E., Kędzierski, M., 2013b. Ichnological characteristics of Late Cretaceous hemipelagic and pelagic sediments in a submarine high around the OAE-2 event: A case from the Rybie section, Polish Carpathians. Palaeogeography, Palaeoclimatology, Palaeoecology, 370, 222-231.

Valenzuela, M., García-Ramos, J.C., Suárez de Centi, C., 1986. The Jurassic sedimentation in Asturias (N Spain). Trabajos de Geología, Universidad de Oviedo, 16, 121-132.

Valenzuela, M., García-Ramos, J.C., Suárez de Centi, C., 1989. La sedimentación en una rampa carbonatada dominada por tempestades, ensayos de correlación de ciclos y eventos en la ritmita

margo-calcárea del Jurásico de Asturias. Cuadernos de Geología Ibérica, 13, 217-235 (in Spanish).

van de Schootbrugge, B., Bailey, T.R., Rosenthal, Y., Katz, M.E., Wright, J.D., Miller, K. G., Feist-Burkhardt, S., Falkowski, P. G., 2005. Early Jurassic climate change and the radiation of organic-walled phytoplankton in the Tethys Ocean. Paleobiology, 31, 73-97. https://doi.org/10.1666/0094-8373(2005)031<0073:EJCCAT>2.0.CO;2

Vialov, O. S. 1971. Mesozoic problematica from Pamir and Caucasus. Paleontologicheskiy Sbornik, 7, 85-93. In Russian.

Vorlicek, T.P., Kahn, M.D., Kasuya, Y., Helz, R.H., 2004. Capture of molybdenum in pyrite-forming sediments: Role of ligand-induced reduction by polysulfides. Geochimica et Cosmochimica Acta, 68, 547–556. https://doi.org/10.1016/S0016-7037(03)00444-7

Wei, W., Algeo, T.J., 2020. Elemental proxies for paleosalinity analysis of ancient shales and mudrocks. Geochimica et Cosmochimica Acta, 287, 341-366.

Wei, W., Yu, W., Algeo, T. J., Herrmann, A. D., Zhou, L., Liu, J., Wang, Q., Du, Y., 2022. Boron proxies record paleosalinity variation in the North American Midcontinent Sea in response to Carboniferous glacio-eustasy. Geology, 50(5), 537-541. https://doi.org/10.1130/g49521.1

West, R. R., Ward, E. L., 1990. *Asteriacites* lumbricalis and a protasterid ophiuroid. En A. J. Boucot (Ed.), Evolutionary paleobiology of behavior and coevolution (pp. 321-327). Elsevier.

Westphal, H., Munnecke, A., Böhm, F., Bornholdt, S., 2008. Limestone-marl alternations in epeiric sea settings-witnesses of environmental changes or diagenesis? In: Pratt, B.R., Holmden, C. (Eds.), Dynamics of Epeiric Seas. Geological Association of Canada, Special Paper 48, pp. 389-406.

Wetzel, A., Uchman, A., 2012. Hemipelagic and pelagic basin plains. In: Knaust, D., Bromley, R.G. (Eds.), Trace Fossils as Indicators of Sedimentary Environments. Developments in Sedimentology Vol. 64. Elsevier, Amsterdam, pp. 673-701.

Wignall, P.B., 1990. Observations on the evolution and classification of dysaerobic communities. The Paleontological Society Special Publications, 5, 99-111.

Wignall, P.B., 1994. Black shales (No. 30). Clarendon Press.

Wignall, P.B., Newton, R.J., Little, C.T., 2005. The timing of paleoenvironmental change and cause-and-effect relationships during the Early Jurassic mass extinction in Europe. American Journal of Science, 305, 1014-1032. https://doi.org/10.2475/ajs.305.10.1014

Wilson, R.D., Schieber, J., Stewart, C.J., 2021. The discovery of widespread agrichnia traces in Devonian black shales of North America: another chapter in the evolving understanding of a "not so anoxic" ancient sea. PalZ, 95, 661-681.

Xu, W., Ruhl, M., Jenkyns, H.C., Leng, M.J., Huggett, J.M., Minisini, D., Ullmann, C.V., Riding, J.B., Weijers, J.W.H., Storm, M.S., Percival, L.M.E., Tosca, N.J., Idiz, E.F., Tegelaar, E.W., Hesselbo, S.P., 2018. Evolution of the Toarcian (Early Jurassic) carbon-cycle and global climatic controls on local sedimentary processes (Cardigan Bay Basin, UK). Earth and Planetary Science Letters, 484, 396-411.

Xia, G., Mansour, A., 2022. Paleoenvironmental changes during the early Toarcian Oceanic Anoxic Event: Insights into organic carbon distribution and controlling mechanisms in the eastern Tethys. Journal of Asian Earth Sciences, 237, 105344. https://doi.org/10.1016/j.jseaes.2022.105344

Zhang, Y., He, Z., Jiang, S., Gao, B., Liu, Z., Han, B., Wang, H., 2017. Marine redox stratification during the early Cambrian (ca. 529-509 Ma) and its control on the development of organic-rich shales in Yangtze Platform. Geochemistry, Geophysics, Geosystems, 18(6), 2354-2369.